NASA SP-118

SPACE-CABIN ATMOSPHERES

Part IV — Engineering Tradeoffs of One- Versus Two-Gas Systems

NATIONAL AERONAUTICS AND SPACE ADMINISTRATION

SPACE-CABIN ATMOSPHERES
Part IV. Engineering Tradeoffs of One- Versus Two-Gas Systems

A literature review by
Emanuel M. Roth, M.D.

Prepared under contract for NASA by
Lovelace Foundation for Medical Education
and Research, Albuquerque, New Mexico

Foreword

THIS REPORT is Part IV, the last volume of a study on *Space-Cabin Atmospheres*, conducted under sponsorship of the Directorate, Space Medicine, Office of Manned Space Flight, National Aeronautics and Space Administration. Part I, "Oxygen Toxicity," was published as NASA SP–47, Part II, "Fire and Blast Hazards," as NASA SP–48, and Part III, "Physiological Factors of Inert Gases," as NASA SP–117.

This document provides a readily available summary of the open literature in the field. It is intended primarily for biomedical scientists and design engineers.

The manuscript was reviewed and evaluated by leaders in the scientific community as well as by the NASA staff. As is generally true among scientists, there was varied opinion about the author's interpretation of the data compiled. There was nonetheless complete satisfaction with the level and scope of scholarly research that went into the preparation of the document. Thus, for scientist and engineer alike it is anticipated that this study will become a basic building block upon which research and development within the space community may proceed.

JACK BOLLERUD
Brigadier General, USAF, MC
Acting Director, Space Medicine
Office of Manned Space Flight

À,

Contents

Introduction

THE SELECTION of an ideal space-cabin atmosphere requires thorough analysis of physiological, physical, and engineering considerations of the problem. Since the basic function of a cabin atmosphere and its control system is to provide an environment for the optimum function of both crew and equipment, the specific interaction between the two must constantly be kept in mind. In this fourth part of the series on Selection of Space-Cabin Atmospheres, an attempt is made to consider this interaction in establishing valid criteria for engineering tradeoffs.

It has been the general practice in this series to avoid relating the analysis of literature to any one specific space mission. This philosophy will be continued in the present study; however, meaningful engineering tradeoffs can be made only with rather well-defined physical constraints on the system. Because the manned-orbiting-laboratory concept allows adequate and realistic constraints to be set, it will be used as a model example in this analysis. Since the success and safety of each mission and crew are to a considerable extent dependent on the choice and design of atmospheric and thermal control systems, synthesis and optimization methods have become essential steps in atmosphere selection. Because every bit of weight and volume must be saved and every fraction of performance extracted from every subsystem, with no loss in reliability, and with economy of effort and at minimum cost, sophisticated analyses have been required for total systems integration. In the past, studies of this type have been of great value to the engineer in presenting heat- and mass-transfer data, as well as chemical process descriptions which include the direct influence of vehicle data, system variables, process selection, and reliability considerations. Very often the gas-specific factors have, by necessity, been included in the analyses, but their roles have not been pointedly delineated. It is hoped that the role of the gas-specific factors and the many biases surrounding their choice does become more clear as a result of the present analysis.

The study begins with an evaluation of the physiological considerations which set boundaries for the physical environment within the cabin (ch. 1). The engineering analysis of chapter 2 is a review of the interaction between the physiological and hardware parameters of the environmental control system. An attempt is made to compare for each subsystem the effect of several physiologically acceptable gas mixtures on the weight and power penalties for missions of different types and durations. In chapter 3, the tradeoff criteria established in chapter 2 are used in an analysis of a typical mission — a two-man orbiting vehicle. The results of tradeoff analyses performed by several groups are compared to demonstrate the sensitivity of the final product to the physical, physiological, and engineering assumptions which were made. This mission was chosen only because of the availability of several completely independent studies of the tradeoffs by the aerospace industry. These independent analyses offer the opportunity for evaluation of assumptions and biases which usually creep into any tradeoff study. It is hoped

that this review will provide an adequate basis for unbiased atmospheric tradeoff studies of future missions.

Several excellent reviews of analytical methods for atmospheric control processes have been used for basic source materials. [24, 20, 80, 95] The unpublished data of the Boeing Co. on engineering tradeoffs of different gas systems were also of great value in establishing the gas-specific variables critical to this study. [12]

At the NASA Manned Spacecraft Center in Houston, there is presently a project on the design of computer-assisted design and tradeoff tools. [48] Such a program should be of great value in simplifying the approach to many of the problems raised in this review.

The nomenclature and units used throughout the paper are presented as appendix A. Tables for use in converting units from one system of units to another are presented as appendix B.

Physiological Considerations

THE BASIC physiological requirements for selection of space-cabin atmospheres have been discussed by many investigators, as well as by the first three parts of the present series.[90, 91, 92] Since exhaustive review of these factors is beyond the scope of this present analysis, only a brief summary will be presented. The major factors are as follows:

    (1) Total pressure
    (2) Oxygen
    (3) Water vapor
    (4) Carbon dioxide
    (5) Diluent gas
    (6) Toxic contaminants and odors
    (7) Dusts, aerosols, and ions
    (8) Circulation of atmosphere
    (9) Temperature control

TOTAL PRESSURE

The boundaries of pressure limitations in space cabins are more dependent on engineering realities than on physiological limits. For the upper limit, it is certainly not necessary to consider pressures greater than 1 atmosphere (760 mm Hg). The establishment of the lower limit is determined by the desire to keep the alveolar partial pressure of oxygen as close as possible to the sea-level equivalent of 104 mm Hg. At sea level, this is attained in a dry air free of carbon dioxide and water vapor with an oxygen ambient partial pressure (p_{O_2}) of 160 mm Hg. In the presence of an alveolar p_{CO_2} of 40 mm Hg and alveolar water vapor of 47 mm Hg, the minimum total pressure of a pure oxygen cabin should be $104 + 40 + 47$, or 191 mm Hg. One must therefore examine the engineering implications of total pressures between 760 and 191 mm Hg.

OXYGEN

An average oxygen consumption rate of 1.8 to 2 lb/man/day can be assumed. Partial pressure of oxygen in a space vehicle should be ideally maintained above a minimum point which allows a blood saturation of at least 95 percent to insure optimum performance. The upper limit of oxygen partial pressure is far from clear.[90] Figure 1 indicates the operational envelope of pressure and oxygen which can be considered in the space cabin. The curve is based on exposure for 1 week or more. To maintain the same degree of oxygen saturation in the blood as in air at sea level when total pressure is decreased, the percentage of oxygen in the atmosphere must increase as shown by the "sea level equivalent" curve.

The unimpaired performance zone (center clear zone) indicates the range of variation that can be tolerated without performance decrement. The maximum oxygen tolerance (definite pathology) for long periods is currently under investigation. The role of nitrogen and trace contaminants on the symptoms of oxygen toxicity in the oxygen range of 90 to 100 percent is still open to question, as shown by the right-hand area.[90]

Prolonged exposure to the low oxygen levels illustrated to the left of the unimpaired performance zone requires special acclimatization. Acclimatization can be accomplished by continuous exposure to successively lower pressures, with little intermediate return to higher pressures. Optimal acclimatization to allow survival at 25 000 feet requires 4 to 6 weeks. The minimum tolerable total pressure is based upon the effective partial pressure of oxygen. Decompression which may occur below a total pressure of 300 mm Hg in the
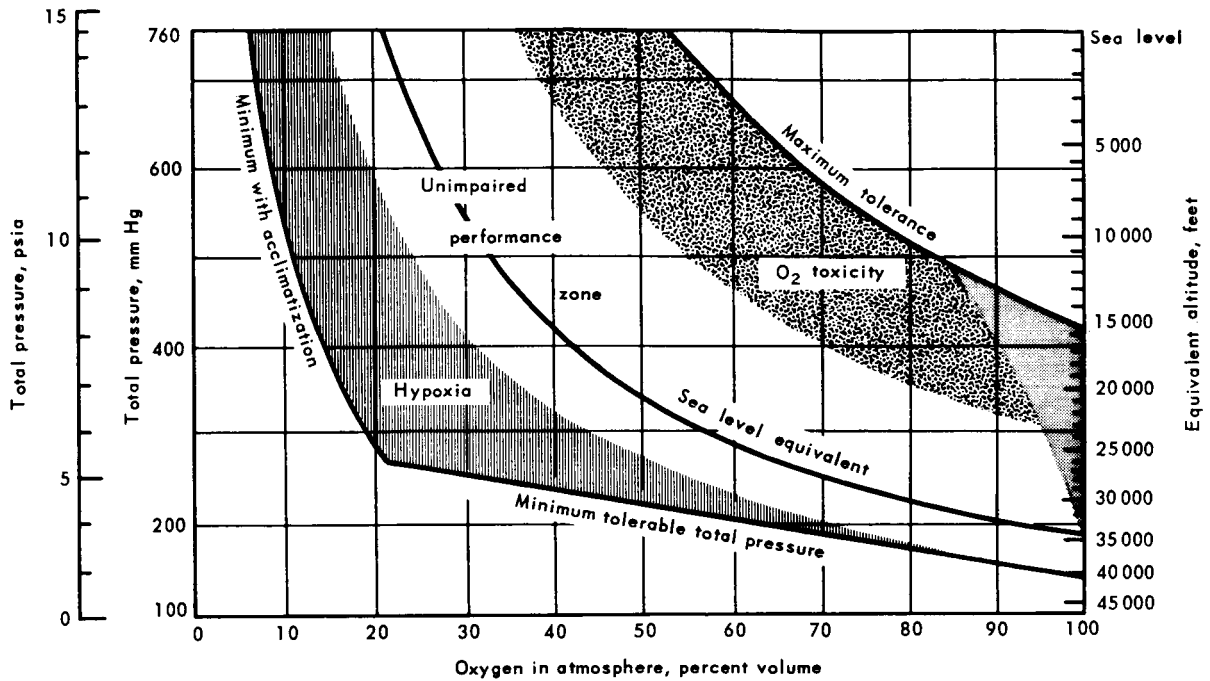
FIGURE 1.—*Oxygen-pressure effects.* (MODIFIED FROM THE NASA BIOASTRONAUTICS DATA BOOK [94] AFTER THE DATA OF LUFT.[82])

absence of adequate denitrogenation is disregarded.

Figure 2 represents the approximate time of appearance of signs and symptoms of oxygen toxicity. The nature of the symptoms varies with the ambient partial pressures of oxygen which cause them. Above 760 mm Hg, the central nervous system is the primary site of defect, with symptoms such as nausea, dizziness, convulsions, and syncope. In the range of 400 to 760 mm Hg, respiratory and nervous system symptoms predominate. These are substernal distress (bronchitis and probably atelectasis), paresthesias, and nausea. In the range of 200 to 400 mm Hg, reported symptoms are respiratory and, possibly, hematological and renal: atelectasis, oxidative hemolytic anemia, and protein and casts in the urine. Studies from the Gemini IV, V, VI, and VII missions suggest that oxygen toxicity has not been entirely ruled out as a factor in the decrease of red blood cells on exposure to the 258 mm Hg (5 psia) p_{O_2} used in these cabins.[9] The role of tocopherol deficiency and plasma lipid peroxides in the hemolytic process is currently under study.[31, 72, 10]

At a recent NASA conference on selection of post-Apollo atmospheres, it was reported that electron-microscopic changes in mitochrondial structure have been seen in the liver and kidney of several animal species after prolonged exposure to 5-psia, 100 percent oxygen.[87] There were no specific symptoms or clinical chemistry findings associated with these lesions, and their meaning is not clear. The U.S. Air Force toxicology studies at the Aerospace Medical Laboratories at Wright-Patterson Air Force Base have recently revealed that most of the abnormal blood chemistries seen in dogs and monkeys early in exposure to 5-psia, 100 percent O_2 return to normal within 6 months.[2] Only blood lactic dehydrogenase (LDH), serum pyruvic glutamic transaminase (SPGT), and serum glutamic-oxalic transaminase (SGOT) remain slightly above the upper limits of the normal range. These slight abnormalities may represent adaptation to 5-psia, 100 percent O_2.

Recent studies on susceptibility of humans to pulmonary atelectasis indicate that the ratio of pulmonary air conductance to lung volume appears to be a significant factor in individual
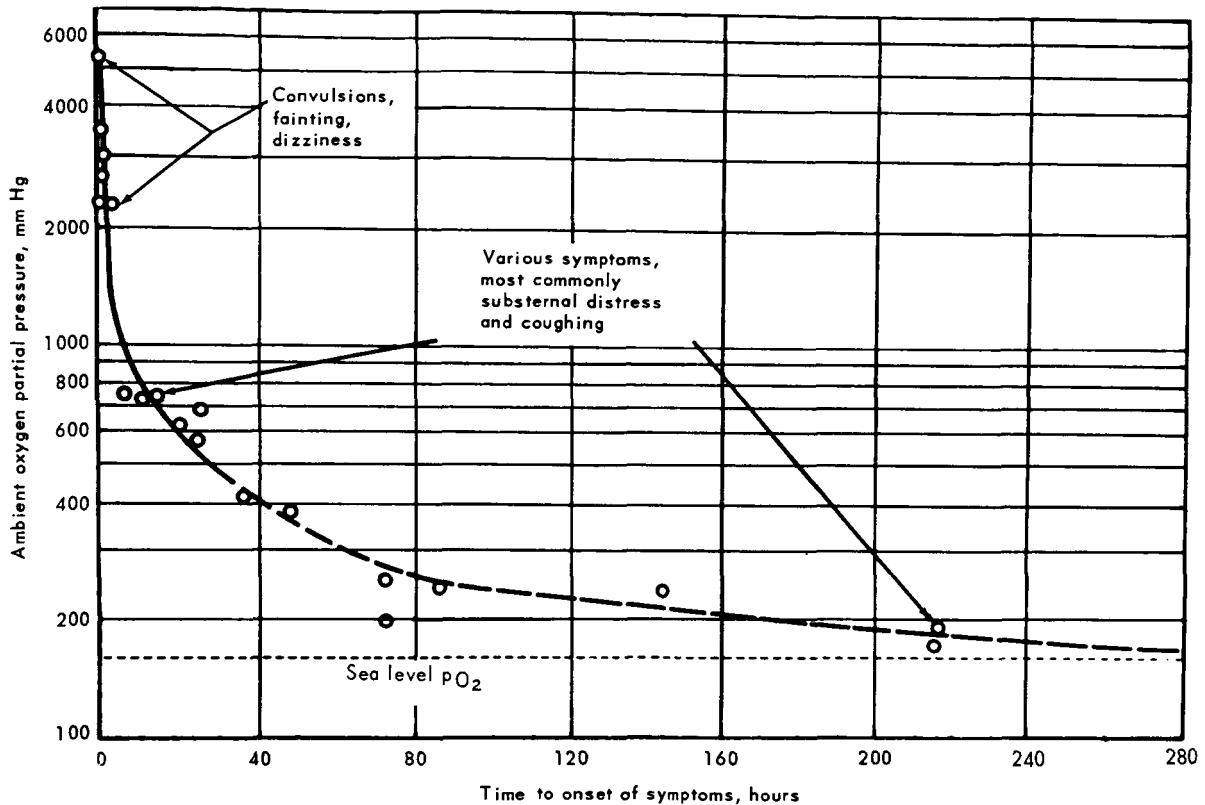
FIGURE 2.—*Time of onset of signs and symptoms of oxygen toxicity.* (AFTER WELCH [113] AND ROTH.[90])

susceptibility.[25] When this ratio, measured in liters-sec^{-1}-cm H_2O^{-1} per liter of lung volume, is less than 0.13, atelectasis is seen after exposure to 5-psia, 100 percent O_2. Fortunately, most "normal" subjects tested have ratios of greater than 0.14. This would suggest that selection of astronauts for resistance to atelectasis in 100 percent O_2 space-cabin environments may be practical. The condition may be ameliorated by recurrent deep-breathing exercise. It was concluded at this conference that 5-psia, 100 percent O_2 would be acceptable for space missions of less than 30 days' duration. For longer exposures in space, ground-based validation experiments may be required for at least the duration of the expected mission.

A partial pressure of pure oxygen at 3.0 to 3.5 psia would appear to eliminate the problem of oxygen toxicity caused by oxygen at 5.0 psia, a p_{O_2} of 100 mm Hg above normal atmospheric partial pressures of oxygen. The near absence of nitrogen should not play a significant role in

the problem, but this factor has not been clearly established.[92] The use of 5.0 psia instead of 3.5 psia in Mercury and Gemini cabins appears to have been dictated by the desire to maintain a pressure high enough to minimize the chance of pulmonary atelectasis, as well as to reduce the chance of decompression sickness. Early in the mission, the residual nitrogen even after several hours of preoxygenation could still cause symptoms.[92] Also, the selection of cabin pressure at 5 psia allows for a backup emergency suit circuit operating at 3.5 psia. This backup mode is automatically initiated when the cabin pressure falls below 3.8 psia. Another factor often mentioned in the choice of the higher pressure is the added safety factor of a longer decompression time in case of puncture of the sealed cabin. It is obvious that some oxygen pressure between 3.5 and 5.0 psia will be the optimum for most mission types, but the exact pressure of choice will be dictated by other physiological and engineering considerations.

WATER VAPOR

A very important constituent in the atmosphere is water vapor. It is customary to plot a psychrometric chart comparing dry-bulb and wet-bulb temperature, saturation temperature, relative humidity, and dewpoi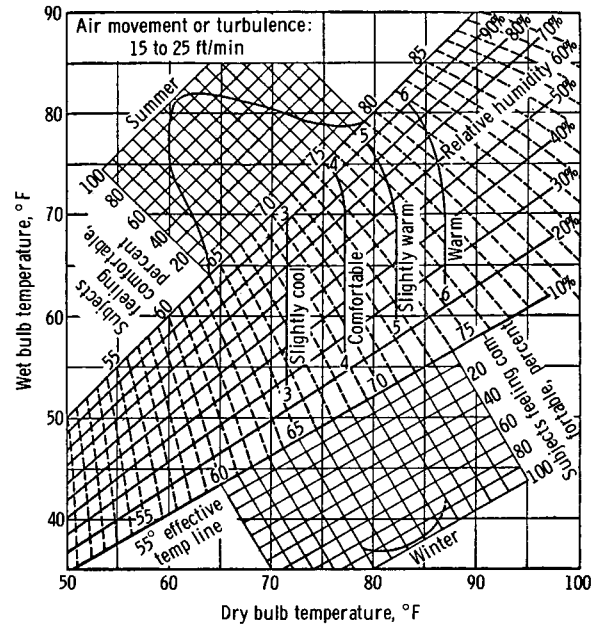nt temperature to delineate the comfort zone. Most graphic representations are useful only at one pressure, usually around sea level. In figure 3(a) this problem is avoided by plotting dry bulb against dewpoint temperature, resulting in saturation and relative humidity lines which are independent of pressure. Figure 3(b) defines comfort zones more clearly. Other psychrometric presentations can be seen in figures 73 and 74 as well as in the "Temperature" section (ch. 7) of the NASA Bioastronautics Data Book.[11] Parameters such as effective temperature and lines of equal comfort are also available.[20, 7]

The humidity acceptable in space vehicles is thus a function of the temperature, but should lie within the vapor pressure range of 5 to 16 mm Hg. The removal of water is a thermodynamic process which constitutes a large percentage of the thermodynamic load on the atmospheric control system. The amount of water vapor added by the occupants can be measured by the so-called latent heat load whereby each pound of water evaporated into the air is represented by about 1050 Btu. Latent personal heat loads of from 70

(b) Summer and winter. (AFTER ASHRAE GUIDE.[1])

FIGURE 3.—Definition of comfort zone—Concluded.

Btu/hr (resting) to about 1000 Btu/hr (severe exercise) can be expected as extreme ranges, with an average of 150 to 200 Btu/hr over a 24-hour period for each person in a multimanned crew. This is a conservative value, considering the 83 Btu/hr reported for the astronauts in Vostok.[109] The biological implications of water metabolism in space vehicles are currently under study.[111]

CARBON DIOXIDE

The carbon dioxide production rate is a function of the oxygen usage rate, and the respiratory quotient of about 0.82 to 0.85. Since an average O_2 consumption rate of 2 lb/man day can be expected, the CO_2 production rate of about 2.2 lb/day can be assumed.

It is generally considered that the best practice is to keep the level of carbon dioxide below 4 mm Hg and to have a maximum allowable level of 7.6 mm Hg. Figure 4 represents the rationale behind this choice by indicating the general symptoms common to most subjects when exposed to mixtures of carbon dioxide in air at a total pressure of 1 atmosphere. Some adaptation to higher concentration is possible
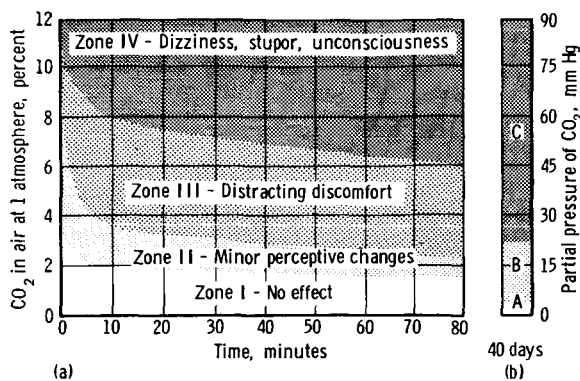

(a) Temperature-humidity effects. (AFTER COE ET AL.[20])

FIGURE 3.—Definition of comfort zone.

FIGURE 4.—*Carbon-dioxide effects.* (FROM DATA OF
KING,[55] NEVISON,[77] AND SCHAEFER.[99])

but not without biochemical alterations in the body.[99] In zone I, no psychophysiological performance degradation or any other consistent effect is noted. In zone II, small threshold hearing losses have been found, and there is a perceptible doubling in depth of respiration. In zone III, the zone of distracting discomfort, the symptoms are judgment errors, mental depression, headache, dizziness, nausea, "air hunger," and decrease in visual discrimination. Zone IV represents marked deterioration leading to dizziness and stupor, with inability to take steps for self-preservation. The final state is unconsciousness.

The bar graph at the right shows that for prolonged exposures of 40 days, concentrations of carbon dioxide in air of less than 0.5 percent (zone A) cause no biochemical or other effects; concentrations between 0.5 and 3.0 percent (zone B) cause adaptive biochemical changes, which may be considered a mild physiological strain; and concentrations above 3.0 percent (zone C) cause pathological changes in basic physiological functions.

DILUENT GAS

The value of an inert diluent gas in decreasing the fire and blast hazard and possibly the oxygen toxicity hazard in space cabins has already been discussed in parts I and II of this series.[90, 91] More recent work is available on the prediction of ignition and burning rates of different materials in pure oxygen and mixed gas systems.[41, 40] A continuing bibliography on fire and blast hazards is also available.[93] The arcing

of electrical equipment in unusual atmospheres is now under study at the Boeing Co.[27] Preliminary results suggest that there is little or no difference between gas mixtures in arcing tendency at a given pressure unless the amount of inert gas is above 75 percent. Neon has a lower breakdown voltage than the others.

Studies of plastics burning in closed chambers containing 100 percent O_2 at 5 psia and in other gas mixtures during zero-gravity parabolic flight maneuvers suggest that the zero-gravity factor in suppressing flame propagation may more than compensate for the increased flammability in 100 percent O_2.[100, 54] However, the lack of forced convection in the closed system during simulation is somewhat unrealistic and may give a false sense of safety. On the other hand, it should be remembered that in actual space vehicles a nearly zero-convection state can be readily attained by merely shutting off circulation fans soon after the fire has been discovered. Future zero-g studies are being planned to include forced convection at levels similar to those expected in operational space cabins. One must, however, always keep in mind the fire hazard during the positive-g phases of launch and reentry.

Presence of inert gases can lead to physiological problems related to decompression sickness, explosive decompression, ebullism, preoxygenation scheduling, thermal control, and voice propagation. These have been covered in great detail in part III of this series.[92] The general conclusion of this study was that nitrogen, helium, and neon were the only gases worth considering from the physiological point of view. There was no overwhelming physiological mandate for the preference of any one of these three diluents.

On theoretical grounds only, neon offers some advantage by potentially minimizing the bends and chokes as well as the more serious neurocirculatory collapse symptoms of decompression sickness. Only minimum diving data support this theoretical conclusion. From empirical studies simulating decompression during early stages of flight in non-steady state gas conditions, it appears that helium is equal to or even more dangerous than nitrogen in causing bends at altitude. Studies under equilibrium conditions

are required.[92, 112, 4] Theoretical and empirical studies, on the other hand, also suggest that helium is less likely than nitrogen to cause neuro-circulatory collapse symptoms after decompression. One must also consider the very low incidence of bends expected in an astronaut population decompressing from a 5- or 7-psia cabin and the even lower incidence of neurocir-culatory collapse expected under these condi-tions.[92] The incidence for older and less physically conditioned scientist-observers in the crew will no doubt be somewhat greater.

Previous opinions notwithstanding, the sub-stitution of helium for nitrogen would produce no overall increase in the decompression safety factor to make helium preferable to nitrogen. The adverse thermal and voice-distortion factors predicted for helium have been shown to be minimal at the pressures and composi-tions suggested for space cabins. The only gross advantage of helium over neon or nitrogen is in minimizing the hazard of lung damage from explosive decompression. The extremely low probability of this event occurring without lethal mechanical injury to other parts of the body indicates that this factor must be weighted quite low among the selection criteria.

From the preceding discussion it would appear that the engineering, and not the physiologi-cal, factors will have to play the major role in the selection decision between the three inert diluents. It is also clear that the lower the partial pressure of inert diluent, the safer is the mixture from the point of view of decom-pression sickness but not fire. The minimal partial pressure of inert diluent required for normal metabolic function over long periods of time has not as yet been determined. [92]

In the presence of a fixed partial pressure of oxygen, the higher the partial pressure of inert gas, the longer is the time of decompression to hypoxic levels, but the more dangerous is the mixture in production of symptoms once de-compression has occurred. As an alternate to the 5-psia, 100 percent oxygen environments already used in space vehicles, one can suggest mixed gas systems ranging from 5 psia with 70 percent oxygen and 30 percent inert gas to 7 psia with 50 percent oxygen and 50 percent inert gas. The 5-psia mixture would be slightly more dangerous from the points of view of increased fire hazard [40] and decreased time of decompression. The 7-psia mixture would have a greater tendency to cause decompression symptoms after total decompression occurred. The engineering factors determining the choice between the three proposed conditions are discussed in chapter 2.

TOXIC SUBSTANCES AND ODORS

The many toxic substances and odors which can be generated by the hardware or human occupants have been discussed in great detail in many studies.[3, 39] A review of these sub-stances and their effect on body performance is beyond the scope of this study.

It is clear that the chemical constituents of the atmosphere can alter the toxic materials generated in the cabin.[90] The nature of these alterations and the effect on humans is currently being studied by the Aerojet-General Corp. and the Aerospace Medical Laboratories at Wright-Patterson Air Force Base.[2]

Provision must be made for continuous reduc-tion of the amount of toxic substances in the cabin atmosphere. This entails the passage of cabin atmosphere through catalytic burners or adsorption devices at relatively low velocities. The gas-specific effect of this requirement on the engineering consideration of cabin atmosphere selection will be discussed subsequently.

DUSTS, AEROSOLS, AND IONS

The zero-gravity environment will increase the hazard of dust, aerosols, and ions over and above that experienced on Earth. Again, the chemical constituents of the atmosphere will alter the hazard presented by these agents. Removal of these materials requires filters and similar de-vices through which the atmosphere must be circulated and imposes gas-specific penalties in atmosphere selection.

AIR CIRCULATION

Absence of convection in zero-gravity states requires that air be circulated through the cabin at relatively high velocities, primarily to dissipate local heat from equipment and crew and also to distribute CO_2 and contaminants from local

sources. The flow rates must be sufficiently designed to accomplish these functions without producing discomforting drafts in the cabin.[62, 8] Because of the relatively high volumes and velocities involved, the physical properties of the atmosphere being circulated play a major role in the engineering considerations.

TEMPERATURE CONTROL

Major physiological factors bearing on engineering tradeoffs of different atmosphere systems are the thermoregulatory parameters of man. Because of the sensitivity of tradeoffs to these parameters, and the somewhat scattered data pertaining to this problem, an attempt is made to analyze in detail the critical data and equations to be used in the presentation of subsequent engineering considerations. Several excellent reviews of thermal physiology have been used in the preparation of this section.[11, 8, 38, 58, 117, 7]

The processes of heat rejection used by man include conduction radiation, convection, and evaporation of moisture from the skin and lungs. Conductive loss in space cabins can be neglected. The convective and evaporative losses may occur under free- or forced-convection conditions. The primary atmospheric parameters that may be varied are temperature, velocity, and humidity of ventilating gas. The primary physiological parameters of the human subject are the metabolic rate; sweating characteristics; peripheral blood flow; body size, position, and temperature distribution; comfort criteria; and the thermal conductivity and water vapor permeability of clothing.

If one assumes no heat storage or loss, the heat balance equation for man in steady-state conditions in a zero-g environment may be written as

$$Q_M - Q_W = Q_r + Q_c + Q_l = Q_s + Q_l \qquad (1)$$

Radiation Heat Transfer

The radiation heat loss equation for man is

$$Q_r = \sigma f_{cw} A_r (T_c^4 - T_w^4) \qquad (2)$$

Calculation of the actual radiation-heat-transfer problem is a complex one involving numerous thermal radiation sources at different temperatures and geometries. By assuming a

single crewman having an effective body surface area of 15.6 sq ft with a uniform clothing surface temperature and an enclosure of greater than 100 sq ft per man, that is, $f_{cw} = \epsilon_c$, a simplified radiation cooling equation can be written as

$$Q_r = 2.65 \times 10^{-8} \, \epsilon_c (T_c^4 - T_w^4) \qquad (3)$$

A sample graph, assuming $\epsilon = 0.9$, is seen in figure 5 where the radiation heat loss to any given environmental temperature is given for several clothing surface temperatures.[78] Figure 6 represents the radiation heat-transfer coefficients (h_r) for different combinations of environmental and clothing temperature. The equation used in this figure can be derived from equations (3) and (5).[23]

Forced Convective Heat Transfer

The correlation between convective heat-transfer processes and mass-transfer processes has been used by many investigators to develop analytic models for forced convective heat ex-
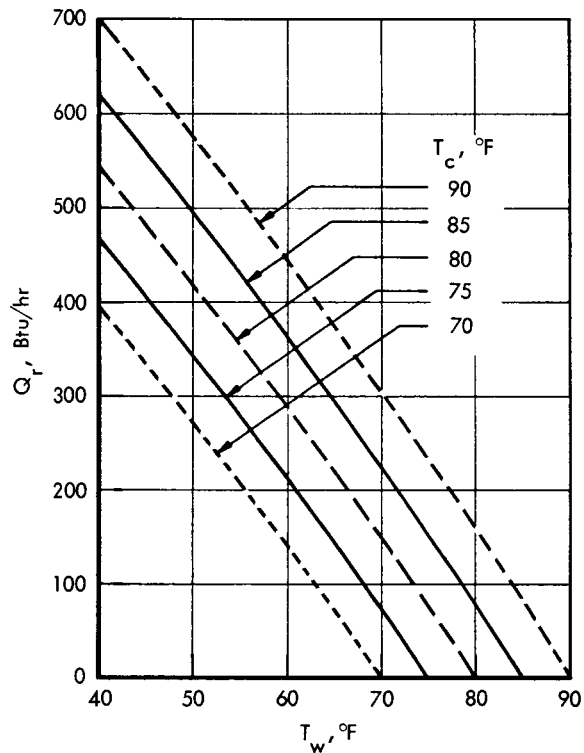

FIGURE 5.—*Radiative heat loss from man to his surroundings.* (AFTER PARKER ET AL.[78])
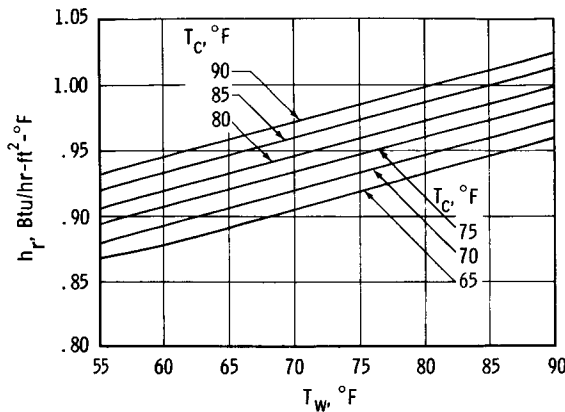
FIGURE 6.—*Radiation heat transfer coefficient.*

$$h_r = \epsilon\sigma\left(\frac{T_c^4 - T_w^4}{T_c - T_w}\right) \epsilon = 0.9; \; T_c \text{ is clothing tempera-}$$

ture; and T_w *is environmental temperature.*
(AFTER PARKER ET AL.[78])

change in man. In the recent analysis of Berenson,[7] the following assumptions were made:

(1) All sensible heat passes through the clothing by conduction, and the clothing heat-transfer area is equal to the skin surface area. Since sensible heat loss occurs from nonclothed skin and since the clothing surface may be up to 40 percent greater than skin surface, these assumptions may be conservative. It must be remembered, however, that even though the area increases, the air pockets which are formed act as thermal and mass transfer resistances. Zero gravity will tend to increase resistance by eliminating convection currents in the pockets.

(2) In the absence of conductive heat loss, the relationship between clothing surface temperature T_c and skin temperature T_s can be determined by the equation:

$$T_c = T_s - \frac{L}{k}\left(\frac{Q_c + Q_r}{A}\right) \qquad (4)$$

The value of L/k is the useful function of clothing heat-transfer resistance, Clo, where 1 Clo = 0.88° F-ft²-hr/Btu.

The rate of heat transfer by convection from clothing surface can be written as

$$Q_c = h_c A (T_c - T_a) \qquad (5)$$

The convective heat-transfer coefficient is actually a complicated function of thermal properties of the fluid, the geometry of the body, and second- or third-order factors of fluid flow. The value of h_c for convective exchange about the whole human body is a critical coefficient to which the gas-specific engineering tradeoffs are sensitive. Unfortunately, there has been some variance between the values used by several different groups in relating the h_c of man to the atmospheric gas velocity. Selection of the appropriate film coefficient or actual heat-transfer coefficient is a difficult problem.[59] A discussion of the implication of different coefficients used in the analysis of forced convection about the human body has been published recently.[53]

The early data of Winslow et al.[116] suggest that for clothed humans sitting in a turbulent air flow the following equation may be used:

$$h_c = 0.153 \bar{V}^{0.5} \left(\frac{\rho}{\rho_{STD}}\right)^{0.5} \qquad (6)$$

This equation is not too different from that derived for rough flat plates.[12]

$$h_c = 1.03 \; k \left(\frac{\rho\bar{V}}{\mu}\right)^{0.5} \qquad (7)$$

Figure 7 represents a summary of several approaches to forced convective heat-transfer coefficients (convective film coefficients). The first three curves represent the h_c values obtained from data on empirical studies of humans.[34, 116, 76] These are compared with four theoretical curves: a cylindrical model of man in crossflow, a flat plate with flow perpendicular to it, a 10-inch diameter cylinder in crossflow, and a cylinder in longitudinal flow (fig. 8). The value of h_c for the cylindrical model of man corresponds closely with those obtained by Nelson[76] and is equivalent to h_c for crossflow about cylinders 5 inches in diameter. The specific equation used for the flat-plate model in figure 7 was not stated but appears to differ from the flat-plate equation noted above[12] which gives results closer to those of the equation of Winslow et al.[116]

Figure 9 shows the effect of gas velocity on the convective heat-transfer coefficient based on the cylindrical model of man for various helium-oxygen and nitrogen-oxygen atmospheres.
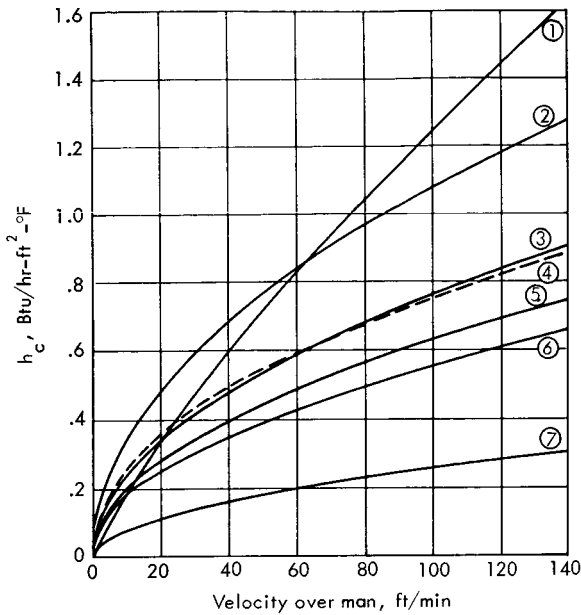
(1) Hall [34]
(2) Winslow et al. [116]
(3) Nelson et al. [76]
(4) Cylindrical model of man in cross-flow (analytical)
(5) Flat plate (Hamilton-Standard)
(6) 10-inch-diameter cylinder in cross flow
(7) Longitudinal flow

FIGURE 7.—*Comparison of forced convection film coefficient for man at ½ atmosphere.* (AFTER PARKER ET AL.[78])

The partial pressure of oxygen of 170 mm Hg is near the sea-level equivalent and is held constant, with the diluent gas ranging from 0 to 400 mm Hg. These curves were generated by taking the heat-transfer coefficient to be proportional to the various fluid properties as follows:

$$h_c \sim k(N_{Pr})^{0.33} \ (N_{Re})^{0.5} \sim k(N_{Pr})^{0.33}\left(\frac{\rho\bar{V}}{\mu}\right)^{0.5} \qquad (8)$$

The values for neon mixtures will lie between those for helium and nitrogen. It is clear from comparing physical properties of the gases that for different mixtures of oxygen and nitrogen, there is little sensitivity of h_c to percent composition of gas (table 4).

The following equation, derived from the heat mass-transfer analog [28] for Prandtl numbers of 0.6 to 15 and Reynolds numbers of 10 to 10^5, approxi-
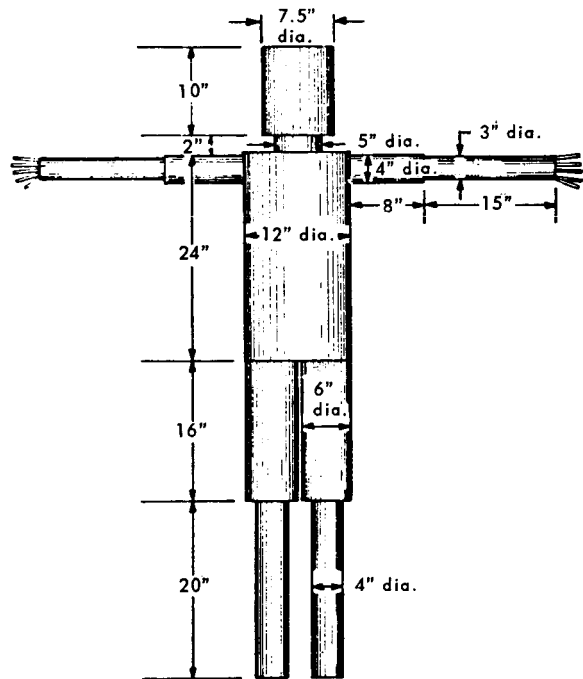
Part	Area, ft^2 [a]
Head	1. 95
Neck	. 22
Trunk	6. 18
Upper legs	4. 19
Lower legs	3. 49
Upper arms	1. 40
Lower arms	1. 96
Fingers	[b]. 67
Total	20. 06

a 19.5 ft^2 used to include some factor of safety.
b Each finger: 3½ inch long by ⅞ inch diameter.

FIGURE 8.—*Cylindrical model of man.* (AFTER PARKER ET AL.[78])

mates the forced-convection cooling rate for nitrogen-oxygen mixtures:[7]

$$Q_c = 0.407\sqrt{P\bar{V}}(T_c - T_a) \qquad (9)$$

Free Convective Heat Transfer

In the presence of a gravitational field, such as that on Earth, planetary surfaces, or rotating space stations, free convection is possible and
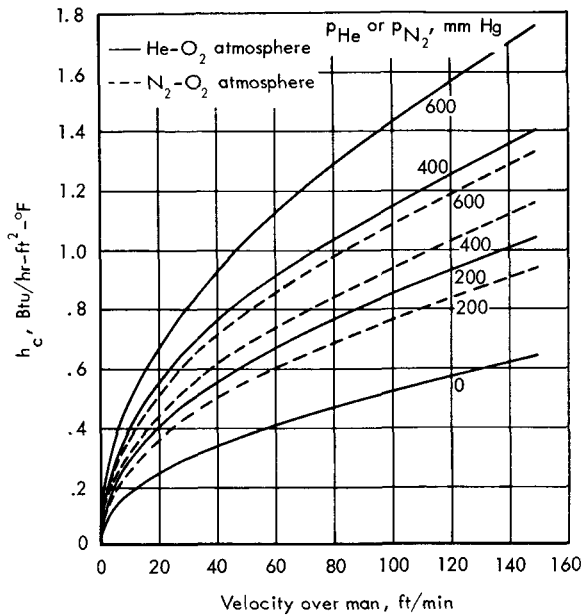
FIGURE 9.—*Heat transfer coefficients of man in mixtures of oxygen and helium and of oxygen and nitrogen at different gas velocities. Conditions: 170 mm Hg of oxygen; p_{He}=partial pressure of helium in atmosphere; p_{N_2}=partial pressure of nitrogen in atmosphere; based on cylindrical model of man.* (AFTER PARKER ET AL.[78])

is the preferred mode of cooling because no additional energy need be expended.

Berenson has combined the general free-convection equations with the assumptions regarding clothing effects to yield an equation for free-convection cooling:

$$Q_c = 1.17[P^2g(T_c - T_a)]^{0.25}(T_c - T_a) \qquad (10)$$

The handling of mixed free- and forced-convection environments can be simplified by the McAdams rule; that is, both the free- and forced-convective heat-transfer coefficients are calculated, and the higher of the two values is used.[63] Berenson has shown that the critical crossover point of the forced convection velocity ($\overline{V}_{crit}$), where the forced-convection heat-transfer coefficient is equal to the free-convection coefficient, can be calculated for oxygen-nitrogen mixtures by equating equations (9) and (10) and solving for

$$\overline{V}_{crit} = 8.3[g(T_c - T_a)]^{0.5} \qquad (11)$$

With a 10° F temperature difference between clothing surface and atmosphere, the critical velocity is 26 ft/min on Earth but only 10.5 ft/min on the Moon.

Evaporative Heat Transfer

In addition to the vasodilation caused by elevated temperature, the body loses heat by evaporation of sweat. At skin temperatures above 91.4° F, the sweat rate appears to depend only on intracranial temperatures. Below this skin temperature, sweating is reduced by decreasing skin temperature.[6] The rate of sweating and humidity loads on the environmental control system have been discussed previously.

Krantz[58] employed the data of Winslow et al.[117] to establish comfort indices for high temperatures and related these data to the percentage of evaporative capacity of the body being used. The metabolic rate is estimated for any given level of activity, and the difference between the metabolic and sensible heat loss is the required evaporative cooling rate. Environmental conditions are evaluated with respect to maximum evaporative cooling capacity of humans. Table 1 represents the expected comfort level relative to the percent of maximum capacity being used. There is some controversy as to the absolute validity of this concept in air and especially in unusual atmospheres and at high total sweat output.[111]

TABLE 1.—*Expected Comfort Level*

Maximum evaporative capacity, percent	Comfort level
0 to 10	Cold
10 to 25	Comfortable
25 to 70	Tolerable
70 to 100	Hot
Over 100	Dangerous

Approximately the first 10 percent of maximum capability represents basal insensible loss from respiration and diffusion. These losses are, of course, a function of the metabolic output and respiratory rate.

Berenson[7] has presented a simplified equation (12) for latent cooling rates as derived from the heat-mass transfer analogy of Eckert[28] and equa-

tion (8). One must keep in mind the effect of inert gas on the coefficients and second-order clothing factors in evaporative transfer.[11, 111]

$$Q_l = h_D h_{fg} AC \left(\frac{P_s - P_a}{RT_s}\right)_{H_2O} \quad (12)$$

Since the heat-transfer properties of nitrogen-oxygen mixtures are independent of the fraction of each component, equation (12) has been reduced by Berenson for all oxygen-nitrogen mixtures in a forced convection environment to yield

$$Q_l = 2.46 CT_a \left(\frac{\overline{V}}{P}\right)^{0.5} (P_s - P_a)_{H_2O} \quad (13)$$

The values of evaporative loss under conditions of $C = 1$ give predicted results slightly higher than actually measured.[19, 111] Since the rate of evaporation and the diffusion coefficient for water vapor are inversely proportional to pressure, it is clear that the latent cooling will increase with decrease in pressure. Sample calculations illustrating the magnitude of the pressure, dew point, and gas-stream-velocity effects at $T_a = 80°$ F

and $T_s = 95°$ F are seen in figure 10. These rates should be taken as the very upper attainable levels.[111] In the temperature range under consideration, the temperature and the dew point have relatively little effect compared with gas-stream velocity and ambient pressure.

For general free convection in nitrogen-oxygen mixtures, the latent cooling equations have also been developed by combining equations for free convection, transport properties of air, and evaporative cooling[7] to yield:

$$Q_l = 25.7 \frac{CT_a}{P} (P_s - P_a)_{H_2O}\{P_g[0.005P(T_c - T_a) + 1.02(P_s - P_a)_{H_2O}]\}^{0.25} \quad (14)$$

Under high workloads at low pressure, respiratory water loss becomes a more significant factor in latent heat loss. Recent data are available on this problem.[120]

Combined Heat Transfer

In any environment, all of the above modes of heat transfer may be used. The ambient dry-bulb temperature, humidity, air velocity, and ambient pressure determine the partition of mechanisms actually used by the body.

Figure 11 represents the changing partition of heat-loss mechanisms at rest with increasing dry-bulb temperature at a constant relative humidity of 45 percent and constant gas velocity.
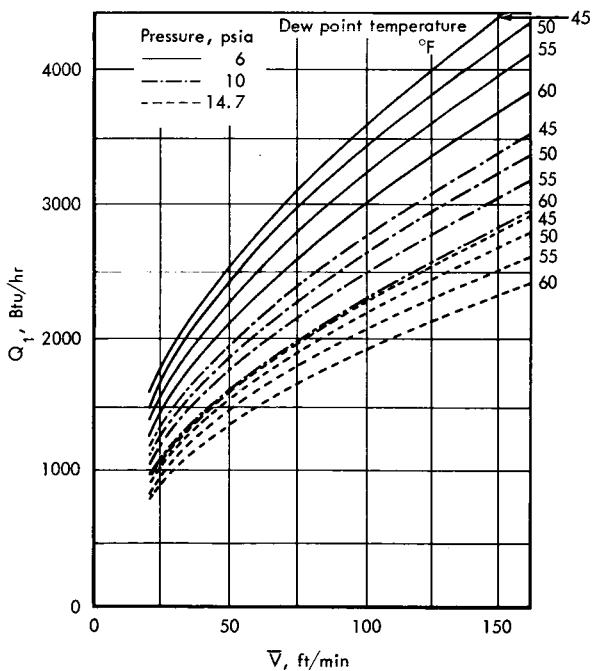

FIGURE 10.—*Maximum evaporation rate in oxygen-nitrogen mixtures.* $Q_l = 246 T_a \sqrt{\overline{V}/P}(P_s-P_a)_{H_2O}$; $T_s = 95°$ F; $T_a = 80°$ F. (AFTER BERENSON.[7])
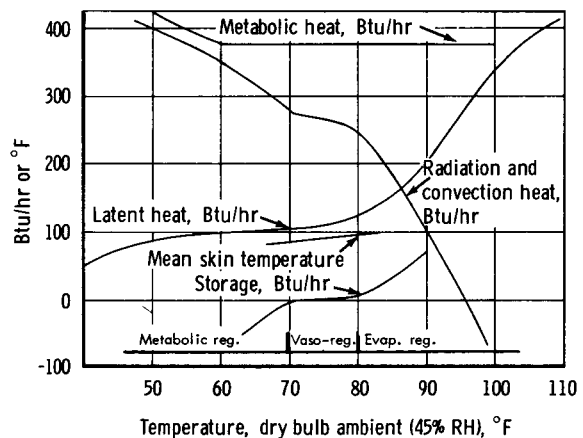

FIGURE 11.—*Typical relation between human heat balance and temperatures for lightly clothed subjects in still air at sea level.* (AFTER JOHNSON.[46])

The regions of primarily metabolic, vasomotor, and evaporative regulation are noted. Specification of the design atmospheric temperature, gas velocity, and humidity will be critical in determining the actual partition of loads on the air-cooling and dehumidifying systems and therefore will affect the gas-specific tradeoffs in question.

The use of liquid-cooled garments or ventilated garments inside the cabin will not be considered as a basic mode of operation.[89, 17] Tradeoffs in contingency modes must take into consideration such interactions between the cabin atmosphere and the suit.

Berenson has calculated comfort-zone predictions for many different atmospheric conditions and gravitational states.[8] These graphs may be consulted for unusual conditions in space vehicles using oxygen-nitrogen atmospheres. For cabins with helium-oxygen atmospheres, other calculations need to be made to determine comfort zones.

The general effect of helium mixtures on thermoregulation in space cabins has been covered in part III of this series.[92] Since the compilation of these data, several studies have been published on the theoretical and empirical aspects of this problem which are pertinent to the present study.

Parker et al.[79] have compared theoretical gas-velocity limits and thermal comfort zones in helium-oxygen and nitrogen-oxygen mixtures of varying total pressure. To avoid the movement of papers at 1 atmosphere in air, a velocity of 50 to 60 ft/min is stated as the tolerable upper limit of velocity above the 40 to 50 ft/min draft threshold

in a 1-g environment. It must be remembered that in zero-g, any velocity can move papers. The velocity threshold for movement is significant only before and during launch and during reentry. Since the force of a gas stream is proportional to $\rho \bar{V}^2$, a table of constant force thresholds equivalent to 50 to 60 ft/min in air can be calculated. Table 2 represents this maximum-force velocity along with the corresponding ambient temperature T_a required to maintain thermal comfort as measured by average skin temperatures T_s at 91° F and 94° F. The development of these comfort-zone temperatures follows.

The thermal comfort zones for different gas velocities of varied mixtures of oxygen and helium and of oxygen and nitrogen in zero-g were calculated by assuming the following conditions:

(1) $T_a = T_w$ (air temperature = ambient temperature = wall temperature)
(2) No body-heat storage
(3) $p_{O_2} = 170$ mm Hg in all cases and p_{N_2} or p_{He} increasing from 200 to 600 mm Hg
(4) Zero-gravity environment
(5) Evaporative heat loss is the same as at 1 atmosphere and 1g,
(6) Convective heat loss is for cylindrical model of man with $(A_c = 19.5$ ft$^2)$ in crossflow (fig. 8)
(7) Metabolic heat generation is for a man seated at rest (400 Btu/hr at 70° F)
(8) T_s = skin temperature in the 91° F range
(9) Clo = 1; $\epsilon_2 = 0.9$
(10) $A_r = 15.6$ ft^2 and $A_r/A_c = 0.8$
(11) Partition of heat loss is similar to that seen in figure 11

TABLE 2.—*Maximum Velocity Over Man in 1-g Environment* [AFTER PARKER AND EKBERG [79]]
[$p_{O_2} = 170$ MM HG]

p_{He}, mm Hg	p_{N_2}, mm Hg	Maximum velocity over man, ft/min	T_a, °F, required for—	
			$T_s = 91°$ F	$T_s = 94°$ F
0	0	100 to 120	56.5 to 58.5	66 to 67.5
200	0	94 to 113	65 to 66.5	72 to 73
400	0	88 to 106	68 to 69	74.4 to 75.5
600	0	84 to 100	70 to 71	76.5 to 77.5
0	200	71 to 86	61.5 to 63	69 to 70
0	400	57 to 69	63.5 to 65	70 to 71.5
0	600	50 to 60	64.5 to 65.5	71 to 72

(12) The clothing temperature T_c is related to atmospheric temperature T_a by the relation

$$T_c = T_a + \frac{1.137\ (T_s - T_a)}{(0.8\ h_r + h_c)\ \text{Clo} + 1.137} \qquad (15)$$

(13) The relation of h_r to T_c is the same as that noted in figure 6; $T_w = T_a$.

In view of equations (13) and (14) which predict that the rate of evaporation is inversely related to the ambient pressure, it appears that assumption (5) is open to question. Since the evaporation probably accounts for less than one-third of the total heat loss at the temperatures in question, the assumption of 1-atmosphere pressure does not present too great an error. As for assumption (4), it is true that in the presence of adequate forced convection, the gravitational factor in equation (14) would play a minimal role in evaporative heat loss and can be neglected in the solution of comfort zone temperatures. The 0.25-power factor in this equation would in itself reduce the overall weighting of gravity effect. Assumption (12) holds only for Clo values in air. Where thermal conductivity is high, as in mixtures with high content of helium, there is much less Clo than calculated for air.[101, 35]

Figure 12 represents the results of these calculations. As would be expected, the helium-oxygen mixtures show a narrower zone of comfort at higher temperatures, especially at lower flow rates than do the nitrogen-oxygen mixtures. This is more marked in the cases with higher content of inert gas (12(c) and 12(d)). The temperature values in table 2 indicate the zone of comfort for the maximum gas velocities calculated for each mixture as determined by figure 12.

Secord and his coworkers have tested some of these predictions of He gas effects in space cabins.[102] The tests were performed in their space-cabin simulator at 5, 7, and 10 psia for a mixture of helium and oxygen and at 5 and 7 psia for a mixture of nitrogen and oxygen. The wall temperature was within 10° F of gas temperature, so no major radiation factor was at play. Figure 13 presents a representative test run for one of the four crew members in helium and oxygen at 5 psia, indicating test peaks and nadirs
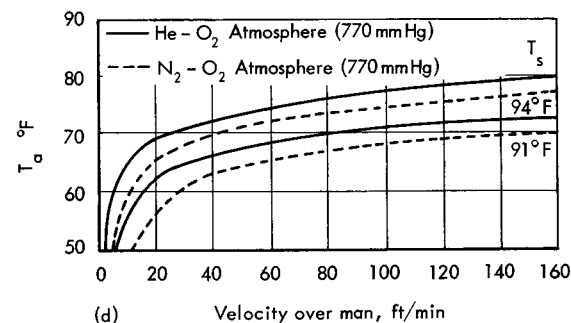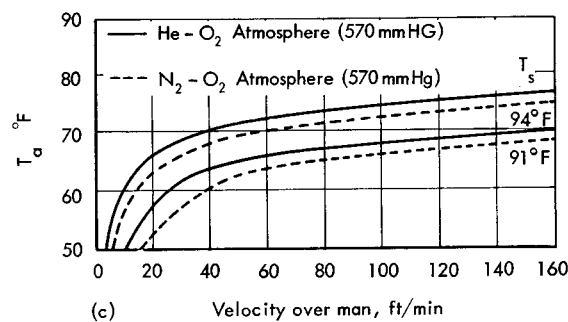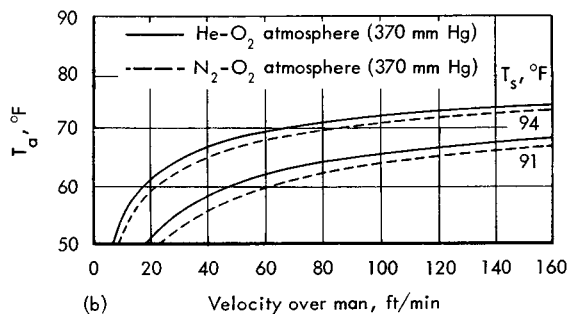

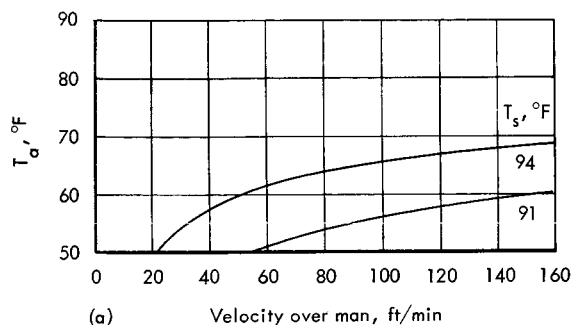FIGURE 12.—*Comfort lines for man seated at rest with 1 Clo.* (AFTER PARKER ET AL.[79]) *(a)* $p_{O_2} = 170\ mm\ Hg.$ *(b)* $p_{O_2} = 170\ mm\ Hg\ and\ p_{He}\ or\ p_{N_2} = 200\ mm\ Hg.$ *(c)* $p_{O_2} = 170\ mm\ Hg\ and\ p_{He}\ or\ p_{N_2} = 400\ mm\ Hg.$ *(d)* $p_{O_2} = 170\ mm\ Hg\ and\ p_{He}\ or\ p_{N_2} = 600\ mm\ Hg.$
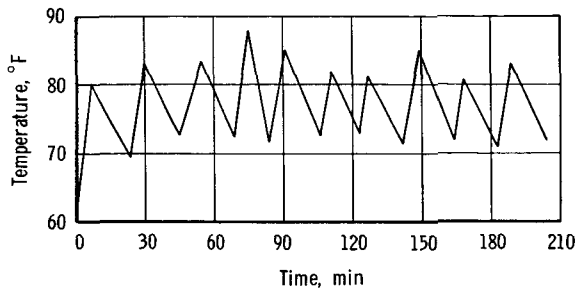
FIGURE 13.—*Representative thermal comfort zone with an air velocity of 50 ft/min, a water partial pressure of 12 mm Hg, a total pressure of 5 psia, a helium-oxygen atmosphere. 0.7 Clo, and 1 experimental subject.* (AFTER SECORD.[102])

of the totally subjective temperature comfort range. Figure 14 represents a summary of the midzone temperatures under several conditions, indicating a significant increase in allowable cabin temperature when helium is used as a diluent. It is also seen that the allowable increase in cabin temperature appears to be a function of the Clo about the subject. The value of Clo was calculated by assuming air at sea level as the interstitial gas. At 0.7 Clo, midzone temperature differences were noted as atmospheric conductivity was increased; at zero Clo (nude), minimal differences were noted.

It is of interest to compare these results with the predictions of figure 12. The atmosphere of figure 12(b), containing 170 mm Hg of p_{O_2} and 200 mm Hg of He and a total pressure of 370 mm Hg (7.1 psia), can be compared with the 7 psia He-O₂ mixture of figure 14. For a gas flow of 50 ft/min and 1 Clo insulation, figure 12(b) indicates an expected average temperature of
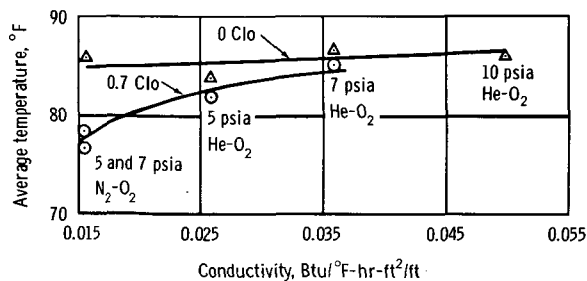
about 65° F. The empirical data of figure 14 for 50 ft/min and 0.7 Clo suggest an average temperature of about 84° F.

The discrepancy cannot be fully accounted for by differences in Clo values in helium,[35] although the direction of the error is correct. The comfort temperature of figure 14 would be expected to be at most only a few degrees higher than that of figure 12(b) if Clo were the only factor. Equations (4) and (5) describe the convective relationship involved. Preliminary data[101] suggest that the Clo value of clothing is approximately inversely proportional to the thermal conductivity of the atmosphere.[101] Since the ratio of k for 5-psia O₂-He/sea level air is 0.027/0.015 = 1.8 (table 4), the effective Clo value would only decrease from 0.70 to about 0.39 Clo. In figure 14, the difference between the comfort temperatures of zero Clo and 0.7 Clo in a 7-psia helium-oxygen mixture is only 1° to 2°. One would therefore expect that the difference between 0.70 and 0.39 effective Clo would lead to an even smaller discrepancy.

There appear to be several flaws in the assessment of comfort in the experimental curves. The size of experimental group is inadequate. The peaks and nadirs were entirely subjective. One of the subjects was a Negro from the Deep South who, in spite of his residence in Los Angeles for some time, had a very high average comfort temperature and tended to skew the upper limit of the comfort zone of the four subjects to higher levels.[101] Since his tolerance to low temperatures was also great, his mean comfort temperature was close to that of the other subjects. No average skin temperature for the four subjects at midcomfort zone was determined. This would help quantify the proposed skewing of comfort temperature curves by helium-oxygen mixtures.

If the data of this one subject were eliminated and a larger sample were studied, the theoretical and empirical comfort temperatures would probably lie closer to one another. This experiment does corroborate the fact that for equivalent partial pressures, the average comfort temperature in helium-oxygen mixtures is higher than in nitrogen-oxygen mixtures but the experimental difference of 7° F is much greater than the 2° to 3° F predicted, for the 5-psia atmosphere of 70 percent oxygen and 30 percent helium.

FIGURE 14.—*Space cabin comfort zone data.* (AFTER SECORD.[102])

The recent studies of Welch and his co-workers [112] tend to shed some light on this problem. Unfortunately, determination of specific comfort ranges were not part of the Welch protocol. Comfort temperatures were recorded as the average cabin temperature set over periods of several weeks by subjects who had control over the thermostat within the cabins. These temperature settings are presented in table 3 for subjects in loose-fitting surgical clothes of about 0.25 to 0.50 Clo (sea-level air).

These data include varied numbers of different subjects being studied under each gas mixture. No windspeed measurements were made during these studies. Welch reports, however, that papers were not rustling and no complaints of wind chill were recorded. If anything, he reports, gas velocity was on the "low side" in the test

TABLE 3. — *Temperatures Selected by Subjects in Space-Cabin Simulators* [AFTER WELCH [112]]

	3.7 psia, 100-percent oxygen	5 psia, 100-percent oxygen	5 psia p_{O_2} — 175 mm Hg p_{He} — 74 mm Hg	7.3 psia p_{O_2} — 150 mm Hg p_{He} — 230 mm Hg	7.3 psia p_{O_2} — 165 mm Hg p_{N_2} — 206 mm Hg
Selected temperature, °F...............	69.3	70.9	74.7	75.4	72.7

cabin simulators. According to table 2, this would indicate maximum expected velocities of less than 100 ft/min in 100 percent oxygen and 70 ft/min in the 7.4 psia, nitrogen-oxygen mixture. The temperature ranges in these experiments fall in between those predicted by figure 12(c) and the data of figure 14. No measurements of average skin temperature were made. It is difficult to determine which skin comfort temperature (T_s) of figure 14 most closely applies to these experiments. Welch does report that some subjects tolerated air temperature as high as 78.1° F in 100 percent oxygen at 5 psia without complaint.

These data seem to corroborate the impression that the data of figure 14 tend to be high. They also suggest that for the 7-psia, 50 percent oxygen condition, the difference between comfort temperature in helium and nitrogen may be closer to 2° to 3° F than to 7° to 8° F indicated by figure 14.

The data of Welch for the 5-psia helium-oxygen mixtures at 0.25 to 0.5 Clo were predicted by the comfort chart of Johnson [46] in figure 15(a). It is also interesting that for the 1 Clo conditions, the predictions of figures 12(c) and 15(a) are remarkably similar. Figure 15(b) presents a comfort chart for 5-psia oxygen paralleling the oxygen-helium chart in 15(a).

The predicted differences between 15(a) and 15(b) are only a few degrees.

When exercise loads are added to the normal routine in mixed gas systems, there is some
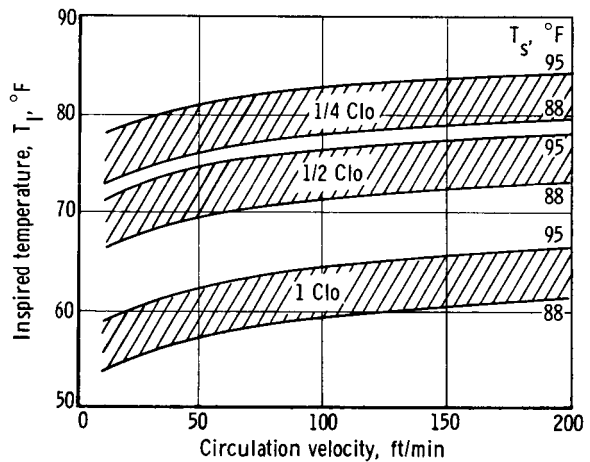
$P_IO_2 = 173$ mm Hg
$P_IHe = 75$ mm Hg
$P_IH_2O = 10$ mm Hg
$P_ICO_2 = 5$ mm Hg

(a) *5-psia oxygen-helium mixture.*

FIGURE 15.—*Human comfort chart.* (AFTER JOHNSON.[46])

$$P_1O_2 = 243 \text{ mm Hg}$$
$$P_1H_2O = 10 \text{ mm Hg}$$
$$P_1CO_2 = 5 \text{ mm Hg}$$

(b) 5.0-psia oxygen.

FIGURE 15.—*Human comfort chart*—Concluded.

advantage in having helium present to decrease the heat-storage index and maintain a lower skin temperature.[29] From this review, one can conclude that accurate comfort-zone temperatures for an average astronaut population under forced-convection, zero-g environments and with variable, atmosphere-dependent Clo values still remain to be determined for the several pertinent gaseous conditions. The importance of controlling Clo values, humidity, and air velocity and establishing more specific comfort zone criteria is apparent.

With the physiological considerations outlined, the next phase of this study considers the interaction of the biological and engineering variables in defining the tradeoff conditions.

Engineering Considerations

THE FOLLOWING is an outline of the engineering considerations which must be covered in developing adequate criteria for tradeoffs:

(1) *Weight*
  (a) Structure of cabin wall
  (b) Atmospheric leakage
  (c) Tankage for gas
  (d) Weight-power penalty for air-conditioning system:
    1. Cabin ventilation fan
    2. Atmosphere processing fan
    3. Equipment cooling fan
    4. Cooling system pumps, reservoirs, tubes, valves, radiator, and heat exchangers
  (e) Reliability factors
(2) *Transient Phenomena*
  (a) Decompression time after puncture
  (b) Transient overloads from environmental control system failure
(3) *Power System Factors*
  (a) Fuel cells
  (b) Solar cells
  (c) Nuclear systems
(4) *Economic and Operational Factors*
  (a) Development time

(b) Use of existing hardware and equipment
(c) Maintenance and convertibility
(d) Crew acceptance
(e) Contaminant buildup
(f) Qualification testing
(g) Environment for inflight experiments
(h) Complexity of design and operation
(i) Cost

In view of the physiological considerations presented in chapter 1, the atmospheres examined from an engineering point of view are limited to those of 5 to 7 psia with pure oxygen, helium-oxygen, or nitrogen-oxygen mixtures. Since the physical properties of neon lie between those of helium and nitrogen and since little is known of their physiological properties, neon mixtures will not be covered in great detail. Where the discussion requires that specific mixtures be compared, the several mixtures representing the limits of the physiological boundaries are used. These limits are 5-psia, 100 percent O_2; 5 psia with 30 percent inert gas and 70 percent oxygen; and 7 psia with 50 percent inert gas and 50 percent oxygen. Table 4 represents some physical properties of these mixtures.[46] Physical properties of the individual inert gases have been summarized in part III

TABLE 4. — *Properties of Candidate Systems, 540° R (80° F)* [AFTER JOHNSON [46]]

Atmosphere	Molecular weight, m	k, Btu/ ft-hr-°R	ρ, lb/ft³	C_p, Btu/ lb-°R	μ, lb/ft-hr	d, ft²/sec (steam) $\times 10^{-3}$	α, ft²/sec $\times 10^{-3}$	N_{Le}, α/d	N_{Pr}, $C_p\mu/k$
14.7-psia air	29	0.0151	0.076	0.24	0.0421	0.264	0.238	0.902	0.67
5-psia O_2	32	.0154	.0283	.222	.0500	.756	.707	.935	.72
5-psia O_2-N_2	31	.0153	.0268	.23	.0465	.756	.707	.935	.70
5-psia O_2-He	24	.0267	.0198	.278	.0520	.862	1.355	1.572	.54
7-psia O_2-N_2	30	.0152	.0362	.23	.0470	.540	.500	.926	.71
7-psia O_2-He	18	.0304	.023	.33	.0512	.705	1.512	2.15	.496

of this series and may be used for calculation of other physical properties of inert gas-oxygen mixtures as the need arises.

WEIGHT CONSIDERATIONS

Structure of Cabin Wall

The weight penalty for the cabin wall must be considered as a function of the thickness required for safe maintenance of total internal pressure as well as a function of the thickness required for. safety against penetration. The specific mission in question is therefore a critical factor in this weight penalty calculation. The greater the dynamic flight loads and the greater the danger of meteorite penetration, the thicker the cabin wall must be. The greater the probability of penetration, the less tolerable is the 100-percent oxygen environment. The less tolerable a 100-percent oxygen environment, the greater percent inert gas must be added, and the greater the internal pressure of the cabin.

One must obviously define the mission in question, the size and shape of the cabin, the mission duration, and the specific cabin-gas system before an appropriate analysis of cabin-wall weight tradeoffs can be established. One must also define the meteorite environment or penetration rate. Figure 16 represents a sample calculation demonstrating these interactions.[12] The basic assumptions are a vehicle with a cabin

volume of 2100 cu ft and a vehicle area of 860 sq ft designed for a mission of 1-year duration with an oxygen-nitrogen system. This cabin is approximately twice the size of the proposed cabin of the U.S. Air Force Manned Orbiting Laboratory.

It can be seen in figure 16 that the weight penalty determined by flight loads is independent of the internal pressure of the cabin. The assumed meteoroid criteria are also indicated. With a 100-percent oxygen environment at 5 psia, it was considered that a criterion of no-penetration probability (P_0) of 0.997 is required. The addition of an inert diluent reduces the cabin-wall weight penalty most strikingly as oxygen content is reduced to 50 percent. Unfortunately, the criteria used for the allowable probability of penetration versus oxygen percentage are not stated. It would appear that curves of fabric burning rate versus total pressure and percent O_2, such as presented in part II of this series, could be roughly used for generating such a relationship. In view of the difficulty in assigning hazard weighting for specific burning rate, the penetration probability assigned to any burning rate would have to be somewhat arbitrary.[91] The recent work covering zero gravity effects on burning rates (see section on diluent gas in ch. 1) suggests that at least from the point of view of fire and blast hazard, the curve of allowable penetration probabilities in figure 16 may be shifted in the direction of higher percentages of oxygen. Because of the uncertainties regarding the absence of forced convection in the zero-g studies to date, the degree of this shift is still uncertain.

In addition to this uncertainty, the relationship between structural weight penalty and probability of no mass penetration requires that appropriate frequency-penetration equations be specified. Unfortunately, there is no indication of the equations which were used. If the curve is indeed shifted much to the left, the flight loads may well tend to be the limiting weight factor at pressures closer to or even below 5 psia.

It should be stated that meteoroid design criteria influence only very long missions. Puncture probability is low enough for missions in the 30- to 60-day class so that special meteoroid protection is not required.
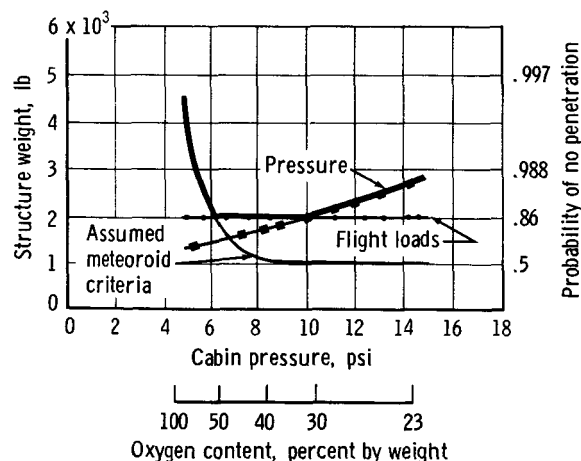

FIGURE 16.—*Structural weight considerations for a vehicle having a volume of 2100 ft³ and an area of 860 ft² for a mission of 1 year and an oxygen-nitrogen system.* (AFTER BOEING.[12])

The curve for structural weight versus internal pressure shows that the weight increase caused by increasing pressure does not become effective until about 10 psia. The heavy black line indicates the locus of weight-limiting factors and suggests that the minimum structural weight is relatively constant at 6 to 10 psia and is determined by dynamic loads. With less stringent criteria for meteorite protection and allowable percentage of oxygen, the minimum structural weight may extend closer to 5 psia. It must also be remembered that the relative weighting of specific penalties will change as the size and mission considerations are altered, but in general, minimum theoretical structural weight is constant for pressures up to 6 or 7 psia. The pressure-dependent weight penalty generally begins above 7 psia but, as in the above case, may not begin until 10 psia.[67] Fortunately, the minumum structural weight range of 5 to 10 psia also covers the physiologically ideal range of 5 to 7 psia.

While it is beyond the scope of this report to present, in detail, the complete structural analysis of a typical cabin wall, it appears appropriate to point out several factors which prevent the weight penalties from being a simple linear function of pressure. Figure 17 represents a study of the partition of wall weight for a space station

FIGURE 17.—*Effect of atmospheric pressure on pressure vessel weight. Conditions: 120-inch-diameter station, 182-inch-long pressure cabin, 140-inch-radius headers, and 2219–T62 aluminum material.* (AFTER PARKER ET AL.[79])

cabin which is a cylinder 120 inches in diameter and 182 inches long; the meteorite penetration and dynamic-load factors were not considered.[79] The problem of minimum gages and sizes for the cylinder headers and rings prevents the theoretical value of zero weight for zero pressure from being attained.

Atmospheric Leakage

The leakage of atmosphere from the cabin must be approached from two points of view. In the acute penetration of cabin wall by meteorites or other missiles, the large ratio of orifice diameter to wall thickness implies a sonic orifice flow. The leakage may well be rapid and the overall safety of the mission dependent on the rate of leak. A slower leak may allow a greater period of time for emergency procedures and possible crew survival.

Another consideration is the slow elastomer-to-metal seal leak which controls the amount of gas which must be taken on board to maintain constant atmospheric pressure over long periods of time. In this case, capillary-type flows must be considered. The following discussion is an extension of the more physiologically oriented review of the problem presented in part III of this series.

In general, it is necessary to distinguish between five different types of flow: [20, 67]

    (1) Reversible-adiabatic choked flow (sonic orifice flow or isentropic flow)

    (2) Isothermal frictionless flow

    (3) Isothermal flow with friction

    (4) Isothermal free-molecular flow

    (5) Capillary flow

Reversible-adiabatic choked flow is the type of flow that exists in an orifice nozzle at or above the critical pressure ratio. In this case, the flow at the throat or the minimum cross section is at sonic velocity or at a Mach number of 1. Choked flow will occur in any leakage where the orifice diameter is greater than wall thickness, provided the pressure ratio is critical or smaller. Isentropic flow involves no change of entropy in the system.

Isothermal frictionless flow occurs when the diameter of the passage is substantially less than the length of the passage. The idealized "frictionless" flow forms the upper limit of flow rates
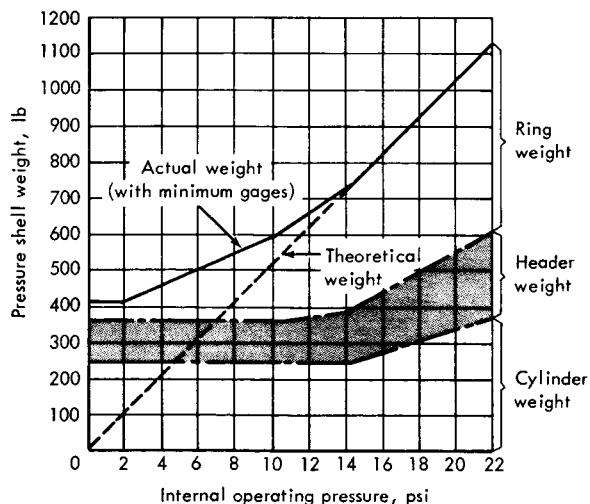
where the maximum velocity in the duct is $1/(\bar{V}_c)^{0.5}$ times the sonic velocity, or 0.845 times sonic velocity. Where great friction is involved through small holes or porous media, the flow rate is a function of both the passage dimensions and the friction factor and does not lend itself to a simple limit.

Isothermal free-molecular flow occurs when the critical hole diameter is so small that the molecules appear to act individually and not as a part of a flow stream. In this case the velocity is $(8/\pi\gamma)^{0.5}(\gamma + 1/2)^{0.5} = 2(\gamma + 1/\pi\gamma)^{0.5} = 1.48$ times the same velocity found for adiabatic choked flow. However, the area to be considered is $1/4/(2/\gamma + 1)^{1/\gamma - 1} = 0.395$ that for adiabatic choked flow. The actual flow rate is therefore $1.48 \times 0.395 = 0.584$ times that for adiabatic choked flow.

Capillary flow is similar in nature to the isothermal free-molecular flow and involves flow through long capillary passages. The intake flow is of laminar continuum type with a transition to the free-molecular flow at the zero pressure end. The problem of choice of an equation for flow through porous or capillary passages has been discussed in part III of this series.[92] There is little empirical data to support any single one. Mason has concluded that a modification of the Knudsen equation appears to best approximate this type of flow. This equation may well hold for orifices of diameter less than 25 percent of cabin-wall thickness. The equation is presented below in discussion of gas tradeoffs for slow seal-leak conditions.

EMERGENCY RAPID GAS LEAKS

Because of the multivariate conditions of gas leakage, it appears appropriate to review the development of generalized equations covering those factors pertinent to the problem at hand— gas specific leakage tradeoffs. These may be used to calculate leak rates for specific variables in question.

The theory of sudden rapid leakage under emergency conditions has been reviewed in great detail by Coe and his coworkers.[20] Only a general review of the concepts and pertinent equations required for tradeoff studies are presented here.

In general, two emergency situations may occur which require attention. A cabin puncture may be small enough to give a slow pressure transient and expose the crew only to the problems of decompression sickness. This may involve isothermal decompression, in that enough time may be available for thermal equilibration. However, even a relatively slow emergency leak from a space vehicle may be isentropic or adiabatic. In a zero gravity environment with no natural convection, the heat-transfer rate may be inadequate to maintain constant temperature and cause adiabatic conditions, although fan circulation should be present. One must also consider explosive decompression (time constants of less than 0.1 sec) where the transients are fast enough to allow the temperature to vary adiabatically or isentropically with the pressure. The physiological implications of these situations have been covered in part III of this series.[92]

Quotient rule differentiation of the ideal gas law $(PV = n_t RT)$ with respect to time yields

$$\dot{n}_t = \left(\frac{V}{R}\right)\frac{\dot{P}T - \dot{T}P}{T^2} \qquad (16a)$$

and solving for $\dot{P}$, the pressure change in a compartment undergoing any form of decompression would be

$$\dot{P} = \frac{n_t RT}{V} + \frac{P\dot{T}}{T} \qquad (16b)$$

The mass leak rate would be expressed by

$$\dot{W}_L = PC_d A \sqrt{\frac{g}{R}} \sqrt{\frac{m}{T}} f_1(\gamma) \text{ lb/sec} \qquad (17)$$

where

$$f_1(\gamma) = \sqrt{\gamma\left(\frac{2}{\gamma + 1}\right)^{\frac{\gamma + 1}{\gamma - 1}}} \qquad (18)$$

In terms of moles/sec,

$$F_L = \frac{\dot{W}_L}{m} = \frac{0.1444 \, PC_d A}{\sqrt{Tm}} f_1(\gamma) \qquad (19)$$

Isothermal Decompression

If the decompression takes place isothermally,

$T = T_0$ and $\tau = 0$. Then the equation (16b) becomes

$$\dot{P} = \frac{\dot{n}_t R T_0}{V} \qquad (20)$$

For the purposes of the present analysis, one can assume that the leak rate is always much greater than the feed rate and the rate of oxygen consumption. This would be certainly true if gaseous feed from storage can be immediately cut out as soon as a sudden pressure drop occurs. Substituting equation (19) into (20) leads to a rate of pressure drop

$$\underline{\dot{P}} = \frac{R T_0 F_L}{V} = -223 \left(\frac{C_d A}{V}\right) \sqrt{\frac{T_0}{m}} f_1(\gamma) P \text{ lb/ft}^2/\text{sec}$$

$$(21)$$

If

$$\alpha = 223 \left(\frac{C_d A}{V}\right) \sqrt{\frac{T_0}{m}} \, f_1(\gamma) \text{ sec}^{-1} \qquad (22)$$

the rate of pressure change becomes

$$\dot{P} = -\alpha P \qquad (23)$$

By integrating equation (23), it is seen that at any given second τ the ratio of pressure to original pressure is:

$$\frac{P}{P_0} = e^{-\alpha \tau} \qquad (24)$$

and the time to reach any given pressure ratio P/P_0 is:

$$\tau = \frac{\ln P_0}{\dfrac{P}{\alpha}} \qquad (25)$$

The upper curve of figure 18 presents a generalized isothermal decompression curve using relationships of equations (22) and (25) with the units $T_0 = {}^\circ\text{R}$, $A = \text{ft}^2$, $V = \text{ft}^3$, $\alpha = \text{sec}^{-1}$, and $\tau = \text{sec}$.

The isothermal decompression curves for the more specific situation where feed gas input,
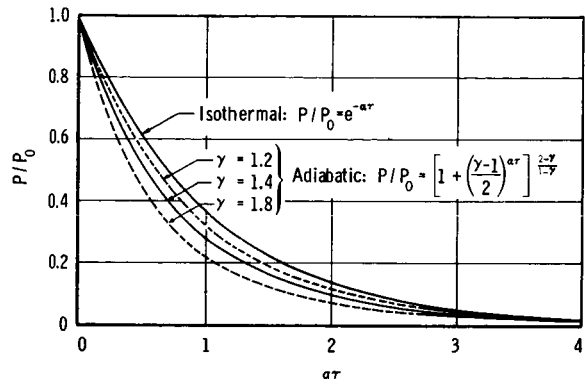
FIGURE 18.—*Generalized decompression curves for space compartments.* (AFTER COE ET AL.[20])

metabolic water and CO_2 production, and oxygen consumption are not neglected may be found in the analysis of Coe et al.[20] These complicated additions to the problem are beyond the scope of the present study and, except for feed gas, would have little effect on the decompression curve for acute emergency situations.

It can be seen from the isothermal curve and the equations (17) and (19) that the rapid, isothermal, mass-leak rate is an inverse function of the square root of the average molecular weight of the gas mixture and the molar leak rate is a direct function of the square root of the average molecular weight.

Adiabatic Decompression

If the decompression occurs adiabatically,

$$T = T_0 \left(\frac{P}{P_0}\right)^{\frac{\gamma-1}{\gamma}} \qquad (26)$$

and

$$\dot{T} = \left(\frac{\gamma-1}{\gamma}\right) \left(\frac{T_0}{P_0^{\frac{\gamma-1}{\gamma}}}\right) \left(\dot{P}/P \frac{1}{\gamma}\right) \qquad (27)$$

By substitution of equation (26) and (27) and rearranging, it can be seen that

$$\dot{P} = \left(\frac{\gamma R T_0}{V}\right) \left(\dot{n}_t \frac{P}{P_0}^{\frac{\gamma-1}{\gamma}}\right) \qquad (28)$$

Again assuming no feed into the system during decompression and substituting equation (26) into equation (19) gives:

$$F_L = \frac{0.1444\, C_d A}{\sqrt{T_0 m}}\, f_1(\gamma) P_0^{\frac{\gamma-1}{2\gamma}} P^{\frac{\gamma+1}{2\gamma}} \qquad (29)$$

Substituting equation (29) into equation (28) with the assumption that there is no feed into the system

$$\dot{P} = -223 \left(\frac{C_d A}{V}\right) \sqrt{\frac{T_0}{m}}\, (\gamma) f_1(\gamma) \left(\frac{P^{\frac{3\gamma-1}{2\gamma}}}{P_0^{\frac{\gamma-1}{2\gamma}}}\right) \qquad (30)$$

$$\dot{P} = -\left[\frac{\alpha\gamma(\phi-1)}{P_0^{\frac{\gamma-1}{2\gamma}}}\right] P^{\frac{3\gamma-1}{2\gamma}} \qquad (31)$$

where α is defined by equation (22). Integrating equation (31):

$$\frac{P}{P_0} = \left[1 + \left(\frac{\gamma-1}{2}\right)\alpha\tau\right]^{\frac{2\gamma}{1-\gamma}} \qquad (32)$$

so that

$$\tau = \frac{2\left[\left(\frac{P_0}{P}\right)^{\frac{\gamma-1}{2\gamma}} - 1\right]}{\alpha(\gamma-1)} \text{ sec} \qquad (33)$$

Figure 19 represents a plot of $f_1(\gamma)$ versus γ as indicated by equation (18).

Assuming specific values of γ, generalized adiabatic decompression curves can be plotted using the relationships of equations (22) and (33) and figure 19, with the units: $T_0 = °R$, $A = \text{ft}^2$, $V = \text{ft}^3$, $\alpha = \text{sec}^{-1}$, and $\tau = \text{sec}$. Figure 18 shows such a family of curves for isothermal conditions. It can be seen from figure 18 that at low values of $\alpha\tau$, the isothermal pressure drop is slower than adiabatic, but as $\alpha\tau$ increases, the adiabatic curves level off more rapidly. The molar rate of flow is again inversely proportional to the square root of the average molecular weight of the gas mixture (eq. (29)) and is related to the ratio of specific heats of the gases by the complex γ and $f_1(\gamma)$ relationship of this equation.

The interaction between the human lung and explosive decompression of the cabin has been reviewed in detail in part III of this series.[92] The same general gas-specific factors appear to
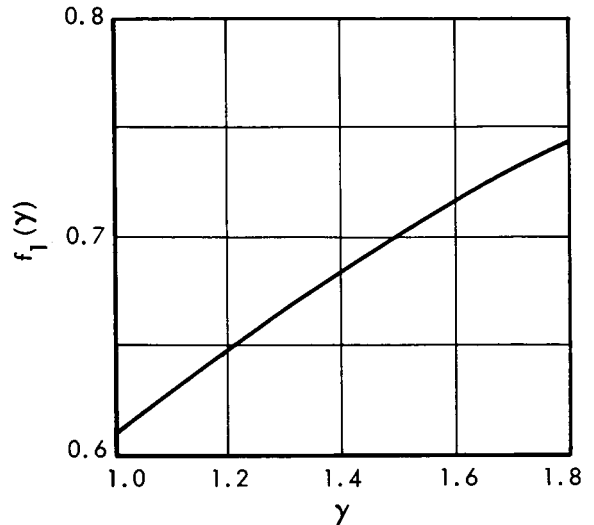
FIGURE 19.—*Specific heat function.* (AFTER COE ET AL.[20])

be at play. The interaction between the rapid leak rate and an active storage system or gas regeneration system is quite complex both from the point of view of pressure stabilization and weight penalty required to cover the open-feed decompression emergency. It is not felt that the present discussion warrants such a detailed analysis. It is also felt that the complexities of pressure caused by the presence of a fire during accidental or deliberate decompression precludes the addition of this concomitant event in the tradeoff analysis. The contribution of temperature rise due to heat liberation, oxygen consumption, and total pressure change due to imbalance between moles of combustion products formed and moles of reactants consumed have been theoretically analyzed by Coe et al.[20] The reader is referred to this study for further details.

What are the gas-specific factors involved in the fast leak situation? Since the amount of time required for a cabin to reach physiologically borderline levels of p_{O_2} is a major consideration in fast emergency leak conditions, it would be appropriate to compare the time it would take the several proposed gas systems to reach this endpoint.

The Boeing Co. has made calculations predicting these critical times.[12] Figures 20 and 21 represent the graphic presentation of variables
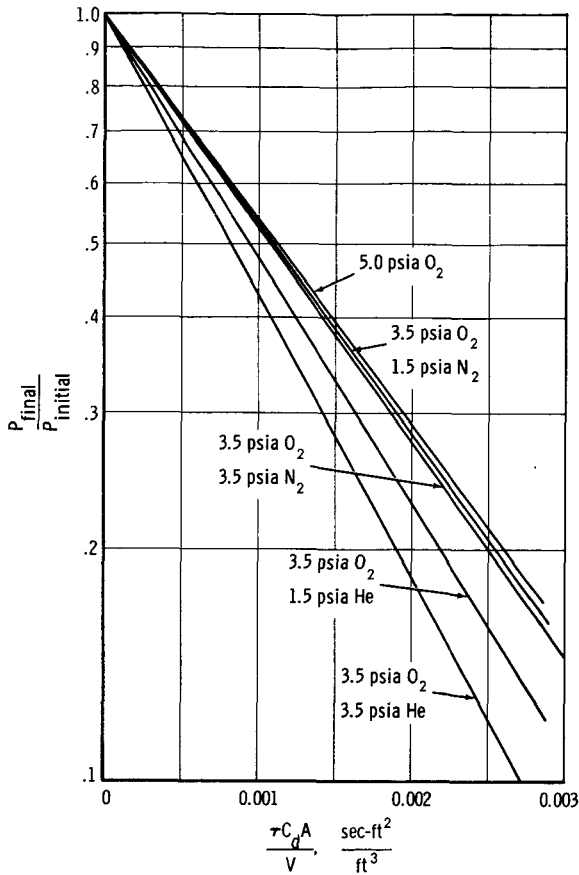
FIGURE 20.—*Isothermal decompression.* (AFTER BOEING.[12])
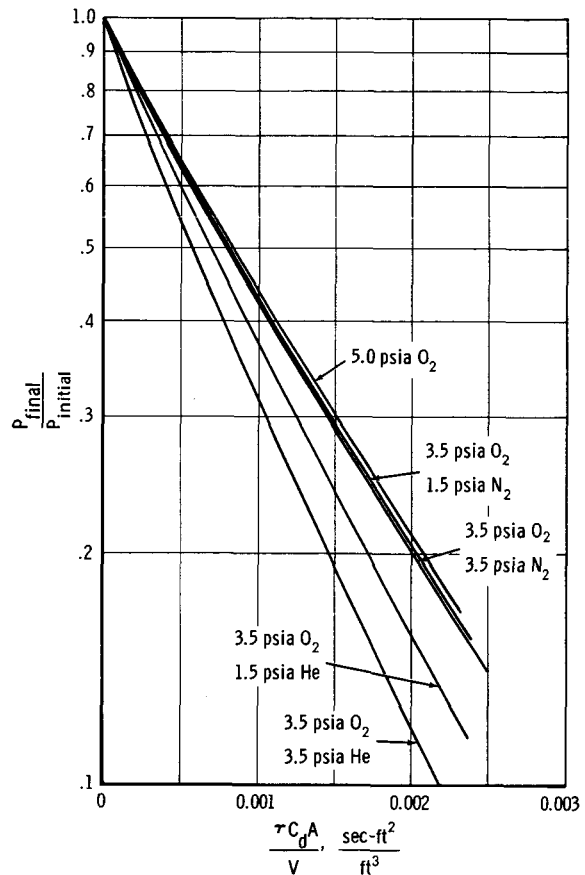
FIGURE 21.—*Isentropic decompression.* (AFTER BOEING.[12])

required for these calculations. From equations (22), (25), and (34), it can be seen that a logarithmic plot of P/P_0 versus $\tau C_d A/V$ will give curves from which the time can be simply determined. These relations are plotted for the isothermal condition in figure 20 and the isentropic or adiabatic condition in figure 21, with $\tau =$ seconds, $A =$ ft², and $V =$ ft³. These represent five specific cases of the generalized decompression curves of figure 18. In order to calculate the physiologically critical times, the minimal tolerable total pressures needed at any percentage of oxygen in the atmosphere can be obtained from figure 1.

A sample calculation can be shown for isothermal flow using figure 20. For a hole ½ inch in diameter, an orifice coefficient (C_d) of 1, and a cabin volume of 770 ft³, the time to reach 3.5-psia total pressure from 0.5-psia oxygen can be determined from figure 20 by using the ratio 3.5 to 5.0 or 0.7 to give:

$$\frac{\tau C_d A}{V} = 0.000575 \left(\frac{\text{sec ft}^2}{\text{ft}^3}\right)$$

and

$$\tau = \frac{0.00575 \times 770}{\dfrac{\pi \times (0.25)^2}{144}} = 325 \text{ sec}$$

The time to reach minimum tolerable partial pressure of p_{O_2} can be calculated by the factors of figure 1. This reduces the available time considerably.

Table 5 represents the time in minutes required to reach 3.5 psia for ½-inch and ¾-inch holes under isothermal and isentropic conditions with five proposed atmospheres. Table 6 represents the times required to meet minimum tolerable total pressures as determined by minimal p_{O_2} levels. It can be seen that in all cases, the

TABLE 5. — *Decompression Time to 3.5 psia* [AFTER BOEING [12]]

[CABIN VOLUME = 770 FT^3; ORIFICE COEFFICIENT = 1]

Leak mode	3.5 psia O_2 3.5 psia N_2 7.0 psia	3.5 psia O_2 3.5 psia He 7.0 psia	3.5 psia O_2 1.5 psia N_2 5.0 psia	3.5 psia O_2 1.5 psia He 5.0 psia	5.0 psia O_2
	Decompression time, min				
Isothermal — 1/2-inch hole...............................	10.0	7.75	5.3	4.59	5.42
Isentropic — 1/2-inch hole...............................	7.64	5.47	3.9	3.25	3.95
Isothermal — 3/4-inch hole...............................	4.5	3.44	2.36	2.04	2.41
Isentropic — 3/4-inch hole...............................	3.4	2.43	1.73	1.45	1.75

TABLE 6. — *Decompression Time to Minimum Tolerable Total Pressure as Determined by Minimum Acceptable* p_{O_2} [AFTER BOEING [12]]

[CABIN VOLUME = 770 FT^3; ORIFICE COEFFICIENT = 1]

Leak mode	3.5 psia O_2 3.5 psia N_2 7.0 psia	3.5 psia O_2 3.5 psia He 7.0 psia	3.5 psia O_2 1.5 psia N_2 5.0 psia	3.5 psia O_2 1.5 psia He 5.0 psia	5.0 psia O_2
	Decompression time, min				
Isothermal — 1/2-inch hole...............................	6.17	4.72	2.25	1.93	5.42
Isentropic — 1/2-inch hole...............................	4.54	3.22	1.62	1.35	3.95
Isothermal — 3/4-inch hole...............................	2.75	2.1	1.0	.86	2.41
Isentropic — 3/4-inch hole...............................	2.03	1.42	.72	.59	1.75

oxygen-nitrogen mixture at 7 psia takes the longest times and 100 percent oxygen takes the shortest time to reach the critical condition. The larger the hole, the less the absolute difference between mixtures. There is no difference between the times for either endpoint criterion for 100 percent oxygen at 5 psia. The lower the pressure of inert gas, the less time required to reach both endpoints and the greater the difference between the two criteria. From the point of view of the human subject, table 6, of course, presents the more valid endpoint. At equivalent composition and pressures, nitrogen has a slight advantage over helium.

The relative weighting of this factor in the overall tradeoff analysis is discussed in chapter 3. The major question raised at this point is the operational significance between the maximally divergent times of 2 minutes and 0.6 minute for the 3/4-inch hole with isentropic flow. If the mission requires at least 2 minutes for donning an emergency suit in a high-risk mission, this difference may well be critical in the selection. The major probability of a penetration producing such a hole size is obviously a major mission-specific factor to be considered.

There are several other minor considerations in the area of fast-flow systems. These are the maximum airlock dumping and repressurization times during extravehicular operations and the maximum rate of cabin pressure dumping during fire emergencies. The dumping of airlock and cabin would, of course, follow the more isentropic type of flow. In the present case, the faster the

flow through the maximum orifice available, the more advantageous the gas mixture. One would therefore have to weigh the advantage of having a more rapid dumping capability for a suited crew against a less-rapid emergency dumping after accidental puncture with an unsuited crew.

The repressurization of an airlock from a vacuum to the pressure of the main compartment is most rapidly accomplished by opening a valve between the two chambers. In most cases, the pressure and temperature of the main compartment is maintained constant by the gas feed system and the compression will be close to isothermal because of the great flow turbulence in the airlock. The flow across the valve starts off as a supercritical pressure ratio and then becomes subcritical when

$$P_c/P_{lk} = \left(\frac{2}{\gamma+1}\right)\frac{\gamma}{\gamma-1}$$

The approximate time required to recompress a lock isothermally from a vacuum can be determined for air of $\gamma = 1.4$ by the equation

$$\tau_t = \frac{V}{130\,C_dA}\sqrt{\frac{m}{T_{lk}}} \qquad (34)$$

This aspect of a space mission will be critical only when a crewman must be retrieved most rapidly through a lock to a cabin. Since the relatively small volume of the lock suggests that the minimum time for recompression will not in any practical way limit the survival potential of the crewman, the effect of atmospheric composition should have little practical effect on the survival. The difference in time, measured by seconds, which will be given the entering crewman by an optimum gas mixture does not appear to warrant a thorough analysis of the problem in the present context. A general analysis of this problem is presented by Coe et al.[20] That the gas-specific factor will probably not be critical is indicated by their calculation from equation

(34) that a lock of 40 ft[3] can be isothermally pressurized by air to 99 percent of the main compartment pressure through a valve of only 0.58 in.[2] in 30 seconds. Doubling the area of the valve can reduce this time to about 15 seconds. Since the time required is proportional to the square root of the molecular weight, substitution of air (molecular weight = 29) by the proposed mixture of lowest molecular weight, helium-oxygen mixture at 7 psia (molecular weight = 18), will reduce minimum compression time by only a few seconds. For larger lock systems, the number of seconds to be saved will increase as will the physiological significance of the savings. However, the valve size can be increased to meet this demand in a large lock.

One must also consider the airlock pumping weight penalties. The airlock may be pumped into a separate storage tank or into the main compartment. The effect of atmosphere composition on this penalty is currently under study at Douglas.[101] Data are also available on a new elastic recovery principle in the design of airlocks.[16]

SLOW SEAL LEAKAGE

The selection of appropriate equations for the description of slow leaks through elastomer-metal seals is a significant factor in calculation of weight penalties for gas storage system. In part III of this series, a preliminary analysis of the problem by Mason of AiResearch was discussed.[92] More recently Mason has expanded his calculations to include analysis for neon and other variables. It appears appropriate to review these calculations and compare them with similar unpublished calculations made by R. K. Moir and J. R. Malcom of the Boeing Co.[12]

The most divergent equations for seal-leak calculations are those for isentropic sonic-orifice flow described above for large holes and those for capillary-free molecular flow. Mason's recent modification of the Knudsen equation for capillary flow of laminar continuum to free molecular transition at a final pressure of zero is

$$q = \frac{5.22\,D^4P'^2}{10^6\mu'L} + \frac{7.42\,D^3P'}{10^6\,L}\sqrt{\frac{T'}{M'}} + \left[\frac{7.44\,D^2\mu'T'}{10^8\,M'L}\right]\left[\ln\left(1+\frac{23.9\,DP'}{\mu'}\sqrt{\frac{M'}{T'}}\right)\right] \qquad (35)$$

where

q pressure × volumetric leakage rate, micron-
      liters/sec

D capillary diameter, microns

P' cabin pressure, 14.7 psia

μ' viscosity, 1.81×10^{-4} poise

L capillary length, cm

T' temperature, 527.7° F

M' molecular weight, 28.97

The number of capillaries required to achieve a 1 lb/day leakage rate with capillary flow of 5 psia oxygen is shown in table 7 for several holes of 1-mm length. Since the number of capilaries multiplied by the diameter represents the possible number of leakage paths along spacecraft seal perimeters, it was pointed out that the most probable hole size is in the range of 1 to 10 microns.

Table 8 represents a comparison of equivalent leakage rates for several physiologically adequate gaseous mixtures based on a 1 lb/day leakage

rate of oxygen at 5 psia; isentropic sonic orifice and capillary flows of the type represented by equations (32) and (35), respectively, are compared.

Table 8 shows that the flow type is not critical and that helium leakage is not as excessive as

TABLE 7. — *Capillary Size and Quantity Required for 1.0 lb/day Leakage From 5-psia Oxygen Atmosphere* [AFTER MASON ET AL.[67]]

Capillary diameter, microns	Number of capillaries of 1-mm length	Number of capillaries × diameter, microns
0.01	1.0×10^{14}	3.3×10^{6}
.1	1.0×10^{11}	3.4×10^{5}
.3	3.9×10^{9}	3700
1.0	9.7×10^{7}	320
3.0	2.7×10^{6}	27
10.0	3.9×10^{4}	0.06
30.0	5.9×10^{2}	0.06

TABLE 8. — *Comparison of Capillary and Orifice Leakage Models* [AFTER MASON ET AL.[67]]

[BASIS: 1 LB/DAY LEAKAGE FROM A 5-PSIA PURE OXYGEN ATMOSPHERE]

	Leakage, lb/day, at pressures of —							
	5 psia		7 psia		10 psia		14.7 psia	
	Capillary	Orifice	Capillary	Orifice	Capillary	Orifice	Capillary	Orifice
Oxygen	0.77	0.83	0.98	0.96	1.19	1.11	1.54	1.29
Helium	.04	.05	.14	.12	.28	.26	.62	.50
Total	.81	.88	1.12	1.08	1.47	1.37	2.16	1.79
Oxygen	0.70	0.76	0.81	0.80	0.92	0.84	1.10	0.87
Neon	.19	.21	.57	.51	1.09	.99	2.23	1.73
Total	.89	.97	1.38	1.31	2.01	1.83	3.33	2.60
Oxygen	0.71	0.71	0.86	0.72	1.03	0.73	1.33	0.73
Nitrogen	.27	.27	.84	.63	1.69	1.18	3.74	2.00
Total	.98	.98	1.70	1.35	2.72	1.91	5.07	2.73

often predicted. There is actually little difference between the weight of these mixtures lost per day in the 5- to 7-psia range. For orifice flow, the leakage rate is nearly proportional to pressure. At pressures less than 7 psia, the same is true for capillary flow. As the pressure and molecular weight increase, equation (35) suggests that the leakage rate becomes proportional to the square of the pressure.

For the range of capillary orifices and cabin atmospheres most suitable from a physiological point of view, the calculated leak rates are indicated in table 9. This table also employs as a basis a leak equivalent to 1 lb/day of O_2 at 5 psia. The number of holes required for this leak rate through capillaries of 1-mm length was determined by table 7 and the leakage rates for other gases were evaluated. Only at the higher

TABLE 9.—*Leakage Rates for Various Atmospheres* [AFTER MASON ET AL.[67]]

[BASIS: 1 LB/DAY LEAKAGE FROM A 5-PSIA PURE OXYGEN ATMOSPHERE]

Capillary diameter, microns	p_{O_2}, mm Hg / $p_{Diluent}$, mm Hg / p_{Total}, mm Hg	Relative leakage rate, lb/day, for—											
		Diluent, helium				Diluent, neon				Diluent, nitrogen			
		180 / 79 / 259 (5 psia)	180 / 200 / 380 (7.35 psia)	180 / 338 / 518 (10 psia)	180 / 580 / 760 (14.7 psia)	180 / 79 / 259 (5 psia)	180 / 200 / 380 (7.35 psia)	180 / 338 / 518 (10 psia)	180 / 580 / 760 (14.7 psia)	180 / 79 / 259 (5 psia)	180 / 200 / 380 (7.35 psia)	180 / 338 / 518 (10 psia)	180 / 580 / 760 (14.7 psia)
0.01	O_2	0.814	0.947	1.061	1.204	0.739	0.775	0.798	0.818	0.710	0.718	0.723	0.725
	Diluent	.045	.132	.249	.485	.205	.543	.944	1.662	.273	.699	1.188	2.045
	Total	.859	1.079	1.310	1.689	.944	1.318	1.742	2.480	.983	1.417	1.911	2.770
0.1	O_2	0.813	0.947	1.058	1.199	0.741	0.774	0.795	0.815	0.710	0.716	0.720	0.727
	Diluent	.045	.131	.248	.483	.205	.543	.942	1.656	.273	.696	1.183	2.050
	Total	.860	1.078	1.306	1.682	.946	1.317	1.737	2.471	.983	1.412	1.903	2.777
0.3	O_2	0.812	0.949	1.069	1.229	0.738	0.777	0.805	0.840	0.710	0.728	0.749	0.785
	Diluent	.045	.132	.251	.495	.204	.544	.954	1.708	.273	.708	1.230	2.215
	Total	.857	1.081	1.320	1.724	.942	1.321	1.759	1.548	.983	1.436	1.979	3.000
1.0	O_2	0.797	0.959	1.113	1.339	0.725	0.789	0.846	0.933	0.711	0.776	0.849	0.978
	Diluent	.044	.133	.261	.539	.201	.553	1.002	1.895	.273	.754	1.395	2.758
	Total	.841	1.092	1.374	1.878	.926	1.342	1.848	2.828	.984	1.530	2.244	3.736
3.0	O_2	0.769	0.977	1.193	1.538	0.702	0.810	0.920	1.099	0.714	0.862	1.031	1.327
	Diluent	.042	.136	.280	.620	.194	.567	1.089	2.233	.274	.838	1.693	3.741
	Total	.811	1.113	1.473	2.158	.896	1.377	2.009	3.332	.988	1.700	2.724	5.068
10.0	O_2	0.734	1.001	1.294	1.794	0.672	0.837	1.014	1.314	0.716	0.972	1.265	1.780
	Diluent	.040	.139	.304	.723	.186	.586	1.201	2.669	.275	.945	2.078	5.018
	Total	.774	1.140	1.598	2.517	.858	1.423	2.215	3.985	.991	1.917	3.343	6.798
30.0	O_2	0.713	1.016	1.356	1.949	0.654	0.853	1.071	1.443	0.718	1.039	1.407	2.055
	Diluent	.039	.141	.318	.785	.181	.398	1.268	2.933	.276	1.009	2.311	5.794
	Total	.752	1.157	1.674	2.734	.835	1.451	2.339	4.376	.994	2.048	3.718	7.849

pressures does the hole size appear significant. The gaseous composition does not appear to be very significant for any hole size in the 5 to 7 psia range. For the smaller holes, nitrogen has a slight advantage; for the larger holes, neon. In the 1- to 10-micron range predicted as most probable by table 7, there is virtually no difference between the inert gas used. Figure 22 summarizes these data graphically for a capillary 3 microns in diameter. Pressure is the major determinant of mass leakage through seals.

Unfortunately, there is little empirical data to corroborate these predictions. Mason reported that preliminary work with a cabin simulator suggests little difference between helium and nitrogen in leakage through inflatable elastomer to metal seals.[66] The variation in leak rate from run to run was too great for any definite conclusion. Only when vacuum grease was applied to the inflatable seal was there any indication that the molal leak rates for a 50-percent oxygen and 50-percent nitrogen mixture and a 50-percent oxygen and 50-percent helium mixture were similar. Mason feels that large mission-to-mission variation in hatch-seal leak rates may be anticipated in operational vehicles.

In the Boeing studies of leak rate through seals, simple isentropic orifice flow, compressible pipe flow, and capillary flow were compared. Because the calculations were approached in a somewhat different way from those of Mason et al., they appear worthy of review. The capillary and isentropic equations which the Boeing groups used were the same equations used by Mason et al. Unfortunately, the specific compressible pipe

flow equation used by the Boeing group was not specified. The Boeing approach was to also assume a given hole size and calculate the number of holes required to leak 2.0 lb/day of oxygen-nitrogen mixture at 7.0 psia. Mason et al., it should be remembered, used 1 lb/day of 5.0 psia O_2 as a basis (table 7). Since the physical flow properties of oxygen and nitrogen are similar, the bases differ only in original pressure (7 versus 5 psia) and leak (1 lb/day versus 2 lb/day). A major difference was the assumption of a $\frac{1}{4}$-inch (6.3 mm) instead of the 1-mm path length of the previous study.

Figure 23 represents the plot of hole diameter versus number of holes required for the assumed leak. It can be seen that for hole sizes of 30 microns, 4×10^3 holes are required to support the model leak with capillary flow. Comparison with table 7 indicates that under the specific assumptions used in the Mason study, 5.9×10^2 holes are required, or only 0.15 the number of holes required under the Boeing assumptions.

The Boeing group discarded orifice flow as a valid model because the calculated hole sizes were so small that it made the orifice assumptions invalid by virtue of the excessive ratio of path length to diameter. Compressible pipe flow was discarded for small hole sizes because the pressure drop was assumed to be so great as to make the flow molecular in nature. Using figure 23 to calculate the number of holes and the hole diameters that will leak 2 lb/day of oxygen-nitrogen mixture at 7 psia, the mass leakage for the other atmospheres was determined assuming capillary flow as indicated by equation (35). Figure 24
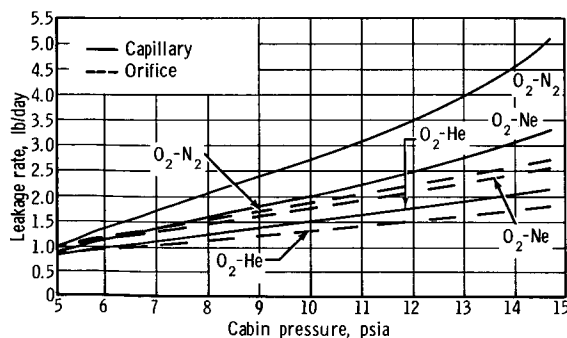

FIGURE 22.—*Leakage rate as a function of pressure. Basis: 1 lb/day leakage for 5-psia oxygen atmosphere.* (AFTER MASON ET AL.[67])
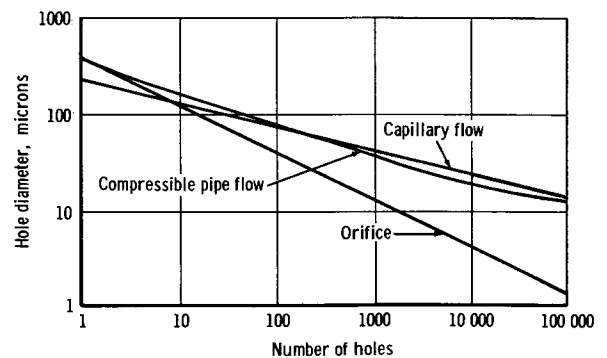

FIGURE 23.—*Variation of hole diameter with number of holes required for the assumed leak.* (AFTER BOEING.[12])
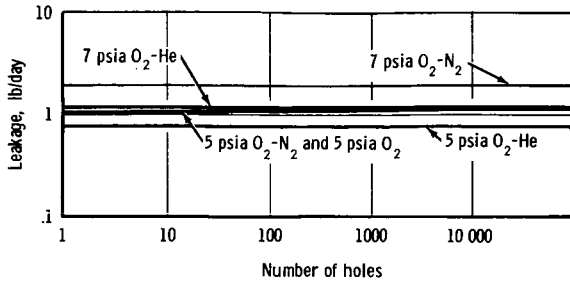
FIGURE 24.—*Sensitivity of leakage to number of holes and atmospheric composition for rates equivalent to 2.0 lb/day of 7.0-psia oxygen-nitrogen mixture.* (AFTER BOEING.[12])

represents the results of these calculations. Even with the greater capillary length of the Boeing study, it can be seen that the relative leakage rates of the different atmospheres is not affected by the assumption of hole size and hence number of holes.

Table 10 compares the mass leak rate through capillaries of 3 microns in diameter for approximately similar mixtures and pressures calculated by the two groups using the different basic assumptions discussed previously. The leak rates appear quite insensitive to the different capillary lengths under study (1 and 6.3 mm). This remarkable agreement may have fortuitously arisen from the interaction between the slightly different pressures and compositions being studied and the differences in path length. In any case, these mass leak rates appear to be adequate for a first-order analysis of the weight tradeoffs of the different gas systems. The oxygen-neon

mixtures appear to be slightly more favorable than the other mixtures for the 3-micron-diameter hole under consideration.

Recent advances in sealing technology in spacecraft design have been reviewed.[107] These principles should be brought to bear on the problem.

Tankage for Gas

The tradeoffs for gas tankage appear to be most sensitive to differences in spacecraft configuration and mission plan. This arises from the dependence of storage efficiency on the size and shape of the container, be it for gaseous or cryogenic systems. There are also major questions regarding the basic weight penalties in cryogenic tankage for small liquid helium and neon systems. In the following section an attempt will be made to define the knowns and the unknowns in storage systems and indicate how they may condition the several tradeoff analyses in the subsequent sections of this report.

GENERAL CONSIDERATIONS

The storage of gases for atmosphere control systems may be classified as (1) high pressure gaseous storage at ambient temperature, (2) cryogenic storage at low or moderate pressures, and (3) for oxygen and nitrogen, storage in chemical form. Each of these approaches will be presented with the minimum detail required for tradeoff analyses.

TABLE 10. — *Comparison of Mass Leak Rates*

Mass leak rate, lb/day, at pressures of —							Study
5 psia				7 psia			
100 percent O₂	70 percent O₂ 30 percent He	70 percent O₂ 30 percent Ne	70 percent O₂ 30 percent N₂	50 percent O₂ 50 percent He	50 percent O₂ 50 percent Ne	50 percent O₂ 50 percent N₂	
1.0	0.811	0.702	0.988	1.13	0.810	1.70	Mason et al.[67]
1.05	.76	....	1.05	1.08	....	2.0	Boeing.[12]
1.0	.72	....	1.00	1.02	....	1.90	Boeing[12] normalized to 5-psia O₂=1 lb/day.

HIGH-PRESSURE GASEOUS STORAGE

The basic role of gaseous storage systems appears to be that of supplemental storage or storage for repressurization of the cabin when long-term storage prior to use makes it more efficient, especially in smaller cabin systems. The need for high delivery rate in repressurization also favors gaseous storage. A comparison with liquid systems under these conditions is presented subsequently.

The basic problem in this approach to gas storage is the minimization of container volume penalties by the use of elevated storage pressures without incurring excessive pressure shell weight. It can be shown that if the fluid stored acts like an ideal gas, the weight of container designed to hold a given charge is essentially independent of pressure while container volume is inversely proportional to pressure. Very-high-pressure storage appears to be the ideal goal. However, gas compressibility factors begin to limit the weight efficiency of storage. At pressures above several thousands of pounds per square inch, gases become less compressible. The decrease in compressibility is less serious for helium and neon than for oxygen and nitrogen.[46]

Thus as pressure is increased, overall vessel volume passes through a minimum and actually increases because of overall shell-wall thickness. Pressure-level optimization studies for oxygen storage vessels conducted by Jacobson,[43] Keating,[51] and Coe et al.[20] indicated an optimum storage pressure of 7500 psia for equal pressure and volume criteria. This level was used in the Project Mercury system.[75] Optimum storage vessels for pressure up to 9000 psia are currently under study by several companies.[66] These vessels will be of greater value for helium and neon where compressibility factors play a lesser role.

If the rough sizing of a vehicle volume is available, the tradeoff between storage weight and volume can be made for any vehicle design. The total storage system penalty effects are estimated by using the relation

$$\frac{dX}{X} = a\frac{dW_T}{W_T} + b\frac{dV_T}{V_T} \qquad (36a)$$

The above relation simply states that the percentage change in overall system penalty X is the weighted sum of storage vessel weight and volume percentage changes. Such a relation holds true over at least a small system size range, with the weighting factors a and b determined by the type of vehicle geometry and structure considered. System optimization then involves minimization of X, where

$$X = W_T{}^a V_T{}^b \qquad (36b)$$

As can be seen, the relative importance of storage vessel weight and volume is expressed by the weighting factors a and b. Thus, for a case where $b = 0$, weight is all important, while volume is all important for the case $a = 0$. For $a = b$, system optimization involves minimization of the product of weight and volume, $W_T V_T$. Storage vessel data given in the following section cover these three cases and also include the cases of minimum $W_T \sqrt{V_T}$ and $V_T \sqrt{W_T}$ (intermediate relative importance levels).

The optimization of weight and volume parameters to be discussed is taken directly from the study of Coe et al.[20] The physical basis for the tradeoff data may be found in this study. In all cases, it is assumed that the nominal fill temperature of the vessel is 530° R and maximum fluid use is 620° R. Storage fluid end pressure is 30 psia.

The gas compressibility factors for oxygen were computed from experimental pressure-volume-temperature data for nitrogen, assuming the law of corresponding states, the accuracy of the basic nitrogen data, and the close similarity of the two gases. Container structural analyses were given for simple geometries and were based upon the assumptions of true geometrical shape and of a low ratio of wall thickness to diameter. It is to be emphasized that more detailed analyses than those presented would be required to optimize structural design in a specific application. Particular attention would have to be given to vessel mounting requirements.

Oxygen

Figure 25 represents the variation with nominal charge pressure of the total weight and volume of spherical oxygen vessels for SAE 4340
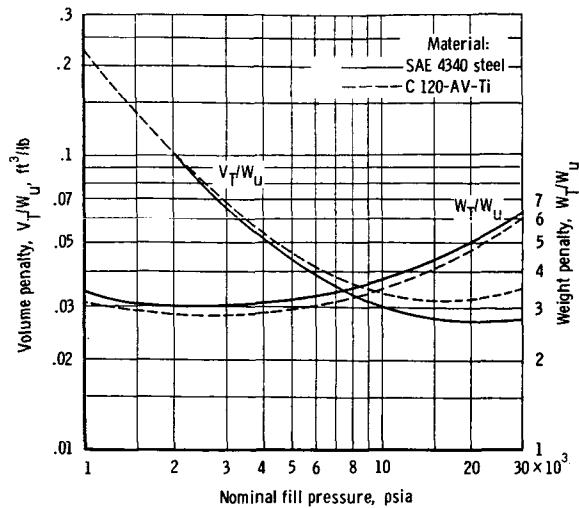
FIGURE 25.—*Weight and volume of spherical oxygen storage vessels for safety factor of 1.88.* (AFTER COE ET AL.[20])

FIGURE 26.—*Optimization of spherical oxygen storage vessels. Material is SAE 4340 steel.* (AFTER COE ET AL.[20])

steel and titanium alloy C120 AV Ti. The safety of titanium pressure vessels for oxygen storage has been questioned in part II of this series,[91] but will be included to show the weight savings. A fatigue failure criterion with a safety factor of 1.88 was used in figure 25.

As discussed above, the weight and volume penalties show distinct minima. Minimum weight occurs at approximately 2500-psia charge pressure, indicating the deleterious effect of charge temperature tolerances on fluid load penalties at low charge pressures. Minimum vessel volume occurs at a charge pressure of approximately 20 000 psia for the steel vessels, showing the effects of increases in vessel wall thickness at higher charge pressures, as well as the increasing compressibility factor for the gas under these conditions. From other calculations, it appears that the pressures at which the weight and volume are minimum are apparently independent of the safety factor used in the design. However, the actual values of the weight and volume are directly related to the safety factor. Similar data for Inconel 718, stainless steel 301A (cryogenically stretched by Ardeforming), and Ti 6A 6V 2S may be found in figure 7–15 of reference 51.

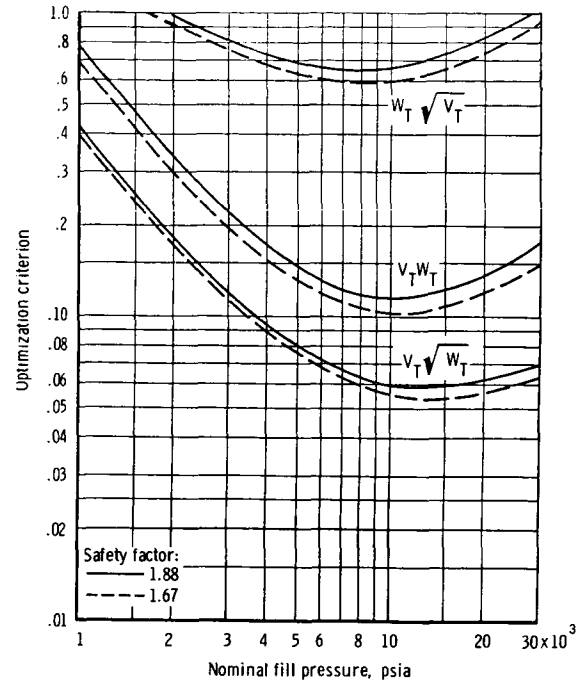The terms $W_T V_T$, $W_T \sqrt{V_T}$, and $V_T \sqrt{W_T}$ are shown on figure 26 as functions of charge pres-

sure level for spherical steel oxygen vessels. The use of these factors is explained by equations (36a) and (36b). The effects of weight and volume weighting factors on optimum charge pressure level can be seen by comparison of figures 25 and 26. It should be noted that the inclusion of unusable fluid weight penalties results in a higher optimum charge pressure (approximately 10 000 psia) than that computed by Keating.[50] (See table 11.)

Nitrogen

Total weights and volumes of spherical nitrogen storage vessels are shown in figure 27 as functions of charge pressure level for the two cases studied. Titanium was used as the vessel material for nitrogen. The results are generally similar to those obtained for oxygen, showing minima in vessel weight and volume in the pressure range studied. Similar data covering pressure up to 3500 psia for Inconel 718, stainless steel 301A (cryogenically stretched by Ardeforming) and Ti 6A 6V 2S may be found in figure 7—15 of reference 51.
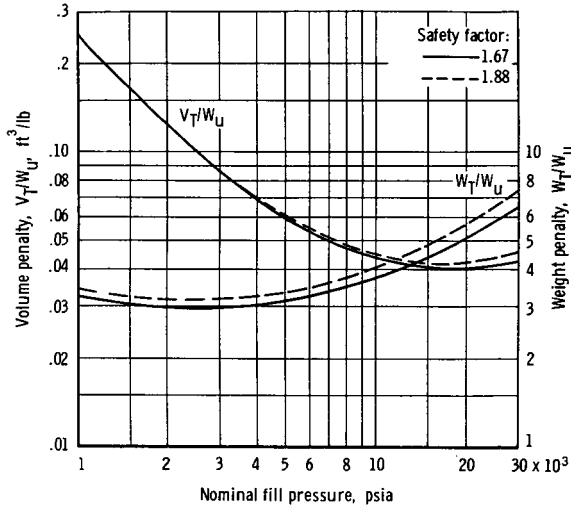
FIGURE 27.—*Weight and volume of spherical nitrogen storage vessels. Material is Ti C–120 AV.* (AFTER COE ET AL.[20])

Figure 28 shows the terms $W_T V_T$, $W_T \sqrt{V_T}$, and $V_T \sqrt{W_T}$ for spherical nitrogen vessels as functions of charge pressure level derived from equations (36a) and (36b). Here, the optimum charge pressure for minimum $W_T V_T$ is approximately 8000 psia in the case considered.

Table 11 summarizes the optimum values of weight and volume for oxygen and nitrogen vessels. It should be noted here that the weights plotted in figures 25 to 28 and table 11 do not include the weight of the lines, brackets, or valves; an allowance should be made for these accessories. The valve weight depends only on the number of vessels and on the number of valves installed on each vessel for redundancy and for installation requirements. (See table 19.) Mounting bracket design depends primarily on the size of the vessel, on the number of vessels,

TABLE 11.—*High-Pressure Gas Storage Optimum Design* [AFTER ROUSSEAU ET AL.[95]]

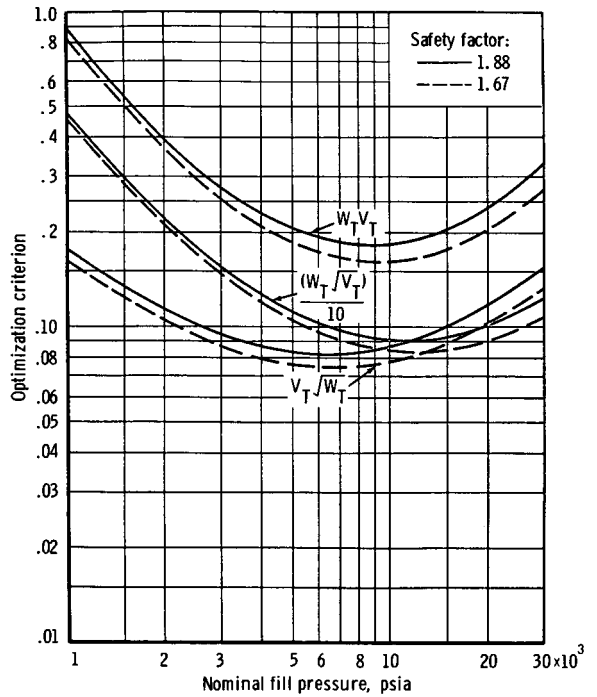| Parameter	Oxygen	Nitrogen
Optimum pressure, psia..................	10 500	9500
Weight penalty, W_T/W_u..................	3.46	3.66
Volume penalty, V_T/W_u, ft³/lb..........	0.0296	0.0446
Optimization criterion..................	0.1025	0.163

FIGURE 28.—*Optimization of spherical nitrogen storage vessels. Material is Ti C–120 AV.* (AFTER COE ET AL.[20])

and on the installation. These weights, in general, are small; an allowance for accessory weight should be made, however, in the total vessel weight.

Helium

The weights and volumes of spherical helium vessels are shown in figure 29 as functions of charge pressure level, using titanium as the pressure shell material. These data are limited to pressures below 6000 psia because of the lack of higher pressure-density data. The tendency of helium to diffuse through the metal may well limit the usefulness of higher pressures. Compressibility is not a factor with helium.

Neon

In the pressure range studied, the compressibility of neon appears to be the same as that of helium, both acting quite close to that of an ideal gas.[44] Since the density of helium at 0° C and 1 atm is 0.178 gm/l and that of neon 0.899 gm/l, the volume per pound of useful load should be reduced by a factor of about 5 and run parallel
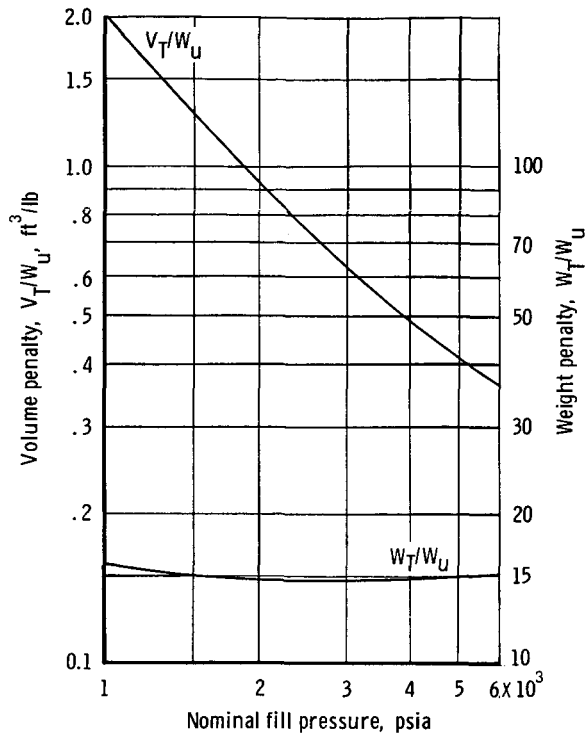
FIGURE 29.—*Weight and volume of spherical helium storage vessels.* (AFTER COE ET AL.[20])

to the upper curve of figure 29. Similarly, the total vessel weights per pound of useful load should also be reduced by a factor of 5 and run parallel to the lower curve of figure 29. A less expensive mixture of 85 percent neon and 15 percent helium may be economically more feasible than pure gaseous neon.[92]

Mixed Gas Storage

The availability of mixed gas storage in one container for repressurization purposes appears to be a great advantage of high pressure gaseous systems. This system is indeed attractive only for this purpose since the requirement for stable use of both constituents precludes its maintenance use in cabins where unavoidable erratic leaks occur. Even in the event of constant-leak systems, the mixed gas form alone is not suitable for cabins where crew occupancy or workload can vary from time to time and no parallel control of leak rate is feasible. Because mixed gas storage is limited to repressurization systems, a thorough weight penalty analysis does not appear warranted in the present context.

CRYOGENIC STORAGE

General Considerations

The cryogenic storage of fluids offers several distinct advantages over high-pressure storage of the low boiling-point fluids such as oxygen and nitrogen. These advantages are a higher fluid storage density at low to moderate pressure, reduced container weight per unit of stored mass, provision of potential refrigeration or cooling sources as heat sinks (170 Btu/lb for liquid oxygen or nitrogen when heated to room temperature).

The major defects are the sensitivity to unexpected heat leaks and the complexity of delivery in zero gravity. These defects require special attention to insulation needs, single-phase fluid expulsion, phase separation for venting, and quantity measurement. Cost, development time, servicing equipment, standby penalties, and limited expulsion capability are other disadvantages.

Two major classes of cryogenic liquid storage systems are used. They specify either mode of storage or method of pressurization. The fluid may be stored as a single phase of fluid or as a two-phase mixture of fluid and vapor requiring special separation techniques. The pressurization may, in turn, be accomplished by use of externally supplied gas or by thermal energy added by means of electric power or a heat exchanger in the storage space.

Because weight tradeoffs are quite sensitive to the specific form of cryogenic storage involved, it appears appropriate to renew briefly for the reader not versed in cryogenics, the several forms of storage systems available. For further details, it is suggested that the reader refer to the discussions of Vance,[108] Cook,[21] Coe et al.,[20] and Christian and Hurlich.[18] The following discussion is taken directly from the Coe paper.

The following three types of systems appear to be most commonly suggested for zero-gravity space cabin use:

(1) Supercritical single-phase thermal pressurization

(2) Subcritical single-phase helium bladder expulsion

(3) Low-pressure two-phase vapor or liquid delivery

Supercritical single phase.—The operation of this type of storage vessel, which avoids zero-gravity phase separation problems, is shown on a schematic fluid temperature-density diagram on figure 30. Figure 31 shows the thermodynamic process operation on a schematic pressure-enthalpy diagram and illustrates one method of tank heat addition.

Tank fill conditions are indicated by point 1 on figures 30 and 31. Here, the storage vessel is assumed incompletely filled with liquid at atmospheric pressure. The storage fluid is thus a mixture of saturated liquid and vapor. After filling, the tank is capped off. Heating before use thus results in pressurization at constant average density. If pressurization continues past point 2 in figures 30 and 31, the storage fluid becomes homogeneous, acting as a compressed liquid. In practice, the tank is heated prior to use until the storage pressure is higher than critical (point 3). Tank temperature rises slightly during this process, but is below critical at point 3.

Fluid delivery starts once supercritical pressure is reached, with pressure being maintained by adding heat to the storage space. Constant pressure operation is indicated by path 3–4′ in

FIGURE 31.—*Pressure-enthalpy diagram for thermally pressurized supercritical storage.* (AFTER COE ET AL.[20])

figures 30 and 31. Here, as long as supercritical pressures are maintained, the storage fluid remains homogeneous. This type of system is thus ideal for the zero-gravity storage of fluid mixtures.

As shown in figures 30 and 31, fluid temperatures rise during operations. When the vessel is almost empty, the storage fluid is a compressed gas. Pressure may thus be allowed to fall at the end of operation without incurring liquid dropout, as shown by path 3–4′. Operation on path 3–4′ permits heating requirements to be relaxed during the last phases of delivery. The resultant lower final density reduces the quantity of fluid which cannot be used.

One method of tank fluid heat addition is illustrated in figure 31. Here, the delivery fluid is first heated to ambient temperatures by, for example, heat exchange with cabin air. The warm, high-pressure fluid then passes through a valve which senses and regulates tank pressure. When tank pressure falls below the regulated value, the warm gas is directed through a heat exchanger in the storage space, where it provides energy for pressurization. This gas is then reheated before use. In practice, the pressure
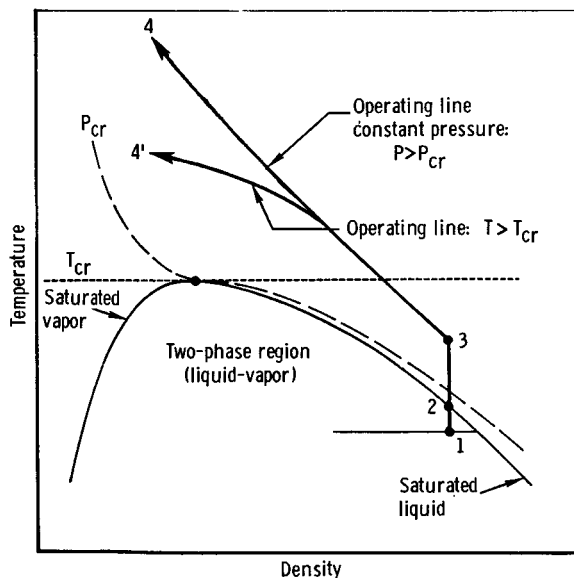

FIGURE 30.—*Temperature-density diagram for thermally pressurized supercritical storage. For $P > P_{cr}$ fluid is single phase regardless of T; for $T > T_{cr}$ fluid is single phase regardless of P.* (AFTER COE ET AL.[20])
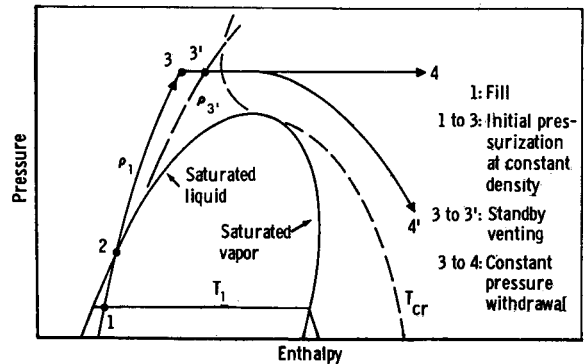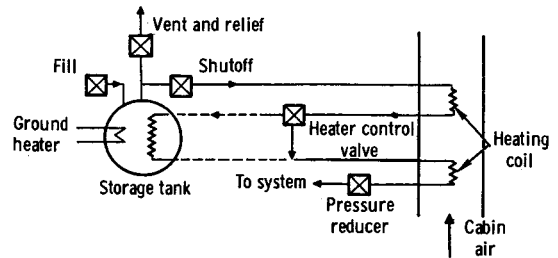
control valve usually acts as a flow modulator, directing a portion of the warm gas to the tank heat exchanger at all times.

Storage quantity determination is simplified in a supercritical storage system because the fluid is homogeneous and the mass of fluid left in the tank is directly proportional to fluid density. The latter may be determined by the use of a capacitance matrix which measures fluid dielectric constant, or by the measurement of the power required to drive a small fan inserted in the tank. Use of such a fan can also eliminate temperature stratification in the fluid and promote higher internal heat-exchanger heat-transfer coefficients.

Subcritical compressed liquid storage with positive expulsion. — A system using the technique of subcritical compressed liquid storage with positive expulsion is shown schematically in figure 32 which also illustrates system thermodynamic operation on a pressure-enthalpy diagram. Here, helium from an external high-pressure source is used to pressurize a flexible bladder within the fluid storage vessel and thereby to expel fluid from the tank. Low fluid-storage pressures are used, so that, with proper design, the fluid masses stored and expelled are liquid.

Generally, it is assumed that the fluid storage space is capped on the ground with saturated liquid in the presence of a certain percentage of vapor at atmospheric pressure, and that the storage pressure is regulated to some value lower than the fluid critical pressure. The fluid fill state is shown as point 1 on figure 32. With the tank completely filled, a slight heat leak will result in compression of the fluid at constant density until tank regulated pressure is reached (point 3). This initial compression takes place with a small fluid temperature rise, as shown on figure 32, so that the liquid is substantially subcooled.

Heat leak into the storage tank during standby can result in venting of liquid at constant pressure, with standby operation between points 3 and 4. This process is accompanied by a rise in the temperature of the fluid mass in the tank, with the result that the degree of subcooling attainable during use is diminished.

System operation during vehicle launch and climb to orbit is shown as path 4–5 on figure 32.
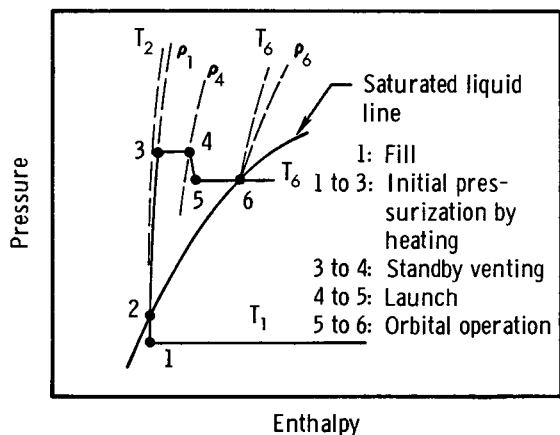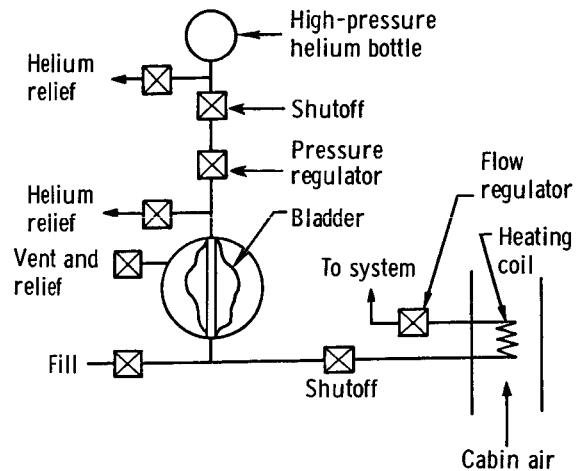

FIGURE 32.—*Liquid storage with positive expulsion.* (AFTER COE ET EL.[20])

The absolute fluid-pressure decreases due to a drop in ambient pressure, assuming a gage type of pressure control. System demand and tank heat input determines the exact path followed in this period; however, with no fluid usage, some fluid will be vented during pressure decay.

Operating conditions during flight at altitude follow path 5–6 in figure 32. Fluid is withdrawn from the tank at constant pressure, with pressure regulation being provided by the helium system.

For stable operation, it is desirable that the storage fluid be kept as a single-phase liquid during use. This requires that the tank liquid temperature be kept below the saturation temperature at the regulated pressure or, to express it differently, that the fluid vapor pressure be kept below the regulated pressure.

It is noted that single-phase storage in this system is possible only if the fluid in the tank is at a uniform temperature. If, for example, energy added through the tank walls in zero gravity is not transferred to the entire mass of fluid stored but is confined to the wall boundary layer, local film boiling can occur with subsequent instability problems. With this system, fluid stored in the tank has fairly constant temperature and enthalpy during use, giving a constant heat-sink capability. Storage quantity measurement is difficult for this system, because of the variety of bladder geometries possible during operation. The following two possible methods of storage quantity determination are:

(1) The volume of helium gas in the bladder can be determined. This could be accomplished indirectly by determining the resonant frequency of the bladder volume when small pressure pulsations are applied from a transducer. Such a method could not be used if the storage fluid contained any vapor bubbles.

(2) Radioisotope counting can be used to determine the rates of fluid used and vented, and instantaneous or periodic flow totalization. This technique would introduce fluid loading complexities.

This positive-expulsion liquid storage system is moderately complex, since it requires two fluid pressure vessels and pressure regulation systems. System reliability at present depends primarily upon the reliability of the thin pressurizing bladder used and its ability to withstand repeated flexing at cryogenic temperature levels. Vessel fabrication problems are also intensified by the use of a bladder, particularly if the bladder is to be replaceable. It is considered that bladder reliability per se is not a critical development problem.

Subcritical pressure, two-phase storage with thermal pressurization.—For vessels having two-phase storage with thermal pressurization the fluid is carried at subcritical pressure and exists as a mixture of liquid and vapor. For zero-gravity applications, special phase-separation provisions are therefore required to permit pressure stabilization during delivery and to prevent the accidental loss of liquid when venting is necessary. A number of phase-separation techniques are being considered. They include the

use of capillaries or semipermeable membranes or even rotation of the storage vessel to create an artificial gravity field. Magnetic fields may be used for liquid-vapor separation in cryogenic oxygen vessels in view of the paramagnetic properties of oxygen.

There are a number of possible vessel designs utilizing two-phase storage. In this report, emphasis is placed upon a particular type of vessel where the fluid is stored as a liquid-vapor mixture but designed for automatic vapor delivery. The fluid delivery method employed can also be used as a zero-gravity vapor vent in other types of storage system.

Figure 33 illustrates the fluid withdrawal process used on a schematic pressure-enthalpy diagram and shows one method of tank heat addition for pressurization. Preuse pressurization is similar to the process described previously. Here, tank operation is of most interest. It is most significant that the storage space fluid
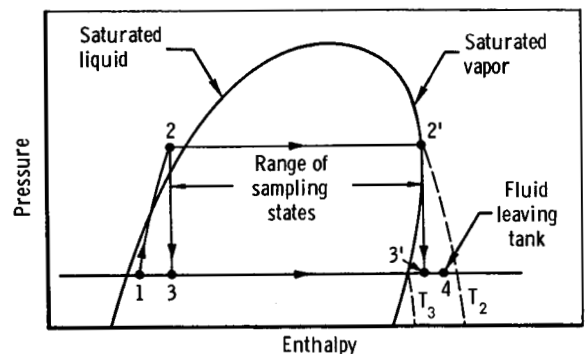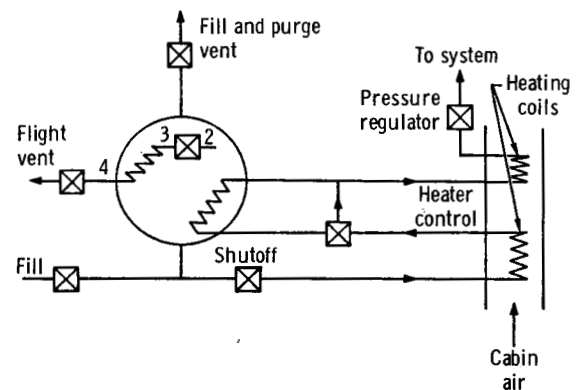

FIGURE 33.—*Two-phase storage with vapor delivery.* (AFTER COE ET AL.[20])

is a mixture of liquid and vapor. In the absence of gravity, the mass sampled at any point in the tank may consist of liquid and vapor in any proportion. Sampling states may thus range from point 2 to point 2' in figure 33. Withdrawal system operation is described below.

The fluid to be delivered is first passed through a valve and throttled to a pressure lower than tank pressure. Referring to figure 33, states before throttling may range from points 2 to 2', and after throttling from points 3 to 3'. The temperature of the fluid after throttling, however, is lower than storage temperature. This passage of the vent fluid through a heat exchanger within the storage space permits a transfer of energy to take place along paths 3 to 4 or 3' to 4 (essentially constant pressure). The fluid can thus be evaporated and superheated slightly before being discharged at a temperature close to that of the storage fluid but at a lower pressure.

Tank heat addition for pressurization is similar to that for supercritical storage. As shown in figure 33, the delivery fluid is heated to ambient temperature and used as an energy source. Fluid quantity measurement is possible by use of a matrix-type capacitance gage.

This withdrawal method provides automatic phase separation during venting and is attractive for long-duration, zero-gravity applications. It is evident that this system has traded a phase-separation problem for a zero-gravity heat-transfer problem. Careful insulation design is required to avoid venting during use when the fluid withdrawn from the tank may be completely liquid. It should be noted that this system is not suitable for the storage of a liquid mixture such as oxygen and a diluent gas because fractional distillation of the two-phase mixture will lead to fluid-composition variations during operation.

Because much of the weight tradeoff data depends on the critical aspects of overall system size, fixation to the spacecraft heat leak, geometry, standby time, etc., it is pertinent to consider hardware components and general design procedures which determine the size and weight requirements for any given spacecraft cryogenic application.

Components. — Cryogenic vessels usually consist of two concentric shells separated by an insulation space. The inner shell contains the cryogenic fluid, while the outer shell is exposed to the ambient atmosphere. The shells can be spherical or cylindrical although, when installation requirements permit, spherical vessels are preferred for minimum size and weight.

In general, a cryogenic storage vessel for space-vehicle use must also incorporate the following components which add considerable weight and obligatory volume to the overall system:

(1) A delivery line from the inner shell to beyond the outer shell.

(2) A venting system from the inner container with a pressure relief valve; the venting system can be complicated in a zero-gravity environment by the fact that only vapor should be permitted to escape through the vent line.

(3) A fill line which, in general, is different from the delivery line for ease of filling and valve installation.

(4) A quantity gage which will measure the content of the vessel under all operating conditions.

(5) An internal heat exchanger or electrical heating coil to insure positive delivery in the case of a thermally pressurized vessel.

(6) A bladder in the case of helium pressurized vessels, with the appropriate lines to the high-pressure helium source.

(7) Support members to transfer the high acceleration loads usually present at launch or reentry to the outer shell and finally to the vehicle.

The major vessel weight items, aside from the fluid load, consist of the inner and outer shells and thermal insulation. It is important to remember that for small vessels, valves and controls introduce sizable heat leaks and weight penalties. Proper selection of all vessel components is necessary, however, to insure proper operation under space flight conditions. Weight tradeoffs should, but do not always, specify these accessories.

Physical properties of the fluid component of the system affect much of the subsequent design procedures. Table 12 summarizes the properties in question.

Design procedures. — An analysis of the general design procedures gives some understanding of second-order criteria which must be applied

TABLE 12. — *Properties of Cryogenic Fluids* [AFTER COE ET AL.[20]]

Fluid	Critical pressure, psia	Critical temperature, °R	Normal (14.7 psia) boiling point, °R	Heat of vaporization (at 14.7 psia), Btu/lb	Liquid density, lb/ft³
Oxygen	736	278	162.3	91.6	71.2
Nitrogen	492	227	139.2	85.2	50.4
Neon	395	80	59.2	37.1	70.5
Helium	40.6	9.36	7.6	8.84	7.8

in the subsequent tradeoff analysis. Given a spherical shape and general type of construction, the first step in design is the estimation of vessel fill load. Here, it is noted that *mission and system specifications fix the useful fluid load* W_u in terms of a required delivery schedule w_u over the vessel operating time τ_u. This specification is expressed as

$$W_u = \int w_u d\tau_u \qquad (37)$$

The fluid fill load W_f is then the sum of the useful load, the amount of fluid lost by venting during the standby and use periods W_V and the amount of residual fluid at the end of operation W_R. Fill load is found as follows:

$$W_f = W_u + W_V + W_R \qquad (38)$$

The residual fluid load depends upon the fluid pressure and temperature at the end of use. These variables fix fluid end density, giving the following relation for W_R:

$$W_R = \frac{\pi d_i^3 \rho_R}{6(1728)} \qquad (39)$$

Fluid venting losses depend, for a given tank design, upon the duration of vessel standby and the external temperature environment of the vessel during standby. Venting losses are also possible during operation at low delivery rates. In some cases, if venting losses are arbitrarily specified, this specification fixes vessel-insulation requirements.

With the fluid fill load fixed or assumed, fluid fill density is selected. The filling operation usually ends with a small amount of vapor present

in the storage space of a cryogenic tank. Fill density ρ_f is thus slightly less than liquid density.

Storage space volume is then fixed as

$$V_f = \frac{W_f}{\rho_f} \qquad (40)$$

For a spherical vessel, pressure shell inner diameter is then given as:

$$D = 12 \left(\frac{6W_f}{\pi \rho_f} \right)^{1/3} \qquad (41)$$

With pressure-shell diameter fixed, a maximum operating pressure is assumed. Pressure-shell weight may then be calculated. A preliminary estimate of shell support configuration is then made, and the line geometries are established. Following these steps, a thermal analysis is made to permit *the selection of the insulation material and estimation of insulation thickness.*

Determination of insulation thickness requires, first, that the vessel thermal design criterion be selected. This is often, as explained above, based upon standby considerations. For thermally pressurized vessels of long use, insulation may be set by the heat required at minimum delivery rate.

A preliminary insulation thickness is first calculated using the assumption that vessel heat leaks through lines and supports are negligible. This fixes vessel geometry. Line and support heat leaks are then calculated, and a second approximation to insulation thickness is obtained.

When insulation is based upon flow requirements during operation, a thermal design analysis is made to determine if fluid vent losses during standby or use result in a useful load less than

specified. If this is the case, a new value of fill load is assumed, and the design is repeated. Tank insulation design is thus an iterative process. With insulation thickness determined, the outer shell diameter and weight may be obtained, giving total vessel weight, less valves and controls. These items can be specified independently.

The above indicate the steps generally taken in storage vessel design analyses.

Some of the major internal and environmental factors determining the design weight of the hardware are:

(1) Inner shell:
  (a) Internal fluid pressures of up to 3000 psia
  (b) Launch and reentry loads
(2) Outer shell:
  (a) Compression load from buckling pressure of atmosphere
  (b) Effect of insulation and vacuum beneath it
  (c) Dynamic loads
(3) Insulation:
  (a) Evacuation required to improve insulation and prevent liquefaction of atmospheric components within the space, with subsequent deterioration of performance
  (b) Temperature and pressure variation inside the craft
  (c) Compressive loads passing from outer to inner shell
  (d) Allowable heat-leak contribution from lines and support members
  (e) Ideal operational thermal requirements: no-loss standby for a given holdup with pressure buildup from fill pressure to maximum pressure; constant pressure operation at minimum delivery rate with no venting in thermally pressurized tanks; and no external heat input other than vessel heat leak

It is quite apparent that all of the above factors must be considered in detail before a gas-specific cryogenic weight tradeoff can be made. Minor variation in assumptions about any of these factors can alter the cryogenic storage penalty in any specific mission.

Storage vessel weight tradeoffs. — In presenting typical cryogenic-system storage weights, the following assumptions are made:

(1) Vessels are spherical.

(2) Control and accessory weights are ignored; this is an important point.

(3) Room temperature properties of materials are used to give weights which could be lowered if this factor becomes critical in a design tradeoff.

(4) Vessel pressurization is achieved by means of electrical heaters, heat exchangers, or simply by heat leakage from the outer shell, resulting in a uniform temperature throughout the mass of the fluid stored. In practice, this condition may not be realized unless suitable means are provided for mixing the fluid inside the container. Especially in a zero-gravity environment, where there are no natural convection currents, considerable temperature stratification may exist within the body of the fluid if the only mechanism for heat transfer were conduction through the fluid itself. A fan or other suitable mixing device is necessary to validate this assumption. Such a device can also be used advantageously to increase the heat-transfer rate from the heat exchanger, thus reducing its size and weight. The one disadvantage of fluid mixing is the additional heat that is dumped into the cryogenic fluid. Obviously, the solution to this problem of fluid temperature uniformity depends on the vessel size, mission duration, and type of storage considered, and can be found only for a particular application. In a general analysis of the type presented here, temperature uniformity must be assumed, although in practice, a computer program can be used to cover the non-uniformity of temperature.[12]

(5) In general, the line and support heat leaks are assumed to constitute a fixed proportion of the insulation heat leaks. This assumption greatly simplifies the calculations, since these heat leaks depend on the geometry of the lines and supports of a particular vessel and can only be calculated exactly when the detailed design of the vessel is performed. Based on previous analysis of lines and supports, it appears that the value of the ratio of line and support heat leaks selected for the numerical examples (0.20 insulation heat leaks) is conservative for large vessels, and can be achieved for small vessels by careful design of the lines and support members.

(6) Heat exchangers, instrumentation, and control valves were not considered in the analysis. They are closely related to mission requirements

and are therefore treated as separate components; as such, these items, together with the storage vessel itself, form a subsystem. An analysis of these subsystems will be presented below in the comparison of the total gas system weight penalties. The subsystem weight should be relatively constant for different gases stored. It should be remembered, however, that for small vessels up to 10 inches in diameter, the weight of such items may in certain applications be an important part of the subsystem weight.

(7) Other assumptions used in the numerical examples, such as constant ambient temperature, constant pressure operation, constant rate of flow, etc., are clearly stated wherever used. The design methods outlined here are general and are not limited in any way by the assumptions made to present typical examples.

The numerical assumptions of table 13 were followed.

One can question the use of magnesium as part of an oxygen storage system in view of the meteoroid and fire hazard. [91] The assumption of 14.7 psia as fluid end pressure may also be considered somewhat liberal.

Tradeoff curves using slightly different assumptions have been published more recently with slight reduction in penalties. [95] The penalty data for these advanced systems are discussed below.

Oxygen Systems

Weight penalties for the three types of oxygen storage vessels are presented in figures 34 to 38. The types of vessels considered have been described previously and include: thermally pressurized supercritical storage; subcritical, compressed-liquid storage with positive expulsion; and subcritical, thermally pressurized storage with vapor delivery. Useful oxygen load is taken as the primary design criterion. Venting losses have been ignored.

Supercritical pressure—thermal expulsion.— Vessel weight and volume penalties for this type of storage are presented in figures 34 and 35 as functions of useful fluid load and minimum delivery rate. As shown, delivery rate has very little effect except in the case of large vessels with low delivery rates. Inner shell weight is the major vessel weight penalty for this type of system.

Subcritical pressure—bladder expulsion.— Vessel weight penalties for this type of system are shown in figure 36 as a function of useful fluid load. Since thermal design of positive-expulsion vessels depends greatly upon flow schedule, an arbitrary value of 1 inch was chosen as the insulation thickness for all calculations. This is a tradeoff assumption which has been questioned. [12] Helium gas stored at 6000 psia and 530° R was used as the pressurization

TABLE 13.—*Sample Data Assumptions for Oxygen* [AFTER COE ET AL.[20]]

Physical parameter	Supercritical storage	Subcritical positive expulsion	Subcritical 2-phase storage
Design pressure, psia	1500	70	150
Fill factor, K_f	0.98	0.98	0.98
Fluid end pressure, psia	14.7	70	14.7
Fluid end temperature, °R	300		162
Ambient temperature, °R	620	620	620
Inner shell material	Al	Al	Al
Outer shell material	Mg	Mg	Mg
Insulation k, Btu/hrft°R	5×10^{-5}	5×10^{-5}	5×10^{-5}
Insulation density, lb/ft³	4.7	4.7	4.7
Minimum insulation thickness, in	0.50	1.0	0.50
Support and line heat leaks, $(q_S + q_{Ls})/q_T$	0.20	0.20	0.20
Shell structure weight allowance, percent	10	10	10
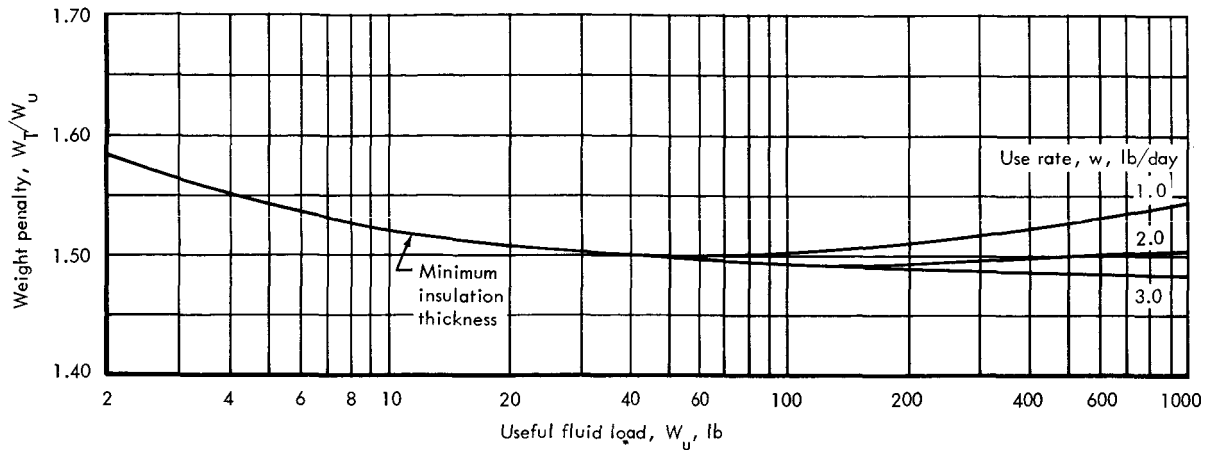
(a) *Supercritical oxygen storage. Vessel pressure: 1500 psia; ambient temperature: 620° R; spherical vessel.* (AFTER COE ET AL.[20])

FIGURE 34.—*Vessel weight penalty.*
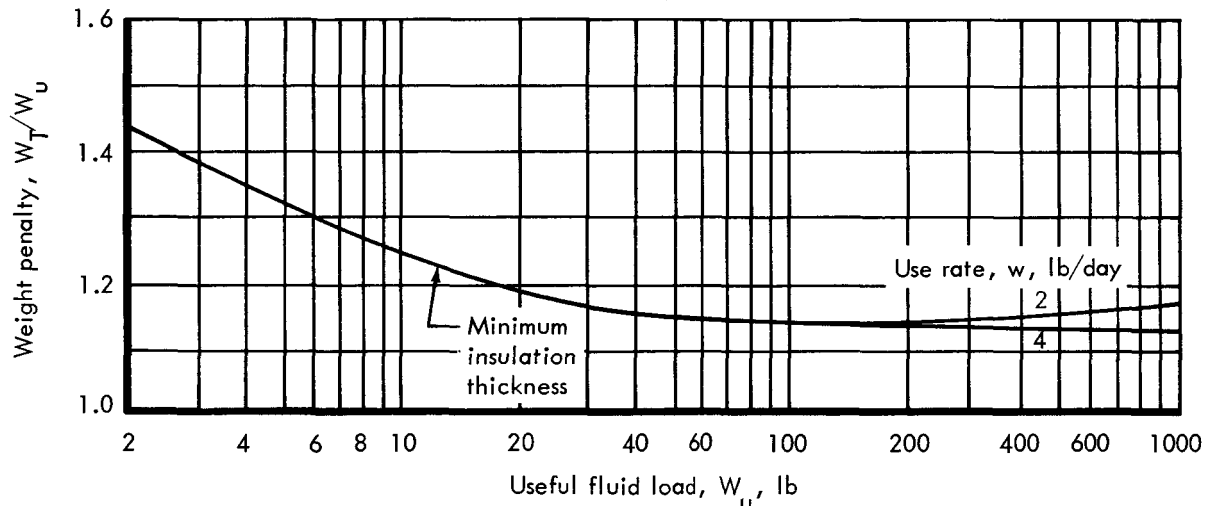
(b) *Advanced supercritical oxygen storage. Note that for flow higher than 4 lb/day, the vessel weight is determined by the minimum insulation thickness.* (AFTER ROUSSEAU ET AL.[95])

FIGURE 34.—*Vessel weight penalty*—Concluded.

fluid; helium vessel weight penalties were obtained from figure 29.

Subcritical pressure two-phase storage. — Weight and volume penalties for this type of vessel are shown on figures 37 and 38 as functions of useful fluid load and minimum delivery rate. Here, the system was assumed to deliver saturated vapor at storage pressure for the purposes of thermal design. This is a tradeoff assumption which has been questioned.[36]

On the whole, subcritical storage appears to present a smaller weight penalty than corresponding supercritical systems. The volume penalties are similar.
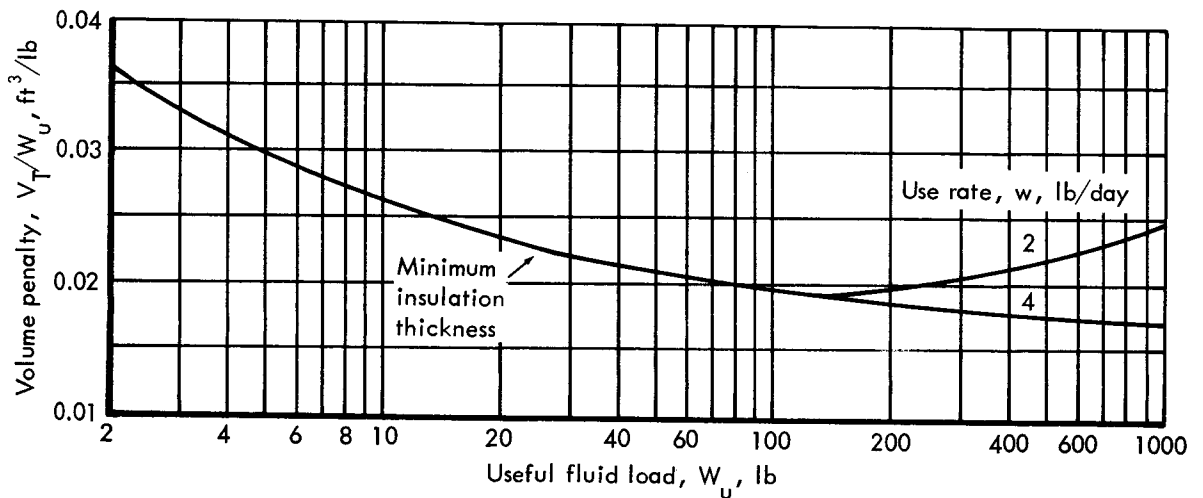
Nitrogen Systems

Data for two types of nitrogen storage vessels are presented in figures 37 to 41. Vessel
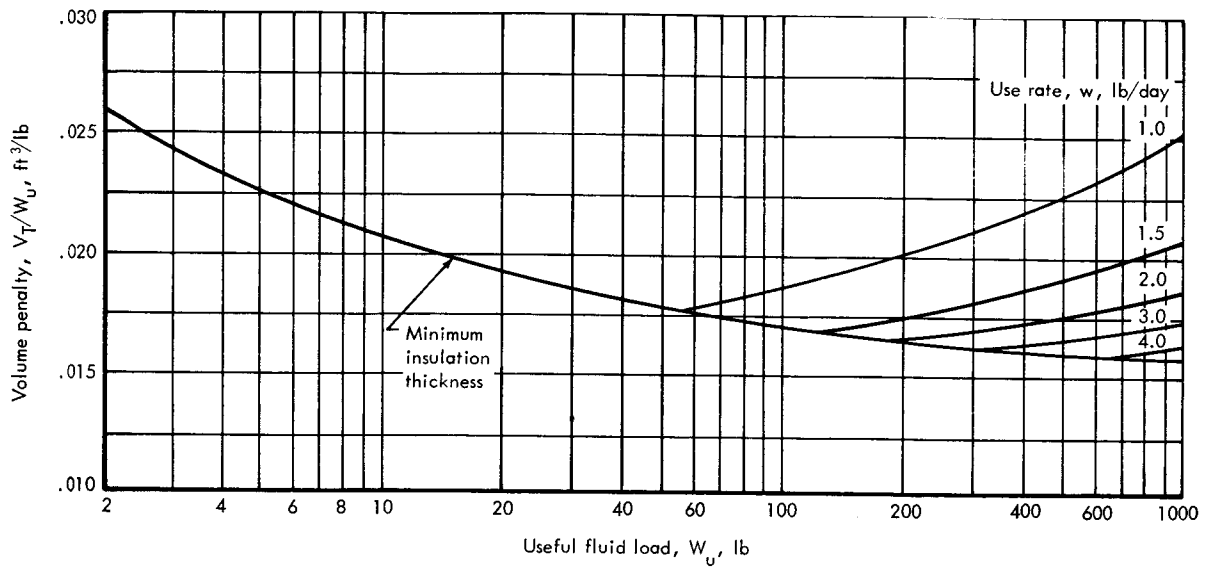
(a) *Supercritical oxygen storage. Vessel pressure: 1500 psia; ambient temperature: 620° R; spherical vessel.* (AFTER COE ET AL.)
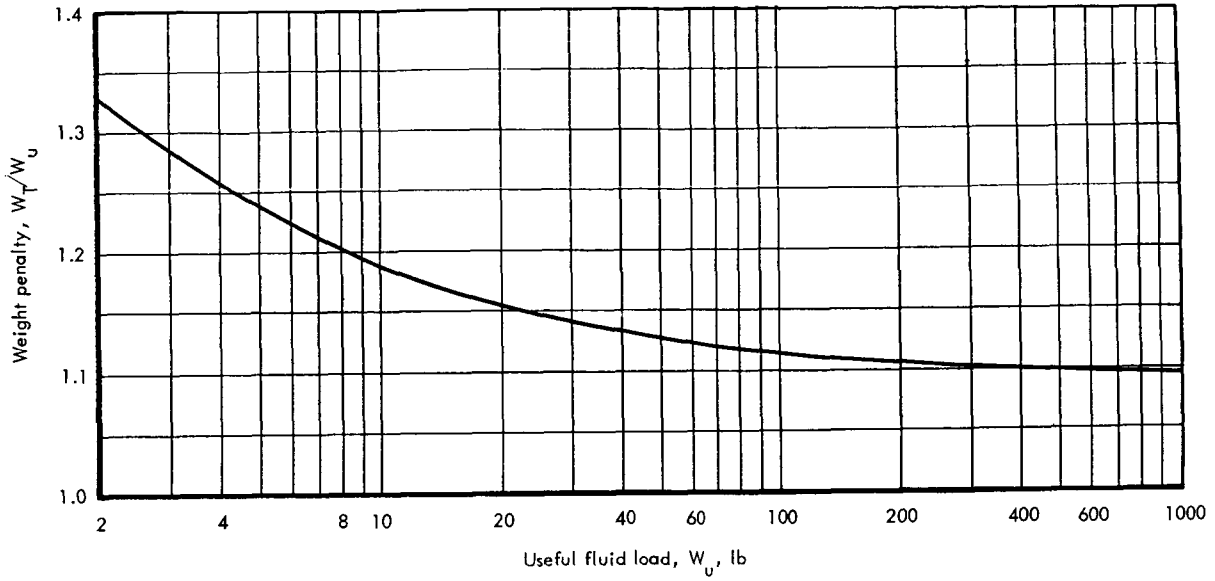
FIGURE 35.—*Vessel volume penalty.*

(b) *Advanced supercritical oxygen storage. Note that for flow rate higher than 4 lb/day, the vessel volume penalty is determined by the minimum insulation thickness.* (AFTER ROUSSEAU ET AL.[95])
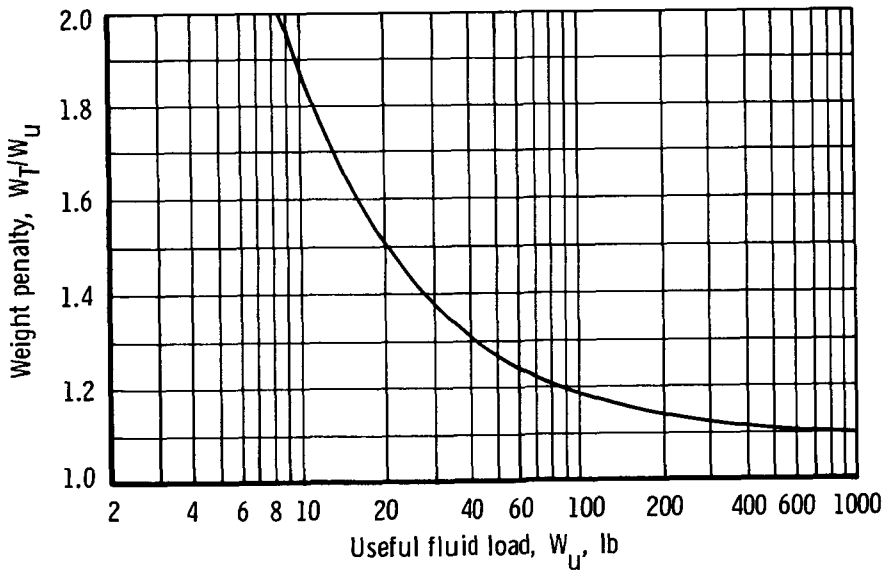
FIGURE 35.—*Vessel volume penalty*—Concluded.

(a) *Subcritical oxygen storage with liquid delivery. Storage pressure: 70 psia; insulation thickness: 1 inch; spherical vessel.* (AFTER COE ET AL.[20])

FIGURE 36.—*Vessel weight penalty.*

(b) *Advanced subcritical oxygen storage.* (AFTER ROUSSEAU ET AL.[95])

FIGURE 36.—*Vessel weight penalty*—Concluded.
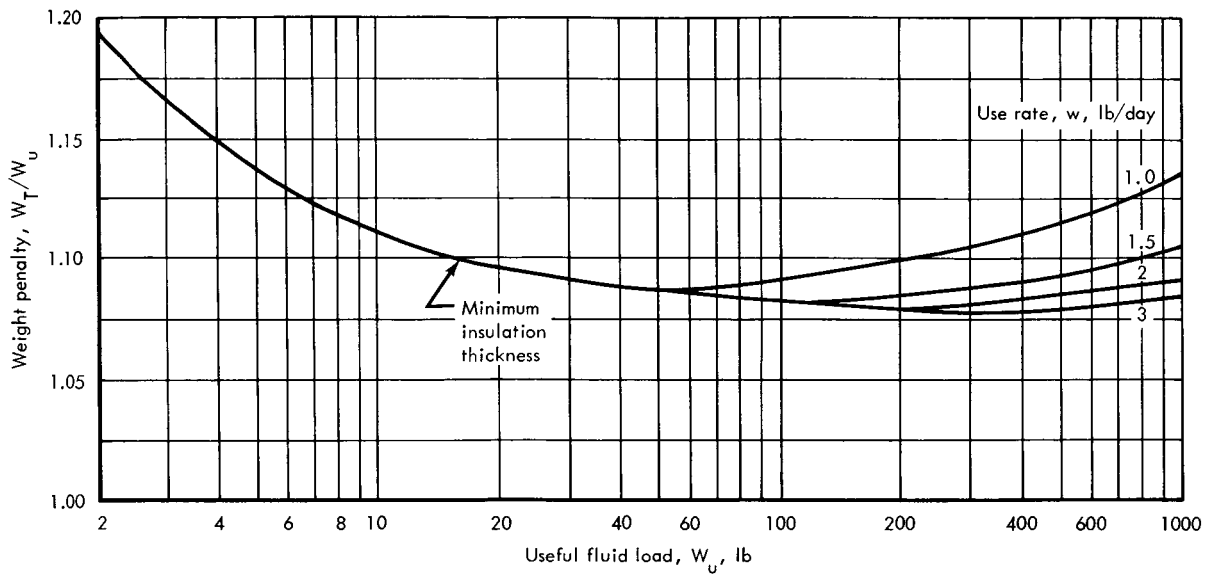
FIGURE 37.—*Vessel weight penalty for subcritical oxygen storage with vapor delivery.   Storage pressure:
150 psia; ambient temperature: 620° R; spherical vessel.   (AFTER COE ET AL.[20])*
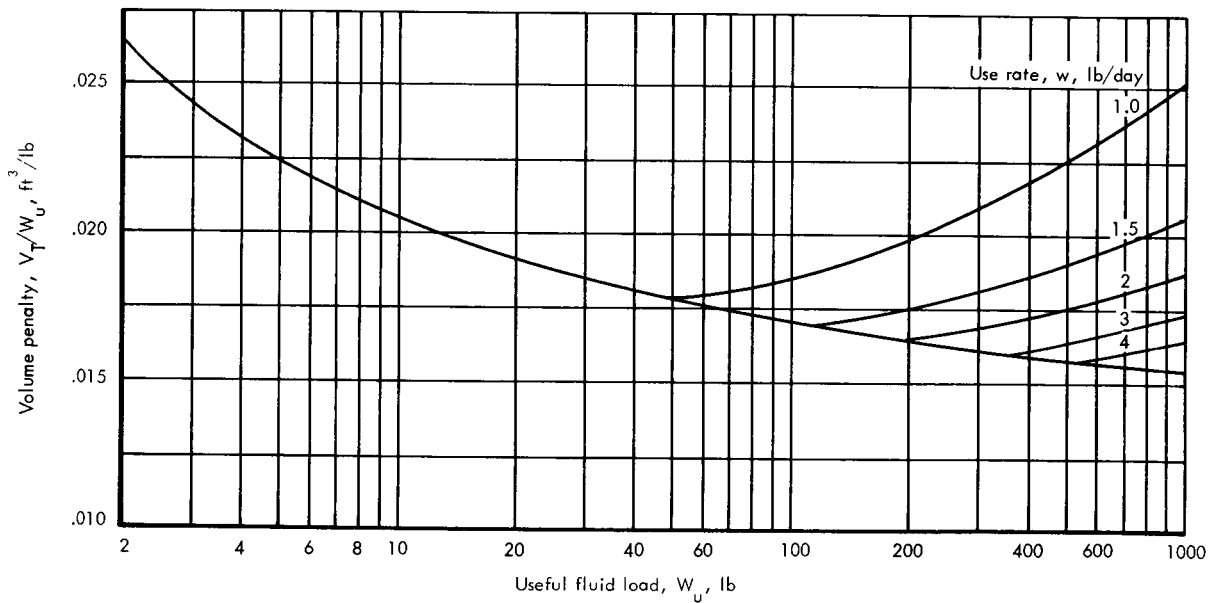

FIGURE 38.—*Vessel volume penalty for subcritical oxygen storage with vapor delivery.   Vessel pressure:
150 psia; ambient temperature: 620° R; spherical vessel.   (AFTER COE ET AL.[20])*

types considered are supercritical storage and two-phase storage with vapor delivery. Assumptions used were generally those given previously for oxygen, except for those recorded in table 14.

TABLE 14.—*Sample Data Assumptions for Nitrogen* [AFTER COE ET AL.[20]]

| Physical parameter	Supercritical storage	2-phase storage
Design pressure, psia..........	1000	150
Fluid end temperature, °R....	300	140
Inner shell material............	Ti	Ti or Al
Outer shell material............	Mg	Mg

Supercritical pressure. — Vessel weight and volume penalties are shown in figures 39 and 40 as functions of useful fluid load and minimum delivery rate. The vessel weights are somewhat lower than shown for oxygen in figure 34. This results from the permissible use of titanium as the inner shell material for nitrogen storage.

A change in the shape of a vessel from spherical to any other form increases the weight penalty. Weight and volume of cylindrical, supercritical storage vessels for nitrogen were also calculated based on the same design conditions. The vessel length-to-diameter ratio was taken as 2.0. The results of these computations are shown in figures 41 and 42. These plots show a much heavier design, which is the penalty paid for shape.

Subcritical pressure, two-phase storage, vapor delivery. Weight penalties for this type of nitrogen storage are shown in figure 43. Volume penalties are essentially the same as those given in figure 40. Here, it should be noted that aluminum is used as the inner shell material where minimum gage thickness is desired, giving a broken weight-penalty curve.

Air mixture. — It is possible to store liquid air for spacecraft use. Supercritical air-storage weight and volume penalties are shown plotted in figures 44 and 45. The calculations were performed for the same conditions as for the nitrogen vessel discussed above. It should be remembered that if uniform gas is desired, the two-phase storage is impossible for oxygen-nitrogen mixtures with the throttling system discussed previously. The bladder and other two-phase systems could be adapted for subcritical two-phase systems.[12]
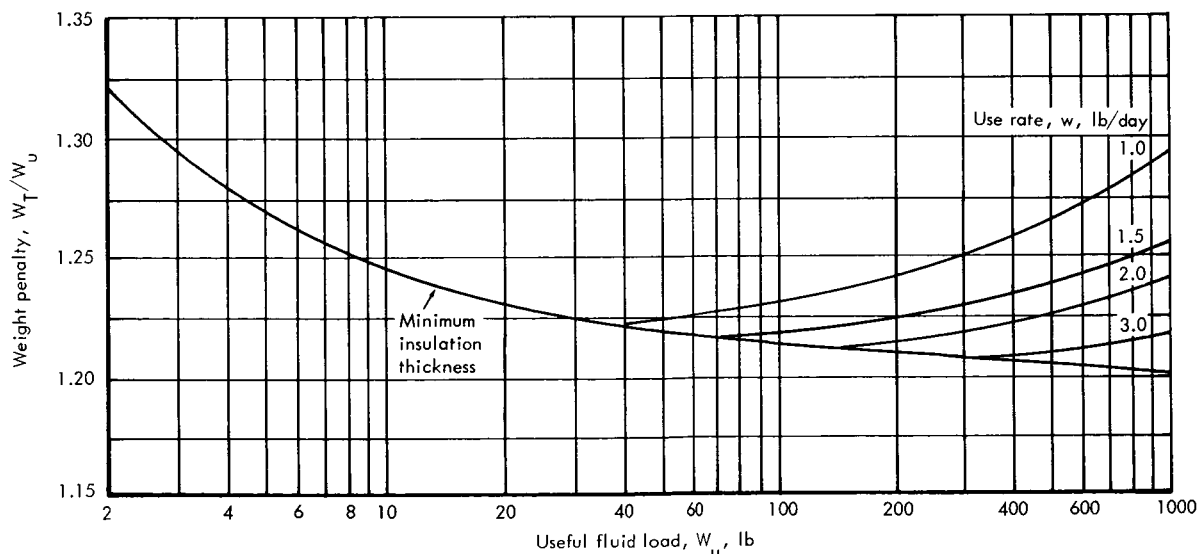
(a) *Supercritical nitrogen storage. Vessel pressure: 1000 psia; ambient temperature: 620° R; spherical vessel.* (AFTER COE ET AL.[20])

FIGURE 39.—*Vessel weight penalty.*
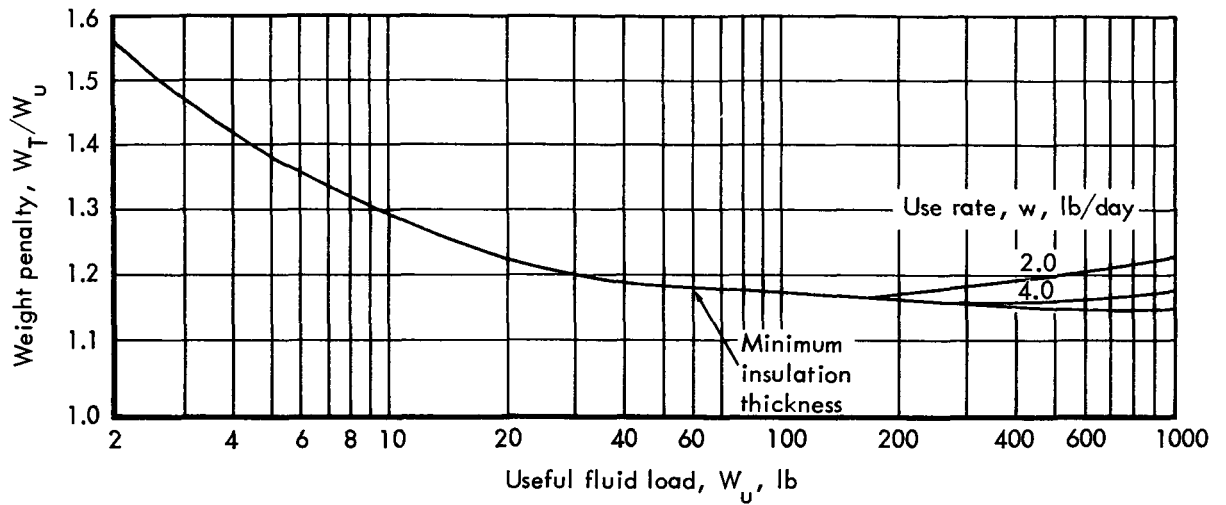
(b) *Advanced supercritical nitrogen storage.* (AFTER ROUSSEAU ET AL.[95])

FIGURE 39.—*Vessel weight penalty*—Concluded.

(a) *Supercritical nitrogen storage. Vessel pressure: 1000 psia; ambient temperature: 620° R; spherical vessel.*

FIGURE 40.—*Vessel volume penalty.* (AFTER COE ET AL.[20])

(b) *Advanced supercritical nitrogen storage.* (AFTER ROUSSEAU ET AL.[95])

FIGURE 40.—*Vessel volume penalty*—Concluded.

FIGURE 41.—*Cylindrical vessel weight penalty for supercritical nitrogen storage. Vessel pressure: 1000 psia; ambient temperature: 620° R; spherical vessel.* (AFTER COE ET AL.[20])

FIGURE 42.—*Volume penalty for supercritical nitrogen storage. Vessel pressure: 1000 psia; ambient temperature: 620° R; spherical vessel.* (**AFTER COE ET AL.**[20])

(a) *Subcritical nitrogen storage with vapor delivery. Storage pressure: 150 psia; ambient temperature: 620° R; spherical vessel.* (**AFTER COE ET AL.**[20])

FIGURE 43.—*Vessel weight penalty.*

(b) *Advanced subcritical nitrogen storage.* (AFTER
ROUSSEAU ET AL.[95])

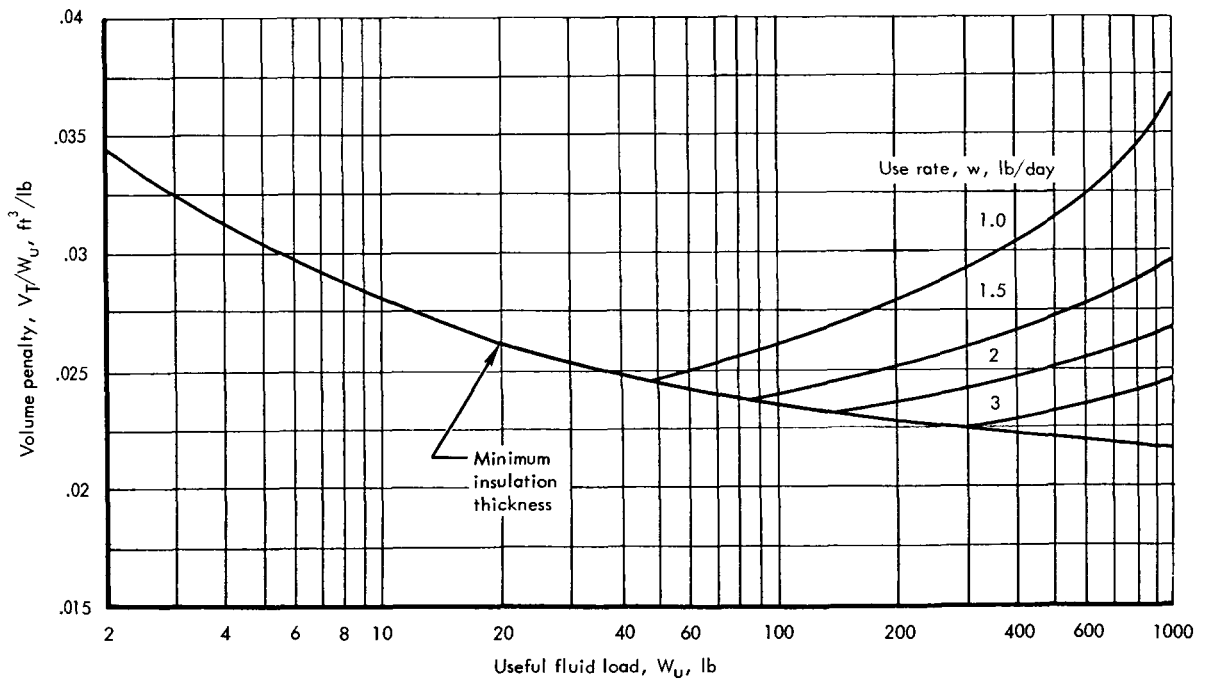FIGURE 43.—*Vessel weight penalty*—Concluded.

FIGURE 44.—*Vessel weight penalty for supercritical air storage. Vessel pressure: 1000 psia; ambient
temperature: 620° R; spherical vessel.* (AFTER COE ET. AL[20])
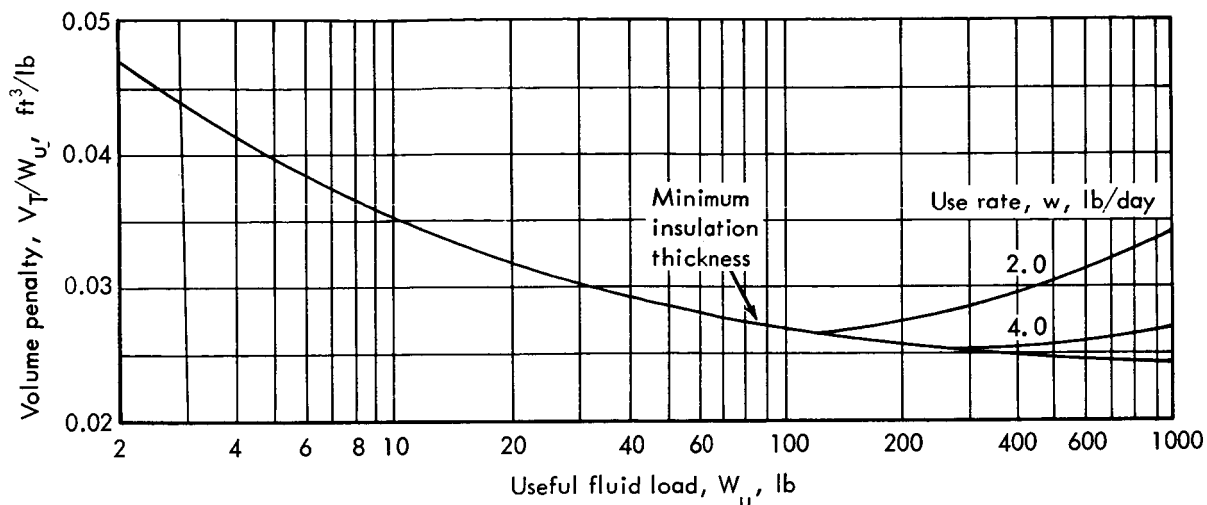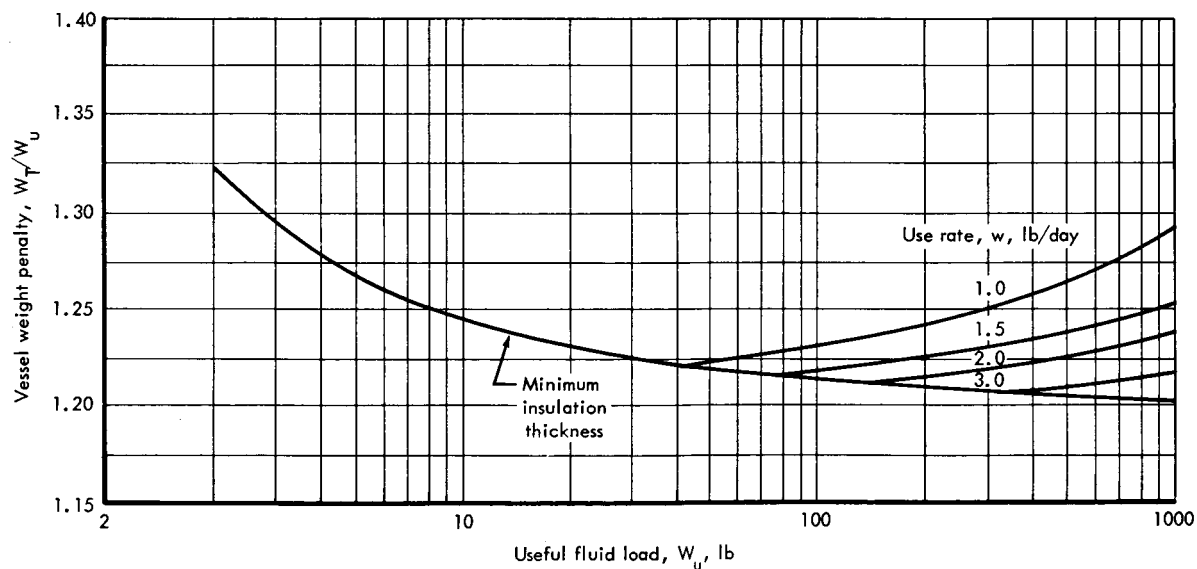
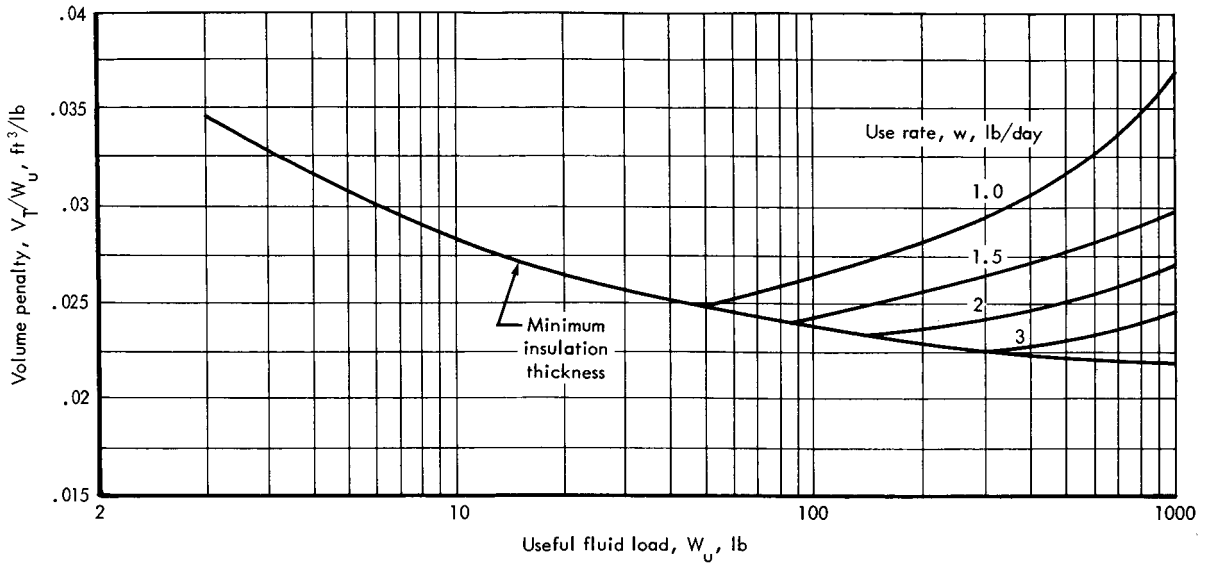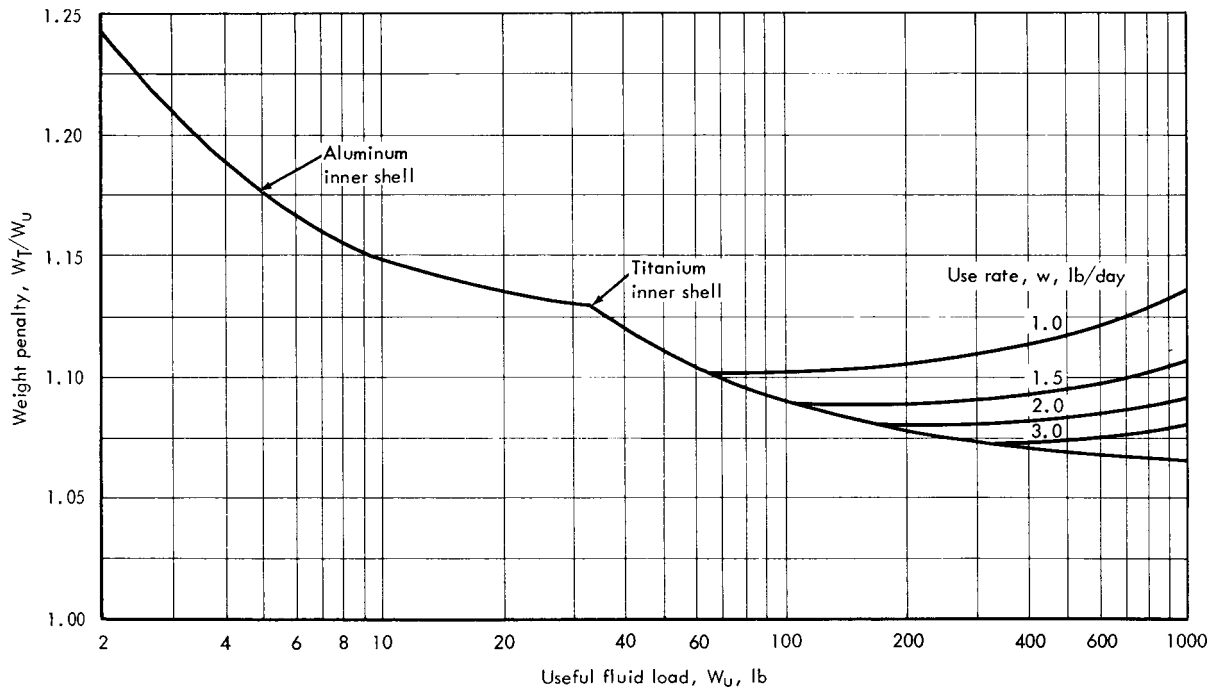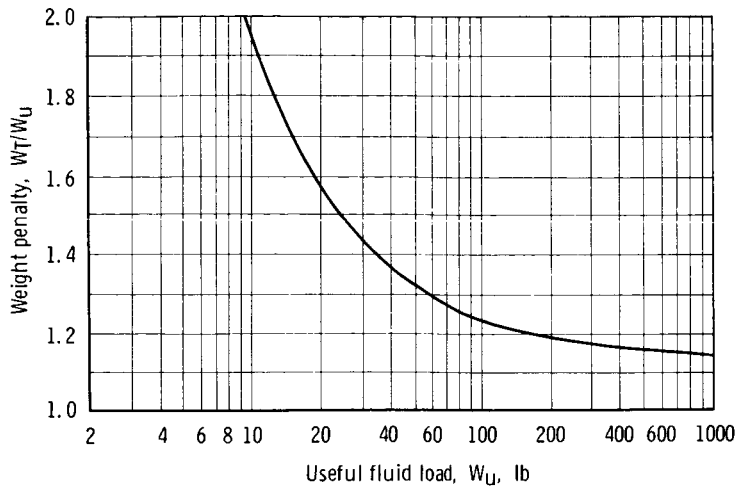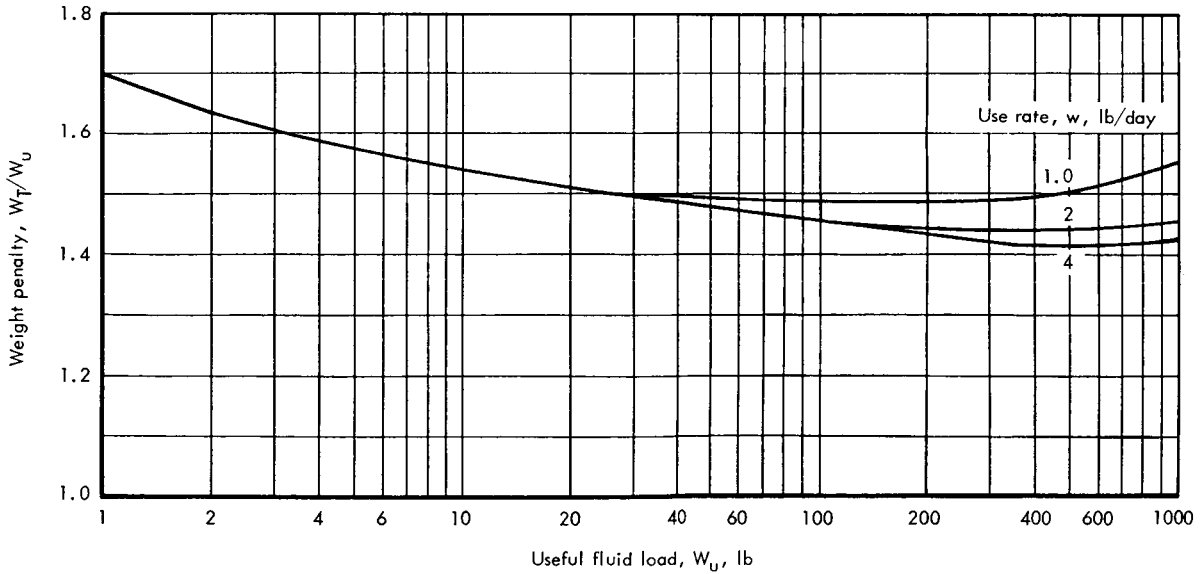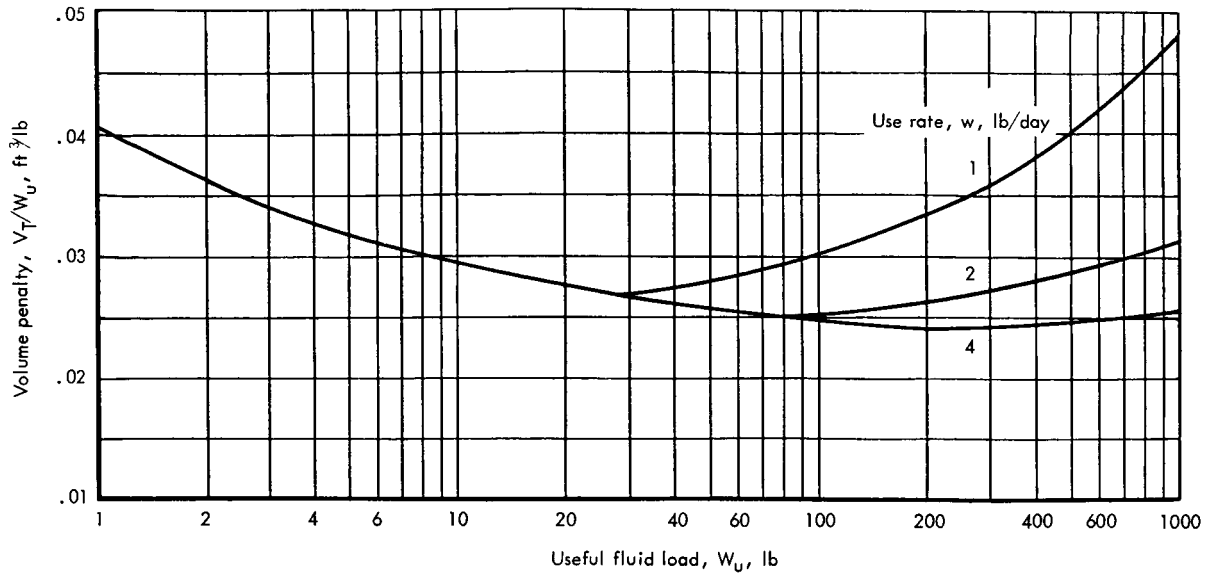FIGURE 45.—*Vessel volume penalty for supercritical air storage. Vessel pressure: 1000 psia; ambient temperature: 620° R; spherical vessel.* (AFTER COE ET AL.[20])

Sensitivity of O_2 and N_2 Cryogenic Storage Penalties to Design Assumptions

Sometime after the cryogenic tradeoffs discussed previously were published, advanced systems were analyzed using different basic assumptions. The pressures of the systems and materials were the major alterations. Table 15 represents these new design parameters. Figures 34(b) and 35(b) represent the weight and volume penalties of the supercritical and subcritical systems for oxygen. Figures 39(b), 40(b), and 43(b) represent the weight and volume penalties for supercritical and subcritical storage of nitrogen. It is of interest to compare these alternate designs with the corresponding figures 34(a), 35(a), 36(a), 39(a), 40(a) and 43(a), and see the effects of these changes in design on the relation between useful weight and weight penalties. This advanced series probably represents the current state-of-the-art for these systems.

Sensitivity of O_2 and N_2 storage penalties to mission-specific variables. — As was discussed above, mission-specific variables have a significant effect on tankage tradeoffs. Several examples of these effects will be presented.

In a study by Hamilton Standard of oxygen tankage for a large, manned, orbiting space station, the effect of standby time on tankage system dry weight was analyzed for several usable fluid weights in supercritical and subcritical storage with no venting.[36] The tanks had a spherical inner shell of Inconel and an outer shell of aluminum. The glass paper-aluminum insulation had a conductivity of 3×10^{-5} Btu/hr-ft-°R. Figure 46 presents the results. The systems can tolerate a 48-hour standby without weight penalty. Initially, subcritical storage offers weight advantages over its supercritical counterpart; however, this advantage diminishes in cases of long standby and small useful fluid payloads. This is due to the fact that the quantity of heat required to pressurize the fluid from 1 atmosphere to an operating pressure at 100 psia is only about 30 percent of that required for supercritical storage at 875 psia. This effect is especially noticeable at small payloads where insulation presents a larger part of the total weight of the system. For long systems having long standby times, venting can be used in both supercritical and subcritical systems. In such cases, a tradeoff between vent fluid and insulation must be made. It should be stated that anticipation of such long standby times for oxygen systems is probably unrealistic, but may be realistic for inert gas systems.[24]

TABLE 15.—*Comparison of Vessel Designs* [AFTER ROUSSEAU ET AL.[95]]

Parameter	Oxygen	Nitrogen
Supercritical vessel design (advanced concept)		
Design pressure, psia	800	725
Maximum pressure, psia	875	850
Inner shell material	René 41	René 41
Minimum insulation thickness, in	0.75	0.75
Insulation density, lb/ft³	5.0	5.0
Outer shell material	Al6061–T6	Al6061–T6
Liquid fraction at fill	0.95	0.95
Vessel shape	Spherical	Spherical
Subcritical vessel design (advanced concept)		
Design pressure, psia	100	100
Maximum pressure, psia	120	120
Inner shell material	Al	Al
Insulation thickness, in	1.0	1.0
Insulation density, lb/ft³	5.0	5.0
Outer shell material	Al6061–T6	Al6061–T6
Liquid fraction at fill	0.95	0.95
Accessory weight (gas bottle). lb	7.0	7.0
Pressurizing gas	Helium	Helium
Liquid residue, percent	3	3
Vessel shape	Spherical	Spherical
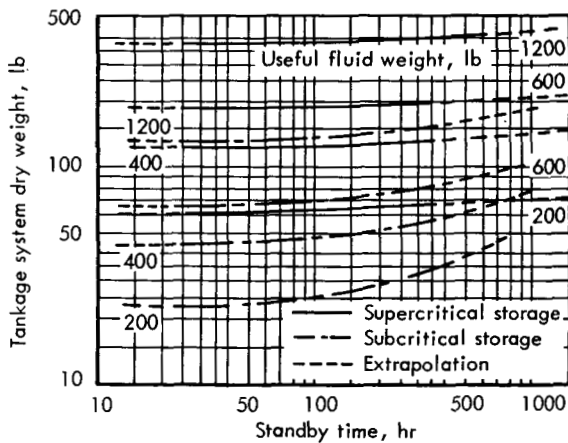
FIGURE 46.—*Weight variation of cryogenic oxygen storage system with standby time. Use rate per tank=8.5 lb/day.* (AFTER HAMILTON-STANDARD.[36])

The sensitivity of total weight of a nitrogen system on rate of usage and usable fluid weight can be seen in figure 47. The same assumptions as those for figure 40 hold true, except that the inner tank was of Inconel instead of titanium. In the case of nitrogen, the use rate is quite low (leakage and repressurization) and becomes the determining factor in the total system weight penalty.

In the case of weight tradeoffs for cabin repressurization systems, the mission duration, repressurization rate, and cabin size are critical determinants for various cryogenic and gas storage systems. The Hamilton Standard Corp. has studied these repressurization system tradeoffs for two given cabin sizes, 7000 ft³ and 70 000 ft³, at 7 psia in very large stations where repressurization penalties become severe unless lock
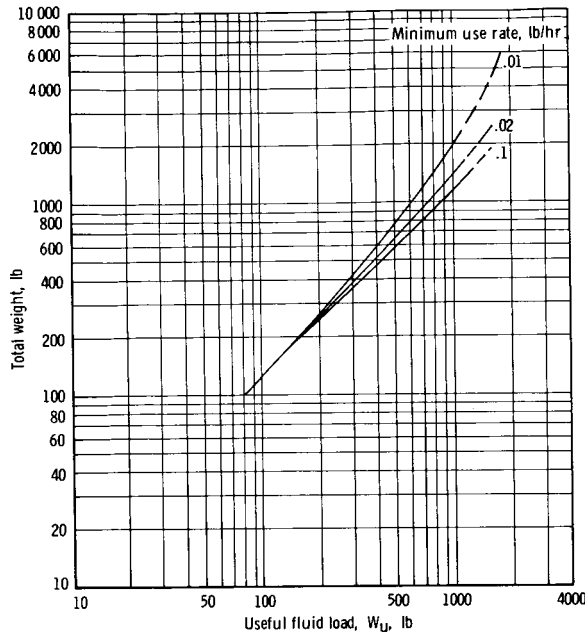
(a) *Subcritical nitrogen storage.*

FIGURE 47.—*Total system weight versus fluid.*
(AFTER HAMILTON-STANDARD.[36])
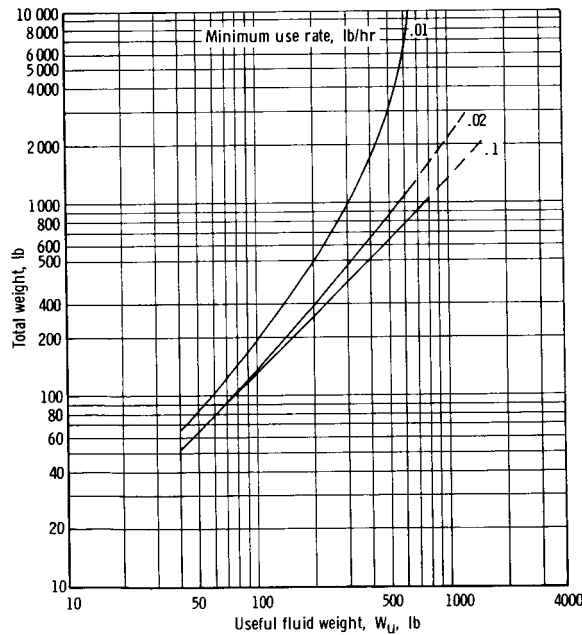
(b) *Supercritical nitrogen storage.*

FIGURE 47.—*Total system weight versus fluid*—
Concluded.

systems are used. Three general methods were compared—high-pressure gas storage, super-critical cryogenic with thermal pressurization, and subcritical cryogenic with thermal pressurization. The study also compared storage of separate gases and mixed gases. The characteristics of the tanks were the same as above with fluid delivery at 30 psia. Figures 48(a) and 48(b) represent the results for the 7000 ft³ cabin, and figures 49(a) and 49(b) the results for the 70 000 ft³ cabin. It can be concluded from these figures that for small fluid payloads and long standby times, gaseous storage looks attractive. The
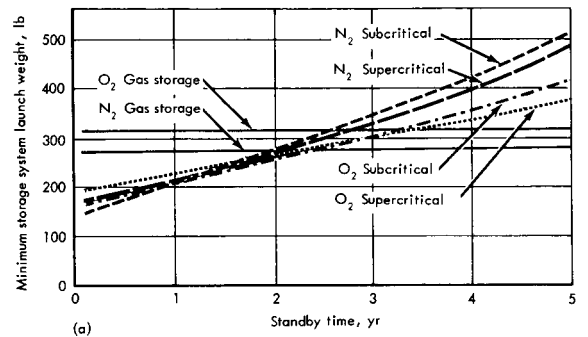
(a) *Minimum storage weight.*

FIGURE 48.—*Weight of repressurization storage system versus standby time. Cabin volume: 7000 ft ³; total pressure: 7.0 psia; useful oxygen required: 138 lb; useful nitrogen required: 120 lb; spherical tankage.* (AFTER HAMILTON STANDARD.[36])
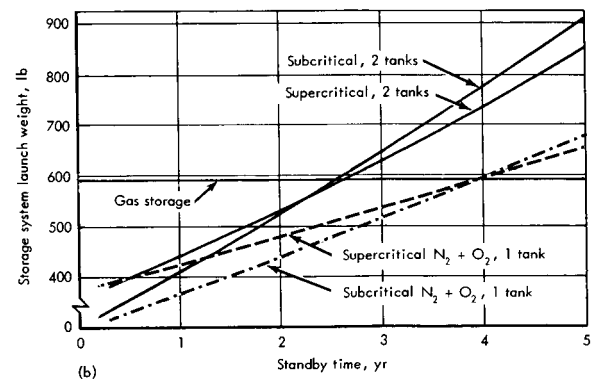
(b) *Total storage weight.*

FIGURE 48.—*Weight of repressurization storage system versus standby time*—Concluded.

gaseous-cryogenic crossover point in figure 48(b) appears at 2.6 years. For larger systems, the crossover point is shifted to longer standby times (fig. 49(b)).

Because the subcritical system has a lower average specific heat input requiring more insulation, the optimum weight of the supercritical systems is less than the subcritical system for long periods of standby (fig. 48(b)). The average specific heat input can be defined as the average heat input required to maintain tank pressure and vaporize the fluid per pound of fluid withdrawn between the 100 percent full condition and

that percent left after standby. For short standby and large fluid payloads, the subcritical storage methods have weight advantage over supercritical (figs. 48(b) and 49(b)).

For repressurization, a considerable weight saving can be attained by mixing the O_2 and N_2 and storing both fluids in the same tank (figs. 48(b) and 49(b)). In general, system weight increases with the increase in the number of tanks needed to store a given payload. Care must be taken in programing the withdrawal to avoid compositional changes in the final gas output.

Helium Systems

Experience with small flight-rated cryogenic helium systems is limited. Because the rate of use of helium will be so low and the heat-leak factor so great in determination of weight trade-offs in helium systems, it appears appropriate to review in detail some of the second-order factors involved in the design of small cryogenic helium tanks. It should be kept in mind that improved technology may alter some of the numerical factors used.

Figure 50 reviews the state of the art in low heat-leak systems. The curve represents the minimal heat leak which can be expected in systems. The modified Gemini oxygen system is of AiResearch design. The helium and nitrogen systems are estimates made by the Cryogenics Group of the Boeing Co. The nitrogen and helium tanks are evaluated for 5-psia and 7-psia cabin-
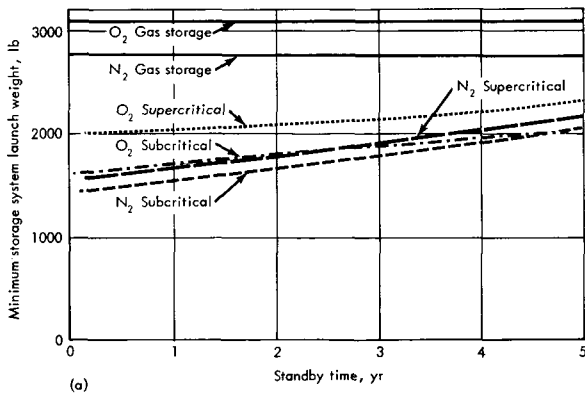
(a) *Minimum storage weight.*

FIGURE 49.—*Weight of repressurization storage system versus standby time. Cabin volume: 70 000 ft³; total pressure 7.0 psia; useful oxygen required: 1380 lb; useful nitrogen required: 1202 lb; spherical tankage.* (AFTER HAMILTON STANDARD.[36])
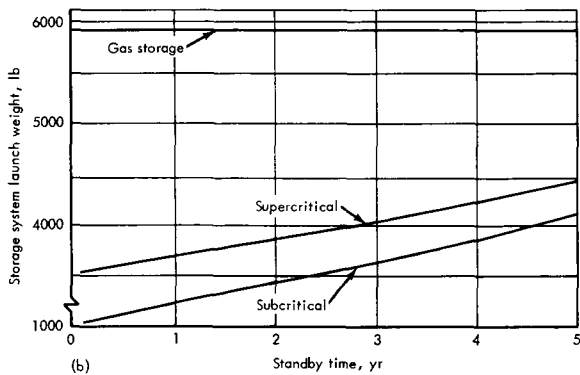
(b) *Total storage system weight.*

FIGURE 49.—*Weight of repressurization storage system versus standby time*—Concluded.
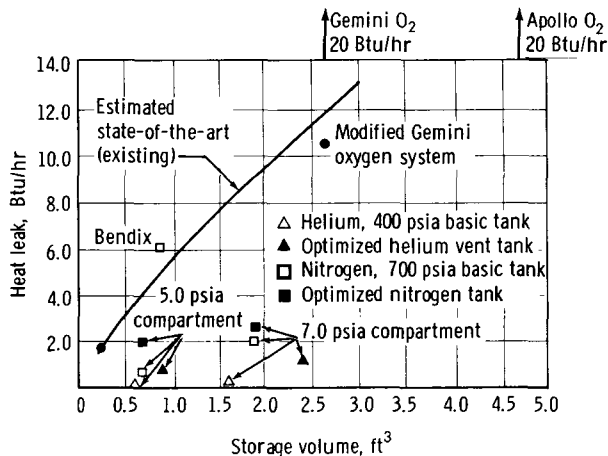
FIGURE 50.—*State-of-the-art tank heat leak.* (AFTER BOEING.[12])

compartment pressures. The helium tanks represented are a basic 400-psia system and an optimized venting tank. This is the minimum pressure at which the helium tank can operate and yet provide, by allowing pressure delay, the flow rates required for compartment repressurization. The nitrogen tanks are represented by the basic 700-psia tanks, as well as an optimized tank of nonventing type operating at 2000 psia. The "basic" tank is at the minimum pressure for supercritical storage. It can be seen that these small tank systems for helium and nitrogen are certainly pushing the state of the art. The small volumes require relatively large percentage penalties for the fill tubes and secondary hardware weight as well as for excessive insulation weight to cover large obligatory heat leaks through fill lines and support structures. Improvement in secondary hardware could certainly effect gross changes in these figures.

Figure 51 represents the effect of pressure on the maximum allowable heat leak and suggests that supercritical operation is required. As the pressure is increased, a higher design heat leak can be tolerated. The nitrogen tanks can take a much higher heat leak than can helium tanks of corresponding volume at any given pressure. The smaller the tank, the smaller the maximum heat leak. The 1.9 ft³ tank, for instance, could probably serve the Apollo mission and sustain a 1.8 Btu/hr heat leak at 700-psia pressure. The basic 400-psia cryogenic helium tank of this same size tolerates a maximum 0.25 Btu/hr leak rate but could tolerate 1 Btu/hr heat leak at 2000 psia. At

first glance, one would think that the heat leak could be avoided by operating at a higher tank pressure or by venting fluid.

Because of the complex nature of the weight tradeoff, however, the total system penalty does not get smaller with increasing pressure. Figure 52(a) represents the role of insulation thickness on the weight tradeoff presented by the Cryogenics Group at Boeing. These leaks were determined by utilizing the optimum secondary support structures for heat-leak resistance available at Boeing.

Total system weights for helium in a two-man orbiting laboratory system is presented for different insulation thickness (spacing between shells) in a 5-psia compartment. Both unvented storage at 2000 psia and vented storage at 1000, 1500, and 2000 psia are plotted for spacings of
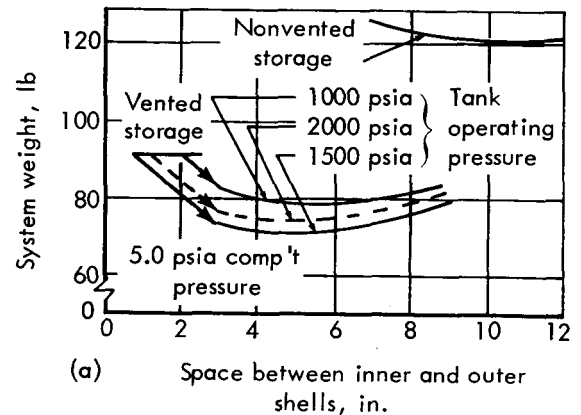
(a)   Space between inner and outer shells, in.
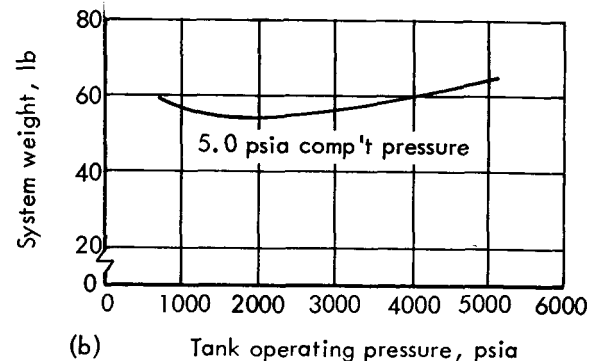
(b)   Tank operating pressure, psia

FIGURE 52.—*Helium storage for 30 days.* (*a*) *Supercritical storage.* (*b*) *Low-temperature gaseous storage.* (AFTER BOEING.[12])

FIGURE 51.—*Maximum allowable heat leak for supercritical nonvented tank.* (AFTER BOEING.[12])

2 to 12 inches between the shells. The system weight includes usable fluid, vent fluid, fill fluid, tank, and the weight equivalent of electric power required for expulsion of the liquid helium. It can be seen that the nonvented storage presents a greater systems weight penalty than does the vented system. There appears to be an optimum range of 3 to 4 inches of inner-to-outer wall spacing for vented tanks and 10-inch spacing for minimum system weight for nonvent design. Increasing the pressure of vented storage systems has little effect on overall system weight. There appears to be a weight minimum at 1500 psia. Calculations for 3000 and 4000 psia indicate progressively greater penalties along a family of curves paralleling the 2000-psia curve.

In figure 53 the effect of compartment pressure on cryogenic storage can be seen to be interacting with insulation thickness to alter total system of nitrogen storage. The lower pressure of 5 psia appears more favorable than 7 psia from this point of view. It should be remembered, however, that the usable quantity of nitrogen is much less

for the 5-psia compartment, and this is the major factor in the weight difference.

The design uncertainties brought about by the acute sensitivity of the small helium systems to heat leak cannot be overemphasized. Figure 54(a) represents the sensitivity of system weight penalty of cryogenic helium to errors in heat-leak calculations. The same components of system weight are included as those in figure 52(a). The system was designed for a 30-day mission at 7.0-psia cabin pressure and is used for the optimized helium tank of figure 50 at 1000 psia. It

(a) Δ Heat leak, Btu/hr

(b) Δ Heat leak, Btu/hr
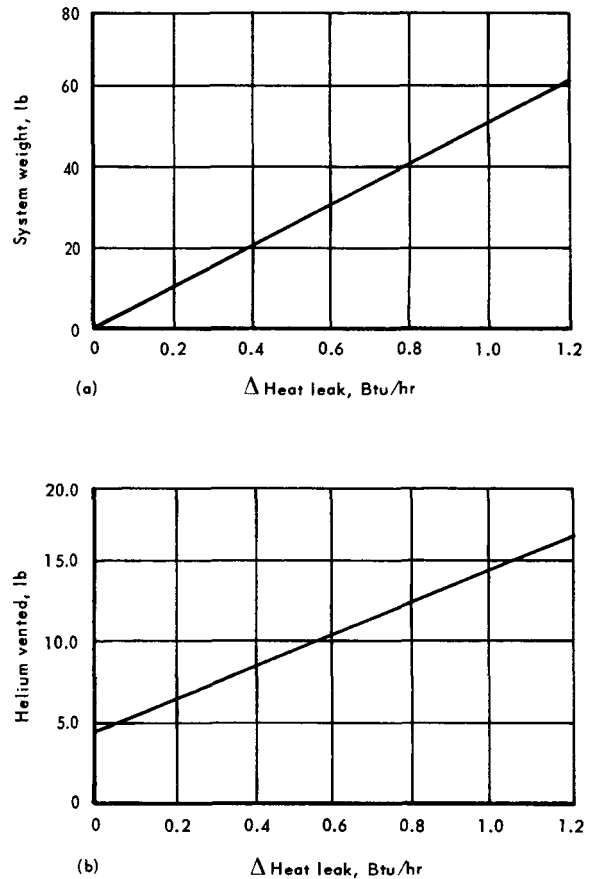
FIGURE 54.—*Helium tank sensitivity to heat leak for 30 days at 7.0 psia. Basic system (optimized) was used: 1000 psia vent tank; 11.8 pounds of usable helium with 4.4 pounds of vent helium; 1.15 Btu/hr heat leak; 2.42 ft³ storage volume; 110-pound system weight. (a) System weight if heat-leak design margin (from 1.15 Btu/hr) is selected. (b) Tank vent fluid if tank heat leak exceeds design value of 1.15 Btu/hr. (AFTER BOEING.[12])*

Space between inner and outer shells, in.

FIGURE 53.—*Nitrogen supercritical storage for 30 days. (AFTER BOEING.[12])*

has an 11.8-pound usable helium weight in a 110-pound system with a 2.42 ft³ storage volume. To account for a predicted heat leak of 1.15 Btu/hr, 4.4 pounds of vent helium is expected. Figure 54(a) shows that an error of only 1 Btu/hr in heat-leak calculation of the design can increase the total system weight by 50 pounds or nearly 50 percent. Figure 54(b) indicates that an actual heat leak of only 1.0 Btu/hr above design value brings about an increase in the vent helium from a predicted 4.4 pounds to 14.6 pounds, thus reducing the usable fluid quantity.

Another approach has been studied by Boeing. If the vehicle has a hydrogen tank for a fuel-cell reactant supply or for a propulsion engine, consideration should be given to mounting the helium tank within the hydrogen tank. This method would result in low-temperature gaseous storage of helium with a fluid storage density comparable to that of liquid helium. The advantage is that the helium tank does not require insulation and therefore the tank design is simply a high-pressure gaseous storage vessel. A thermodynamic analysis must be made for each mission to establish the minimum expulsion rate, final density, and optimum storage pressure. For the same usable fluid quantities and mission as the supercritical tanks shown in figure 52(a), figure 52(b) shows the resulting system weight versus helium storage pressure. This penalty also includes the penalty to the hydrogen tank for installation of the helium tank. The hydrogen tank for this study was a 30-cubic-foot supercritical tank supplying a fuel cell during the 30-day mission. The energy needed to expel the helium is transferred into the helium from the hydrogen; therefore, no heaters or blowers are required in the helium tank. In the

structural design of the helium tank the failure mode with the hydrogen-tank pressure of zero must also be considered. For the quantities of helium stored in this study, however, the internal helium maximum pressure resulted in a vessel capable of withstanding this condition.

Table 16 indicates the weight tradeoff of the several helium systems studied by the Boeing Co. for a manned orbiting laboratory for a 30-day mission. The system weight includes vent fluid, unavailable fluid, fill tolerance fluid, dry tanks, valves, heaters, and the energy-weight penalty for electrical thermal expulsion. The tradeoffs for the cryogenic helium system proposed and the heat-leak uncertainty factors are noted in figures 52 and 54. The penalty is about 9 pounds of total system weight per pound of useful fluid. These are compared with the more certain tradeoffs for nitrogen. The leak values of study 2 in table 10 were used to determine usable fill weights.

It can be seen in table 16 that the supercritical, nonvented storage of helium in a 5-psia cabin requires 71 pounds, the lowest total storage-system weight penalty for the cryogenic systems under study. The low-temperature gaseous storage in the liquid hydrogen tank gives the lowest value of 53 pounds.

Another major factor which must be considered in the helium tradeoffs is the duration of mission. As discussed in the case of nitrogen systems, both the size of the helium system and the stand-by times interact in determining the specific weight penalty. Each cannot be considered alone. The Cryogenics Group at AiResearch has recently reviewed this problem.[66] Four different mission durations were selected for study: 30 days, 60 days, 90 days, and 180 days. They are

TABLE 16. — *Diluent Tankage System Weights for 30-Day, 2-Man Mission* [AFTER BOEING [12]]

Storage method	Nitrogen system weight, lb		Helium system weight, lb	
	5.0-psia cabin with 32 lb of useful fill	7-psia cabin with 85 lb of useful fill	5.0-psia cabin with 4.5 lb of useful fill	7-psia cabin with 11.8 lb of useful fill
Supercritical — vented..	108	174	121	180
Supercritical — nonvented...	113	175	71	110
Low-temperature gaseous storage in liquid-hydrogen tank........			53	105

listed in table 17 along with the corresponding crew size, minimum use rate, and standby times. The constant 0.005 lb/hr is determined by the leak rate which is assumed to be the same in all vehicles. The first three missions are identical except for differences in duration. The fourth is for a lunar shelter with 90 days of standby time before use.

TABLE 17.—*Helium Tankage Reference Conditions* [AFTER MASON AND POTTER[66]]

[MINIMUM USE RATE = 0.005 LB/HR]

Mission length, days	Number of men	Usable weight, lb	Standby duration, days
30	2	5.8	2
60	3	11.6	2
90	3	17.4	2
180	3	34.8	[a]90

[a] Lunar stay.

Because the Cryogenics Group at AiResearch has had the most practical experience with small cryogenic storage systems for helium, a close analysis of the approach appears warranted. The general designs of cryogenic helium tankage for all these missions are the same. They are flight weight, vacuum-jacketed, supercritical pressure vessels with superinsulation and a vapor-cooled shield. The inner vessel is of Ti-5Al-25Sn-ELI. The vapor-cooled shield is of Al 6061 and the outer shell and mounting ring is of Al 2219. Compressed fiber glass is used for the inner-shell support and the insulation is aluminized Mylar. The delivery systems for all the tanks are similar. The fluid leaving the tank intercepts heat being transferred through the insulation at the vapor-cooled shield. The fluid is then heated to atmospheric temperature in a warmup-heat exchanger before reaching the shutoff valve. A pressure relief valve operating at atmospheric temperature is employed.

There are two modes of operation for this cryogenic system — isobaric and pressure variant. The pressure-variant mode leads to a lighter system. In operation of the pressure-variant mode, the tank pressure is allowed to increase slowly during the mission. A portion of the energy transferred into the liquid is used to expel the demand and thereby to reduce the insulation requirement. For the 30-, 60-, and 90-day missions the pressure-variant tanks have a maximum pressure of between 850 and 1000 psia and have the same weight penalty. At first glance it would appear that tanks for the longer mission would be larger and would entail a greater weight penalty because of the same demand flow to cover a constant leak rate. However, the greater quantity of fluid stored in the longer mission allows a greater amount of energy to be absorbed by the stored cryogenic per unit increase in pressure. This counteracts the other factors mentioned above.

It should be pointed out that utilization of the pressure-variant mode may not be acceptable if helium is to be capable of supplying the high flow rate for compartment repressurization in the launch or orbit-stabilization phases of a space mission.

Figure 55 represents the data for the isobaric and pressure-variant cryogenic systems and shows that their weight penalties are more favorable than that of the gas-phase storage at 3000 psia. The 180-day mission has a 90-day standby time which must really be considered apart from
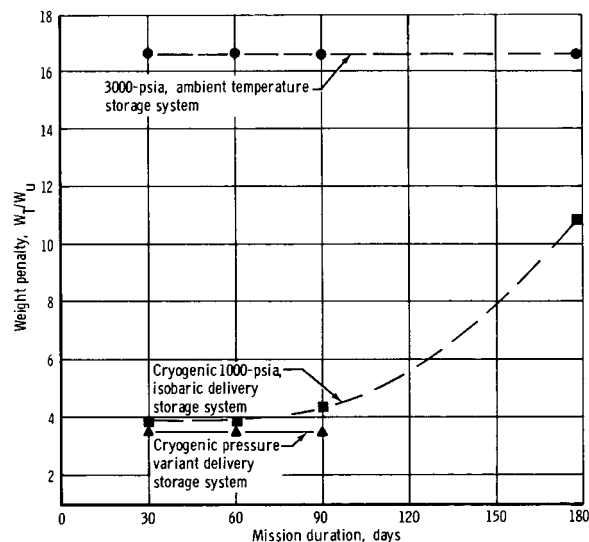

FIGURE 55.—*Weight penalty for helium storage systems.* (AFTER MASON AND POTTER.[66])

the other three missions which have only 2-day standby times.

Because of the long standby time, venting during the later portion of the standby period must be considered. In view of this venting, a pressure variant operation proposed for the shorter missions is not applicable. The tank represented in figure 55 for the 180-day mission undergoes approximately 35 days of non-vented standby and then vents at 1000 psia for the remainder of the 55 days before beginning mission operation.

In these considerations, flow rates are critical. If the use rates were to be increased, the weight penalties will decrease. To indicate the change in penalty involved, the 30-day mission with isobaric tank was further analyzed. The reference quantity of usable weight shown in table 16 was increased in proportion to the increase in minimum demand flow. Figure 56 represents the improvement in W_T/W_u from 3.8 to 2.75 as demand flow increases from 0.005 to 0.15 lb/hr.

It is of interest to compare the weight ratio W_T/W_u of 3.8 presented by AiResearch (fig. 56) with the 9.3 value predicted for the 7-psia cabin by the Cryogenic Group at the Boeing Co. (table 16). The chief difference is probably the fact that the Boeing group includes vent fluid, heater power, accessory structures in their penalty; while AiResearch includes only the basic tank and useful fluid. (See table 19.) There is also a
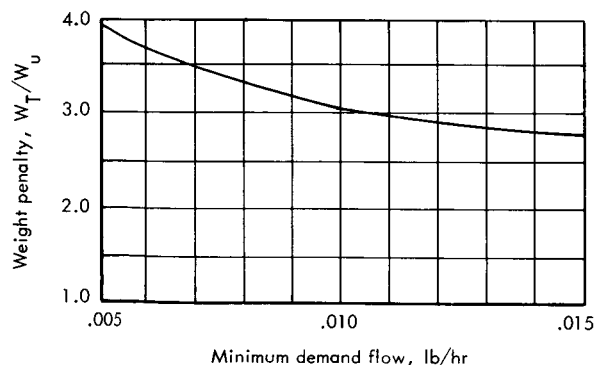
FIGURE 56.—*Weight penalty change due to minimum demand flow increase for 30-day mission, 1000-psia isobaric operation.* (AFTER MASON AND POTTER.[66])

difference in the assumption regarding minimum heat leaks which can be tolerated by optimized insulating support systems for the tankage. By improving this parameter, the heat leak may be decreased, and the total system weight penalty can be greatly improved by the relationships presented in figures 54(a) and 54(b).

Work in progress on the ground-support helium tank for the Apollo lunar excursion module and on small cryogenic vessels may give a more definitive answer to the problem. Because of the lack of operational experience with small cryogenic helium systems in spacecraft and the indicated sensitivity of the system to small design errors, it would be wise to approach helium tradeoffs with great caution.

Neon Systems

Unfortunately, little work has been done on flyable neon cryogenic systems. The Linde Division of Union Carbide Corp. has made small cryogenic neon units for laboratory use.[68] AiResearch is currently studying neon cryogenic systems but no published data are available.[66]

Neon appears to be a much more favorable liquid for cryogenic storage than is helium. Matsch reports that because of the high heat of vaporization and liquid density (table 10), much less boiloff of neon occurs.[68] In commercial containers of 25-liter size (8 to 12 lb of liquid), the normal evaporation rate of nitrogen is 1.9, neon is 6.3, and helium is 18.1 ft³ (STP) per day.

The percentage of boiloff per day is 0.33 percent for liquid nitrogen, 0.54 percent for liquid neon, and 3.0 percent for liquid helium. The gross weights for 1000 ft³ (STP) of gas are 92 pounds for nitrogen, 63 pounds for neon, and 31 pounds for helium. On a volume basis, neon also offers 3.5 times more refrigeration than does liquid hydrogen and 40 times more than liquid helium.

A preliminary review of the data at AiResearch [66] indicates that a subcritical system designed for 30 days of minimum leakage at 0.012 lb/hr with an initial charge of 20 pounds and a pressure-variant operating mode from 450 psia to 1500 psia will have a dry weight of only about 17 pounds. Therefore, $W_T/W_u=37/20=1.85$

for neon compared with an optimized 3.8 for helium and about 1.2 for nitrogen.

Since the boiling point of liquid neon is above that of liquid hydrogen, gaseous storage in a liquid hydrogen tank is impossible. Because of the favorable aspects of neon from a physiological point of view, more work on the cryogenic storage of this gas appears appropriate. The problem of storage of the technical grades of neon contaminated with 15 percent helium also requires further study.

SOLID CHEMICAL STORAGE

Because relatively stable forms of chemical compounds containing a high percentage of oxygen and nitrogen are available, this mode of storage appears particularly suitable for cabin pressurization, erection of inflatable structures, emergency breathing supplies, spacesuit backpacks, and nitrogen supplies for missions requiring small units with long standby time prior to operation. Several excellent reviews of the subject are available.[20, 65, 83, 81, 13, 74, 14, 64, 82, 84]

Chemical Oxygen Supplies—General Considerations

Oxygen producing chemicals can be divided into four major groups:

(1) Alkali and alkaline earth peroxides, superoxides, and ozonides

(2) Alkali and alkaline earth chlorates and perchlorates

(3) Hydrogen peroxide

(4) Water electrolysis

Table 18 shows some of the pertinent physicochemical properties of oxygen-producing chemicals suitable for space cabin use. Lithium peroxide is not available commercially, and calcium superoxide, because of its low yield per pound in commerically available material (50 percent impurity), is of value only in extravehicular suit backpacks where its resistance to fusion is of merit.

Potassium and sodium peroxides are compounds of primary interest in the first category. They absorb water and carbon dioxide and produce carbonates, bicarbonates, and oxygen. In terms of oxygen storage capacity, the ozonides are superior to corresponding superoxides. (See table 15.) The potassium and sodium ozonides are readily prepared.[83] As with the superoxides, lithium ozonide theoretically has the most desirable characteristics in terms of oxygen availability (0.73 lb/lb of compound), but all attempts at synthesis have failed.[83] Lithium peroxide has been synthesized. Chlorate candles are stable materials which can be burned in generators to produce oxygen at a constant rate. Hydrogen peroxide is a strongly oxidizing liquid which can

TABLE 18.—*Comparison of Oxygen-Producing Chemicals* [AFTER COE ET AL.[20] AND PETROCELLI[81]]

	KO_2	NaO_2	Li_2O_2	NaO_3	$LiNO_3$	$LiClO_4$	$NaClO_3$	H_2O_2	H_2O_2
Available O_2 (theoretical), weight percent.....	33.8	43.6	34.8	56.3	23.2	60.1	45.1	47.1	47.1
Purity.................................	....	0.90	(^{a})	....	1.00	1.00	....	0.90	0.98
Available O_2, lb/lb........	0.32	0.392	0.375	0.56	0.232	0.601	0.40	0.423	0.461
Density, lb/in.^{3}...............	0.0237	....	0.0774	....	0.0861	0.0878	0.0815	0.0502	0.0515
Heat of reaction, Btu/lb ^{b}...................	^{c} 415	^{d} 635	^{e} −363	+1515	−488	−596	+422	+1106	1214
H_2O balance, lb/lb........	−0.0207	−0.0246	....	−0.136	0	0	0	+0.577	+0.539
H_2O balance, lb/lb O_2.....	−0.0862	−0.0862	....	−0.225	0	0	0	+1.34	+1.17
CO_2 balance lb/lb.........	0.31	0.40	0.96	0.31	....	....	....	....	....

^{a} 10 percent Li_2O_4.

^{b} + Indicates exothermic reaction; − indicates endothermic reaction.

^{c} $2 KO_2 + 1.23 CO_2 + 0.23 H_2O = 0.77 K_2CO_3 + 0.46 KHCO_3 + 1.5 O_2$.

^{d} $2 NaO_2 + 1.23 CO_2 + 0.23 H_2O = 0.77 Na_2CO_3 + 0.46 NaHCO_3 + 1.5 O_2$.

^{e} Li_2O_2.

be decomposed catalytically to generate oxygen, water vapor, and heat.

Superoxides, Ozonides, and Peroxides

The reactions of superoxides with water vapor and carbon dioxide to form oxygen have been reviewed by Petrocelli and much of the following discussion is based on his work.[81] These reactions can be expressed by the following equations:
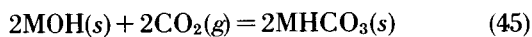
$$2MO_2(s) + H_2O(v) = 2MOH(s) + {}^3/_2O_2(g) \quad (42)$$

and

$$2MO_3(s) + H_2O(v) = 2MOH(s) + {}^5/_2O_2(g) \quad (43)$$

where

s	solid
v	vapor
g	gas
l	liquid
M	alkali earth element

In turn, carbon dioxide is removed from the breathing atmosphere through reactions with the product hydroxide which cause the formation of carbonates and bicarbonates:

$$2MOH(s) + CO_2(g) = M_2CO_3(s) + H_2O(l) \quad (44)$$

$$2MOH(s) + 2CO_2(g) = 2MHCO_3(s) \quad (45)$$

On the basis of these stoichiometries, the theoretical respiratory quotient (RQ), capable of being obtained with superoxide systems, ranges from 0.67 (carbonate formation only) to 1.33 (bicarbonate formation only). With ozonide systems, the theoretical RQ range is 0.40 to 0.80 for the corresponding stoichiometries.

The early concern about RQ mismatch with humans has been resolved by analysis of alternate reaction mechanisms. At first, superoxides were evaluated on the basis of a stoichiometry which involved the formation of the metal carbonate only (eq. (44)). Thus, the RQ of the system was expected to be 0.67 and oxygen overproduction was expected. The other factor which contributed to doubts about the superoxides is based on the experience gained from the use of potassium superoxide canisters in self-contained breathing apparatus for firefighting and mine rescue. Such canisters resulted in very inefficient

utilization (about 80 percent) of the superoxide charge. The inefficiency of such canisters can be attributed to the formation of a hard crust of potassium hydroxide on the reaction surface of the superoxide, thereby preventing water vapor in the exhaled breath from contacting the unreacted superoxide. The discovery that bicarbonate does form under certain conditions of temperature and relative humidity has shown that the problem of oxygen overproduction, anticipated when only carbonates were thought to be formed, is insignificant. Semipassive superoxide systems have been designed to incorporate control of flow rates and relative humidity to achieve better than 90-percent oxygen recovery from the superoxide supply.[69, 52, 51]

In effect, the following stoichiometry can be achieved in a properly designed superoxide reactor.

$$2MO_2(s) + 1.23CO_2(g) + 0.23H_2O(v)$$
$$= 0.77M_2CO_3(s) + 0.46MHCO_3(s) + 1.5O_2(g) \quad (46)$$
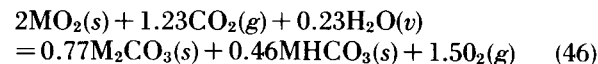
Lithium peroxide (Li_2O_2) is of interest as an air vitalization material because in the presence of moisture it can be caused to react directly with carbon dioxide to yield oxygen and lithium carbonate: [74]

$$Li_2O_2(s) + CO_2(g) = Li_2CO_3(s) + {}^1/_2O_2(g) \quad (47)$$

Thus, it is possible to remove 0.96 pound of carbon dioxide with each pound of lithium peroxide from a closed breathing system and, at the same time, to return 0.35 pound of oxygen to the system. The RQ for a system employing only lithium peroxide would be 2.0. As a result, the use of this chemical would require an additional source of oxygen. The theoretical capacity of lithium peroxide for carbon dioxide is about 4 percent greater than the capacity of lithium hydroxide for carbon dioxide.

In 1964, Markowitz demonstrated that, in the presence of water vapor, carbon dioxide absorption and oxygen evolution by lithium peroxide does occur, but oxygen generation lags far behind the amount anticipated on the basis of equation (47).[74] Yet Markowitz was able to explain his results by showing that the absorption of carbon dioxide and the evolution of oxygen

proceed by two different reactions; lithium peroxide and water vapor first reacting to yield the active carbon dioxide absorbents, LiOH, LiOH · H_2O, and hydrogen peroxide:

$$Li_2O_2(s) + 2H_2O(v) = 2LiOH(s) + H_2O_2(l) \quad (48)$$

and

$$LiOH(s) + H_2O(v) = LiOH \cdot H_2O(s) \quad (49)$$
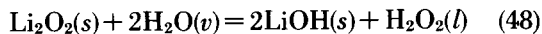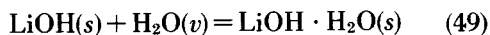
Carbon dioxide is then absorbed via:

$$2LiOH(s) + CO_2(g) = Li_2CO_3(s) + H_2O(l) \quad (50)$$

and

$$2LiOH \cdot H_2O(s) + CO_2(g) = Li_2CO_3(s) + 2H_2O(l). \quad (51)$$
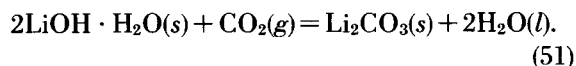
Oxygen is evolved as a result of the decomposition of the H_2O_2:

$$H_2O_2(l) = H_2O(v) + \tfrac{1}{2}O_2(g) \quad (52)$$
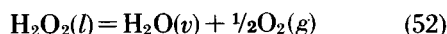
Markowitz points out that in order to achieve theoretical yields of oxygen, it will be necessary to develop a catalyst to insure the decomposition of all the H_2O_2 formed in equation (48).

In 1964, Dobrynina published a monograph on lithium peroxide in which she thoroughly reviewed the state of the art with respect to its chemistry.[22] Ducros and Beranger have also reviewed their preliminary respiratory exchange studies with this compound.[26] These studies show that the state of the art of lithium peroxide, as an air revitalization material, is not nearly as advanced as it is for superoxides. Continued basic research is necessary in order to optimize lithium peroxide as a carbon-dioxide absorber and oxygen source.

Lithium superoxide (LiO_2) if it exists in a stable form would be of great value for air regeneration. Lithium superoxide potentially represents the lightest alkali metal oxide in terms of weight of agent per weight of oxygen produced. Experimental efforts to produce this compound have given ambiguous results. An effort has been made to estimate the thermodynamic properties of this compound to determine whether further experimental efforts are worthwhile, to predict suitable experimental conditions, and to draw conclusions about the stability of the compound. [103]

The free energy of lithium superoxide was calculated from estimated values of the heat of formation, entropy, and heat capacity. The estimates were based on graphical comparison with properties of other oxides. (See fig. 57.) The heat of formation was also determined from calculation of the lattice energy by means of the Born-Haber cycle, as -65 kcal as compared to -38 kcal for lithium peroxide and about -20 kcal for the other superoxides (fig. 57). From the Born-Haber result and other estimated data, the free energy at room temperature is -53 ± 5 kcal.

Consideration of the free energies of various decomposition reactions showed that the tendency to decompose corresponds to 15 kcal from 100° to 300° K. This tendency is so much greater than the uncertainty of the estimates that lithium superoxide can be considered unstable at all temperatures. Furthermore, none of the usual methods of promoting stability are sufficiently

FIGURE 57.—*Heats of formation of oxides of alkali metals and hydrogen.* (AFTER SNOW.[103])

effective to overcome this instability. Substances can be stabilized by putting them into solid solution. For example, phase data have shown the exi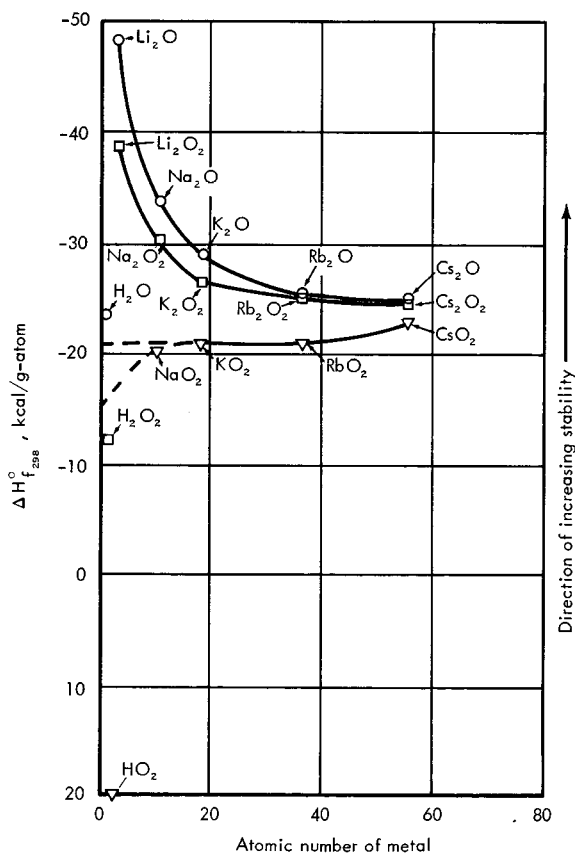stence of solutions of sodium superoxide in sodium peroxide. It has been shown that, theoretically, no significant concentration of lithium superoxide can be stabilized in this way.[103] This conclusion might be different if a mixed compound that has a definite heat and free energy of formation is formed. Such compounds do not usually have sufficient free energy to overcome the instability of lithium superoxide. Further attempts to prepare lithium superoxide do not appear promising. Even if the compound were prepared, it would tend to decompose spontaneously. It would not be safe to carry such an unstable compound in a manned space cabin.

Weight and Volume Tradeoffs of Alkaline Earth Superoxide and Peroxide Systems

Because of several operational interactions with other systems, determination of weight tradeoffs for superoxide systems is most difficult. In the presence of leaks and the resultant waste of oxygen, supplementary oxygen systems will probably be required. The simultaneous requirement for extra cooling capacity, on the one hand, and provision of carbon dioxide absorbtion, odor control, and sterilization of air, on the other, alters the requirements for weight and power ordinarily allocated for these purposes. Inclusion of these factors in tradeoffs is feasible only in final systems-integration steps.

The use of superoxides is very similar to that of LiOH in that they are packaged as granular beds through which the cabin gas is circulated. Figure 58 is a schematic of the system with the appropriate water and carbon dioxide controls required for adequate control of system RQ and CO_2 absorbtion. The filtered granular beds must be of stainless steel or other metal protected by polyethylene or polyfluorocarbon coatings.

Test results for the superoxide systems suggest that utilization efficiencies of 0.90 are attainable.[20] Since the purity of the NaO_2 and KO_2 are about 0.95, the consumption rates for CO_2 control are 5.46 and 6.9 lb/man day, respectively. The flow characteristics for CO_2

absorption are assumed to be the same as those for LiOH systems in figure 59. Using these flows and assuming that all the heat of reaction is all dumped into the process airstream, the temperature rise of air flowing through the superoxide bed can be determined for any cabin p_{CO_2}. This relationship is recorded for both
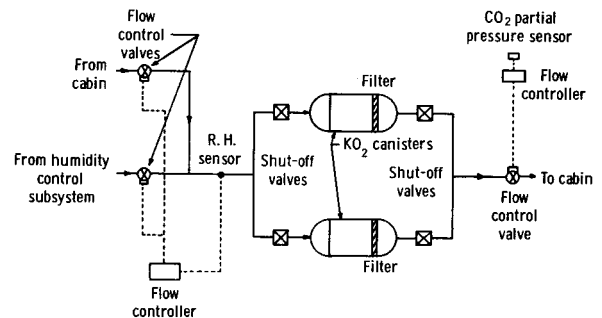
FIGURE 58.—*Alkali metal superoxide subsystem diagram.* (AFTER ROUSSEAU ET AL.[95])

CO_2 partial pressure in cabin, mm Hg
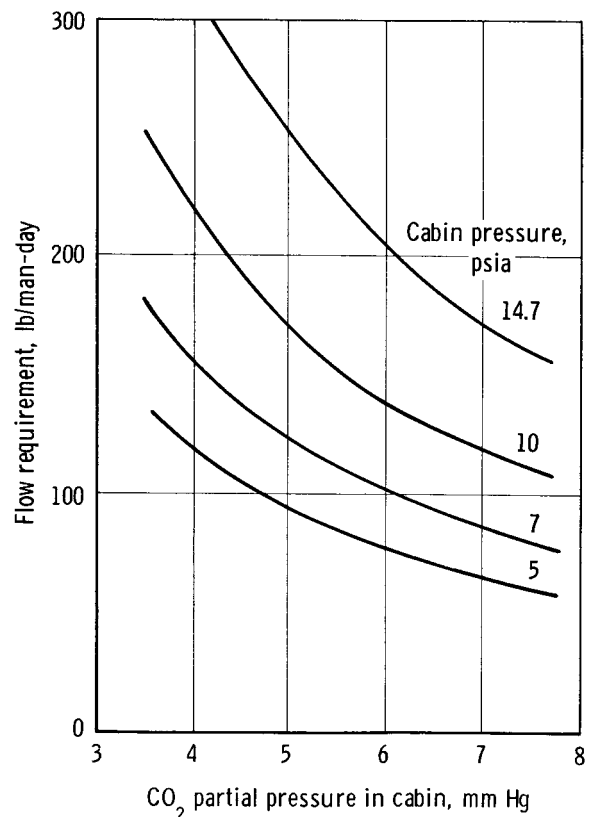
FIGURE 59.—*Lithium hydroxide subsystem flow requirement.* (AFTER ROUSSEAU ET AL.[95])

NaO_2 and KO_2 at several cabin pressures. [95] The additional cooling power to handle this heat must be accounted for in final weight tradeoffs.

The design equations for superoxide canisters may be found in the studies of Coe et al. [20] and Rousseau. [95] Figure 60 represents the canister weights of NaO_2 and KO_2 required for different numbers of crew members. Since the expendable superoxide weight of the potassium subsystem is considerably greater than the sodium, only the latter is discussed further. Potassium superoxide give slightly lower pressure drops in the canister and heat rejection load, but they account for only a small part of the overall subsystem equivalent weight. The total subsystem equivalent weight is the total of the sodium superoxide consumption, the canister weight, accessory weight, power-loss penalty, heat-rejection penalty, and material balances weight. Then a deficit of water exists, the material balance requires additional water and causes a penalty. However, oxygen which is added by the system can be subtracted from the consumption weight by a factor of W_{O_2} = 2.28 $N\tau$, where N is the crew size. The system equivalent weight penalty is

$$W_e = (W_{NaO_2} - W_{O_2} + W_{H_2O}) + W_{can} + W_{acc} + W_P + W_Q$$

$$W_e = (5.52 - 2.28 + 0.185)N\tau + 3.423N^{2/3} + (5.2 + 1.79\sqrt{N}) + [(PL)_t(PP)] + 1.70N(RP) \quad (53)$$

This equation has been solved for a typical set of conditions defined by the assumptions: cabin pressure = 10 psia; p_{CO_2} = 7.6 mm Hg; heat rejection = 10 percent vehicle power penalty in lb/watt; pressure losses other than NaO_2 bed = $0.8\sqrt{N}$ in. of H_2O. The subsystem accessory weights are in the neighborhood of 8 pounds for a three-man system.

Figure 61 is a plot of the subsystem equivalent weight for sodium superoxide as a function of time for one to five crew members. There was no material balance credit for water or oxygen and power penalties of 0.1 to 0.4 lb/watt were used. In figure 62 the same parameters are plotted with credit for oxygen and a penalty for water upon assuming a 0.171 lb/man-hr water
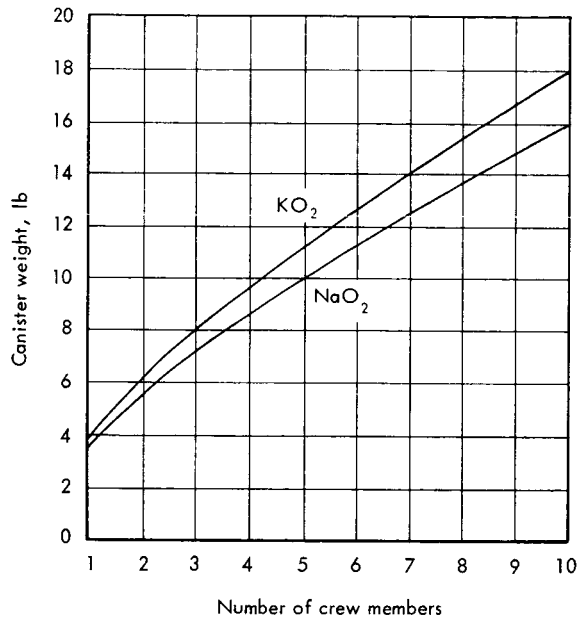
FIGURE 60.—*Alkali metal superoxide canister weight.* (AFTER ROUSSEAU ET AL. [95])
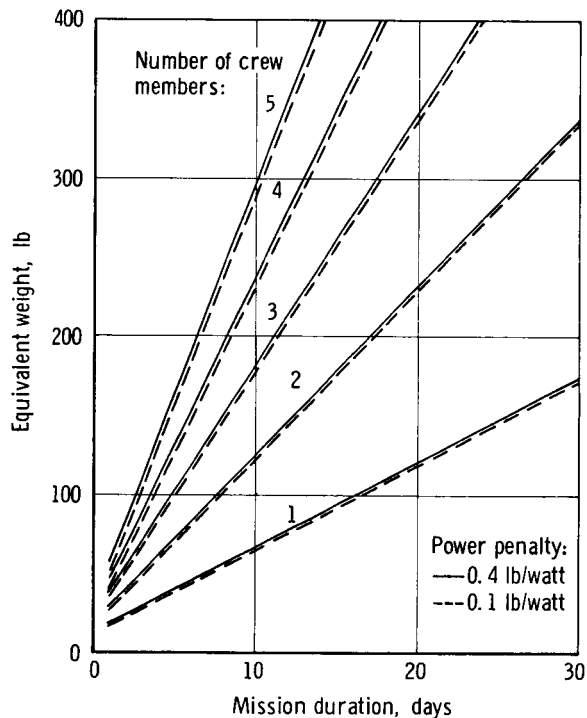
FIGURE 61.—*Equivalent weight for sodium superoxide subsystem with no credit for oxygen production.* (AFTER ROUSSEAU ET AL. [95])
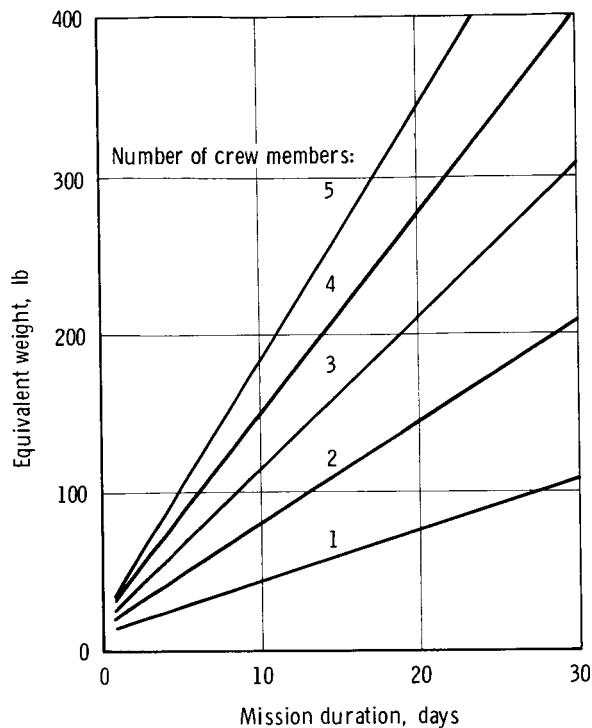
FIGURE 62.—*Equivalent weight for sodium super-oxide subsystem credited with oxygen production. Power penalty is 0.1 lb/watt.* (AFTER ROUSSEAU ET AL.[95])

FIGURE 63.—*Comparison for carbon dioxide absorption subsystem (superoxide credited for water).* (AFTER ROUSSEAU ET AL.[95])

consumption rate by the superoxide process. Any less water produced by the crewman would be considered a penalty.

In any tradeoff study, a comparison must ultimately be made between the equivalent weight of carbon dioxide absorption by super-oxide and LiOH with water and oxygen creditation. Figure 63 shows this plot with the same assumptions as above and for a three-man cabin. This plot indicates that when oxygen is credited to the superoxide system, the weight penalty for equivalent carbon dioxide absorption is still greater than that for the LiOH subsystem.

Much remains to be done on the optimum design of the canister system. Several new approaches to the problem show some promise in specific applications.[83,14]

Chlorate Candles

This discussion of oxygen generation by de-composition of lithium perchlorate and hydrogen peroxide has been taken directly from the dis-cussions of Coe et al.[20] and Rousseau.[95]

Lithium perchlorate decomposes into lithium chloride liberating oxygen (60.1 percent by weight). The following equation describes the chemical reaction.

$$LiClO_4 \rightarrow LiCl + 2O_2 \qquad (54)$$
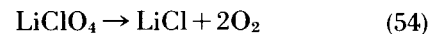
The temperature necessary to initiate the reaction is approximately 720° F, which is approximately 280° F higher than the melting point of the perchlorate. A heat input of 991 Btu/lb of oxygen produced is required to sustain the reaction.

A problem of separating the gaseous oxygen from the liquid compound in the decomposition chamber arises in a zero-gravity environment. Separation can possibly be achieved by use of a porous diaphragm. The rate of oxygen pro-duction appears difficult to control, since little is known about the decomposition mechanism. This can probably be achieved, however, by controlling the heat input into the decomposi-tion chamber.

Chemical sources of oxygen do find a specialized application in portable life support systems where storability and compactness are decisive advantages. In such applications perchlorates are potentially promising because of high oxygen yield, but to date they have shown an unfavorable side reaction leading to the evolution of chlorine gas. Present chemical oxygen development effort is concentrated on sodium chlorate, $NaClO_3$. This chemical will be used as a source of oxygen in an advanced portable life-support backpack now under development. [66]

A rough estimate of the weight of a simple lithium perchlorate decomposition system is shown here as figure 64. The calculations from which this plot was obtained are based on the following data assumptions:

(1) Ullage: 50 percent
(2) Decomposition chamber wall: stainless steel, 0.050 inch thick
.(3) Decomposition chamber insulation: fiber glass, 1.0 inch thick
(4) Porous diaphragm for phase separation: ceramic, 0.15 inch thick

Even with this simple system, lithium perchlorate does not appear on a weight basis alone to be competitive with other sources of oxygen for use aboard space vehicles.

Oxygen Generation by Decomposition of Hydrogen Peroxide

Hydrogen peroxide is available commercially at a concentration of 90 weight percent or lower. A concentration of 98 percent is now available on a semicommercial basis. Higher concentrations are desirable since they have a higher content of oxygen and greater stability.

To generate oxygen, hydrogen peroxide decomposes according to the following equation:

$$H_2O_2 \text{ (liq.)} \rightarrow H_2O \text{ (liq.)} + \frac{1}{2}O_2 \text{ (gas)} + 1242 \text{ Btu lb} \quad (55)$$
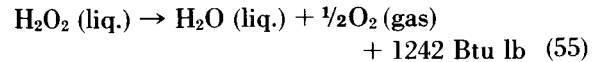
The water produced in the reaction may be useful in the vehicle water-management system. Catalysts are required for smooth and rapid decomposition of hydrogen peroxide. These materials have been thoroughly investigated in connection with propellant uses of hydrogen peroxide so that few problems remain. Silver-screen packs appear to be the most advanced catalyst at the present time. Zero-gravity conditions increase the complexity of the decomposition and feed system.

Disadvantages of hydrogen peroxide include its high toxicity. Concentrated peroxide blisters the skin on contact. Vapors and aerosols entrained with the oxygen are deleterious to the respiratory system. On contact with most structural materials, the decomposition of peroxide is catalyzed. Storage in pure aluminum appears practical for long durations in vented tanks. However, accidental contamination could be disastrous.

Figure 65 shows an arrangement of a peroxide decomposition system. Hydrogen peroxide is

FIGURE 64.—*System weight for oxygen generation by lithium perchlorate.* (AFTER COE ET AL.[20])
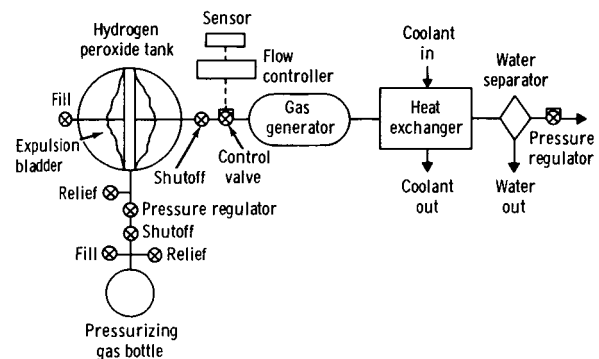
FIGURE 65.—*Chemical oxygen supply using hydrogen peroxide.* (AFTER ROUSSEAU ET AL.[95])

stored in a positive-expulsion tank and expelled through a silver-screen gas generator. The water vapor and oxygen produced are then circulated through a heat exchanger where the water vapor is condensed and subsequently removed as a liquid.

The temperature of the gas at the outlet of the gas generator depends on the heat leaking from the generator and on the purity of the hydrogen peroxide used. The adiabatic temperature of decomposition of a 90-percent purity solution is estimated to be 1364° F.

An estimate of the weight of the hydrogen peroxide storage vessel and pressurizing system was made based on the following assumptions:

(1) Spherical storage vessel
(2) Hydrogen peroxide purity: 0.90
(3) Tank material: aluminum
(4) Utilization efficiency: 0.98
(5) Pressurizing gas: helium
(6) Pressurizing gas subsystem control valves: 7.0 pounds
(7) System is credited for the water evolved in the reaction

The results of these calculations are given in figure 66, where the hydrogen peroxide storage vessel weight penalty is plotted against the useful oxygen load. It should be noted that the weight penalty plotted is lower than the tankage and pressurization subsystem weight by 1.125 pounds per pound of oxygen generated due to the credit given to the water of reaction which is potable.

Oxygen Generation by Electrolysis of Water

Electrolytic processes have been treated in detail in the study of Coe et al.[20] The electrolytic cell considered here is an ion membrane type cell which appears promising for zero-gravity operation.

Reported parameters for a system satisfying the oxygen metabolic requirements of a three-man vehicle are as follows: power input, 702 watts; weight, 112 lb; and volume, 1.97 ft³.

It is believed that the voltage across the cell electrode was on the order of 1.8 volts, and that the gases were delivered at approximately 50 psia. The heat rejected by the three-man cell is estimated to be 447 Btu/hr, and the cell operating temperature is estimated as 122° F. Water is pumped to the electrode by means of a wick.

The weight of an ion-membrane electrolytic cell, including a positive expulsion type water storage subsystem, has been estimated from the data given above with the following assumptions:

(1) Water storage vessel pressurizing gas: helium
(2) Pressurizing gas subsystem control valves: 7.0 pounds
(3) Hydrogen is discharged overboard and no credit is given for its production
(4) Water storage tank material: aluminum

The results of these computations are plotted in figure 67.

This oxygen production technique does not appear competitive on a weight basis with the

FIGURE 66.—*Storage weight penalty for hydrogen peroxide. Hydrogen peroxide tankage is credited for the water of reaction.* $W_{H_2O}/W_u = 1.125$. (AFTER ROUSSEAU ET AL.[95])
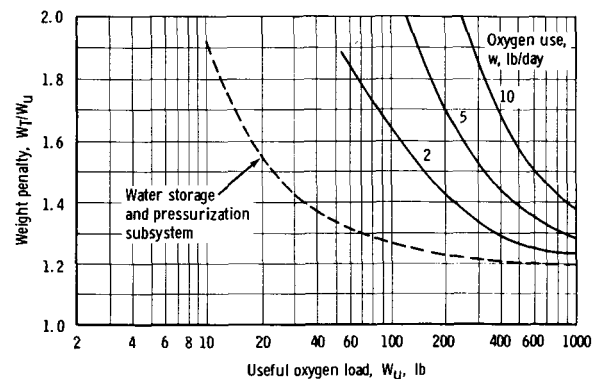
FIGURE 67.—*Electrolytic cell subsystem weight penalty. Weights include valves and control system.* (AFTER ROUSSEAU ET AL.[95])

other storage methods discussed previously, especially for short-duration missions. In addition, the high power requirements of the electrolytic cell are presently a serious disadvantage for space-vehicle installation.

Nitrogen Generation by Decomposition of Lithium Azide

On decomposition at 550° F, lithium azide yields 85.8 percent nitrogen and 95 Btu/lb. To provide heat for initiation and maintenance of decomposition, a reactant can be provided which produces a more stable lithium compound as reaction product. Oxidants such as lithium nitrate or fluorocarbons have been used to form nitrogen-producing solid propellants. In the case of lithium nitrate, the chemical reaction is given by the following equation:
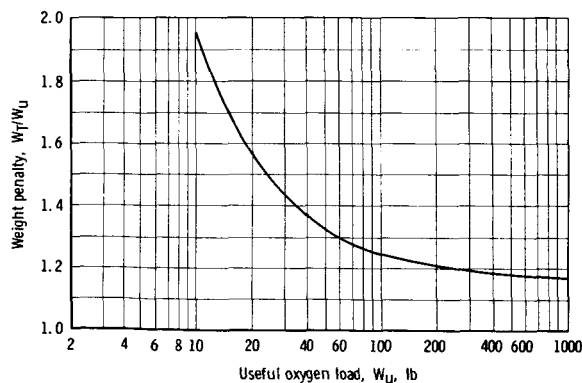
$$5LiN_3 + LiNO_3 \rightarrow 3Li_2O - 8N_2 + p720 \text{ Btu/lb} \quad (56)$$
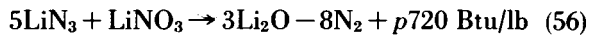
This reaction produces 71.5 percent nitrogen. For practical use, extensive filters must be provided to remove lithium oxide; and heat exchangers, to cool the product nitrogen. Because the reaction operates more smoothly at elevated pressures, the nitrogen-producing mixture would be used to pressurize a small storage tank, the required nitrogen being obtained through a pressure-regulating valve on the tank. A major disadvantage is the fact that the nitrogen-producing azide mixture burns like a solid propellant and is not amenable to simple control.

Material balance alone, without considering any weight penalty for the storage of the azide or the disposal (or storage) of the lithium oxide, shows a weight penalty (W_t/W_{N_2}) equal to 1.14 and is not competitive with the cryogenic methods described previously. In addition, the reaction is difficult to control and presents a safety problem which makes the process prohibitive for space-vehicle use.

COMPARISON OF GAS STORAGE AND SUPPLY SYSTEMS

Component Integration

In addition to the storage vessels and their pressurization subsystem, other components, such as valves and heat-transfer equipment, are integral parts of the complete gas-supply subsystems. Since these accessories can contribute

a large percentage of the total system weight of the gas supply, comparison of the various storage techniques discussed previously can only be made on an integrated basis.

The weight and size of the accessories are, in general, independent of the size of the storage vessel and, in most cases, of the delivery flow rates. While this is true of valves and sensors, it does not apply to items such as heat exchangers where weight is a direct function of the flow rates in the system. Table 19 is an example of current system component weights for several gaseous and cryogenic systems. These must be added to the appropriate storage tradeoffs for total-system integration. Sometimes these weights are included in the basic tankage.[12]

Subsystem Comparison of Weight Penalties

Since weight is usually the determining factor in the selection of a space vehicle system, a plot of several subsystem weights for gas supplies considered in this report is presented for comparison in figure 68. This plot has been prepared using the accessory weights of table 19 and the total storage vessel curves of figures 34(a), 36(a), 66, and 67. The curves are given for oxygen only, since the conclusions drawn from it also apply to nitrogen storage vessels.

Other parameters of importance in system selection are listed in table 20. These include maximum subsystem pressure (excluding the pressurizing gas components), maximum esti-
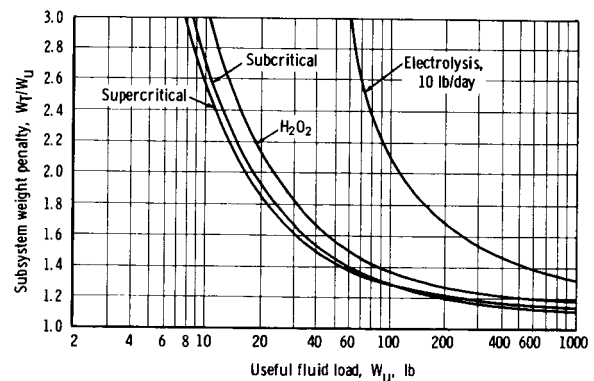
FIGURE 68.—*Comparison of gaseous oxygen supply subsystem weight. Weight penalty for high-pressure gas storage subsystem*$=3.46+7.7/W_u$. (AFTER ROUSSEAU ET AL.[95])

TABLE 19.—*Typical Gas Supply Subsystems Accessory Weights* [AFTER ROUSSEAU ET AL.[95]]

Accessory	Weight, lb	Accessory	Weight, lb
1. High-pressure gas storage, fig. 26:		3. Subcritical cryogenic storage, figs. 36(*b*) and 43(*b*):	
(a) Pressure relief valve	0.3	(a) Helium pressurization subsystem (accounted for in storage vessel weight)	
(b) Fill valve	1.1	(b) Transducer	0.4
(c) Transducer	.4	(c) Fluid quantity indicator	.4
(d) Quick disconnect and shutoff valve	.2	(d) Vent valve	.2
(e) Filter	.1	(e) Fill valve	.3
(f) Check valve	.2	(f) Vessel shutoff valve	.2
(g) High-pressure regulating valve	.9	(g) Heat exchanger	.7
(h) Demand pressure regulating valve	1.4	(h) Check valve	.2
(i) Partial pressure sensor	.2	(i) Demand pressure regulating valve	2 × 1.4
(j) Flow controller	2.5	(j) Partial pressure sensor	.2
(k) Shutoff valve	.4	(k) Flow controller	2.3
		(l) System shutoff valve	.4
Total weight	7.7		
		Total weight	8.3
2. Supercritical cryogenic storage, figs. 34(*b*) and 39(*b*):			
(a) Vessel vent and pressure relief valve	0.2	4. Hydrogen peroxide storage, fig. 66:	
(b) Pressure controller	.4	(a) Helium pressurization subsystem (accounted for in storage vessel weight)	
(c) Electrical heater	.8	(b) Vent valve	0.2
(d) Internal heat exchanger	.9	(c) Fill valve	.3
(e) Fluid quantity capacitance sensor	.5	(d) Vessel shutoff valve	.2
(f) Capacity indicator	.6	(e) Flow control valve	1.5
(g) Fill valve	.3	(f) Partial pressure sensor	.2
(h) Vessel shutoff valve	.2	(g) Flow controller	2.5
(i) External heat exchanger	.5	(h) Gas generator	2.2
(j) Flow control valve	1.2	(i) Heat exchanger	2.5
(k) Check valve	.1	(j) Water separator	1.3
(l) Check valve	.2	(k) Pressure regulator	1.4
(m) High-pressure regulating valve	2 × .9		
(n) Demand pressure regulating valve	2 × 1.4	Total weight	12.3
(o) Partial pressure sensor	.2		
(p) Flow controller	2.5		
(q) System shutoff valve	.4		
(r) Pipes and fittings	.50		
(s) Bosses	.30		
Total weight	14.4		

mated temperature in the subsystem, power requirements, the heat evolved, and the heat-sink potential of the subsystem. Also listed in table 20 is the water consumed (or produced) by the subsystem. Complete system evaluation cannot be made without taking into account these parameters. Normally, the gas supply subsystem would be penalized (or credited) for each one of the items listed above.

On a weight basis, cryogenic fluid-storage subsystems are superior to all the other subsystems considered, except possibly superoxides. This weight advantage increases markedly as the capacity of the supply system increases. At a total fluid load of 100 pounds, the weight of the two cryogenic subsystems is about the same. Above 100 pounds of fluid storage capacity, the subcritical system is slightly higher than its supercritical counterpart. Below 100 pounds, this weight picture is reversed. The weight difference is so small that system selection must be based on other considerations, such as the mission du-

TABLE 20. — *Oxygen Gas Supply Subsystem Characteristics* [AFTER ROUSSEAU ET AL.[95]]

Subsystem	Maximum system pressure, psia	Maximum system temperature, °F	Power requirement, watts/lb O_2	Heat evolved, Btu/lb O_2	Heat sink potential, Btu/lb O_2
High-pressure gas................	10 500	Ambient...........	None	None	None
Supercritical storage.............	875	Ambient...........	None	None	90 at 270° R [a]
Subcritical storage...............	[b] 100	Ambient...........	None	None	155 at 170° R
Hydrogen peroxide decomposition.	[b] 50	1360	None	2610	None
Water electrolysis.................	[b] 50	122	117	75	None

[a] Average.

[b] Pressurizing gas stored at 2000 psia.

ration, standby time, repressurization sequence, and cabin volume, which were discussed above in the appropriate sections.

The weight penalty of the high-pressure gas storage subsystem for oxygen and nitrogen is approximately three times as large as that of cryogenic subsystems at large fluid loads. For this reason, high-pressure gas storage vessels are not very attractive for space vehicle applications other than emergency or repressurization gas supply. In this case, maximum reliability, indefinite standby periods, and short-duration usage are the design criteria, and weight is a secondary consideration. At a stored weight lower than approximately 6 to 8 pounds, the high-pressure oxygen and nitrogen gas subsystems show a lower weight penalty than all the other subsystems analyzed.[95]

Considerable savings may be gained by integrating both gaseous (table 16) and cryogenic storage with the other cryogenic materials stored on the spacecraft for engineering needs. A very comprehensive review of this approach is available.[104, 57, 33, 45]

Several tradeoff studies comparing gaseous and cryogenic oxygen storage with superoxide systems have been recently performed. The one using the most recent superoxide technology is shown in table 21, which compares the weight and volume characteristics for 90-day missions of several different systems. These are based on a man consuming 1.87 lb/day. The fixed weight and volume estimates were said to be based on the same criteria as the present study,[20, 95, 98, 84] but no specific choice of penalties was stated. The sodium superoxide system compares favor-

TABLE 21. — *Weight and Volume Characteristics for Advanced State-of-the-Art, Nonregenerative Air Revitalization Systems* [AFTER PETROCELLI [81]]

System	Fixed weight, lb [a]	90 man-day mission total weight, lb	Fixed volume, ft³ [a]	90 man-day mission total volume, ft³
LiOH (alone)............................	12	269	2	8
Liquid oxygen (150 psi) (50 percent loss).	20	209	1	11
O_2 spheres (3000 psi) (SAE 4340 steel, safety factor 1.88).	10	534	1	13
Liquid (50 percent loss)/LiOH.........	32	667	3	19
O_2 spheres/LiOH........................	22	803	3	21
KO_2..	12	769	2	17
NaO_2.......................................	12	598	2	13.5

[a] Fixed weight and fixed volume estimates include blowers, manifolds, regulators, control device, and miscellaneous piping and tubing.

ably with the liquid-oxygen (50-percent loss)/ LiOH combination. However, a 50-percent loss of liquid-oxygen is assumed with no justification for this value. From the discussion of cryogenic systems, it would appear that little or no venting would be necessary for 90-day missions with even the older subcritical oxygen systems. Subcritical vessels with vapor-cooled shields, designed for two men, would definitely require no venting over a 90-day period.[66] Also, from consideration of the section on gaseous oxygen spheres, use of a higher pressure (10 000 psia instead of 3000 psia) for the oxygen in the oxygen spheres/LiOH weight column may make this system more competitive.

In view of the uncertainties of the data, it is felt that final judgment should be reserved until more concrete tradeoffs regarding the superoxide system are available. Table 21 has been included to show the great importance of one's initial assumptions in estimating storage-systems weight penalties when making comparison with other systems.

Figure 69 represents a time-dependent study of the same type with estimates for a three-man total regenerative system in the 280- to 600-pound range. Included is the estimated power requirement of 2 kilowatts. Although it is not stated, it is presumed that a nuclear power source is being used to give a power penalty of 300 lb/kw. Approximately 600 pounds must therefore be added to the basic estimated weights of the regenerative systems. The estimated power re-

quirement of nonregenerative systems is on the order of only 0.1 kilowatt, and only 30 pounds for power supply need be added to their basic system weight. Figure 70 presents the system volume figures as a function of mission length.

These figures imply that an active chemical system employing sodium superoxide offers the least weight and volume penalty of any of the nonregenerative systems considered and may be competitive with regenerative systems for missions up to 125 to 180 man-days in length. The same objections to the assumed 50-percent loss in liquid oxygen and 3000 psia storage hold as above. Comparison of the superoxide versus regenerative system appears more valid.

Except for the superoxide system discussed previously, none of the chemical systems are competitive on a weight basis with either of the cryogenic storage techniques. No suitable chemical-generation method for nitrogen supply has been found to date.

Oxygen generation from hydrogen peroxide decomposition could find a use in vehicles in which the water-management subsystem shows a water deficit. This situation would occur in missions of short duration when water is not recovered from the waste or wash products. In this case, however, the small requirement for gas-storage capacity and the high weight of the hydrogen peroxide subsystem offset the advantages of water generation as a byproduct of oxygen production. In addition, hydrogen-peroxide systems for a breathing oxygen supply
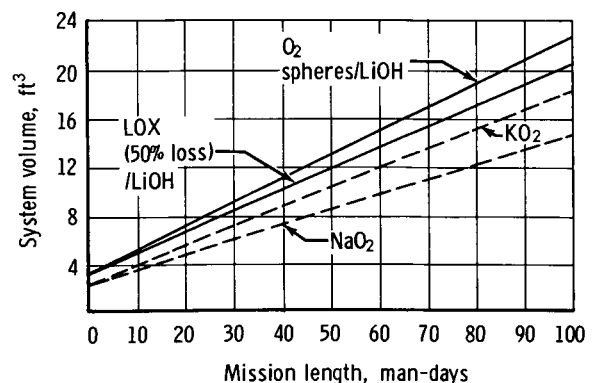

FIGURE 69.—*Variation of weight penalties with mission length.* (AFTER PETROCELLI.[81])

FIGURE 70.—*Variation of volume penalties with mission length.* (AFTER PETROCELLI.[81])

are comparatively underdeveloped, are not easily controlled, and lack safe operational characteristics.

Because of the high electrolytic cell weight, oxygen production from water by electrolysis is attractive only for missions in excess of 1 year. The weight of this system (fig. 67) greatly improves if, in the overall vehicle material balance, an excess of water is produced which can be used for the electrolysis process. The weight plotted can, in this case, be reduced by the amount of excess water production. In a mission of this type, it is very likely that vehicle electrical power would be derived from nuclear or solar sources and that a very low penalty would be paid for supplying power to the electrolytic cell. This type of gas supply system, therefore, offers potentialities for long mission duration, especially if hydrogen is required for carbon dioxide reduction.[95]

Air-Conditioning System

The design of the "air-conditioning" system of a space cabin depends quite clearly on the nature of the atmosphere being studied. Comfort of the crew is the prime consideration. Once the physical requirements for the comfort zones have been established, one can proceed in an orderly fashion to optimize the equipment required for establishing these requirements. The basic physiological considerations have already been covered in chapter 1. In this section, the interaction between these physiological requirements and engineering variables is discussed. A parametric analysis of the several weight-limiting functions of the system is made for the five acceptable gas mixtures. The final product is a specific power and weight tradeoff for the air-conditioning subsystem of a two-man orbiting laboratory system with 30-day capabilities.

GENERAL CONSIDERATIONS

Chapter 1 demonstrated that the parameters of radiant wall temperature, air temperature, relative humidity, and air circulation may be combined in several ways to produce a comfortable crew environment. Because of the relative power penalties and equipment weight associated with

these parameters, the optimum combination of parameters for a zero-g, shirtsleeve, artificial atmosphere environment differs from the combination of parameters considered standard for a sea-level, 1-g, comfort environment. In addition to weight penalties for average comfort temperatures, other factors to be considered are the requirement for accommodating high metabolic rates for short periods of time; the need for simple and responsive controls; and the need for air circulation for subjective comfort, as well as for removal of waste products and contaminants from the atmosphere.

Several previous studies form a basis for the present review. The analytic procedures developed by Coe et al.,[20] Rousseau et al.,[95, 96] Paselk,[80] Boeing Co.,[12] and Johnston[48] form a foundation for the present study. Computer codes using many of these analytic techniques are available. It is obvious that many of the weight and power tradeoffs depend on the integration of the environmental control system with other systems of the spacecraft.[80] The type of spacecraft radiator system, the degree of integration of cooling modes for equipment and crewmen, the power source, and myriads of other factors determine both the absolute power and weight penalties and the relative penalties for different gas mixtures. Because such a complex analysis is far beyond the scope of the present study, it was felt that a valid approximation would suffice if typical integration factors and weight penalties for power could be entered into the study at appropriate points. It is clear that estimation of these factors is the weakest part of the analysis. Wherever possible, the errors and biases presented by these integration factors are pointed out and the sensitivity of the specific tradeoff to these factors is estimated.

To simplify the gas specific tradeoff factors, the Boeing Co.[12] has broken down a typical environmental control system into a few major component parts. Figure 71 represents this breakdown. The atmosphere control fan moves air through a water removal, CO_2 removal, and trace contaminant absorption system. The suit circuit runs parallel to this. Characteristics of this system are low flow and high pressure drop (ΔP). The ΔP of the suit is one of the most
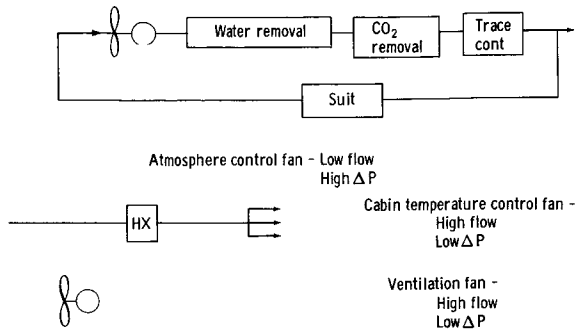
FIGURE 71.—*Typical environmental control system.* (AFTER BOEING.[12])

critical factors. If there is an emergency mode with the requirement for the cabin blower to handle the suit loop with its high ΔP, the weight penalty increases greatly. The cabin temperature-control system has a fan of high flow and low ΔP passing air through a heat exchanger. The cabin ventilation circuit is also of high-flow, low-ΔP type. The major problem at hand is to determine the weight, power, and volume tradeoffs of such a system and to relate them to different atmospheres in question. The criteria of cost, reliability, development status, and interfaces with other systems must also be evaluated. Rousseau et al.[95] have summarized the major criteria in the following paragraphs.

Weight

Weight must include the weights of fixed equipment, ducts and connecting fixtures, any supplies, such as activated charcoal, and silica gel, necessary to the operation of the system, as well as related control mechanisms and instrumentation. In addition, the power requirement is considered in terms of the weight required for the power sources, of whatever kind. As seen below, the weight equivalent of power is the common base for gas-specific tradeoffs. Competing systems and subsystems are usually compared on an equivalent weight basis. The equivalent weight is made up of several terms and is defined algebraically by the equation:

$$W_E = W_H + W_P + W_Q + W_{MAT} \qquad (57)$$

The terms of equation (57) are in turn defined and discussed as follows:

(1) W_H is the system hardware weight comprising heat exchangers canisters, valves, ducts, etc. This weight is the actual system weight, including all its components and associated hardware such as sensors and system-flow controllers.

(2) W_P is the weight of the vehicle power source chargeable to the system under consideration. It can be expressed as the product of the system power requirement by the vehicle power penalty. The system power requirement includes the power expended to circulate the process air through the circuit, the power necessary for system control, and the power required for heating or any other process used in the system.

The vehicle power penalty depends mainly on the size of the vehicle power installation and on the duration of the mission. Nuclear or large solar power sources for short missions have relatively high specific weight, with a minimum of 400 lb/kW of installed power. On the other hand, for long mission durations, the nuclear or solar power penalty is lower, in the range of 200 to 300 lb/kW. This difference is a major factor in overall tradeoffs using these systems.

(3) W_Q is the weight of the vehicle cooling system that can be charged to the particular system or subsystem considered. W_Q is the product of the vehicle cooling system specific weight in lb/W, and the system heat rejection load in watts. However, this penalty depends not only on the size of the heat load but also on the temperature level at which the heat load is rejected to the cooling system. This temperature level must be taken into account when determining the term W_Q.

As mentioned above, final systems integration is a most critical aspect of this problem. An example of the mission dependence of vehicle cooling system is shown in figure 72. This figure represents different heat sink potentials as a function of mission duration and thermal load. Hydrogen must be treated as an expendable when it is also used as a fuel. In the shaded area, active radiators can be used if power is supplied by fuel cells; passive radiators if power is supplied by solar cells.

Thermal transport may be provided by a coolant fluid circulated between the heat producing equipment and the heat sink, with the
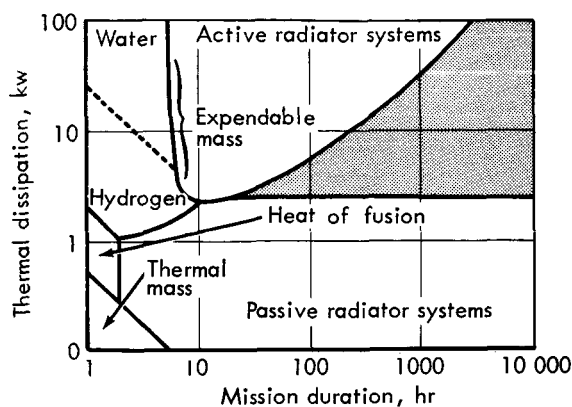
FIGURE 72.—*Heat sinks as a function of mission duration and thermal load.* (AFTER ROWLETT AND LEE.[97])

heat transferred from the equipment to the coolant through cold plates or through circulating pressurization gas and then transported to a radiator or evaporator. Electrical equipment alternatively can be cooled by forced convection of the pressurization gas, which, in turn, generally is cooled in a heat exchanger using an expendable evaporant as its heat sink.

(4) W_{MAT} depends on the system material balance. As an example, if a nonregenerable absorbent is used for the removal of water from the cabin atmosphere, the weight of the absorbent must be charged against the system. Also, if water is used in a system, either permanently absorbed or evacuated overboard, then the system, in certain cases, must be charged for this amount of water expended. On the other hand, if a system produces water or oxygen, it can, depending on the application, be credited for the production of these materials.

Power Requirements

Power requirements include mechanical or pneumatic power for circulation of the atmosphere, heat power for use in a catalytic burner, mechanical or pneumatic power for a water separator, and pneumatic or electrical power for operation of control elements and instrumentation. Mechanical power may come from electric motors, and heat power may come from electric resistance elements; that is, the entire power supply may be electrical. Pneumatic power is customary in capsule pressure controls and pressure relief valves.

The preferred type of power will depend upon the design of the equipment and upon the relative availability of the different types. For continuously rotating devices, such as compressors, electrical power may be better than pneumatic, while for periodically actuated devices, such as water separator sponges or control valves, pneumatic power may have distinct advantages. One must consider off-design as well as on-design modes. Both the maximum rate at which power will be used and the average rate must be considered. The penalty imposed by any power source will be a combination of the influences of the maximum rate and the average rate times the use.

Two philosophies can be used in computing power.[95] The first, which is machine oriented, is to set up the flow circuit and then compute the total gross power required by the components to maintain operation of the circuit. In practice, one assumes a flow rate, composition, density, and temperature. The pressure drops of the individual equipment and ducts are computed and added to give the total pressure drop in the circuit. A compressor capable of providing a specified flow rate at a pressure rise equal to the computed pressure drop is then chosen. The power required by the compressor (an electric motor) is then said to be the power required to maintain the desired fluid circulation in the circuit.

The second method, which is function-oriented, determines with respect to each equipment and duct section, the power equivalent, at 100 percent efficiency, of the pressure drop in the device. The resulting total power equivalent is then modified to reflect attainable power conversion efficiencies, and the required total power is found. This function-oriented method has two drawbacks when compared with the machine-oriented method. The resulting calculations are more complex without being more accurate. Also, unless great care is used, violation of the principles of continuity and conservation of energy may occur, resulting in meaningless values.

Volume

The volume of an atmospheric control system is relatively difficult to determine at an early

, stage of the program. This is due to the fact that a substantial percentage of the total volume is necessarily devoted to ducts and fittings, the actual sizes of which are very dependent upon the layout or arrangement of components. The total volume of the atmosphere control system can include the following:

(1) Core volume or volume of heat exchanger element, or volume of reacting substance, such as lithium hydroxide

(2) Volume of the supports for the core

(3) Volume of the pans and manifolds

(4) Volume of associated or integral ducts

(5) Volume of auxiliary items, spare parts, tools, and replacement chemicals such as lithium hydroxide

(6) Volume, space clearance necessary for access to equipment and for repairs, on the ground or in flight

Because of the complexity of the geometries involved, it is essential that a layout, or better a mockup, be used to arrange circuit components for minimum volume. This requirement precludes a precise evaluation at an early stage necessary for atmospheric selection, and therefore systems volumes are not usually considered in gas-specific tradeoffs.

Humidity Control

As is discussed below, the design of the humidity control system appears to determine much of the hardware and power weight penalty of the atmosphere control loop. A brief comparison of the two most advantageous systems appears to be in order. It is taken directly from Rousseau et al.[95]

Humidity control of a space vehicle cabin atmosphere involves the removal of the water vapor produced by the crew members. As discussed in chapter 1 of this report, the rate of production of water vapor by respiration and perspiration varies greatly, depending on the occupants' metabolic rate and also on their activity. For normal operations the rate of water vapor emitted is taken to be an average of about 4 to 6 lb/man-day. If water is produced at a rate higher than average, as in decompression modes with ventilated suits at about 10 lb/man-day, cabin relative humidity will rise slightly. This

does not present any disadvantage, since the requirements for relative humidity are very broad, as seen by the comfort zone definition in figure 3.

The water recovered from the cabin atmosphere is relatively pure when compared with urine or wash water. To be made potable, however, it must undergo treatment.

Figure 73 represents psychrometric charts for several pressures of oxygen which are of value in establishing humidity-control design. Figure 74 represents similar charts for gas systems of nitrogen-oxygen and helium-oxygen mixtures.

Moisture can be removed by two methods: (1) Adsorption on to silica gel or molecular sieves or absorption by chemicals, or (2) cooler-condensation methods. Rousseau et al.[95] have demonstrated that humidity control by solid adsorbents, such as silica gel or molecular sieves, is more attractive than water removal by chemical absorbents. No heat of reaction is involved in the process, and the heat of adsorption released is roughly the heat of vaporization of the water. The saturated adsorbents can be regenerated by adding heat to the bed at a much lower temperature level than that required to regenerate the chemical absorbents. A temperature of 250° F is usually quoted for silica gel. Regeneration also can be partially achieved by evacuating the bed to vacuum. This process, however, is relatively slow, and its dynamic characteristics are not well known at the present time but are under study. It appears that heat addition to the saturated bed, coupled with evacuation to vacuum, would be very satisfactory for systems in which water is dumped overboard. A desorption temperature of 150° F is sufficient in this case.

Water absorption by chemicals was covered briefly in the section on superoxides. Because of the general inefficiency of the chemical absorption process from a systems point of view, no further discussion is necessary in the present context.[95]

Silica-Gel Adsorbent System

It has been shown that in general, silica gel is far superior to molecular sieves for space cabin dehumidification operations.[95] A typical silica-gel system may be seen in figure 75. Two
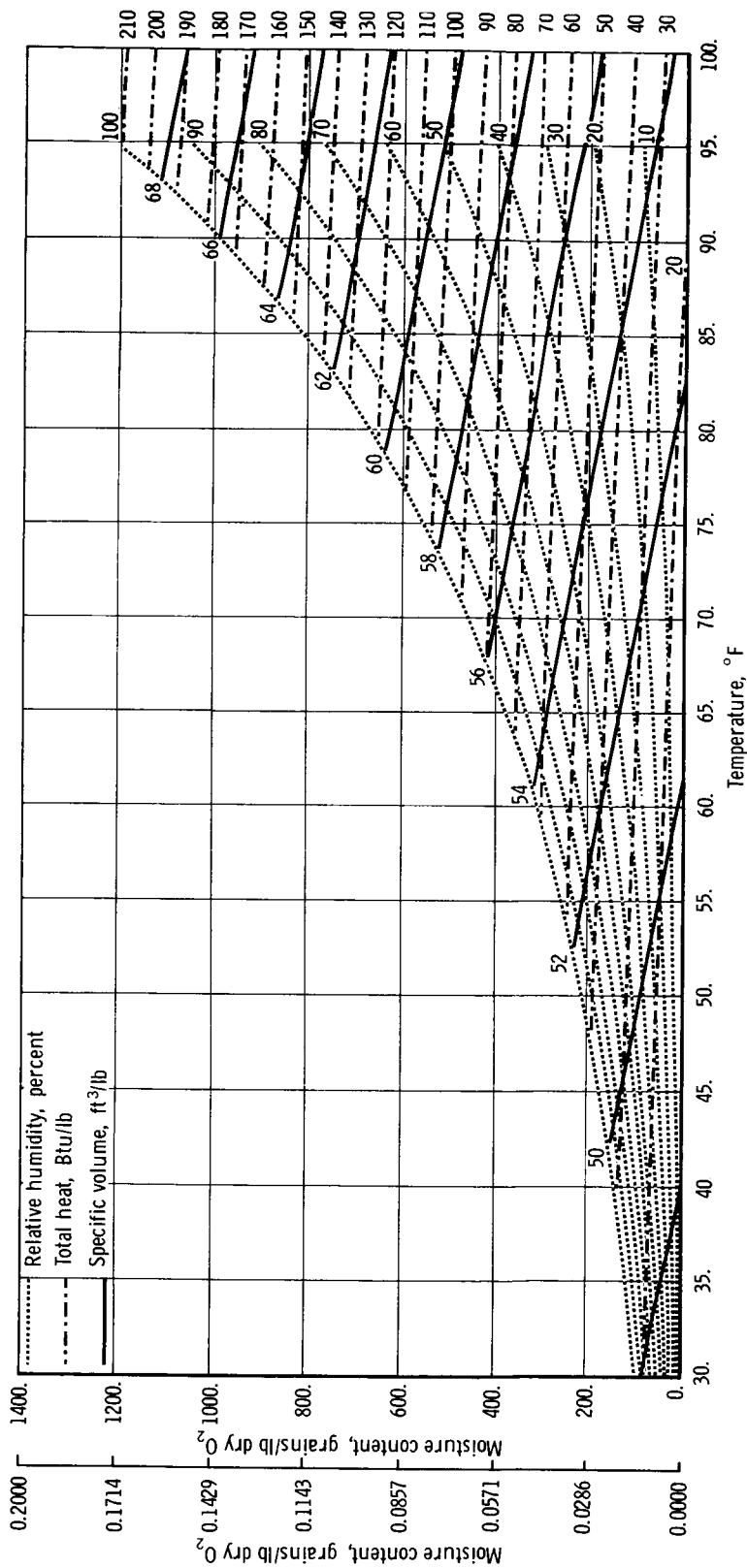
(a) 3.5 psia (180 mm Hg).

FIGURE 73.—Psychrometric chart for oxygen.   (AFTER GREEN.[32])
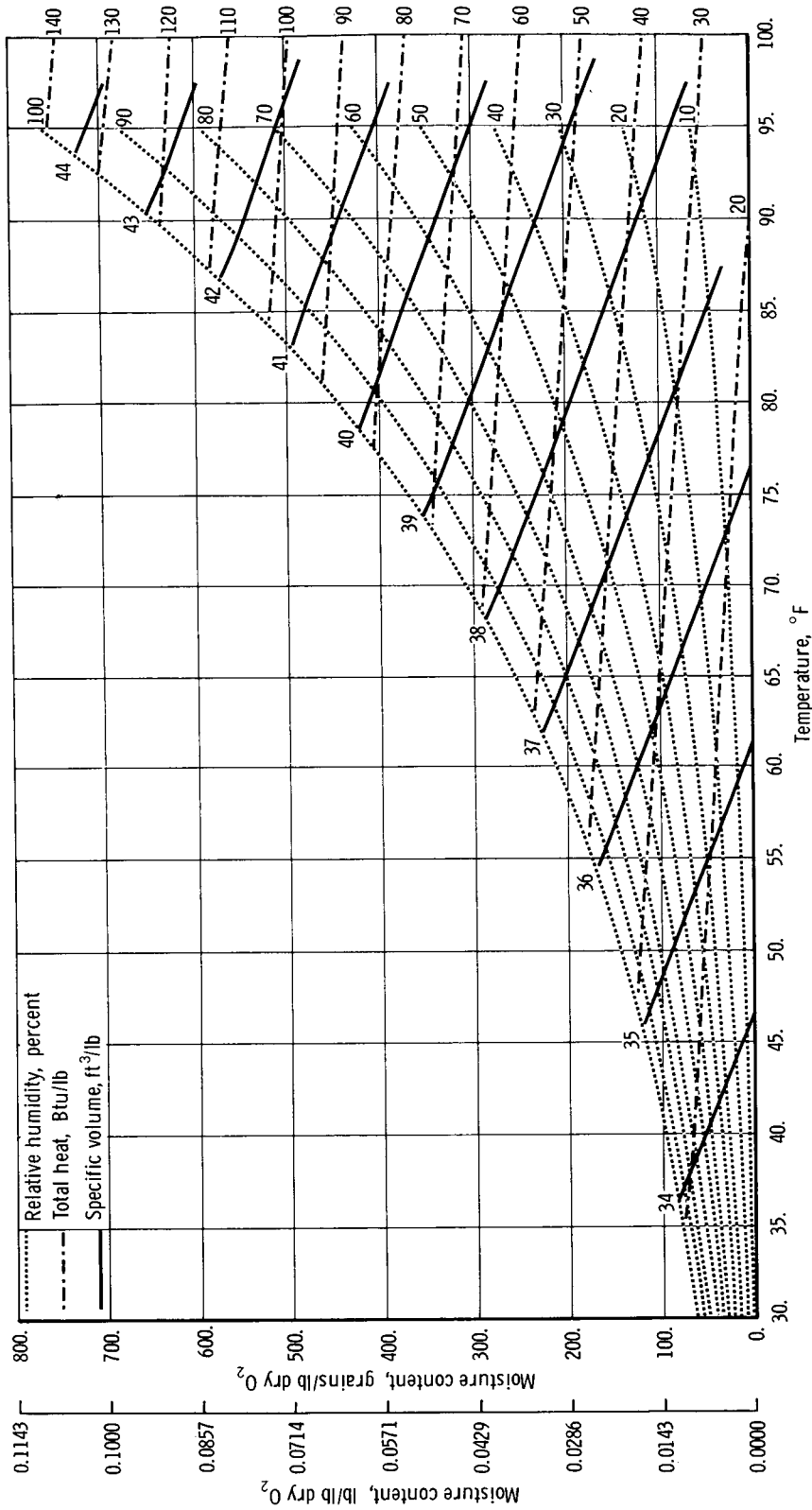
(b) 5.0 psia (258 mm Hg).

FIGURE 73.—Psychrometric chart for oxygen—Continued.
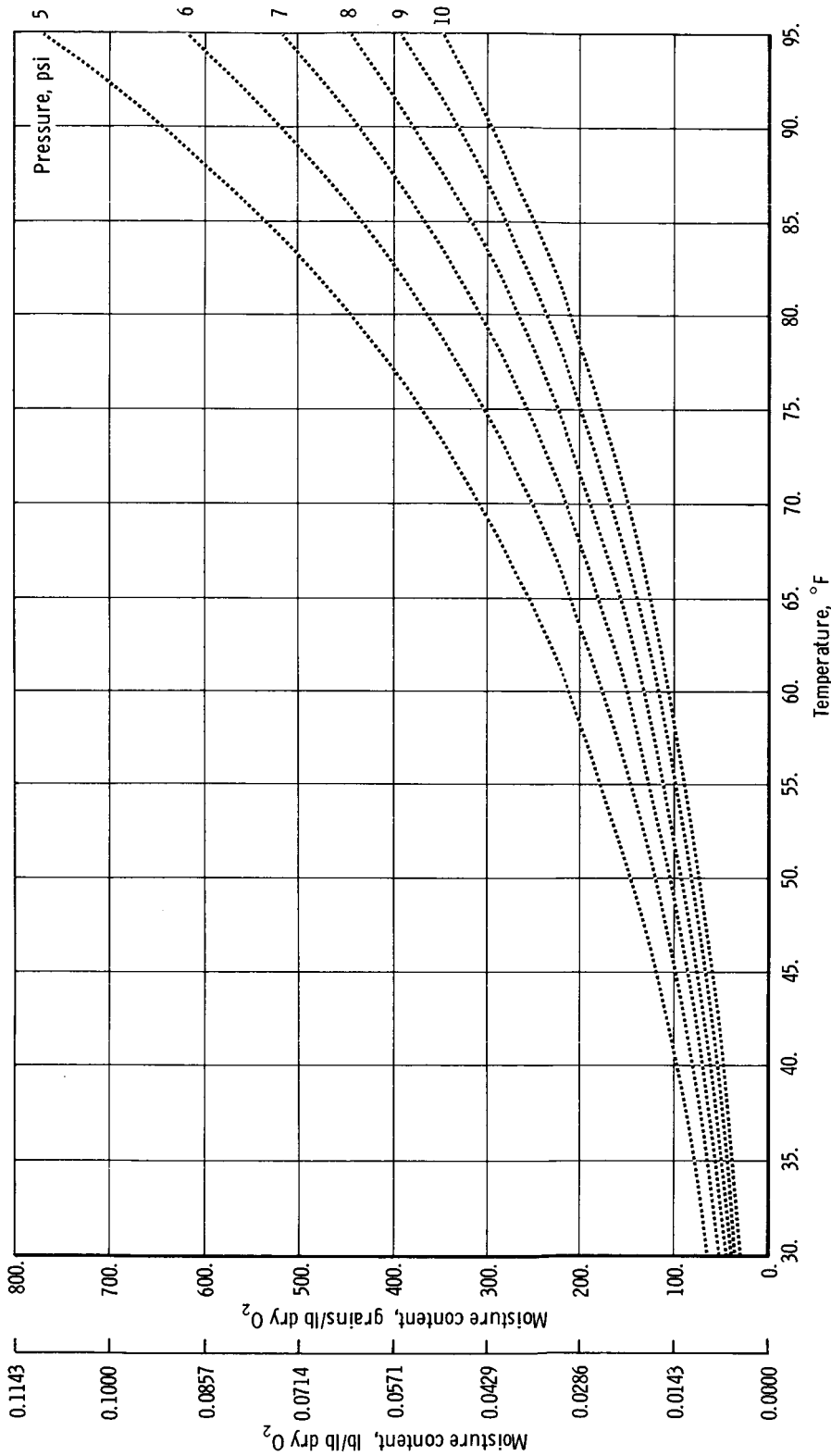
(c) 5.0 to 10.0 psia (258 to 517 mm Hg).

FIGURE 73.—Psychrometric chart for oxygen—Concluded.
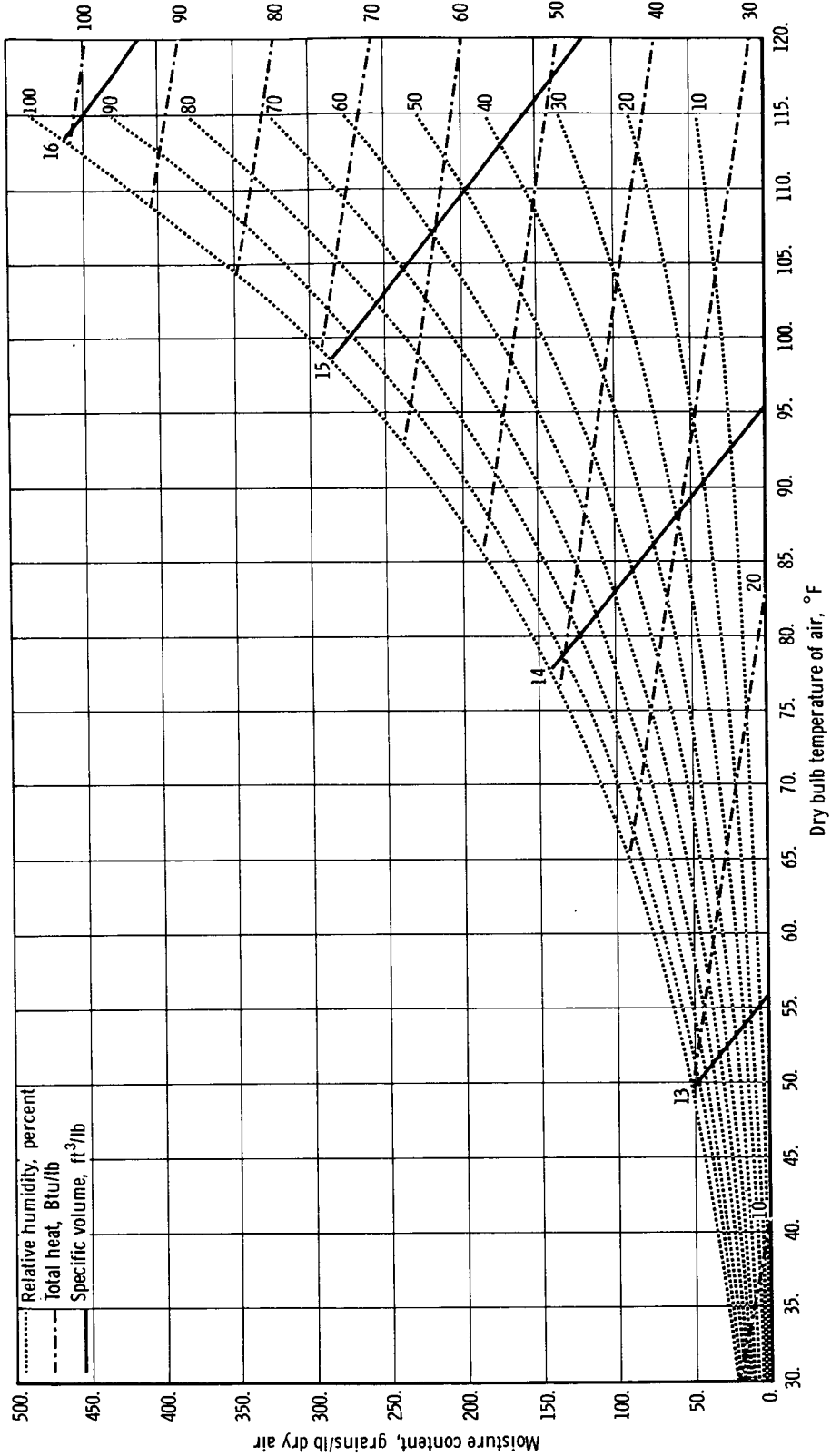
(a) *Air at sea level (14.7 psia).*

FIGURE 74.—*Psychrometric chart for mixed gases.* (AFTER GREEN.[32])
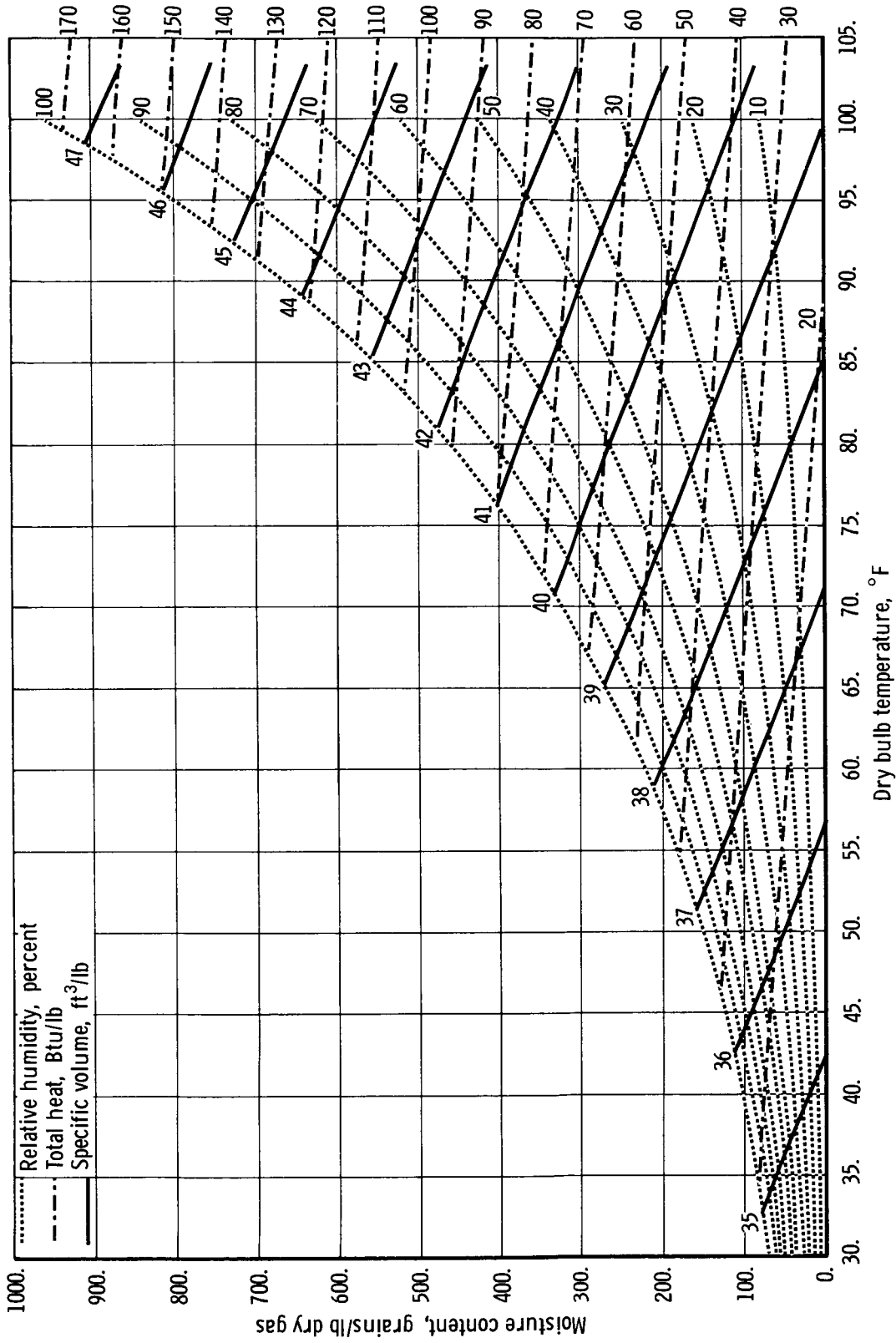
(b) 70 percent oxygen at 3.5 psia (180 mm Hg) and 30 percent nitrogen at 1.5 psia (77 mm Hg).

FIGURE 74.—Psychrometric chart for mixed gases—Continued.
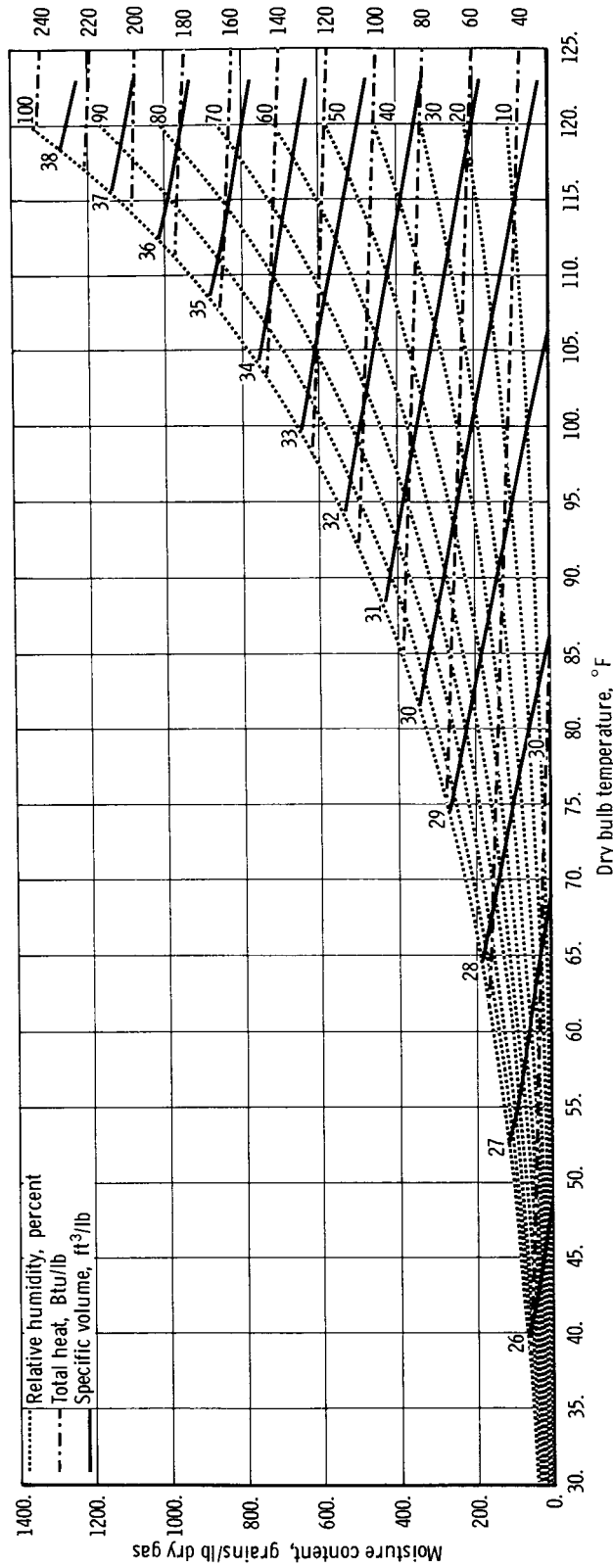
(c) 50 percent oxygen at 3.5 psia (180 mm Hg) and 50 percent nitrogen at 3.5 psia (180 mm Hg).

FIGURE 74.—Psychrometric chart for mixed gases—Continued.
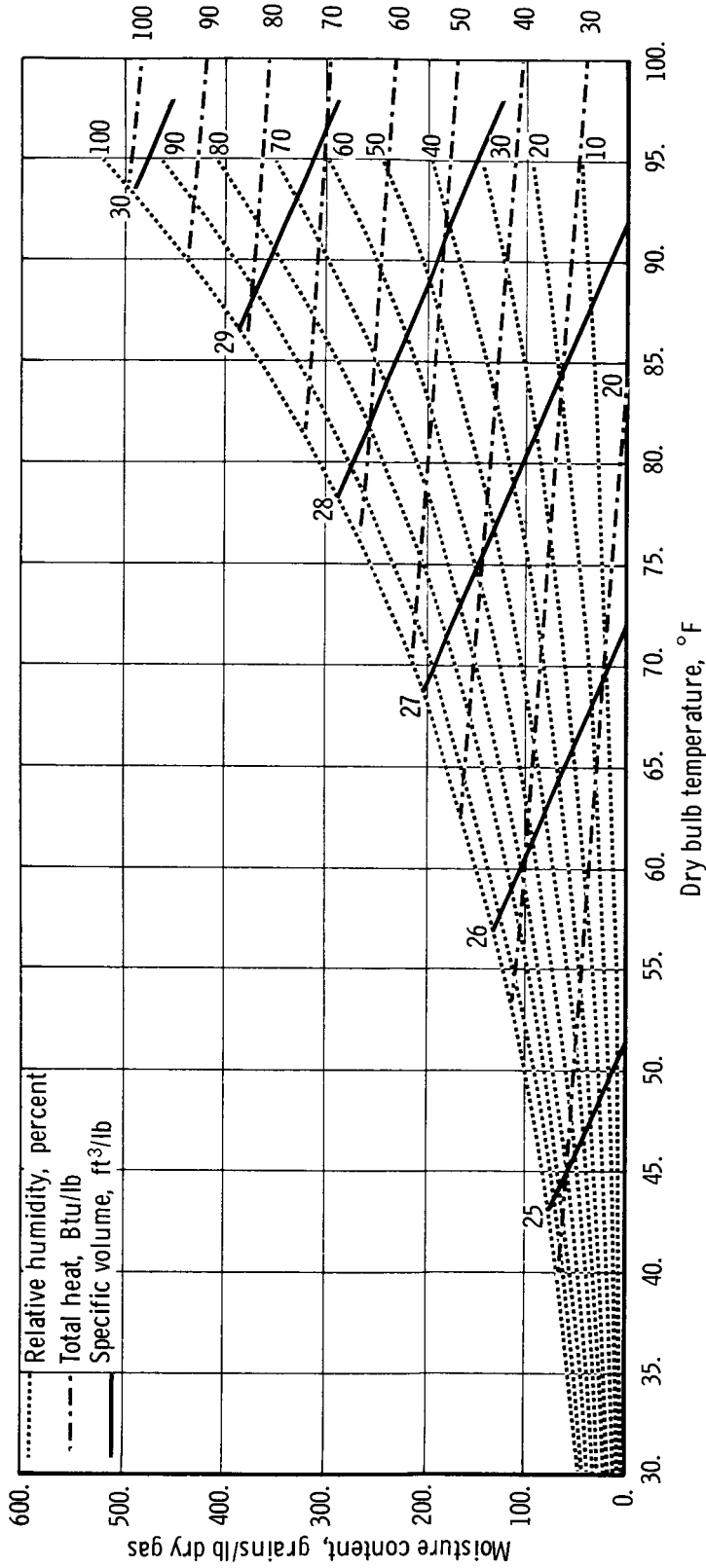
(d) 47 percent oxygen at 3.5 psia (180 mm Hg) and 53 percent nitrogen at 3.9 psia (200 mm Hg).

FIGURE 74.—Psychrometric chart for mixed gases—Continued.
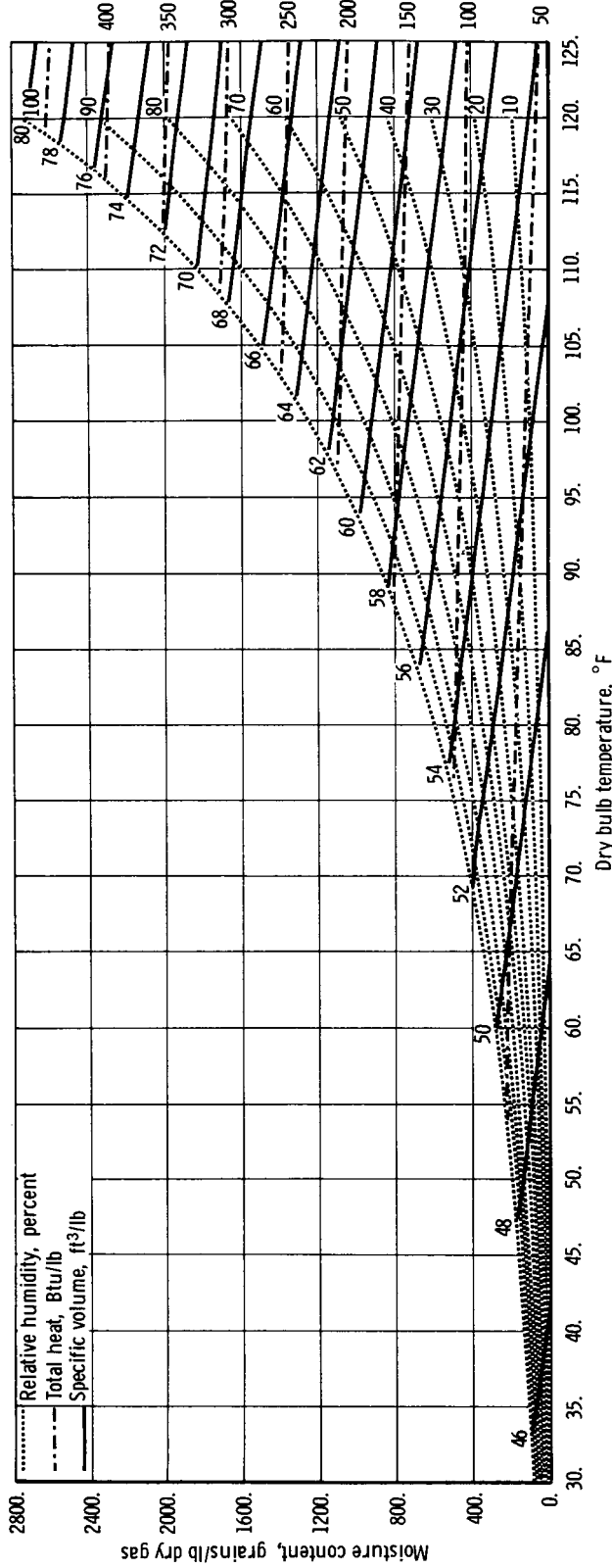
(e) 70 percent oxygen at 3.5 psia (180 mm Hg) and 30 percent helium at 1.5 psia (77 mm Hg).

FIGURE 74.—Psychrometric chart for mixed gases—Continued.
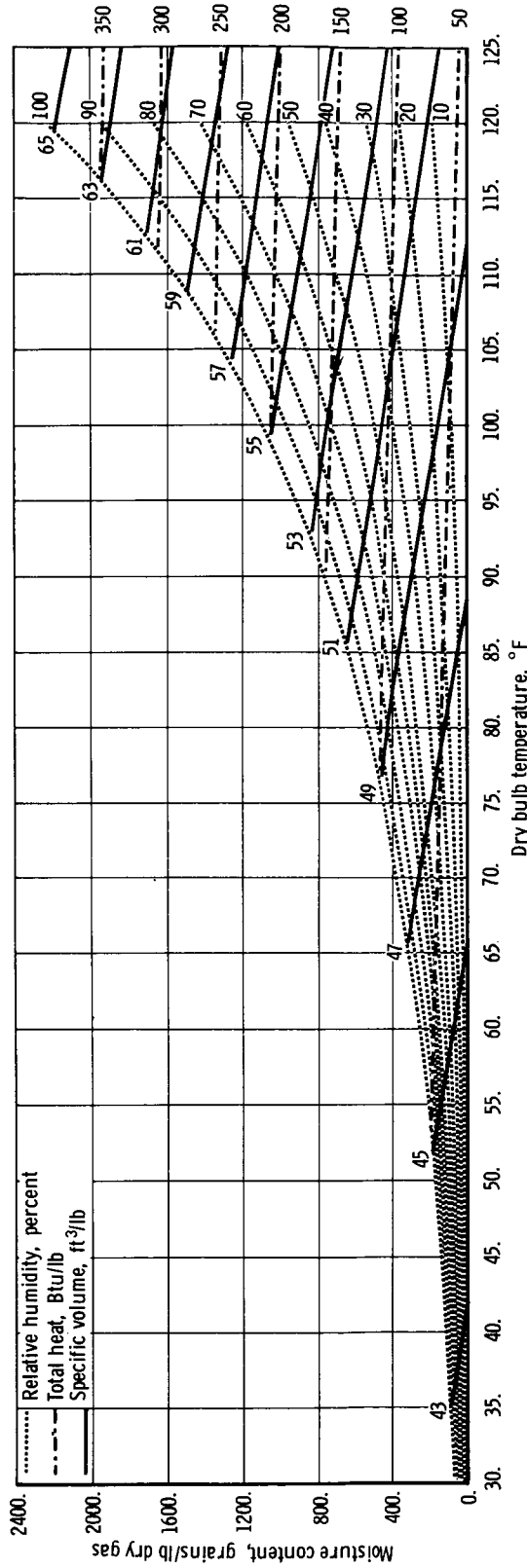
(f) 50 percent oxygen at 3.5 psia (180 mm Hg) and 50 percent helium at 3.5 psia (180 mm Hg).

FIGURE 74.—Psychrometric chart for mixed gases—Concluded.
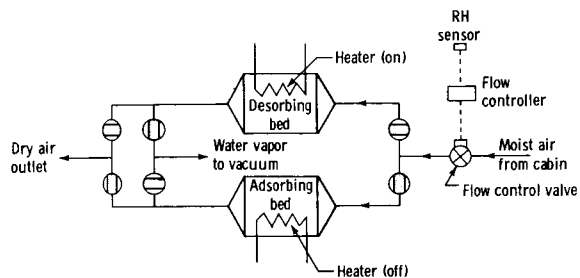
FIGURE 75.—*Humidity control subsystem for regenerable silica gel.* (AFTER ROUSSEAU ET AL.[95])

FIGURE 76.—*Cooler-condenser humidity control subsystem.* (AFTER ROUSSEAU ET AL.[95])

identical silica gel beds are required, one adsorbing and the other desorbing. The operation is fairly simple. When the process water concentration at bed outlet reaches a certain preset value, all the valves of the system are turned 90° from the position shown and heat is applied to the saturated bed, which is then evacuated to vacuum. The process air is routed through the other silica-gel bed. Water vapor from the saturated bed is dumped overboard. The valves are usually automatically switched at fixed time intervals. The valve-actuating mechanism can be a cam shaft driven by an electric motor.

The heater provided for bed desorption can serve a dual purpose: It can be used for removing the heat generated in the bed during the adsorption period, thus increasing the capacity of the silica gel. However, this adds to system complication and is possible only when the heat of desorption is provided by a hot fluid. Often, no suitable fluid loop at the temperature required for desorption (150° F) is available aboard the vehicle and electrical power must be used.

It is to be noted that water is not easily recovered from a saturated bed and must be evacuated overboard. If the regenerable silica-gel system is considered for installation aboard a vehicle in which no excess water is produced, the system must be penalized by the amount of water dumped overboard.

Cooler-Condenser System

A relatively simple method of controlling the humidity of the cabin air is to condense the moisture in a heat exchanger and to remove the condensate from the process airstream. Figure 76 is a schematic diagram of such a system. Water from the moist airstream condenses on the surface of the cooler-condenser and is blown downstream by the air flowing through the heat exchanger. Part of the liquid water droplets are separated from the main airstream in a water separator. The air is then returned to the cabin or to another subsystem for further processing. The condensate is channeled to a reservoir (shown as a bellows), pumped to the water management subsystem, and dumped overboard or returned to the cold side of the cooler-condenser where it is evaporated at low pressure to provide part of the heat sink for humidity condensation.

The system diagram illustrates a possible arrangement for the collection and disposal of the water separated, suitable for operation in a zero-gravity environment. The condensate is ducted by means of wicks from the water separator to a bellows-type reservoir. As the water in the reservoir accumulates, an electrical contact activates a solenoid actuator which compresses the bellows and thus pumps the water through a check valve to the water management subsystem. As the bellows are depressed, the contact is broken and the cycle repeated.

Comparison of Silica-Gel vs. Cooler-Condenser Systems

Equations for the operating parameters and subsystem weight penalties of these two systems are beyond the scope of this present study. The analyses of Coe et al.[20] and Rousseau et al.[95] cover these most adequately. Comparison of the system equivalent weights of these two processes is of value. Table 22 presents the comparison

TABLE 22.—*Comparison of Subsystem Characteristics* [AFTER ROUSSEAU ET AL.[95]]

Parameter	Silica-gel subsystem	Cooler-condenser subsystem
Hardware weight, lb..................	28.1	10.3
Pumping losses, W..................	1.55	4.81
Heat rejection load, Btu/hr, at 70° F.	439	....
Heat rejection load, Btu/hr, at 45° F.	....	569
Heating requirement, Btu/hr, at 150° F.	439	....
Water balance, lb/day..............	[a]−6.6	[b]+6.6

[a] Dumped overboard.
[b] Recovered.

(1) No heat-rejection, heating, or water-consumption penalty.
(2) No heating or water-consumption penalty.
(3) No heating penalty.

FIGURE 77.—*Humidity control subsystem comparison.* (ROUSSEAU ET AL.[95])

of the hardware weight, heat rejection load, heating requirement, power consumption, and water balance for the cooler-condenser and the silica gel subsystem for the following typical vehicle and mission parameters:

(1) Cabin pressure: 7 psia
(2) Cabin relative humidity: 60 percent
(3) Number of crewmembers: three
(4) Cooler-condenser subsystem air outlet temperature: 45° F

The equivalent weight of the subsystem is plotted in figure 77 for various penalties considered. Here it is assumed that the heat rejection penalty (RP), in lb per watt, is 10 percent of the power penalty (PP).

From this plot, it is seen that even in the best light, the silica-gel subsystem is heavier than the cooler-condenser subsystem for vehicle power penalties below 300 lb/kW. If heat-rejection load is taken into account, and more so if the water balance is introduced, the silica-gel subsystem is not competitive with the simple cooler-condenser subsystem on a weight basis.

Even at high vehicle power penalty, the slight weight advantage of the silica-gel system (in ideal conditions) is not enough to offset the advantages of the simpler cooler-condenser system. The cooler-condenser subsystem also is orders of magnitude more reliable than the regenerable silica-gel subsystem. Operation of the silica-gel

subsystem valves requires a complex mechanism. The number of valves, in itself, makes the system unreliable. In addition, all the valves seal against the vacuum to which the bed is desorbed; this presents a serious safety problem. In practice, two valves in series would be installed everywhere. Although single valves are shown in the subsystem diagram of figure 75, the accessory weight estimate is based on the use of two.

Another undesirable feature of the regenerable silica-gel subsystem is the temperature cycling of the process air at subsystem outlet. At the start of the adsorption period, the bed is hot, near 150° F, and the process air temperature will rise through the bed, approaching the temperature of the bed at the outlet. As the bed is cooled, the air temperature will decrease. The cyclic temperature of the outgoing air depends on the bed dynamic characteristics.

Removal of the moisture from the cabin air by cooler-condenser offers the possibility of integration of the humidity control and cabin-temperature control subsystems. This greatly reduces the installation of a number of components as well as control complexity. In actual practice, these two functions, humidity control and temperature control, are unified and effected in the same atmospheric control loop. For the purpose of clarity and to assess better the penalties in-

volved in the process of controlling cabin humidity, humidity control was assumed to be divorced from temperature control.

PARAMETRIC ANALYSIS OF GAS SPECIFIC FACTORS IN THE AIR-CONDITIONING SYSTEM

Often in a study of air-conditioning tradeoff values, there are several core requirements which form the basis of the study. The more common factors such as equal comfort, minimum weight, availability of equipment, and reliability are usually considered. In the case of the air-conditioning system, power and the resulting weight are usually most crucial. In designing for minimal horsepower required, several factors have to be held constant in any tradeoff analysis. These design requirements are volume flow, pressure drop, mass-flow — pressure drop, air velocity, mass flow, heat-flow — temperature gradient, and specific humidity.

Table 23 represents these system requirements. Critical for each of these requirements are design factors in the form of physical properties of the gas and the configuration of the ducts. These are also shown in table 23 along with the effect of the different gas mixtures on the fulfillment of the requirement. The value for a mixture of 50 percent oxygen and 50 percent

nitrogen at 7 psia is taken as 1 and the other mixtures normalized to this value. Thus, let us consider the second requirement $\dot{W}$, ΔP. For the same mass-flow rate and pressure drop, the power required for the reference mixture varies with that required for any other mixture as the ratio of the density of the reference mixture, ρ_1, to that of any other mixture, ρ_2. Since the product of the factors CFM and ΔP both occur in the horsepower equation

$$\text{Fan horsepower} = \frac{62.3(\text{CFM}) \cdot \Delta P(\text{in. H}_2)}{33\,000\eta \times 12} \tag{58}$$

this requirement has no gas factor dependence.

Derivation of the critical gas factors is, of course, crucial to the analysis. Assuming that $\eta = 1$, equation (58) indicates that fan power $\sim$ CFM $\cdot \Delta P$.

Parker et al.[79] have shown that a system can be analyzed for either constant CFM or constant heat transfer rate, Q.

Constant CFM, constant size system. — The fan power is $\sim \Delta P$. In turn, $\Delta P =$ the sum of the duct friction and resistance due to flow transitions. This sum can be expressed as

TABLE 23. — *Horsepower Equation* [AFTER BOEING [12]]

[Values are normalized for 50 percent oxygen and 50 percent nitrogen at 7 psia = 1]

Requirements	Factors		Oxygen-nitrogen system		Oxygen-helium system		Oxygen system
	Gas	Duct configuration	7.0 psia	5.0 psia	7.0 psia	5.0 psia	5.0 psia
CFM $\cdot \Delta P$			1.0	1.0	1.0	1.0	1.0
$\dot{W}$, ΔP	$\dfrac{\rho_1}{\rho_2}$		1.0	1.43	1.68	1.82	1.38
$\bar{V}$	$\dfrac{\rho_2}{\rho_1}$	$\dfrac{A_2}{A_1}\dfrac{D_1}{D_2}$	1.0	.70	.59	.55	.72
$\dot{W}$	$\left(\dfrac{\rho_1}{\rho_2}\right)^2$	$\left(\dfrac{A_1}{A_2}\right)^2 \dfrac{D_1}{D_2}$	1.0	2.05	2.82	3.32	1.9
Q, ΔT	$\left(\dfrac{\rho_1}{\rho_2}\right)^2 \left(\dfrac{C_{p_1}}{C_{p_2}}\right)^3$	$\left(\dfrac{A_1}{A_2}\right)^2 \dfrac{D_1}{D_2}$	1.0	2.12	1.05	2.46	2.56
CFM, ΔP	$\dfrac{\rho_2}{\rho_1}$	$\dfrac{D_1}{D_2}$	1.0	.70	.59	.55	.72
Φ	$\dfrac{P_2}{P_1}\left(\dfrac{T_2}{T_1}\right)^2 \dfrac{R_1'}{R_2'}$		1.0	.73	.61	.41	.77

$$\Delta P = 4f \frac{L}{D} \rho \frac{\overline{V}^2}{2g} + \frac{k \rho \overline{V}^2}{2g} \qquad (59)$$

where

$$4f \frac{L}{D} \frac{\rho \overline{V}^2}{2g}$$

is the pressure loss due to duct friction, and

$$k \frac{\rho \overline{V}^2}{2g}$$

is the pressure loss due to flow transition—elbows, diameter changes, and bends. The factors L, D, $\overline{V}$, g, and k are constant; therefore

Fan power $\sim f\rho + \rho$.

For turbulent flow,

$$f = \frac{0.04}{N_{Re}^{0.16}} = \frac{0.04}{\left(\rho \frac{\overline{V}D}{\mu}\right)^{0.16}} \sim \frac{\mu^{0.16}}{\rho^{0.16}} \qquad (60)$$

Therefore,

Fan power $\sim \dfrac{\mu^{0.16}}{\rho^{0.16}} \rho + \rho \sim \mu^{0.16} \rho^{0.84} + \rho$

Since the pressure drop due to flow transitions (latter term) should be larger than the pressure drop due to duct friction (first term), the variation of power with viscosity, $\mu^{0.16}$, can be neglected and $\rho 0.84$ can be approximated by ρ. Therefore,

Fan power $\sim \rho$ for constant flow systems.

For constant heat transfer, constant size system.—Heat removal rate can be expressed by:

$$\dot{Q} = \dot{W} C_p \Delta T \qquad (61)$$

where ΔT = temperature difference of (air in — air out). Since ΔT and Q are constant,

$$\dot{W} C_p = \text{constant} = A \text{ and } \dot{W} = \frac{A}{C_p}.$$

Since

$$\text{CFM} = \frac{\dot{W}}{\rho} = \frac{A}{\rho C_p} \sim \frac{1}{\rho C_p},$$

Fan power $\sim$ CFM $\Delta P \sim \dfrac{\Delta P}{\rho C_p}$;

and if equation (59) holds true:

$$\Delta P \sim f\rho \overline{V}^2 + \rho \overline{V}^2.$$

For turbulent flow, the relationship of equation (60) holds again.
Since

$$\overline{V} = \frac{\text{CFM}}{A} \sim \text{CFM} \sim \frac{1}{\rho C_p},$$

Fan power $\sim \dfrac{1}{\rho C_p} \left[\dfrac{\mu^{0.16}}{\rho^{0.16} \overline{V}^{0.16}} \dfrac{\rho}{\rho^2 C_p} + \dfrac{\rho}{\rho^2 C_p^2} \right]$

$$\sim \frac{\mu^{0.16}}{\rho^2 C_p^{2.84}} + \frac{1}{\rho^2 C_p^3} \qquad (62)$$

Since the first term (duct friction) should be small compared with the latter term (flow transitions), $\mu^{0.16}$ can be neglected, and $C_p^{2.84} \approx C_p^3$.

$$\text{Fan power} \sim \frac{1}{\rho^2 C_p^3}$$

Fan power generally will be required to accomplish two functions: (1) contaminant removal which requires a constant CFM output, and (2) the cabin cooling which optimally requires a constant heat-rejection capability by the ventilating fan. Thus, for the contaminant fan, power $\sim \rho$, and for the cabin heat exchanger, fan power $\sim 1/\rho^2 C_p^3$.

It should be pointed out that different conclusions with regard to the role of gas-specific factors can be reached if different assumptions are made. For example, in considering flow in ducts and manifolds, the assumption of Parker [79] that friction pressure loss is small compared to duct transition pressure appears reasonable. For flow in heat exchangers or sorbent beds, friction may be a major factor in power analysis. [66]

The value of specific or absolute humidity arises in evaluation of power required for water removal (eq. (67)). The value of ϕ is most sensitive to R', which is the gas constant divided by the molecular weight (table 23). The R' value for air $= 53$, $O_2 = 48$, $N_2 = 55$, He $= 386$. The significance of these values is presented in subsequent paragraphs.

Analysis of the Gas-Specific Factors of the
Cabin Ventilating Fan

The cabin ventilating fan must be considered from several points of view: crew comfort, equipment cooling, and wall temperature. Each of these in turn is affected by many design variables. Those most pertinent to the present analysis are shown in table 24. It should be remembered that radiant cooling affects both man and equipment. Integration of devices controlling the temperature of the wall and the instrument cold plates with the external heat sink can be a major design factor.

One can compare the different gas mixtures in convective cooling capacity by use of equations (6) and (7). If h_{c_1} is the convective heat-transfer coefficient of a baseline gas and h_{c_2} is the convective heat transfer coefficient of any other mixture,

$$h_{c_2} = h_{c_1} \left(\frac{k_2}{k_1}\right) \left(\frac{\rho_2 \overline{V}_2 \mu_1}{\rho_1 \overline{V}_1 \mu_2}\right)^{0.5} \qquad (63)$$

The equations for the convective heat transfer of several gas mixtures can be obtained by the relations in table 25. It is assumed that a mixture of oxygen and nitrogen at 5 psia has the same h_c as oxygen at 5 psia and that a mixture of oxygen and nitrogen at 7 psia is known. Table 25 also shows the calculation for the velocity, $\overline{V}$, of the several mixtures required to give the same convective heat transfer coefficient as a mixture of oxygen and nitrogen at 7 psia. This is obtained from the relationships indicated by equation (6) that:

TABLE 24. — *Major Factors Influencing Power Requirements of Cabin Ventilation Fan* [AFTER BOEING [12]]

Crew comfort	Equipment cooling	Wall temperature
Sweat rate	Q_{output}	T_g
T_w	T_w	$\overline{V}$
T_g	T_g	Distribution of walls
Relative humidity	Location	$T_{condenser}$
$\overline{V}$	$\overline{V}$	Relative humidity
Clo	Distribution of cooling elements	Interaction with external radiator
Distribution of crew		
Noise		

TABLE 25. — *Convective Heat Transfer Coefficients of Several Gas Mixtures and Velocities Required for* $h_{c_1} = h_{c_2}$ [AFTER BOEING [12]]

Mixture	Heat transfer coefficient	Velocity
Oxygen and helium at 7 psia	$h_c = 2.13\ h_{c_{O_2 N_2 - 7}} \left(\dfrac{\overline{V}_{O_2 He - 5}}{\overline{V}_{O_2 N_2 - 7}}\right)^{0.5}$	$\overline{V} = 0.215\ \overline{V}_{O_2 N_2 - 7}$
Oxygen and helium at 5 psia	$h_c = 1.36\ h_{c_{O_2 N_2 - 7}} \left(\dfrac{\overline{V}_{O_2 He - 5}}{\overline{V}_{O_2 N_2 - 7}}\right)^{0.5}$	$\overline{V} = 0.54\ \overline{V}_{O_2 N_2 - 7}$
Oxygen and nitrogen at 5 psia, or 100-percent oxygen at 5 psia	$h_c = 0.85\ h_{c_{O_2 N_2 - 7}} \left(\dfrac{\overline{V}_{O_2 N_2 - 5}}{\overline{V}_{O_2 N_2 - 7}}\right)^{0.5}$	$\overline{V} = 1.36\ \overline{V}_{O_2 N_2 - 7}$

$$\overline{V}_2 = V_1 \left(\frac{k_1}{k_2}\right)^2 \left(\frac{\rho_1}{\rho_2}\right) \quad (64)$$

By determining the different velocities required for a constant convective transfer coefficient, one can calculate the power required for equal convective heat loss by the following reasoning:

From equations (58) and (6), it is evident that fan horsepower HP is $\sim$ CFM $\cdot \Delta P$ and CFM $\sim \overline{V}$. Since $\Delta P \sim \rho$, HP $\sim \rho \overline{V}$. Table 26 indicates the values of k, ρ, and $\overline{V}$ for constant h_c and the rela-

tive horsepower penalties for the different gas mixtures.

Analysis of the Gas-Specific Factors Limiting the Atmospheric Control Loop

In the analysis of gas-specific factors influencing the atmosphere control loop (fig. 71), one is concerned with a system having a low constant-flow rate and a high ΔP (about 8 inches of water). The major considerations are water absorption, trace contaminant removal, carbon dioxide removal, and suit circuit. Table 27 outlines the major factors which influence these considera-

TABLE 26.—*Parameter Values for Different Gas Mixtures* [AFTER BOEING [12]]

	O_2-N_2		O_2-He		O_2
	7.0 psia	5.0 psia	7.0 psia	5.0 psia	5.0 psia
k, Btu/hr-ft-°F	0.0153	0.0153	0.0386	0.0286	0.0155
ρ, lb/ft³	0.0365	0.0268	0.022	0.0206	0.0279
$\overline{V}$, ft/min	47	64	12.5	25	60
Power, watts	63	62	10	19	61
Relative power	1	0.98	0.16	0.30	0.97

TABLE 27.—*Major Factors Influencing Power Requirements of Atmosphere Control Fan*
[AFTER BOEING [12]]

Water		Trace contaminant		CO₂		Suit
$\dot{W}_g = \dfrac{\dot{W}_{H_2O}}{\eta(H_2 - H_1)}$		$\dot{W}_g = \dfrac{\dot{W}_{tc}}{\eta}\dfrac{P}{RT}\dfrac{1}{MAC}$		$\dot{W}_g = \dfrac{\dot{W}_{CO_2}P_t m_g}{\eta P_{CO_2} m_{CO_2}}$		
$\dot{W}_{H_2O}$	Metabolic rate T_w T_g, P, k, R Clo V Radiation Relative humidity Leakage	$\dot{W}_{tc}$	Material, man Chemical processes in man and materials Atmospheric gas	$\dot{W}_{CO_2}$	Diet Metabolic rate Leakage	Q_l Q_c Type ΔP
		η	Leakage Equipment T.C. partial pressure	η	Type equipment CFM CO₂ level Gas	
ΔP	P_t Gas Relative humidity T_g	MAC	Accumulative effects			
η	Type separator $\dot{W}$ Relative humidity					

tions, the required mass gas flow ($\dot{W}_g$), and, ultimately, the horsepower requirements of the atmosphere control fan. The general equations which determine the relationships are also indicated. There are many obvious interrelationships between components within the equation. For instance, the efficiency of the water separator η will ultimately influence $\dot{W}_{H_2O}$ and ΔH. Since the cabin calls for a shirtsleeve environment, no suit factors are considered in the analysis of the cabin tradeoffs. It is assumed that the suit circuit will have its own fan and power.

A specific analysis of the absolute weight of cabin gas needed to handle the different loads of the atmospheric-control system is beyond the requirements of this paper but may be found in Coe et al.[20] and Rousseau et al.[95, 96] From these considerations, the estimated flows of an oxygen-nitrogen mixture at 7 psia required for the several control functions are presented in table 28.

It can be seen that the water removal requires the greatest mass flow of cabin gas. The value for trace-contaminant removal from a "dirty cabin" is the highest expected. The clean cabin represents the "average space cabin."

It is clear, therefore, that the removal of water from the cabin atmosphere will require the greatest mass flow of gas and will determine the power requirements of the atmosphere control loop. Figure 78 indicates that as the temperature of the gas increases, the weight of gas which must be blown through a condenser-cooler with fixed outlet temperature of 50° F to remove 6 pounds of water per day decreases along the
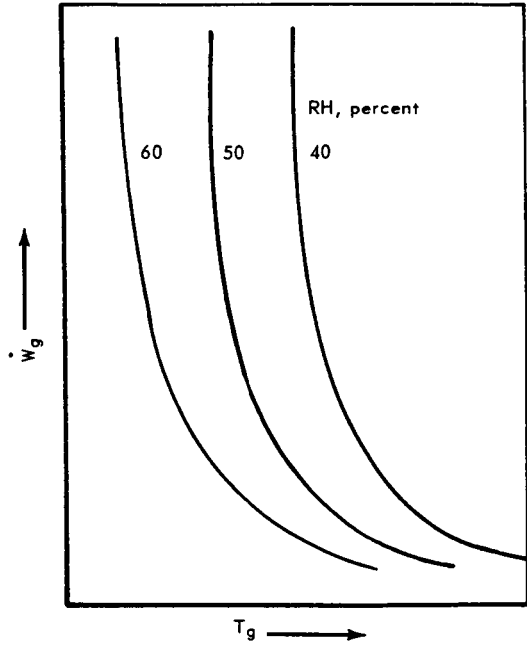
FIGURE 78.—*Mass flow of gas required to remove 6 pounds of water per day at different gas temperatures and relative humidities.* $T_{cond}=50°$ *F.* (AFTER BOEING.[12])

specific relative humidity curves noted. The higher the relative humidity, the less the mass flow of air required per mass of water removed per day and the lower the power requirement.

The relative power requirement for water removal from the several gas mixtures is the next step in the tradeoff analysis. A baseline power value for an oxygen-nitrogen mixture at 7 psia can be determined from the following assumptions and calculation of power:

$\dot{W}=1$ lb/min, empirical resistance constant $=3.9$
$\Delta P=8$ inches of H_2O
Power $= 0.0001575\dot{W}_g$, $\Delta P=100$ watts

These assumptions should handle the assumed water load of 6 lb/day for two men which is a borderline low value. Comparative power for other atmospheres can be determined from equation (58) which indicates that HP $\sim$ CFM $\cdot \Delta P$. The mass flow of gas required to remove water from any atmosphere is inversely related to the specific humidity of the atmosphere. Therefore, comparing any two gases:

TABLE 28.—*Estimated Mass Flow of Gas Required per Day for Atmospheric Control in a 2-Man Cabin* [AFTER BOEING [12]]

Function	Mass flow of gas, $\dot{W}_g$, lb/min
Water removal	0.6 to 1.0
Trace contaminant removal:	
Clean cabin	0.4
Dirty cabin	1.0
CO_2 removal	0.23 to 0.40
Suit loop (liquid cooled—gas augmented, 6 CFM).	0.5

$$\dot{W}_{g_2} \sim \dot{W}_{g_1} \left(\frac{\phi_1}{\phi_2}\right) \qquad (65)$$

The relative ΔP for a gas flow system is related to the $\dot{W}_g$ as follows:

$$\Delta P \sim \frac{\dot{W}_g{}^2}{\left(\dfrac{\rho}{\rho_{\text{STD}}}\right)} \qquad (66)$$

Since relative power for any gas may therefore be determined by the relationship, power $\sim \dot{W} \Delta P / \rho$,

$$\begin{aligned} \text{Power}_2 = \text{Power}_1 &\left(\frac{\dot{W}_{g_2}}{\dot{W}_{g_1}}\right) \left(\frac{\rho_1}{\rho_2}\right) \frac{\Delta P_2}{\Delta P_1} \\ &= \left(\frac{\phi_1}{\phi_2}\right) \left(\frac{\rho_1}{\rho_2}\right) \left(\frac{\Delta P_2}{\Delta P_1}\right) = \frac{m_2}{m_1} \qquad (67) \end{aligned}$$

The final step of this equation is developed in equations (68) to (72) on page 105.

The specific humidity, ϕ, is directly proportional to R'. The power required for any gas to remove water from the stream under the assumed conditions of flow can be calculated from equation (67) relative to an oxygen-nitrogen mixture at 7 psia = 100 watts. Table 29 shows this relationship.

Table 29, along with tables 23 and 26, shows the relative factors required to perform power and other tradeoffs in the design of an air-conditioning system for a space cabin of any type once the appropriate values are known for a reference gas such as 50-percent oxygen and

TABLE 29. — *Power Required To Remove Water From a Gas Stream* [AFTER BOEING [12]]

[Relative to 7-psia oxygen-nitrogen system = 100 watts]

System	Power, watts	
	7 psia	5 psia
Oxygen-nitrogen............................	100	72
Oxygen-helium..............................	60	53
Oxygen..	....	72

50-percent nitrogen at 7 psia. It is obvious that many second and third order interactions have been omitted. However, except for very unusual design limitations, these interactions should not greatly influence the relative tradeoff values.

Absolute Weight Penalties for the Air-Conditioning Subsystem

The next step in the process of establishing total system weight penalties for different gas mixtures in the design of air-conditioning systems is to determine the absolute penalty for the reference mixture, oxygen and nitrogen, at 7 psia. At this stage of the tradeoff analysis, some basic assumptions must be made about the volume of the craft, crew size, and mode of heat sink and power sources. The complex relationships between these variables have been discussed above. In order to establish these interactions, a systems analysis of the entire vehicle is required.

The Boeing Co.[12] has performed such an analysis for a two-man, 30-day, orbiting laboratory. The study has included the integration of cryogenic, power, and environmental control systems with an analysis of the sensitivity of the power-weight penalty of multiple changes in design. A critical factor in this analysis was the determination of a conservative value of 1.25 lb/watt for a 30-day mission. Depending on specific design limitations relating to power source-cryogenics interactions, the calculated 30-day penalties ranged from 0.7 to 1.14 lb/watt. An analysis for a similar system by AiResearch Corp. arrived at 1.2 lb/watt as the power weight penalty. Since these two independent groups agree so well, it is safe to proceed with a conservative value of 1.25 lb/watt.

It is felt that a step-by-step analysis of this absolute power penalty will be of great value. The internal tradeoffs between the critical thermal control, dehumidifying, and ventilating loops have been very graphically presented by the group. It is only through such an analysis that one can appreciate the sensitivity of the total air-conditioning power penalty to on-design assumptions and off-design contingencies. Since these factors ultimately play a significant part in the evaluation of any inert gas tradeoff a detailed review of the study appears warranted.

The model of physiological heat transfer in chapter 1 was used to calculate the heat transfer by each mode for a range of parameters of radiant wall temperature, air velocity, air temperature, and effective wetted surface under a fixed metabolic rate. A power weight estimate was then prepared for each mode of heat transfer. The equipment weight was considered to be the same for the range of parameters investigated. The most promising alternate combinations were examined to determine their sensitivity to higher and lower metabolic rates for off-design peaks in metabolic loading. The power weights then provided a means for evaluating the weight implications of the various gas mixtures.

The following assumptions were made:

(1) A balance is required between body heat production and rejection to keep the body at an average skin temperature of 91° F without sweating or shivering.

(2) To cover a variable exercise load in the orbiting laboratory, the average heat rejection capability of 490 to 520 Btu/hr must be provided in the design. The value of 400 Btu/hr accepted as the average sedentary level was too low for the laboratory operations specified in the mission description.

(3) During normal activity the humidity must be maintained between 40 and 60 percent.

(4) Crew comfort must be provided for in either a 5-psia or 7-psia environment. The lab compartment in a cabin is about 750 ft³; the lock compartment is 450 ft³.

(5) Body surface of a crewmember is 20 ft².

(6) The clothing insulation of the crew can be adjusted from 0.05 to 0.15 Clo. This selected value was on the low side. The underwear worn in Gemini 7 had a Clo value of "less than 0.25 Clo." [85] During the waking hours, this was the preferred mode of dress for general comfort. For sleep, the crew preferred a double layer of underwear and a coverall to protect them from the cold in the dark portion of the orbit. General sensitivity of the comfort zone to Clo value can be estimated from the oxygen-helium predictions of figure 15(a). Since future space cabins with more operating volume will probably have astronauts in coverall garments, a Clo value of 0.5 would probably have been more appropriate

for on-design, average cabin conditions. The lower Clo value tends to increase the comfort-zone temperature and decrease the power penalty of the atmospheric cooling system (fig. 15) for all gas mixtures. It is certain that the region of from 0.05 to 0.15 Clo will give a minimum system weight for air conditioning.

Heat balance.—Figure 79 represents the radiant, convective, and evaporative heat rejection partition which will be required for a crewman working at 520 Btu/hr with a wetted skin fraction of 10 percent and a clothing temperature of 89° F in a 7-psia oxygen-nitrogen atmosphere for several air velocities. Lung losses were not included. It can be seen that increasing the air velocity from 20 to 80 ft/min at 70° F will double the convective heat loss (fig. 79(b)). Also, decreasing
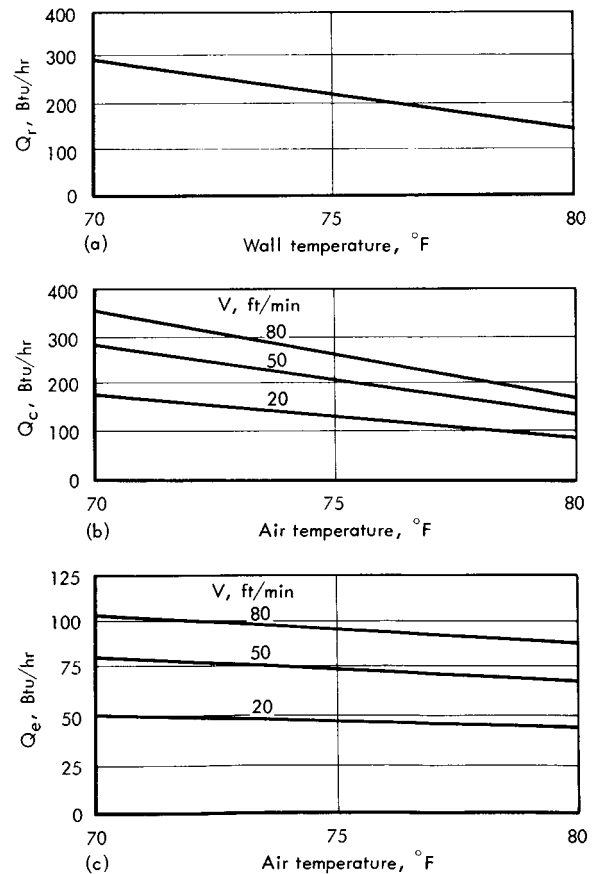

FIGURE 79.—*Heat rejection modes.* $Q_m = 520$ *Btu/hr;* $f_s = 10$ *percent;* $T_c = 89°$ *F;* $P = 7.0$ *psia.* (a) *Radiation.* (b) *Convection.* (c) *Evaporation (lung loss not included).* (AFTER BOEING.[12])

the air temperature from 80° to 70° F at constant air velocity will double convective heat loss. Air temperature has little effect on evaporative heat loss in the temperature zone of 70° to 80° F of vasomotor regulation. This can be seen more clearly in figure 11. Figure 79(c) does show that increase in air velocity from 20 to 80 ft/min results in a twofold increase in evaporative loss (see also fig. 10). The values of figure 79(a) appear very much lower than the corresponding values of figure 10 but it must be remembered that the former is assuming 10 percent skin wetting while the latter assumes 100 percent wetting. A mass transfer coefficient of

$$1.35 \times 10^{-4}(\rho_{actual}\overline{V})^{0.5}/(P_{actual}/P_{standard})^{0.335}$$

was used for these calculations (see eq. (12)).

The analytical approach is to select an air temperature, wall temperature, and relative humidity and to determine the radiant loss (fig. 79(a)) and the air velocity required to provide a balance of heat loss through convection (fig. 79(b)) and evaporation (fig. 79(c)). The resultant air velocity requirements are shown in figure 80 as a function of air temperature and wall temperature. Minimum air velocity requirements are realized with low air and wall temperatures.

Air flow requirements through the humidity control system (outlet temperature of 45° F) as a

function of air temperature and wall temperature are given in figure 81. The increase in flow requirements with a decrease in air temperature is caused by a decrease in the specific humidity of the lower temperature air. Because of the increased heat lost via radiation and decreased loss of latent heat, the inflow requirements are decreased with a decrease in wall temperature.

Both the power weight required to provide the necessary air flow through the humidity control to achieve the necessary evaporative heat rejection rates and the power weight to provide the air circulation to achieve the necessary convective heat rejection rates at three different wall temperatures are shown in figure 82. The power weight penalty of 1.25 lb/watt for the 30-day mission was used. The combined power weight penalty is shown as a function of air temperature and wall temperature in figure 83. An air temperature of 73° to 75° F results in the lowest power penalty for the range of wall temperatures considered.
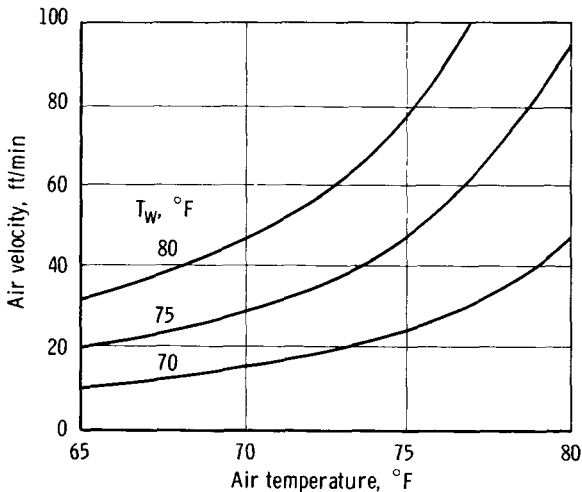

FIGURE 80.—*Air velocity requirements.* $Q_m = 520$ *Btu/hr; RH=50 percent; P=7.0 psia; $f_s=10$ percent.* (AFTER BOEING.[12])
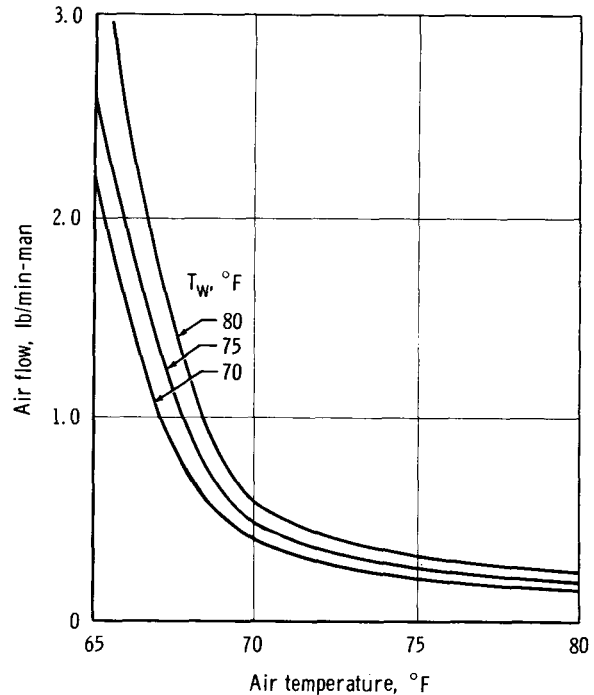
FIGURE 81.—*Humidity control requirements.* $T_{cl}=89°$ *F; heat production=520 Btu/hr; P= 7.0 psia; $T_{cond}=45°$ F; and $f_s=10$ percent.* (AFTER BOEING.[12])
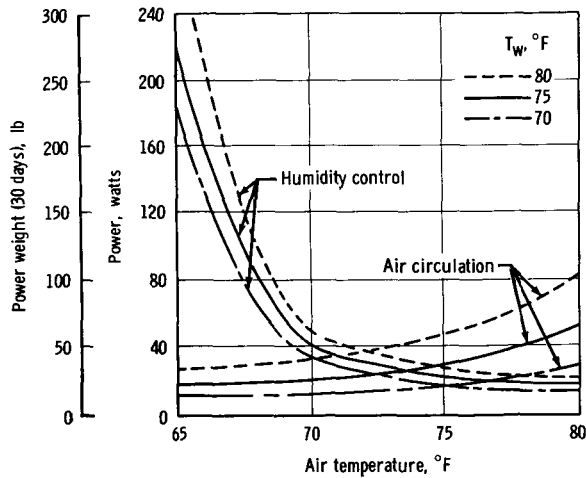
FIGURE 82.—*Humidity and air circulation power requirements.* $Q_m = 520$ *Btu/man-hr.* (AFTER BOEING.[12])

FIGURE 84.—*Temperature control margins.* (AFTER BOEING.[12])

Wall temperature.—Figure 83 indicates that the power weight penalty decreases with decreasing wall temperature. Even at an optimum value of T_a, 50 pounds or more of weight are at stake. The total weight penalty could be doubled. However, in the selection of wall temperature one must consider, in addition to weight implications, the effect of higher, off-design metabolic rates and the system control concept. Figure 84 shows the allowable range of temperatures to prevent condensation on the vehicle walls and

FIGURE 83.—*Combined humidity and air circulation power requirements.* $Q_m = 520$ *Btu/man-hr.* (AFTER BOEING.[12])

equipment. From an independent study of wall heat leak, the minimum surface temperature allowable in the compartments was selected at 65° F. This temperature allows a margin of 5° between equipment temperature and the maximum dew point. A $\pm 4°$ allowance was made for locations above and below the mean radiant temperature and a control tolerance of $\pm 1°$ F was selected. This establishes a minimum temperature of 70° F for air and mean radiant temperature.

Figure 85 compares the capability of two systems to accommodate high, off-design metabolic rates. System A is designed for a T_a of 75° F and a T_w of 70° F; system B is designed for a T_a of 75° F and a T_w of 75°. A comparison of figures 85(a) and 85(b) shows that system B can accommodate higher metabolic rates than system A at equal values of f_s (effective sweating area fraction). The crew duty cycles showed that the system chosen must have the ability to absorb 780 Btu/hr for 1.5 hours. System B accommodates this rate (fig. 85(b), point P) with approximately 20 percent of the body covered with perspiration if the wall and air temperature is 70° F. At the same heat load, system A requires that approximately 50 percent of the body perspire. In addition, system B accommodates the heat output during exercise (1400 Btu/hr).

Evaporative losses during normal activities
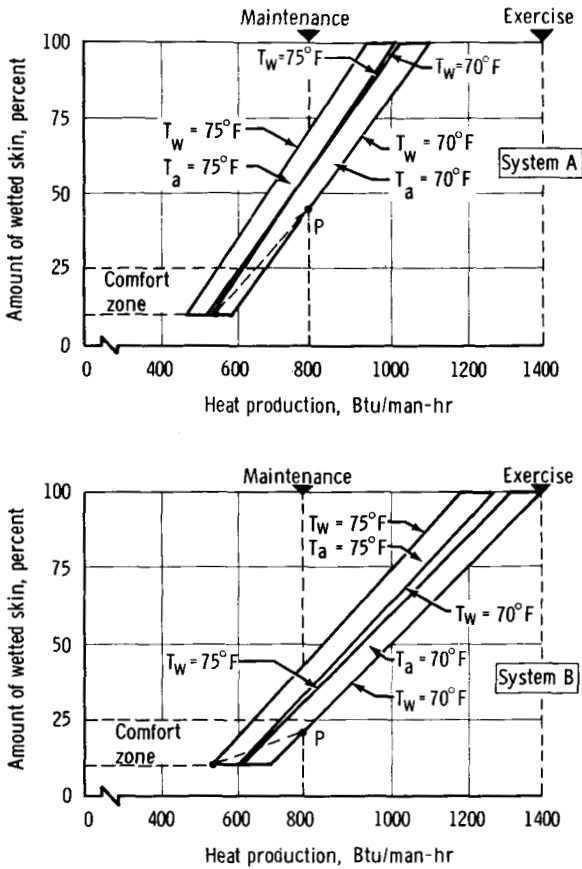
FIGURE 85.—*Wetted skin plotted against heat production. System A: $T_a=75°$ F; $T_w=70°$ F; $V_a=25$ ft/min. System B: $T_a=75°$ F; $T_w=75°$ F; $V_a=47$ ft/min.* (AFTER BOEING.[12])

FIGURE 86.—*Heat rejection distribution. $T_a=75°$ F; $P=7.0$ psia; $V_a=47$ ft/min; $T_{cl}=89°$ F.* (AFTER BOEING.[12])

with air velocity at 47 ft/min and air and wall temperature at 75° F represent approximately 20 percent of the total cooling requirement indicated in figure 86. Table 1 suggests that lightly exercising men are comfortable when evaporative capacity is between 10 and 25 percent. The effect of lowering the wall temperature during increased activity is also shown in figure 86. Lowering the wall temperature from 75° to 70° F increases the radiative losses from 220 to 295 Btu/hr, thereby allowing man to work at an increased rate without increased evaporative losses. Beginning at a work activity corresponding to a heat production of approximately 605 Btu/hr, the evaporative losses increase to maintain a heat balance. At 605 Btu/hr the man's skin may be approximately 10 percent wet. Further increase in activity results in increased wetness and eventually

heavy sweating occurs. The exact quantitation of the fractional wetness factor in exercising individuals in altered environments requires further study. These periods of high activity are expected to be short, such as those in a programed exercise period. During periods of lower activity, the crewman may have to don more clothing above 0.15 Clo in order to remain comfortable, especially during sleep.

It was assumed that wall temperature can be controlled by varying the temperature of radiant panels mounted in the crew compartment. The surface temperatures of many of the consoles and equipment cabinets can be controlled by mounting cold plates on the cabin side of the electronic packages. Any surfaces without cold-plate temperature control such as storage cabinets can, if necessary, be shielded from the crewmembers by radiant panels which are kept at the desired temperature. Since the pressure drop in the panels is very low and the panels are incorporated into the water loop, no power penalty is assessed against the crew temperature control system for radiant temperature control. The weight of the panels does not depend on the operating temperature, which is controlled by varying the water-flow rate and temperature. Therefore, the weight penalty for radiant temperature control is constant and does not influence the optimum radiant temperature. How-

ever, if the wall-temperature design of 70° F is selected, obviously the wall-temperature could not be lowered if condensation on the wall is to be avoided (fig. 84). In this instance control of higher metabolic rates would require a variable air velocity. This design approach requires a multiple-speed blower or multiple blowers which would introduce problems of hardware availability, development cost, reliability, and system complexity.

Returning again to figure 85, one sees that under design conditions, the system for $T_w = 70°$ F requires an air velocity of approximately 25 ft/min and the system for $T_w = 75°$ F requires an air velocity of approximately 47 ft/min. The weight penalty of 20 pounds for the 75° F design is largely due to the power penalty associated with the higher air velocity. A pertinent unresolved physiological problem is the determination of minimum velocity requirements under zero gravity for subjective comfort, aside from thermal balance considerations. Although there is no experimental evidence to substantiate a conclusion, it was assumed that either system A or system B provided adequate air velocity because both systems met or exceeded normally acceptable sea-level air-velocity values (15 to 25 ft/min).

The factors influencing the selection of wall temperature are summarized as follows:

	System A $T_a=75°$; $T_w=70°$	System B $T_a=75°$; $T_w=75°$
Weight penalty, lb........	0	+20
f_t at 780 Btu (maximum sustained level), percent.	45	20
Control concept for peak metabolic rates.	Air temperature and additional equipment	Air and wall temperature
Air velocity, ft/min.......	25	47

As a result of the above evaluation, a wall temperature of 75° (system B) was selected as an on-design value.

Humidity control.—Relative humidity maintained between 40 and 60 percent is desirable due to both physiological and engineering considerations. It was suggested that below 40 percent for prolonged periods some people tend to suffer discomfort such as dry skin and chapped lips.

Air at 75° F and 60 percent relative humidity has a dewpoint temperature of 60° F. The lower limit for wall temperature has been established as 70° F as noted in figure 84. Consideration of these two design parameters provides a 5° F margin of safety before condensation on the wall can occur. To permit humidity control over a range of metabolic activities, it is desirable to control the condensing temperature. As illustrated in figure 87, a system designed for a relative humidity of 50 percent and a condensing temperature of 45° F has twice the capacity when relative humidity is increased to 60 percent and condensing temperature is lowered to 40° F.

Air circulation.—The power requirements for the air circulation system are given in figure 82 for a 7-psia mixed-gas atmosphere. The circulation system consists of two fans and a single-fan heat exchanger combination. One fan is directed over each crewmember at the control console to provide the air velocity required for cooling. The fans are assumed to provide 5 ft³/min of air flow for each watt of power consumed, a value typical of the fans considered for this application.

The cabin ventilation fan-heat exchanger unit provides overall air circulation in the cabin and maintains the air temperature at the desired level. The heat exchanger removes the heat transferred by convection to the air from the crewmembers and the heat dissipated by the two fans. The air-flow rate through the fan-heat exchanger unit is determined by allowing a temperature drop of 10° F across the unit. Equations for fan design and power tradeoffs can be found in the study by Coe et al.[20]

A single-fan circulation system is being considered as a substitute for the three-fan system.
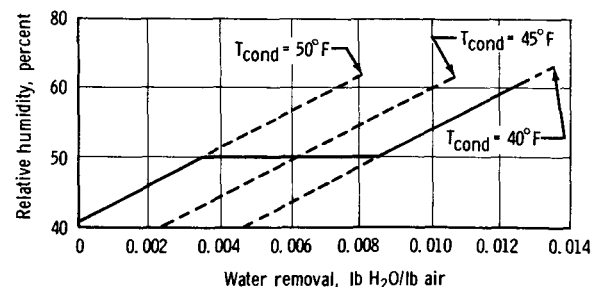

FIGURE 87.—*Humidity control flexibility.* $T_a=75°$ F; $P=7.0$ psia. (AFTER BOEING.[12])

Preliminary scale-model tests at Boeing have shown that a circulating-flow pattern can be obtained by employing a centrally located ceiling inlet with a single outlet located on the opposite face near the outer wall. The air from the inlet flows along the ceiling at a relatively high velocity, entraining flow from the center of the chamber. The resulting circulation pattern is maintained and is not destroyed by the outflow when the outlet is located near the outer wall on the wall opposite the inlet.

Conclusion. — Based on this study an air temperature of $75° \pm 5°$ F, a relative humidity of 50 ± 10 percent, a mean radiant temperature (wall temperature) of $75° \pm 5°$ F, and an air velocity of approximately 47 ft/min were recommended. This recommendation is based on the crew wearing clothes with an insulation factor equal to 0.10 Clo. During periods of normal activity, the air and wall temperature are maintained at 75° F and relative humidity is a nominal 50 percent. At periods of higher activity the air and wall temperatures are decreased to 70° F. During periods of extremely high activity, such as exercise, the crew is permitted to sweat. At periods of lower activity, the crew has the option of adding more clothing or increasing air and wall temperature. In all cases, relative humidity control is maintained by adjustment of condensing temperature in the humidity control system.

Thus, the mission subtask of high exercise conditions the selection of air temperature and wall temperature and mode of control during peaks. The basic power penalty of figure 83 for T_w of 75° F can then be assumed as the on-design point for the mission. Figure 83 indicates that these assumptions give a total power penalty of about 56 watts/man for the water removal and cabin ventilation systems. This is equivalent to about 68 lb/man over the 30-day mission or about 136 pounds for the overall mission.

Unfortunately, another requirement on the designer was to include the possibility of a suited man in the atmosphere-control loop during emergency situations. This would impose a ΔP of 8 inches of water which was assumed in table 29. Therefore, it was felt that the tradeoffs should include the suit-in-the-loop values of tables 26 and 29. Table 30 compares the values for sub-

system power, total power, and total weight assuming the conservative power-weight-penalty of 1.25 and the most optimistic value of 0.70 lb/watt.

As predicted from the Q, ΔT requirement of table 23, table 30 indicates that the power for the suit and humidity control is much less sensitive to gas specific factors than is ventilation power. Analysis of the total power of the air-conditioning system indicates that under the specific design assumptions in question, oxygen-helium mixtures at both 5 and 7 psia require equal power and that this power is less than that for the other gas mixtures. At least 90 watts may be saved by going from an oxygen-nitrogen mixture at 7 psia to any one of the helium mixtures. This represents 114 pounds for the conservative power weight penalty but only 55 pounds for the optimistic penalty of 0.7 lb/watt. Thus, the power penalty conditions the absolute weight differentials between gases. It is also clear that the design contigency of a suit-in-the-loop increases the weight differential between gases. By increasing the total power penalty for two men from 112 lb/mission (fig. 83) to 163 lb/mission (table 30), the suit contingency increases the baseline from which the other values are determined. In comparing gas-specific tradeoffs, one must keep such seemingly minor, yet sensitive factors in mind.

A new approach to gas circulation in space cabins has been suggested by Keating.[49] This technique makes use of the energy obtained by isentropic expansion in the circulation process. The technique may decrease the fan-power penalties which can be a considerable part of the overall weight penalty of the environmental control system.

RELIABILITY — WEIGHT INTERACTIONS AND GAS CONTROL SYSTEMS

Reliability is an important criterion in evaluating the weight specific factors in atmospheric control systems. In certain cases, there is little information on which to base component failure rates. However, the use of good engineering judgment will tend to give reasonably valid system reliabilities, especially when these results are to be used primarily in a relative rather than an absolute comparison.

TABLE 30. — *Weight and Power Tradeoffs of the Air-Conditioning System for a 2-Man Orbiting Laboratory* [DATA FROM BOEING [12]]

[RATIOS AND PENALTIES BASED ON A 7.0-PSIA OXYGEN-NITROGEN SYSTEM]

	7 psia		5 psia		
	3.5 psia O_2 3.5 psia N_2	3.5 psia O_2 3.5 psia He	3.5 psia O_2 1.5 psia N_2	3.5 psia O_2 1.5 psia He	5 psia O_2
Humidity control power (suit in loop)					
Power, watts..	100	60	72	53	72
Ratio..	1	0.60	0.72	0.53	0.70
Power penalty, watts...............................	0	−40	−28	−47	−28
Ventilation power					
Power, watts..	63	10	62	19	61
Ratio..	1	0.16	0.98	0.30	0.97
Power penalty, watts...............................	0	−53	−1	−44	−2
Total power					
Power, watts..	163	70	134	72	133
Ratio..	1	0.43	0.90	0.44	0.80
Power penalty, watts...............................	0	−93	−29	−91	−30
Weight penalty (1.25 lb/watt)					
Weight, lb..	201	87	167	90	166
Ratio..	1	0.43	0.82	0.44	0.81
Weight penalty, lb..................................	0	−114	−34	−111	−35
Weight penalty (0.70 lb/watt)					
Weight, lb..	104	49	94	50	93
Ratio..	1	0.43	0.82	.0.44	0.89
Weight penalty, lb..................................	0	−55	−10	−54	−11

Reliability studies should be made with full cognizance of the critical nature of specific malfunctions and the results of failures of parts and systems. Advantage should be taken, and reflected in the reliability calculations, of the possibilities of redundancy and of replacement

and repair of components when a human operator is present. Unfortunately, reliability factors cannot always be included in the preliminary design phase of a program where tradeoffs of gas-specific factors need to be made.

The reliability of partial-pressure sensing instruments is an issue of great pertinence to the selection of cabin atmospheres. Little reliability data of this type are available on the most recent sensing systems.

The cabin with 5-psia oxygen has a very reliable control system based on a simple sensor for total cabin pressure. As oxygen is consumed and carbon dioxide is absorbed, the cabin pressure drops and more oxygen is allowed to enter the cabin to offset this pressure drop. Mixed-gas cabins require partial-pressure sensors for one of the two gases in order to maintain a constant percentage of both gases in the face of simultaneous oxygen consumption by the crew and variable, mixed-gas leakage from the cabin.

Many different p_{O_2} sensors are available, but no device with ruggedness and long-term reliability of the simple anaeroid sensor of the 5-psia oxygen system has been developed.[86] A flyable, ultraviolet-absorption p_{O_2} meter is currently under development for the NASA by the Perkin Elmer Co.[42] There are still some unresolved problems in the area of the interference by water vapor and carbon dioxide in the ultraviolet band being sampled. Polarographic sensors all appear to have a limited duration of performance without adjustments or replacement of the sensor elements.[47] Chromatographic techniques are available but these are costly in terms of weight and are not as reliable as might be desired in flight equipment. A flyable chromatograph is under development by the Beckman Instrument Co.[5, 114, 115] Time-of-flight mass spectrometers also have the same problems of reliability and flight worthiness.[5] A coincidence mass-spectrometer suitable for flight operations is also under development by the Johnson Laboratories of Baltimore for the AiResearch Corp. but no reliability data are available as yet.[66]

The General Electric Co. is developing fuel-cell sensors which may operate as part of the hydrogen-oxygen fuel cell of the main power supply or be self-contained instruments. Again,

no reliability data are available.[60] Flyable hardware is now under development.[110]

Two new approaches to flyable oxygen sensing devices appear encouraging. A zirconium-oxide solid-electrolyte cell with high temperature operation is under development by the Westinghouse Electric Corp.[105] and a thin-film metal oxide process is under study at the Research Triangle Institute of North Carolina.[119] No reliability data are as yet available.

Sensing inert gas components is another approach to the problem. Helium, by virtue of its unusual physical properties, presents the greatest opportunity for flyable instrumentation. Such physical approaches as thermal conductivity, sound resonance, mass and coincidence spectrometry, and others, offer good potential, but no flight hardware has been developed. An ionization gage has been developed for analysis of helium-oxygen mixtures in gas dynamics laboratories.[70] In spite of the complexity of the circuitry, the modification of such a device for spacecraft use may be a fruitful approach.

A thermal conductivity meter has been used by Meneely and Kaltreider[71] in physiological experiments to separate helium from other respiratory gases and contaminants. An acoustic gas analyzer of the National Instrument Laboratories has also been used by Faulconer and Ridley[30] in respiratory physiology.

The weight penalty and reliability factors associated with the additional controls as well as the sensors in mixed gas systems must also be accounted for. Several control instruments for mixed-gas control are available.[88, 15, 73] It has been estimated that additional weight for a mixed-gas control above that for 5-psia oxygen will range from 12 to 15 pounds.[46, 79] It has also been estimated that for the Apollo spacecraft, substitution of a 7-psia oxygen-nitrogen system for the present 5-psia system would increase the total gas systems weight penalty, including sensors, controls, and tankage, by only 52 pounds or about 10 percent.[66]

TRANSIENT PHENOMENA

Several transient phenomena influence gas-specific tradeoffs. The first has already been covered in the discussion of rapid leakage of gas

from the cabin in a previous section of this chapter. Figures 20 and 21 and table 5 compare the approximate time available to the crewman prior to the onset of physiological symptoms of hypoxia after exposure to the several different gas mixtures in question. The problem of lock repressurization rates in emergencies was also covered in a previous section of this chapter.

Failure of the environmental control system can produce transient problems. Failure of the control system for p_{O_2} may result in periods of progressive hypoxia before repairs can be made. In such a case, the time available for action by the crewman will depend only on the original p_{O_2} in the cabin. Under such circumstances, the cabin with the highest p_{O_2}, pure oxygen at 5 psia, will allow the longest time. There will be no time difference between the other mixtures since they all have the same p_{O_2} of 3.5 psia. After any failure of this type, the amount of time available will, of course, depend on the volume of cabin per man.

As was discussed previously, transient exercise loads in the cabin can condition the selection of cabin and wall temperatures and thus influence gas-specific power penalties.

POWER SYSTEM FACTORS

The power-weight penalties for several systems have been discussed. In general, the larger the system, the lower the power-weight penalty. For missions of long duration, solar-cell and nuclear-power weight penalties are about 200 to 300 lb/kW. Smaller vehicles and shorter flight durations require 400 or more lb/kW. Since little or no flight experience has been gained with larger solar cells or nuclear reactors, these estimated penalties must be used with much reservation. There is a recent review on the availability and reliability of several different power-generation systems in spacecraft.[106]

Fuel-cell penalties are closely dependent on the cryogenic systems. Integration of fuel cell and life support systems is a complex factor which has received much study.[13, 57, 33, 45, 96, 80, 48] Integration of the total power system with life support equipment has also been reported.[37, 118, 48] A review of this problem is beyond the scope of the present study. The role of cryogenic integration in possibly reducing the power penalty

for the 30-day, two-man, orbiting laboratory from 1.25 to 0.7 lb/watt has been discussed.

There is presently at the Manned Spacecraft Center in Houston, a project on the design of computer-assisted design and tradeoff tools.[48] This study should be of great value in system integration.

ECONOMIC AND OPERATIONAL FACTORS

In an overall evaluation of atmosphere selection, economic and operational factors must always be considered. These factors are treated very briefly here and specifically noted for each mixture in chapter 3.

Development Time

The development status of each component and subsystem should be determined to provide an evaluation as to the probability that the total system can be developed within the known limitations of time and budget. For example, the design of some components, such as heat exchangers and ducts, is so well advanced that they may be assumed to perform as required with little or no development. On the other hand, development of helium and neon tankage or regenerative chemical systems for space application will require extensive development, together with some risk that it will not be possible to reach the goals at the desired time. A closely related problem is the adaptability of the system to different mission profiles, a requirement which is becoming ever more essential.

Uses of Existing Hardware and Equipment

Uses of existing hardware and equipment are closely related to development time. Whenever possible, off-the-shelf hardware should be considered in evaluating system weight, reliability, and costs in gas-specific tradeoffs. The most obvious lack of this type of equipment is in small flightworthy helium and neon tankage and mixed gas controls.

Maintenance and Convertibility

The maintenance and convertibility factor relates primarily to the control systems involved. There is a big gap between the simple aneroid controls for the 5-psia oxygen system and the

complex controls of the mixed gas systems, but except for diluent sensors, very little difference exists between the individual mixed gas systems.

Crew Acceptance

In view of the discussions regarding the physiological factors in parts I, II, and III of this series [90, 91, 92] and in chapter 1 of this present report, there is little to suggest that any of the gas mixtures will cause problems as far as crew acceptance is concerned. There may be problems of aural and pulmonary atelectasis in longer missions with 5-psia oxygen, but they have not appeared as yet in the limited flight experience up to 14 days. The more subtle metabolic problems hypothesized for 5 psia oxygen or for the lack of nitrogen in the helium or neon mixtures also require further experimentation and flight testing before evaluation of crew acceptance can be made.

Contaminant Buildup

There is a definite interaction between 5 psia oxygen atmospheres and the toxic contaminant problem.[90, 2] Current experimentation by the Aerojet-General Corp. and the Toxic Hazards Branch of the 6570th Aerospace Medical Research Laboratories of Wright-Patterson Air Force Base, Ohio, should answer the many questions along these lines. There is no reason to suspect that the slightly reduced p_{N_2} in the oxygen-nitrogen mixtures or presence of helium and neon in the other mixtures will significantly alter the toxic contaminant hazard.[92]

Qualification Testing

This factor will extend development programs for the mixed gas systems, especially helium and neon beyond those required for 5-psia oxygen.

Environment for Inflight Experiments

There is always a problem of comparing results of inflight physical and physiological experiments with the controls performed on the ground in sea-level air environments. The need for simulation chambers for ground controls does add an expense and nuisance factor. From an overall point of view, the 7-psia oxygen-nitrogen environment should least influence this requirement. The 5-psia oxygen, oxygen-helium, and oxygen-neon environments will exert a slightly greater effect. In any case, where the gaseous environment will interfere with interpretation of results, appropriate simulated ground controls will be required for any of these mixtures. In a practical sense, this factor should in no way discriminate between the gas mixtures in question.

Complexity of Design and Operation

Aside from the partial pressure control system of all the mixed gases and the design of small, flyable cryogenic tankage for helium and neon, there appears to be little major difference between the different gas systems in complexity of design. There are second-order design and operational factors which may arise in systems integration or mission analysis which would require gas-specific orientation. All of these must ultimately be taken into consideration in arriving at conclusions relative to the advantages and disadvantages of competing gas systems. Interfaces also may be considered as placing restraints or requirements on the system. Many of the interfaces have already been covered. Typical of the often unconsidered interfaces are the following: [95]

(1) Thermal loads to and from other vehicle systems, including vehicle structure.

(2) Power requirements (including quality, type, amount, and variation of rate of secondary systems).

(3) Metabolic inputs from occupants, carbon dioxide, water vapor, and odors in normal and in off-design modes.

(4) Vibration and shock loads, including those generated within the system and those received from outside.

(5) Noise generated by operation of the system.

(6) Control linkages for operation of the atmospheric control system itself.

(7) Space and relative location requirements within the vehicle. The resolution of this item usually requires the use of mockups and tradeoff studies with other spacecraft systems.

(8) The ground checkout system.

(9) Onboard display instrumentation.

(10) Instrumentation providing information to be telemetered.

(11) Provision for supplying an atmosphere for use in a backpack to provide atmospheric control for a pressure suit used for extravehicular operations.

(12) Provision for the use of an airlock to enable occupants in pressure suits to leave and reenter the space vehicle and resulting repressurization needs.

(13) Prompt detection of malfunctions within the system and the transmission of the information to the astronauts.

(14) Interaction with operator; manual control required; extent and scheduling of operator's time; special skills required.

(15) Mechanical support of system components on vehicle load-bearing points.

Cost

The cost factor may loom large in a tradeoff analysis, although it often is not as large as in a basic decision regarding launch-vehicle function. The least expensive is no doubt the 5-psia oxygen system. Availability of hardware and simplicity of controls dictate this factor. Development costs of oxygen-nitrogen systems will no doubt be less expensive than corresponding helium and neon systems. Because of the overall weight savings which may be possible with the helium or neon, the long-range, operational and total program costs may more than make up the difference.

Comparative Analysis of Atmosphere Tradeoffs of the Environmental Control System

IN THE FIRST TWO CHAPTERS, basic data and analytic techniques for performing tradeoff analysis of atmosphere-related environmental control subsystems were presented. An attempt was made to reduce the data to readily available tabular or graphic form and to outline the pitfalls of analysis in each subsystem. The absolute weight penalties determined by the Boeing Co. for a 30-day two-man orbiting laboratory with a volume of about 1200 ft^3 (divided into 750 and 450 ft^3 compartments) were presented in detail. The diluent gas storage tradeoffs were presented in table 16, and the overall air-conditioning tradeoffs were presented in table 30. To arrive at a total system weight penalty, an analysis of the usage rates and total weight of oxygen and diluents must be determined. To these are added the pertinent storage weight penalties to arrive at the total gas-storage subsystem penalty. By adding the total air-conditioning subsystem power-weight penalties to the total storage subsystem weight penalties and adding control weight differences, one can arrive at the gas-specific penalties for the total environmental control system.

The total expendable gas weight was determined by the Boeing Co.,[12] who analyzed the normal requirements for metabolic consumption and leakage as described in chapters 1 and 2. To this was added the estimated oxygen consumed in extravehicular trips, and consumed in the Gemini trips including leakage. An additional weight of gas was needed to cover gas lost in the carbon dioxide removal process and in the catalytic burner. It was also required to account for the gas lost in cabin repressurizations when the air-lock compartment or whole vehicle was used for extravehicular operations. To these expendable requirements was added a 10-percent reserve. Table 31 represented the tabulation of these estimates.

It can be seen that for oxygen, metabolic utilization in the spacecraft cabin was the single greatest usage factor, followed by the Gemini leakage and extravehicular trips. For diluent, spacecraft cabin leakage was the greatest factor, followed by extravehicular trips and laboratory repressurization.

The approximate tankage penalty for oxygen may be determined by entering the graph for supercritical oxygen (fig. 34(b)) and noting that in the range of 315 and 344 pounds of oxygen the tankage penalty is 1.13 pounds of total weight per pound of oxygen stored. This is lower than the older equivalent penalty figure of about 1.5 pounds per pound of fill seen in figure 34(a). It also includes no accessory weights. For the helium diluent tankage penalty of table 31, the data for low-temperature gaseous storage in table 16 were used. The values in parentheses were calculated using the supercritical nonvented storage penalty of 3.8 lb/lb determined by Mason and Potter for pressure variant delivery.[66] For the nitrogen diluent tankage penalty, the values for supercritical vented storage in table 16 were used. The values in parentheses are the tank penalties calculated from the advanced state-of-the-art value of supercritical nitrogen from the data of Rousseau et al.[95] in figure 39(a) where the penalties for 86 and 32 pounds of fill are 1.18 and 1.20, respectively. The two different sets of

TABLE 31.—*Expendable Fluid Requirements and Total Environmental Control System Weight Penalties for a 30-Day, 2-Man Orbiting-Laboratory Mission* [CALCULATED FROM THE DATA OF BOEING,[12] ROUSSEAU ET AL.,[95] AND MASON AND POTTER [66]]

[ALL VALUES IN POUNDS]

Function	7 psia		5 psia		5.0-psia O_2
	3.5-psia O_2 3.5-psia N_2	3.5-psia O_2 3.5-psia He	3.5-psia O_2 1.5-psia N_2	3.5-psia O_2 1.5-psia He	
Oxygen use:					
Extravehicular trips	32.4	32.4	32.4	32.4	46.3
Gemini trips	2.4	2.4	....	....	....
Laboratory repressurization	18.0	18.0	18.0	18.0	25.7
Metabolic	120.0	120.0	120.0	120.0	120.0
Leakage	32.1	29.0	22.9	21.6	31.5
CO_2 removal	13.6	13.6	13.6	13.6	19.5
Catalytic burner	5.0	5.0	5.0	5.0	5.0
Gemini leakage	75.0	75.0	75.0	75.0	75.0
Reserve, 10 percent	29.9	29.5	28.7	28.6	32.3
Total	328.4	324.9	315.6	314.2	355.3
Diluent use:					
Extravehicular trips	20.0	2.86	8.58	1.23	
Gemini trips	2.1	.3	....	....	
Laboratory repressurization	15.8	2.26	6.78	.97	
Leakage	27.9	3.58	8.6	1.14	
CO_2 removal	11.9	1.7	5.1	.73	
Reserve, 10 percent	7.8	1.1	2.9	.41	
Total	85.5	11.8	31.96	4.48	
Tankage:					
Oxygen	42.7	42.4	41.0	40.9	46.3
Diluent	89 (15.4)	93 (32.8)	76 (6.4)	48.5(12.4)	....
Total	131.7(58.1)	135.4(75.2)	117 (47.4)	89.4(53.3)	46.3
Gas storage:					
Total O_2 system	372	367	357	355	402
Total diluent system	174 (101)	105 (44.6)	108 (96)	53 (17.0)	....
Total	546 (482)	472 (412)	465 (453)	408 (372)	402
Fan power:					
Dehumidification	100	60	72	53	72
Ventilation	63	10	62	19	61
Total	163	70	134	72	133
Controls	15	15	15	15	....
Total ECS penalty	724 (660)	557 (497)	614 (602)	495 (459)	535
ΔW	0 (−64)	−167 (−227)	−110 (−122)	−229 (−265)	−189
ΔW	+189 (+125)	+22 (−38)	+79 (+67)	−40 (−76)	0

diluent tankage weights and total weights seen in table 31 represent a difference in approach often found in tradeoffs. The tankage penalty not in parentheses, all of which were taken from table 16, include, along with the dry tank weight, the weight of vent fluid, unavailable fluid, fill tolerance fluid, valves, heaters, and heater power weight. The values in parentheses include only dry tank weight with none of the accessories and controls. The latter are most often used in tradeoff studies. Differences in total storage weight and in total weight penalty reflect these differences in basic assumptions regarding gas storage.

At the bottom of table 31, the differences in total gas-specific weights for the environmental control system are tabulated with both 7-psia oxygen-nitrogen mixtures and 5-psia oxygen as baselines. The lightest weight penalty for the environmental control system was 459 pounds for the 5-psia oxygen-helium mixture. This was determined for optimum supercritical helium operating in the nonvented, pressure variant mode with an accessory-free penalty of 3.8 pounds total weight per pound of useful fill. The total penalty for an environmental control system using

gaseous storage cooled in liquid hydrogen with all the accessories added to the weight penalty was 36 pounds heavier at 495 pounds. The maximum difference of 265 pounds is between 7-psia oxygen-nitrogen mixture and 5-psia oxygen-helium mixture. The lightest system was 76 pounds lighter than the 5-psia oxygen system currently being employed.

What is the projected weight penalty for an oxygen-neon system? Liquid neon with an accessory-free tankage penalty of 1.85 pounds per pound of useful fill as opposed to 3.85 for liquid helium, (both supercritical and pressure variant mode) should reduce the diluent tankage below that of helium by a factor of only about $12.4 - 1.85 \times 4.48 = 3.9$ pounds. This is calculated by assuming the mass leak rates are similar (table 10).

The dehumidifying system is assumed to be of constant water removing capacity with respect to power penalty. The power ratios of the dehumidifying fans for oxygen-neon/oxygen-helium can be estimated by the ratios in equation (67).

$$\frac{\mathrm{HP}_{O_2\text{-Ne}}}{\mathrm{HP}_{O_2\text{-He}}} = \frac{\dot{W}_{g_{O_2\text{-Ne}}}}{\dot{W}_{g_{O_2\text{-He}}}} \times \frac{\rho_{O_2\text{-He}}}{\rho_{O_2\text{-Ne}}} \times \frac{\Delta P_{O_2\text{-Ne}}}{\Delta P_{O_2\text{-He}}} \tag{68}$$

From equation (66),

$$\frac{\mathrm{HP}_{O_2\text{-Ne}}}{\mathrm{HP}_{O_2\text{-He}}} = \frac{\dot{W}_{g_{O_2\text{-Ne}}}}{\dot{W}_{g_{O_2\text{-He}}}} \times \frac{\rho_{O_2\text{-He}}}{\rho_{O_2\text{-Ne}}} \times \left(\frac{\dot{W}_{g_{O_2\text{-Ne}}}}{\dot{W}_{g_{O_2\text{-He}}}}\right)^2 \times \frac{\rho_{O_2\text{-He}}}{\rho_{O_2\text{-Ne}}} \tag{69}$$

Since

$$\frac{\dot{W}_{g_2}}{\dot{W}_{g_1}} = \frac{\phi_1}{\phi_2} = \frac{R'_1}{R'_2} = \frac{m_2}{m_1} \tag{70}$$

and

$$\frac{\rho_2}{\rho_1} = \frac{m_2}{m_1} \tag{71}$$

$$\frac{\mathrm{HP}_{O_2\text{-Ne}}}{\mathrm{HP}_{O_2\text{-He}}} = \left(\frac{\dot{W}_{g_{O_2\text{-Ne}}}}{\dot{W}_{g_{O_2\text{-He}}}}\right)^3 \times \left(\frac{\rho_{O_2\text{-He}}}{\rho_{O_2\text{-Ne}}}\right)^2 = \left(\frac{m_2}{m_1}\right)^3 \left(\frac{m_1}{m_2}\right)^2 = \left(\frac{m_2}{m_1}\right) \tag{72}$$

therefore,

$$\frac{\mathrm{HP}_{O_2\text{-Ne}}}{\mathrm{HP}_{O_2\text{-He}}} = \frac{m_{O_2\text{-Ne}}}{m_{O_2\text{-He}}} = \frac{25.4}{23} = 1.1 \tag{73}$$

The ventilating system is a constant Q and ΔT system with respect to power penalty. According to table 23 the ventilating power ratios of the O_2-Ne/O_2-He should be:

$$\frac{HP_{O_2\text{-Ne}}}{HP_{O_2\text{-He}}} = \left(\frac{\rho_{O_2\text{-He}}}{\rho_{O_2\text{-Ne}}}\right)^2 \left(\frac{C_{p\,O_2\text{-He}}}{C_{p\,O_2\text{-Ne}}}\right)^3 \qquad (74)$$

Since the heat capacity of helium and neon are the same, the C_p factor drops out of the ventilation ratio. The relative power for ventilation becomes:

$$\frac{HP_{O_2\text{-Ne}}}{HP_{O_2\text{-He}}} = \left(\frac{1}{1.1}\right)^2 = (0.83) \qquad (75)$$

A rough estimate of the total weight of a 5-psia oxygen-neon system may be obtained from table 31:

$$355 + 1.85\,(4.48) + 1.1\,(53)$$
$$+ 0.83\,(19) + 15 = 452 \text{ pounds.}$$

This estimate suggests that the total weight for a 5-psia oxygen-neon system of 452 pounds is slightly less than that for an oxygen-helium system (459 lb) under the given design assumptions. It must be emphasized again that the estimated penalties of table 31 and the extrapolation to neon hold only for the specific 30-day, two-man orbiting laboratory under study.

Now these weight penalites are compared with those calculated independently by two other groups: the Lockheed Aircraft Corp.[61] and the Aerospace Corp.[46] Unfortunately, no textual material was available to explain the final tabular tradeoffs which are presented in tables 32 and 33. Both of these tables were for a 30-day, two-man orbiting laboratory of the same general size and mission as that of table 31. It is clear, however, that different assumptions were made regarding several critical parameters.

A comparison of tables 31 and 32 shows that there was a difference in major oxygen-leakage parameters assumed for the mission. There is a difference in diluent leakage and the tankage penalties for both oxygen and diluents. Fortuitously, the total gas-storage penalties are in the same general range, and the ratios between the different gas mixtures are quite similar.

In table 32, there was no partition between the dehumidification and ventilation functions. Also, fan weights of 11 pounds are included. Total fan power weights are higher in table 31. The ratios of the total fan-power weights are similar, with the only exception being the oxygen-helium mixtures. In table 32, the 7 psia has a higher weight than the 5 psia and in table 31, a slightly lower weight. The total environmental control system weights are quite similar; those of table 32 run slightly higher. The weight differences between the gases are quite similar, with the oxygen-helium mixture at 5 psia having the most favorable and oxygen-nitrogen mixture at 7 psia, the least favorable penalty.

Table 33 is far less complete than the others. Leakage was very much lighter, and repressurization gas usage was much heavier than in table 31. This may be a result of differences in interpretation and optimization of mission tasks. Unfortunately, no tankage penalties were recorded. There is, therefore, much weight unaccounted for when the total vehicle penalties are balanced against recorded data. Not all of this could possibly be tankage. The power weights were calculated by assuming a penalty of 2.4 lb/W. This is twice as high as that used in table 31 and, probably, in table 32 as well. The total weight penalties for the environmental control subsystem are generally higher than those recorded in either tables 31 or 32. This may be due to the higher power weight penalty and possibly a higher tankage penalty.

Table 33 is optimized for a circulation velocity of 50 ft/min. Figure 88 represents the pressure sensitivity of the total weight penalty for the vehicle, including tankage and power at the optimum velocity for each gas. The alveolar p_{O_2} is constant at 102 mm Hg in the mixed gas systems and increases with pressure in pure oxygen.

Once again, as in tables 31 and 32, the 5-psia oxygen-helium system had the lowest total environmental control subsystem penalty, and 7-psia oxygen-nitrogen system had the highest. The 7-psia oxygen-nitrogen system was slightly higher than the 5-psia oxygen-nitrogen system. Although the absolute values are not equal, all three tables appear to show similar weight ratios. The 5-psia oxygen system seems to have an intermediate penalty between 7-psia oxygen-helium system and 5-psia oxygen-nitrogen system. The significance of the similarity of results in all three

TABLE 32. — *Expendable Fluid Requirements and Total Environmental Control System Weight Penalties for a 30-Day, 2-Man Orbiting-Laboratory Mission* [AFTER LOCKHEED [61]]

[ALL VALUES IN POUNDS]

Function	7 psia		5 psia		5.0-psia O_2
	3.5-psia O_2 3.5-psia N_2	3.5-psia O_2 3.5-psia He	3.5-psia O_2 1.5-psia N_2	3.5-psia O_2 1.5-psia He	
Oxygen use:					
Metabolic	120	120	120	120	120
Leakage	45	55	41	49	60
Molecular sieve loss	10	10	10	10	15
Repressurization of laboratory	84	84	84	84	120
Repressurization of Gemini B	12	12	12	12	12
Reserve, 10 percent	27	28	27	28	33
Total fluid stored	298	309	294	303	360
Diluent use:					
Leakage	43	7.5	16	3	
Molecular sieve loss	8	1.2	4	.5	
Repressurization of laboratory	73	10.5	31	4.5	
Reserve, 10 percent	12	1.9	5	.8	
Total fluid stored	136	21.1	56	8.8	
Tankage:					
Oxygen tank penalty	89	93	88	91	108
Diluent tank penalty	74	87	31	36	....
Total tankage	163	180	119	127	108
Gas storage:					
Total O_2 system	387	402	382	394	468
Total diluent system	210	108	87	45	....
Total	597	510	469	439	468
Fan system:					
Fan weight	11	11	11	10	11
Fan power	246	142	180	107	180
Total	257	153	191	117	191
Total ECS penalty	854	663	660	556	659
ΔW	0	−191	−188	−298	−195
ΔW	+195	+4	+1	−103	0

studies will be more meaningful when the intermediary calculations are made available.

EFFECT OF MISSION LENGTH ON OVERALL ENVIRONMENTAL CONTROL SUBSYSTEM TRADEOFFS

At many points during the discussion of chapter 2, the effect of mission duration on sub-system penalties was demonstrated. It was made clear that as the duration of mission increases, the size and weight efficiency of many systems increase. Long standby times do penalize liquid storage. It is of interest now to compare the effects of mission duration on the total vehicle weight imposed by cabin factors such as structural weight, oxygen storage, diluent storage,

TABLE 33.—*Expendable Fluid Requirements and Total Environmental Control System Weight Penalties for a 30-Day, 2-Man Orbiting-Laboratory Mission* [AFTER JOHNSON [46]]

[ALL VALUES IN POUNDS]

Function	7 psia		5 psia		5.0-psia O_2
	3.5-psia O_2 3.5-psia N_2	3.5-psia O_2 3.5-psia He	3.5-psia O_2 1.5-psia N_2	3.5-psia O_2 1.5-psia He	
Oxygen use:					
Metabolic	120	120	120	120	120
Leakage	31.4	40.3	30.5	35.3	42.0
Repressurization	63.3	83.7	63.3	73.4	87.2
Total	214.7	244.0	213.8	228.7	249.2
Diluent use:					
Leakage	25.8	4.7	10.9	1.8	
Repressurization	53.6	9.7	22.6	3.8	
Total	79.4	14.4	33.5	5.6	
Gas storage:					
Tankage penalty	?	?	?	?	
Additional gas controls	15.0	15.0	15.0	15.0	
Total	?	?	?	?	
Power (optimized at $\bar{V}$ = 50 ft/min):					
Heat transfer	74.5	35.2	142.0	103.1	169.8
Circulation	216.1	138.0	160.9	119.0	169.8
Total	290.6	173.2	302.9	222.1	339.6
(Unaccounted weight)	325	313	231	223	220
Total vehicle penalty:	926	760	793	694	809
ΔW	0	−166	−133	−232	−117
ΔW	+117	−49	−16	−115	0

and fan and expulsion power. Figure 89 represents these interactions for cabins of pressures varying from 5 to 7 psia.[12] Basic vehicle weights of 10 000 and 13 000 lbs were used for mission durations of 30 and 60 days, respectively. An oxygen-helium mixture was used, with the helium being stored in gaseous form within the hydrogen tank (table 16). The weight effects of the increased hydrogen tank size are accounted for in the power penalties for atmosphere circulation. Because the study was performed at an earlier stage of design, the penalties are somewhat

higher than those used for the corresponding 30-day vehicle of table 31.

It can be seen that even for the 60-day mission, the maximum total environmental control subsystem penalty is only 17 000 pounds, or about 13 percent of the total vehicle weight. The maximum weight differences between designs are in the order of only 3 percent of the vehicle weight. In the longer missions there are some savings in environmental control subsystem weight from the more efficient storage of cryogenic fluids. The increase in structural weight conditioned
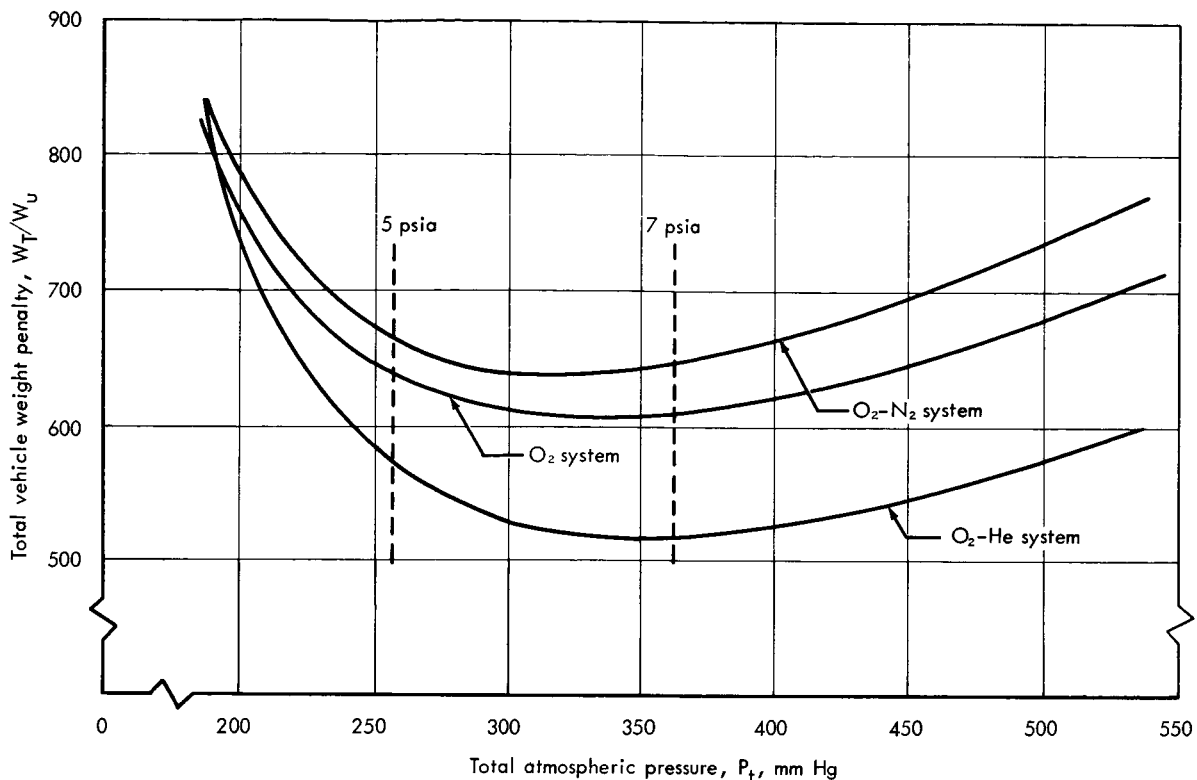
FIGURE 88.—*Total vehicle weight penalty for different gas systems with gas velocity optimized for each system.* (AFTER JOHNSON.[46])

by the higher pressure is minimal. The weight penalty of the diluent is almost equal to that of the fan and cryogenic expulsion power and is only slightly more sensitive to total pressure changes. Increased leakage at higher pressure probably accounts for the increase in diluent penalty.

It thus appears that the relative effect of different atmospheres on total vehicle weight is minimal. For a 30-day, two-man orbital mission, several hundred pounds are at stake. These few hundred pounds, however, may be quite significant in appreciation of total mission success.

SUMMARY OF TRADEOFFS IN THE SELECTION OF SPACE-CABIN ATMOSPHERES

In the several parts of this series, an attempt has been made to develop scientific criteria for the selection of space cabin atmospheres. The many interacting variables preclude a bold statement regarding a single optimum atmosphere.

At all levels of interest, there are mission-specific variables which strongly condition the optimization process.

In tables 34, 35, and 36 an attempt has been made to summarize the comparative values of each system. References to figures and tables in this study and to other parts of this series are included to aid the reader in reviewing the nature of the interaction involved. In the columns headed "Selection," an attempt has been made to place the five gas mixtures in a descending order of desirability. Those mixtures of equal desirability are placed in parentheses.

The remarks covering oxygen-helium systems also apply to oxygen-neon mixtures. The only major differences are the theoretical superiority of neon over helium in reducing bends and neurocirculatory collapse and increasing survival time after ebullism. Dehumidification power weight is slightly greater for oxygen-neon mixtures, while ventilation power weight is slightly less than that for oxygen-helium mixtures.
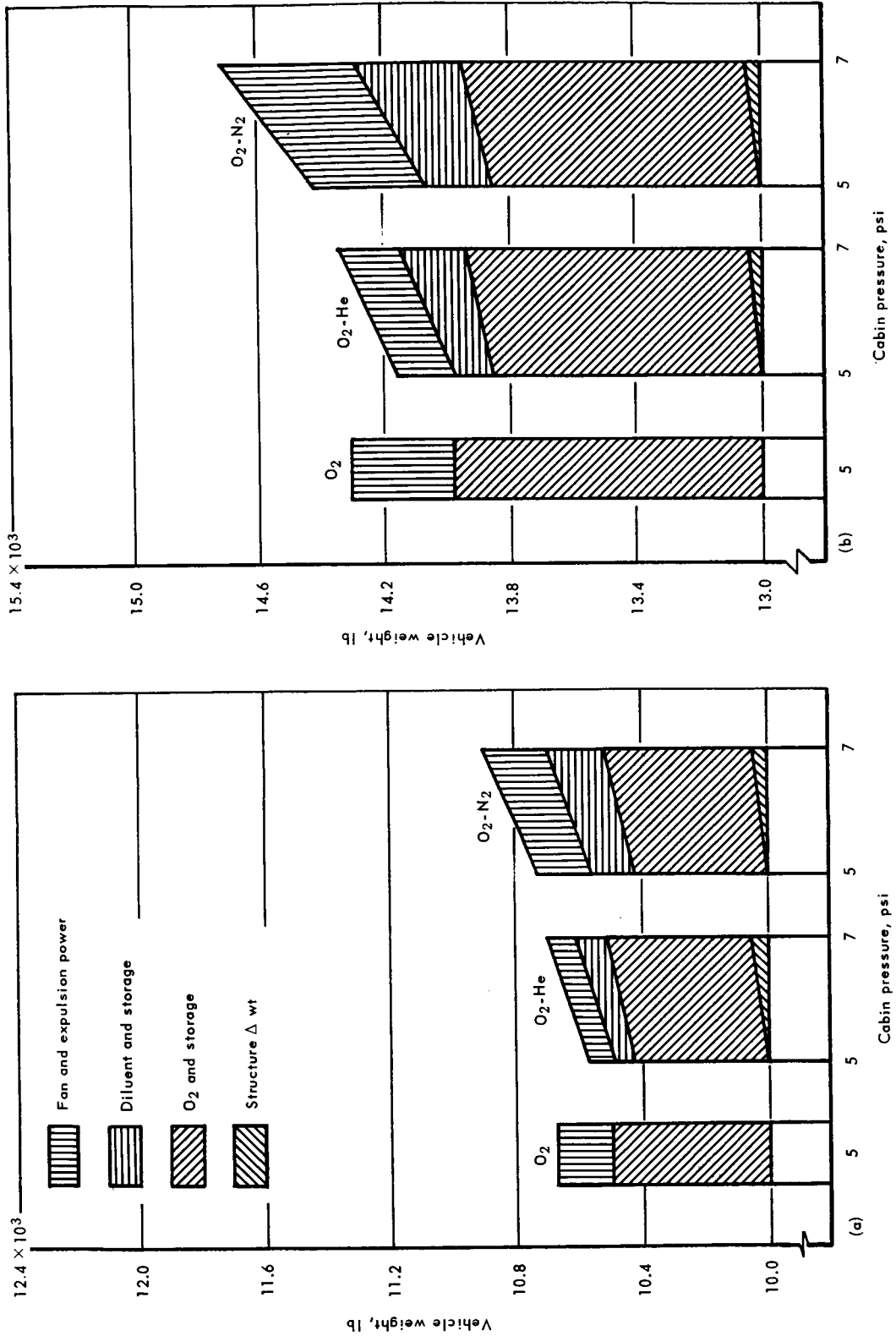
FIGURE 89.—*Total vehicle weight penalties for two-man orbiting laboratory.* (a) *30-day mission.* (b) *60-day mission.* (AFTER BOEING.[12])

TABLE 34. — Physiological Factors

Factor [a]	Mixed 7-psia		Mixed 5-psia		Single 5-psia	Selection order [b]
	1. 3.5-psia O_2 3.5-psia N_2	2. 3.5-psia O_2 3.5-psia He	3. 3.5-psia O_2 1.5-psia N_2	4. 3.5-psia O_2 1.5-psia He	5. 5-psia O_2	
1. Aural atelectasis (Part I) (fig. 2)	No problem	No problem	No problem	No problem	Does occur in laboratory	(1 2 3 4) 5
2. Pulmonary atelectasis (Part I) (fig. 2)	No problem	No problem	No problem	No problem	Does occur in laboratory	(1 2 3 4) 5
3. Vital capacity reduction (Part I) (fig. 2)	No problem	No problem	No problem	No problem	Does occur in laboratory	(1 2 3 4) 5
4. Hemolytic anemia (Part I)	No problem	No problem	No problem	No problem	Has occurred in laboratory; ? significance	(1 2 3 4) 5
5. Urinary abnormalities (Part I)	No problem	No problem	No problem	No problem	Has occurred in laboratory; ? significance	(1 2 3 4) 5
6. Radiation sensitivity (Parts I and III)	No change	No change	No change	No change	No change at this pressure	(1 2 3 4 5)
7. Voice pitch change (Part III)	Insignificant	Minimal	Insignificant	Minimal	Insignificant	1 (3 5) (4 2)
8. Decompression time prior to symptoms of hypoxia (table 6).	Longest available	Intermediate	Next to shortest	Shortest available	Intermediate	1 (5 2) 3 4
9. Alteration of trace contaminant effects (Part II).	None expected	None expected	None expected	None expected	Has occurred in laboratory	1 3 2 4 5
10. Abdominal gaseous distress	Least, same as 2	Least, same as 1	Most, same as 4 and 5	Most, same as 3 and 5	Most, same as 3 and 4	(1 2) (3 4 5)
11. Decompression sickness:						
(a) Bends (Part III)	Rare but most susceptible	Extremely rare; Intermediate susceptibility	Very rare intermediate susceptibility	Same as 3	Probably will not occur when fully denitrogenated	5 (4 3) (1 2)
(b) Neurocirculatory collapse (Part III)	Extremely rare; most susceptible		Very extremely rare	Insignificantly low possibility	Probably will not occur when fully denitrogenated	5 4 3 2 1
(c) Ebullism survival time (Part III)	Least time	Intermediate time	Intermediate time	More time	Most time	5 4 (2 3) 1
12. Explosive decompression (Part III)	Extremely rare; most susceptible	Extremely rare; low susceptibility	Extremely rare; Intermediate susceptibility	Extremely rare; lowest susceptibility	Extremely rare; Intermediate susceptibility	4 2 (3 5) 1
13. Blast overpressure (Parts II and III)	Intermediate lung damage; Worst gas emboli	More favorable than 1	More lung damage; less dangerous emboli than 2	More lung damage; less dangerous emboli than 2	Same lung damage; less dangerous emboli than 3	(2 4) 5 3 1
14. Flash blindness from meteoroid penetration. (Part II).	Least dangerous	Same as 1	Intermediate	Intermediate	Most dangerous	(1 2) (3 4) 5
15. Possible metabolic side effects (Part III)	Least	Slightly more than 4	Slightly greater than 1	Slightly less than 2	Most likely	1 3 4 2 5
16. Tolerance of high air temperature (table 3).	Least	Most	Slightly more than 1	Next to 2	Same as 3	2 4 (3 5) 1
17. Changes in bacterial flora of skin and mouth	Least	Same as 1	Much less expected than in 5	Much less expected than in 5	Does occur in laboratory	(1 2) (3 4) 5

[a] Parts I, II, and III refer to SP-47, SP-48, and SP-117 which are parts of the Space-Cabin Atmospheres series and are listed as references 90, 91, and 92 in this report. Tables and figures cited are in this report.

[b] Mixtures are presented in descending order of desirability; those within parentheses are equally desirable.

TABLE 35.—*Fire and Blast Hazards*

Factor [a]	Mixed 7-psia		Mixed 5-psia		Single 5-psia	Selection order [b]
	1. 3.5-psia O$_2$ 3.5-psia N$_2$	2. 3.5-psia O$_2$ 3.5-psia He	3. 3.5-psia O$_2$ 1.5-psia N$_2$	4. 3.5-psia O$_2$ 1.5-psia He	5. 5-psia O$_2$	
1. Burning rate of fabrics and plastics (Part II) and (ref. 40)	Slowest rate	Greater than 1 but hardest to ignite by contact with hot solid	Slightly greater rate than 2	Greater than 3 but harder to ignite by contact with hot solid	Fastest burning rate	(2 1) (4 3) 5
2. Flame temperature of burning hydrocarbon vapor (Part II)	Lowest	Probably same as 1	Slightly higher than 1	Probably same as 3	Highest	(2 1) (4 3) 5
3. Decompression time to extinguish flame (Part II) (table 6)	Longest	Intermediate	Next to shortest	Shortest	Intermediate	4 3 (2 5) 1
4. Selectivity of cabin materials (Part III)	Least restrictive	Same as 1	Intermediate	Same as 3	Most restrictive	(2 1) (4 3) 5
5. Flash oxidation from meteorite penetration (Part II) (See no. 14 of table 34)	Least dangerous	Slightly more dangerous than 1	Slightly more dangerous than 1	Slightly more dangerous than 3	Most dangerous	1 2 3 4 5
6. Reduction of fire hazard by zero-gravity (Part II)	Slightly more reduced than 3	Probably most reduced; most diffusible inertant at flame front.	Slightly less than 4	Slightly less than 2	Markedly reduced but least susceptible to zero-gravity effects	2 4 1 3 5
7. Toxicity of oxidation products of atmosphere (Part II)	Most toxic; oxides of nitrogen	Least toxic	Slightly less than 4	Least toxic	Same as 4	(2 4 5) (3 1)
8. See no. 13 of table 34						
9. Overall fire hazard (Part II)	Least severe	Same as 1	Intermediate	Intermediate	Most severe	(1 2) (3 4) 5

[a] Parts I, II, and III refer to SP-47, SP-48, and SP-117 which are parts of the Space-Cabin Atmospheres series and are listed as references 90, 91, and 92. Tables and figures cited are in this report.

[b] Mixtures are presented in descending order of desirability; those within parentheses are equally desirable.

TABLE 36.—Engineering Factors for 30-Day, 2-Man Orbiting Mission

Factor [a]	Mixed 7-psia		Mixed 5-psia		Single 5-psia	Selection order [b]
	1. 3.5-psia O$_2$ 3.5-psia N$_2$	2. 3.5-psia O$_2$ 3.5-psia He	3. 3.5-psia O$_2$ 1.5-psia N$_2$	4. 3.5-psia O$_2$ 1.5-psia He	5. 5-psia O$_2$	
1. Gas storage:						
Overall tankage weight penalty (figs. 34 to 43 and table 31).	Less than 2	Greatest	More than 5	Less than 1	Least	5 3 4 1 2
Weight of diluent gas used (table 31)........	Most	Slightly more than 4	Slightly less than 1	Least used	None	5 4 2 3 1
Total gas storage weight. (table 31)........	Most	Intermediate	Intermediate	Least	Slightly more than 4	4 5 (2 3) 1
2. Fan power weight (table 23):						
Atmosphere control (tables 27 to 30)........	Most	Slightly more than 4	Intermediate	Least	Intermediate	4 2 (3 5) 1
Ventilation and heat transfer (tables 24 to 26, 30).	Most (same as 3 and 5)	Least	Most (same as 1 and 5)	More than 2	Most (same as 1 and 3)	2 3 (5 4 1)
3. Controls, weight and complication........	More complicated than 5	Same as 1	Same as 1	Same as 1	Least weight and complication	5 (1 2 3 4)
4. Total ECS weight penalty (tables 31, 32, 33)........	Most	Intermediate	Intermediate	Least	Intermediate	4 5 (2 3) 1
5. Development time and cost........	Intermediate	High	Intermediate	Slightly more than 2 (if small diluent tankage)	Least	5 (1 3) (2 4)
6. Reliability of hardware........	Less than 5	Less than 1	Same as 1	Less than 3	Most	5 (1 3) (2 4)
7. Compatibility with current reentry modules........	Least	Same as 1	Intermediate	Intermediate	Most	5 (3 4) (1 2)
8. Sensitivity to extension of active missions to 90 days.	Little	Some increase in storage efficiency less than 4	Little	Value does gain slightly because of increased storage efficiency	Little	4 2 (1 3 5)
9. Sensitivity to standby operations........	Gaseous storage insensitive, cryogenic is same as 3 and 5	Sensitive due to greater heat sink of cryogenic helium; gaseous may leak at high pressure	Same as 1	Slightly greater than 2 due to greater heat leak; gaseous may leak at high pressure	Same as 1	(1 3 5) 2 4

[a] Tables and figures cited are in this report.
[b] Mixtures are presented in descending order of desirability; those within parentheses are equally desirable.

Tankage penalties for liquid neon are about half those for liquid helium. For the 30-day, two-man orbiting laboratory, the increased power weights almost match the decreased storage weights to give the oxygen-neon mixture a minimal advantage over the oxygen-helium mixture in total environmental control system weight penalty.

References

1. American Society of Heating, Refrigerating and Air Conditioning Engineers. ASHRAE Guide and Data Book. Fundamentals and Equipment for 1965 and 1966. ASHRAE, New York, 1965.
2. BACK, K. C.: Toxic Hazards Branch, 6570th Aerospace Medical Research Laboratories, Wright-Patterson AFB, Ohio. Biochemical effects of chronic exposure of animals at 100 percent oxygen environments. Unpublished data presented at the NASA Workshop Conference on Criteria for Selection and Evaluation of Space Mission Atmospheres, 1965.
3. BACK, K. C.; THOMAS, A. A.; and PINKERTON, M. K.: Toxicology, in Bioastronautics Data Book, P. Webb, (ed.), NASA-SP-3006, 1964, pp. 17-29.
4. BEARD, S. E.; ALLEN, T. H.; MCIVER, R. G.; et al.: Comparison of Helium and Nitrogen in Production of Bends in Simulated Orbital Flights, in Preprints of Scientific Program, 37th Annual Scientific Meeting, Aerospace Medical Association, Apr. 1966 (Las Vegas, Nev.), 1966, pp. 43-44.
5. Beckman Instruments, Inc.: Proposal for Gas Analyzer. Rept. CS-62-227, Fullerton, Calif., 1962.
6. BENZINGER, T. H.: The diminution of thermoregulatory sweating during cold-reception at the skin. *Proc. Nat. Acad. Sci.*, 47: 1683-1688, 1961.
7. BERENSON, P. J.: General Analysis of Human Thermal Comfort. Rept. No. SS-3245, AiResearch Mfg. Co., Los Angeles, Calif., 1965.
8. BERENSON, P. J.: Prediction of Human Thermal Comfort in Oxygen-Nitrogen Atmospheres, in Physiological and Performance Determinants in Manned Space Systems, Vol. 5., P. Horowitz (ed.), American Astronautical Soc., Baltimore, 1965, pp. 1-29.
9. BERRY, C. A.; COONS, D. O.; CATTERSON, A. D.; et al.: Man's Response to Long-Duration Flight in the Gemini Spacecraft, Gemini Midprogram Conference Including Experiment Results. NASA-SP-121, 1966, pp. 235-261.
10. BINDER, H. J.; HERTING, D. C.; HURST, V.; et al.: Tocopherol deficiency in man. *New Eng. J. Med.*, 273: 1288-1297, 1965.
11. BLOCKLEY, W. V.: Temperature, in Bioastronautics Data Book, P. Webb (ed.). NASA-SP-3006, 1964, pp. 103-131.
12. Boeing Company, ECS Flight Technology Group: Engineering Tradeoffs of Different Gas Systems Pertaining to the Selection of Space Cabin Atmospheres. Seattle, Wash., 1965 (unpublished data).
13. Boeing Company: Manned Environmental System Assessment. NASA-CR-134, 1964.
14. BOLLES, T. V.; SPEZIALI, V. A.; and THOMSON, G. W.: Microcontractor Utilizing High-Density Metallic Superoxide. NASA-CR-57021, General Dynamics Co., Electric Boat Div., Groton, Conn. (Rept. No. U413-64-164), 1964.
15. BOSTICK, C. R.: AiResearch Mfg. Co., Department 93-3, Los Angeles, Calif., personal communication, 1965.
16. BRINK, N. O.. Research on an Expandable Airlock Utilizing the Elastic Recovery Principle. NASA-CR-351, 1965.
17. BURTON, D. R.: Performance of water conditioned suits. *Aerospace Med.*, 37: 500-504, 1966.
18. CHRISTIAN, J. L.; and HURLICH, A.: Physical and Mechanical Properties of Pressure Vessel Materials for Application in a Cryogenic Environment—Part II. ASD-TDR-62-258, Pt. 2, General Dynamics/Astronautics, San Diego, Calif., Apr. 1963.
19. CLIFFORD, J.; KERSLAKE, D. McK.; and WADDELL, J. L.: The effect of wind speed on maximum evaporative capacity in man. *J. Physiol.*, 147: 253-259, 1959.
20. COE, C. S.; ROUSSEAU, J.; and SHAFFER, A.: Analytical Methods for Space Vehicle Atmospheric Control Processes. ASD-TR-61-162, Pt. II, AiResearch Mfg. Co., Los Angeles, Calif., Nov. 1962.
21. COOK, G. A. (ed.): Argon, Helium, and the Rare Gases: The Elements of the Helium Group. Vol. I: History, Occurrence, and Properties. Vol. II: Production, Analytical Determination, and Uses. Interscience Publishers, 1961.

22. DOBRYNINA, T. A.: Lithium Peroxide, Moscow, 1964.

23. DOHNER, C. V., Supervising Engineer, HTT-Thermodynamics Technology Component, Missile and Space Division, General Electric Co., Philadelphia, Pa., personal communication, 1966.

24. DRYDEN, C. E.; HAN, L. S.; HITCHCOCK, F. A.; et al.: Artificial Cabin Atmosphere Systems for High Altitude Aircraft. WADC–TR–55–353, Ohio State Univ. Research Foundation, Columbus, Ohio, Nov. 1956.

25. DUBOIS, A. B.; TURAIDS, T.; MAMMEN, R. E.; et al.: Pulmonary atelectasis in subjects breathing oxygen at sea level or at simulated altitude. *J. Appl. Physiol., 21:* 828–836, 1966.

26. DUCROS, H.; and BERANGER, S.: Use of Lithium Peroxide as an Agent for Purification of Tainted Air. FTD–TT–65–1792, 1 + 2 + 4, Foreign Technology Division, Wright-Patterson AFB, Ohio, Jan. 1966.

27. DUNBAR, W.: Corona Onset Voltage of Insulated and Bare Electrodes in Rarefied and Other Gases. AF–APL–TR–65–122, Boeing Co., Seattle, Wash., 1966.

28. ECKERT, E. R. G.; and DRAKE, R. M., JR.: Heat and Mass Transfer, McGraw-Hill Book Co., Inc., 1959.

29. EPPERSON, W. L.; QUIGLEY, D. G.; ROBERTSON, W. G.; et al.: Observations on Man in an Oxygen-Helium Environment at 380 mm Hg Total Pressure: III. Heat Exchange. SAM–TR–66–233, USAF School of Aerospace Medicine, Brooks AFB, Tex., May 1966.

30. FAULCONER, A.; and RIDLEY, R. W.: Continuous quantitative analysis of mixtures of oxygen and ether with and without nitrogen. I. Acoustic gas analyzer for mixtures of first three gases. *Anesthes., 11:* 265, 1950.

31. FISCHER, C.: Manned Space Center, National Aeronautics and Space Administration, Houston, Tex., personal communication, 1966.

32. GREEN, F. H.: Psychrometric Data. ARMC–66–537, AiResearch Mfg. Co., a division of the Garrett Corp., Los Angeles, Calif., May 15, 1966.

33. HALL, G. M.; and TREIRAT, E.: Study of Integrated Cryogenic Fueled Power Generating and Environmental Control Systems. Vol. III: Power Generating Equipment Study. ASD–TR–61–327, Vol. 3, Kidde (Walter) & Co., Belleville, N.J., Nov. 1961.

34. HALL, J.: Copper Manikin Regional Loss and Cooling Constants. Memo Rept. MCREXD–696–105P, Wright-Patterson AFB, Oct. 1950.

35. HALL, J. F.; BUEHRING, WILLI J.; and STROBL, W. W.: Effects of Various Gases on Handgear Insulation. AMRL–TR–65–4, Aerospace Medical Research Labs., Wright-Patterson AFB, Ohio, Dec. 1965.

36. Hamilton Standard Div. of United Aircraft Corp.: Manned Orbiting Space Station. Vol. 4: Environmental Control and Life Support System Study, Final Report, NASA–CR–65088, May 1964.

37. HANSON, K. L.: Thermal Integration of Electrical Power and Life Support Systems for Manned Space Stations. NASA–CR–316, Nov. 1965.

38. HARDY, J. D. (ed.): Temperature. Its Measurement and Control in Science and Industry. Pt. 3: Biology and Medicine, Reinhold Pub. Corp., 1963.

39. HONMA, H.; and CROSBY, H. J. (eds.): A Symposium on Toxicity in the Closed Ecological System. Research Laboratories, Lockheed Missiles & Space Co., Palo Alto, Calif., 1963.

40. HUGGETT, C.; VON ELBE, G.; and HAGGERTY, W.: The Combustibility of Materials in Oxygen-Helium and Oxygen-Nitrogen Atmospheres. SAM–TR–66–85, USAF School of Aerospace Medicine, Brooks AFB, Tex., 1966.

41. HUGGETT, C.; VON ELBE, G.; HAGGERTY, W.; et al.: The Effects of 100 percent Oxygen at Reduced Pressure of the Ignitibility and Combustibility of Materials. SAM–TR–65–78, USAF School of Aerospace Medicine, Brooks AFB, Tex., 1965.

42. HULL, W.: Crew Systems Division, Manned Spacecraft Center, National Aeronautics and Space Administration, Houston, Tex., personal communication, 1965.

43. JACOBSON, S. L.: Engineering of the Sealed Cabin Atmosphere Control System. Presented at the 30th Annual Meeting of the Aeromedical Association, Apr. 27–29, 1959.

44. JENKINS, A. C; and COOK, G. A.: Gas Phase Properties, *in* Argon, Helium, and the Rare Gases: The Elements of the Helium Group. Vol. I: History, Occurrence, and Properties. G. A. Cook (ed.), Interscience Publishers, 1961, pp. 173–243.

45. JENNINGS, A. J.; and HALL, G. M.: Study of Integrated Cryogenic Fueled Power Generating and Environmental Control Systems. Vol. V: Integration and Control Studies. ASD–TR–61–327, Vol. 5, Kidde (Walter) & Co., Belleville, N.J., Nov. 1961.

46. JOHNSON, A. L.: Aerospace Corp., Manager, Life Support Section, Los Angeles, Calif., unpublished data. To be published in the Diluent Selection Study for the MOL Program, 1966.

47. JOHNSON, L. F., JR.; NEVILLE, J. R.; BANCROFT, R. W.; et al.: Physical Transducers for Sensing Oxygen. Review 8–63. USAF School of Aerospace Medicine, Brooks AFB, Tex., Aug. 1963.

48. JOHNSTON, R. S.: The Douglas G–189 Program for Calculating the Performance for Environmental Control in Life Support Systems. Chief, Crew Systems Division, Manned Spacecraft Center, NASA, Houston, Tex., personal communication, 1966.

49. KEATING, D. A.: Application of Gas Expansion to Fluid Circulation Devices in Manned Space Assemblies. AMRL–TR–65–26, Air Force Systems Command, Aerospace Medical Division, Wright-Patterson AFB, Ohio, Apr. 1965.

50. KEATING, D. A.: Design Study of High Pressure Oxygen Vessels. WADC–TR–59–767, Wright Air Development Center, Aerospace Medical Division, Wright-Patterson AFB, Ohio, Feb. 1960.

51. KEATING, D. A.; WEISWURM, K.; MEYER, C. M.; et al.: Manned Testing of a Semipassive Potassium Superoxide Atmosphere Control System. AMRL–TR–65–194, Aerospace Medical Division, Wright-Patterson AFB, Ohio, Nov. 1965.

52. KEATING, D. A.; and WEISWURM, K.: Potassium Superoxide Passive Air Regeneration Studies for Manned Sealed Environments. WADD–TR–60–707, Aerospace Medical Division, Wright-Patterson AFB, Ohio, 1960.

53. KERSLAKE, D. MCK.: Errors Arising From the Use of Mean Heat Exchange Coefficients in the Calculation of the Heat Exchanges of a Cylindrical Body in a Transverse Wind, in Temperature. Pt. 3: Biology and Medicine, J. E. Hardy (ed.), Reinhold Pub. Corp., 1963, pp. 183–190.

54. KIMZEY, J. H.; DOWNS, W. R.; ELDRED, C. H.; et al.: Flammability in Zero-Gravity Environment. NASA–TR–R–246, 1966.

55. KING, B. G.: High concentration-short time exposures and toxicity. J. Indust. Hyg. & Toxicol., 31: 365–375, 1949.

56. KINSLOW, M.; and MAJOR, B. M.: Systems of Units and Conversion Tables. AEDC–TDR–62–6. von Karman Gas Dynamics Facility, ARO Inc., Arnold Air Force Station, Tenn., Feb. 1962.

57. KNIGHTS, A.; JENNINGS, A.; and FORTE, M.: Study of Integrated Cryogenic Fueled Power Generating and Environmental Control Systems. Vol. IV: Environmental Control and Attitude Control Studies. ASD–TR–61–327, vol. 4, Kidde (Walter) & Co., Belleville, N.J., Nov. 1961.

58. KRANTZ, P.: Calculating human comfort. ASHRAE J., 1964, pp. 68–77.

59. KREITH, F.: Principles of Heat Transfer. International Textbook Co., 1962.

60. LAWTON, R. W.: General Electric Co., P.O. Box 8555, Philadelphia, Pa., personal communication, 1965.

61. Lockheed Missiles & Space Co., Bioastronautics Div., Sunnyvale, Calif., personal communication, 1965.

62. LUFT, U. C.: Data on Oxygen Pressure Effects Compiled for the Garrett Corp. The Lovelace Foundation, Albuquerque, N. Mex., 1962.

63. MCADAMS, W. H.: Heat Transmission. McGraw-Hill Book Co., Inc., 1954.

64. MCGOFF, M. J.: Potassium Superoxide Atmosphere Control Unit. AMRL–TR–65–44, MSA Research Corp., Callery, Pa., 1965.

65. MARKOWITZ, M. M.; and DEZMELYK, E. W.: A Study of the Application of Lithium Chemicals to Air Regeneration Techniques in Manned, Sealed Environments. AMRL–TDR–64–1, Foote Mineral Co., Exton, Pa., Feb. 1964.

66. MASON, J.; and POTTER, J.: AiResearch Mfg. Co., Los Angeles, Calif., personal communication of unpublished data, Mar. 1966.

67. MASON, J. L.; WAGGONER, J. N.; and RUDER, J.: The Two-Gas Spacecraft Cabin Atmosphere Engineering Considerations. Presented at the International Astronautics Federation Meeting (Athens, Greece), Sept. 13–19, 1965.

68. MATSCH, L. C.: Associate Technical Director, Linde Division, Union Carbide Corp., Tonawanda, N.Y., personal communication, Mar. 1966.

69. MAUSTELLAR, J. W.; MCGOFF, M. J.; KEATING, D. A.: and WEISWURM, K.: Superoxide Atmosphere Control System for Manned Space Assemblies. Presented at the 36th Annual Meeting of the Aerospace Medical Association (New York), Apr. 1965.

70. MELFI, L. T., JR.; and WOOD, G. M., JR.: The Use of an Ionization Gage as a Quantitative Analyzer for Bi-Gaseous Mixtures. NASA–TN–D–1597, Dec. 1962.

71. MENEELY, G. R.; and KALTREIDER, N. L.: Volume of lung determined by helium dilution. J. Clin. Invest., 28: 129, 1949.

72. MENGEL, C. E.: KANN, H. E.; HEYMAN, A.; et al.: Effects of in vivo hyperoxia on erythrocytes. II: Hemolysis in a human after exposure to oxygen under high pressure. *Blood*, 25: 822–829, 1965.

73. MICKELSON, W. F.; and HYPES, W. D.: Oxygen-Nitrogen Indicator-Controller and Space Cabin Outboard Leak Simulator. AMRL–TDR–64–25, Aerospace Medical Division, Wright-Patterson AFB, Ohio, June 1964.

74. MILLER, R. R.: and PIATT, V. R.: The Present Status of Chemical Research in Atmosphere Purification and Control on Nuclear-Powered Submarines. NRL–5465, U.S. Naval Research Lab., Washington, D.C., Apr. 1960.

75. National Aeronautics and Space Administration, Manned Spacecraft Center, Houston, Tex.: Mercury Project Summary Including Results of the Fourth Manned Orbital Flight, May 15 and 16, 1963. NASA–SP–45, May 1963.

76. NELSON, N.; EICHNA, L. W.; HORVATH, S. M.; et al.: Thermal exchanges of man at high temperatures. *Amer. J. Physiol., 151:* 626–652, 1947.

77. NEVISON, T. O., JR.: Letter Report to the Garrett Corp. The Lovelace Foundation, Albuquerque, N. Mex., Jan. 1962.

78. PARKER, F. A.; EKBERG, D. A.; WITHEY, D. J.; et al.: Atmosphere Selection and Control for Manned Space Stations. Presented at the International Symposium for Manned Space Stations (Munich, Germany), 1965.

79. PARKER, F. A.; EKBERG, D. R.; and WITHEY, D. J.: Atmosphere Selection and Environmental Control for Manned Space Stations. General Electric Co., Philadelphia, Pa., July 23, 1964.

80. PASELK, R. A.: Integration and Optimization of Space Vehicle Environmental Control Systems. ASD–TR–61–175, pt. II, North American Aviation, Inc., Los Angeles, Calif., Apr. 1963.

81. PETROCELLI, A. W.: Progress in the Development of Active Chemicals for Use as Air Revitalization Materials. Presented at the International Astronautics Federation Meeting (Athens, Greece), Sept. 1965.

82. PETROCELLI, A. W.; and CAPOTOSTO, A., JR.: The Synthesis and Utilization of Low-Molecular Weight Ozonides for Air Revitalization Purposes. NASA–CR–135, Nov. 1964.

83. PETROCELLI, A. W.; and CHIARENZELLI, R. V.: The inorganic ozonides. *J. Chem. Ed., 39:* 557–560, 1962.

84. PRESTI, J. B.: Semi-Passive Potassium Superoxide Air Revitalization System, Annual Report. Rept. No. U–413–64–202, General Dynamics Corp., Electric Boat Div., Groton, Conn., Dec. 1964.

85. RADNOFSKY, M. I.: Crew Systems Division, National Aeronautics and Space Administration, Houston, Tex., personal communication, Feb. 1966.

86. REED, A.: Evaluation of Gas Composition Detection Methods in Manned Space Vehicles. Rept. ADR–04–06–62.1, Grumman Aircraft Engineering Corp., Bethpage, N.Y., Dec. 1962.

87. ROBERTS, D. K.: Brief Outline Summarizing Electron Microscopic Studies on "Oxygen Toxicity." Unpublished data: NASA Workshop Conference on Criteria for Selection and Evaluation of Space Mission Atmospheres, Nov. 1965.

88. ROSS, M. D.: Space/Defense Corp., Birmingham, Mich., personal communication, Feb. 1965.

89. ROTH, E. M.: Bioenergetics of Space Suits for Lunar Exploration. NASA–SP–84, 1966.

90. ROTH, E. M.: Space-Cabin Atmospheres. Part I: Oxygen Toxicity. NASA–SP–47, 1964.

91. ROTH, E. M.: Space-Cabin Atmospheres. Part II: Fire and Blast Hazards. NASA–SP–48, 1964.

92. ROTH, E. M.: Space-Cabin Atmospheres. Part III: Physiological Factors of Inert Gases. NASA–SP–117, 1967.

93. ROTH, E. M.: Supplementary Bibliography on Fire and Blast. A: Combustion Studies. B: Secondary Effects. Contract NASr–115, Lovelace Foundation for Medical Education and Research, Albuquerque, N. Mex., Feb. 1966.

94. ROTH, E. M.; and BILLINGS, C. E., JR.: Atmosphere, in Bioastronautics Data Book, P. Webb, (ed.), NASA–SP–3006, 1964, p. 5.

95. ROUSSEAU, J.; BURRISS, W. L.; COE, C. S.; et al.: Atmospheric Control Systems for Space Vehicles. ASD–TDR–62–527, Part I, AiResearch Mfg. Co., Los Angeles, Calif., Mar. 1963.

96. ROUSSEAU, J.: OLSON, R. L.; COE, C. S.; et al.: Atmospheric Control Systems for Space Vehicles. ASD–TDR–62–527, Pt. II, AiResearch Mfg. Co., Los Angeles, Calif., Feb. 1964.

97. ROWLETT, B. H.: and LEE, R. H.: Environmental control. *Space/Aeronautics, 42:* 106–109, Sept. 1964.

98. RUSS, E. J.: Atmospheric Stores System Evaluation for Space Flights of One Year Duration. Report 64–26213, General Dynamics/Astronautics, San Diego, Calif., Oct. 1963, rev. Sept. 1964.

99. SHAEFER, K. E.: A concept of triple tolerance limits based on chronic carbon dioxide toxicity studies. *Aerospace Med., 32:* 197–204, 1961.

100. SCHREIHANS, F. A.; and DRYSOL, D. E.: Flammability Characteristics of Some Organic Spacecraft Materials in Zero Gravity. NAA–SID–65–640, North American Aviation, Inc., Downey, Calif., May 1965.

101. SECORD, T. C.: Chief, Life and Environmental Systems Branch, Douglas Aircraft Corp., Santa Monica, Calif., personal communication, Feb. 1966.

102. SECORD, T. C.; and BONURA, M. S.: Life Support Systems Data from 62 Days of Testing in a Manned Space Laboratory Simulator. Douglas Paper No. 3397, Douglas Missile & Space Systems Division, Santa Monica, Calif. (Presented to AIAA Fourth Manned Space Flight Meeting, St. Louis, Mo., Oct. 11–13, 1965.)

103. SNOW, R. H.: Thermodynamic Evaluation of the Possibility of Lithium Superoxide Production. WADD–AMRL–TR–65–126, Illinois Inst. of Technology, Chicago, 1965.

104. SPIETH, C. W.; BELL, J. E.; HUNTER, B. J.; et al.: Power Generating and Environmental Control Systems. Vol. II: Cryogenic Tankage Investigation. ASD–TR–61–327, Vol. 2, Beechcraft Research & Development, Inc., Boulder, Colo., Nov. 1961.

105. STERNBERGH, S. A.; and HICKAM, W. M.: Flight Type Oxygen Partial Pressure Sensor. NASA–CR–534, Aug. 1966.

106. TONELLI, A. D.; and SECORD, T. C.: Auxiliary Power Generating System for a Large Space Laboratory. DAC–P–1993, Douglas Missile & Space Systems Division, Douglas Aircraft Co., Inc., Huntington Beach, Calif., Sept. 1964.

107. TROUT, O. F., JR.: Sealing manned spacecraft. *Astronautics and Aerosp. Engr., 1:* 44–6, 1964.

108. VANCE, R. W. (ed.): Cryogenic Technology. John Wiley & Sons, 1963.

109. VORONIN, G. I.; GENIN, A. M.; and FOMIN, A. G.: Physiological and Hygienic Evaluation of the Life Support Systems Used on Vostok and Voskhod Spacecraft. (Translation from paper presented at the 2d International Symposium on Basic Environmental Problems of Man in Space, Paris, June 14–18, 1965.) NASA–TT–F–9424, July 1965.

110. WARNER, H.: Oxygen partial pressure sensor. *Med. Electron. Biol. Engng., 1:* 79–84, 1963.

111. WEBB, P.: Human Water Exchange in Space Suits and Capsules. Study in preparation under NASA Contract NASr–115, Lovelace Foundation for Medical Education and Research, Albuquerque, New Mexico, 1966. (To be published as a NASA CR.)

112. WELCH, B. E.: Chief, Environmental Systems Branch, USAF School of Aerospace Medicine, Aerospace Medical Division, Brooks AFB, Tex., personal communication, Mar. 1966.

113. WELCH, B. E.; MORGAN, T. E., JR.; and CLAMANN, H. G.: Time concentration effects in relation to oxygen toxicity in man. *Fed. Proc. 22:* 1053–1065, 1963.

114. WILHITE, W. F.: The Development of the Surveyor Gas Chromatograph. TR–32–425, California Institute of Technology, Jet Propulsion Lab., Pasadena, Calif., May 1963.

115. WILHITE, W. F.; and BURNELL, M. R.: Lunar Gas Chromatograph. *ISA Journal, 10:* 53–59, 1963.

116. WINSLOW, C.-E. A.; GAGGE, A. P.; and HERRINGTON, L. P.: The influence of air movement upon heat losses from the clothed human body. *Amer. J. Physiol., 127:* 505–518, 1939.

117. WINSLOW, C.-E. A.; HERRINGTON, L. P.; and GAGGE, A. P.: Relations between atmospheric conditions, physiological reactions and sensation of pleasantness. *Amer. J. Hyg., 26:* 103–115, 1936.

118. WOODS, R. W ; and ERLANSON, E. P.: Thermal Integration of Electric Power and Life Support Systems for Manned Space Stations. NASA–CR–543, Sept. 1966.

119. WORTMAN, J. J.: A Feasibility Study of a Thin Film Oxygen Partial Pressure Sensor. NASA–CR–66084, 1966.

120. WORTZ, E. C.; DIAZ, R. A.; GREEN, F. H.; et al.: Reduced Barometric Pressure and Respiratory Water Loss. SAM–TR–66–4, USAF School of Aerospace Medicine, Brooks AFB, Tex., Feb. 1966.

Nomenclature

A	area, sq ft
C	fraction of maximum evaporative capacity
C_d	coefficient of discharge
C_p	molar heat capacity at constant pressure, Btu/mole-°R or Btu/mole-°F
C_v	molar heat capacity at constant volume, Btu/mol-°R of Btu/mole-°F
CFM	$\dot{V}$, ft³/min
Clo	clothing heat transfer resistance, 1 Clo = 0.88° F-ft²-hr/Btu
D	diameter
d	diffusion coefficient
e	base of natural logarithms
F	mole rate of flow, moles/day or moles/sec
f	fanning friction factor or gray-body view factor
f_s	fraction of wetted surface of skin

$$f_1(\gamma) = \sqrt{\gamma \left(\frac{2}{\gamma + 1} \right)^{\frac{\gamma+1}{\gamma-1}}}$$

G	mass velocity, lb/sec-ft²
g	acceleration due to gravity, g = 32.2 ft/sec²
H	humidity
h	heat transfer coefficient, Btu/hr-ft²-°F
h_D	mass transfer coefficient, ft/hr
h_{fg}	heat of vaporization, Btu/lb
k	thermal conductivity, Btu/hr-ft-°F
L	clothing thickness, or length, ft
M	metabolism
MAC	maximum allowable concentration
m	molecular weight, lb/mole
N_{Le}	Lewis number
N_{Pr}	Prandtl number, $C_p\mu/k$, dimensionless
N_{Re}	Reynolds number
n	number of moles of gas
P	pressure, psia
PL	power loss, watts
PP	vehicle power penalty
p	partial pressure, psia
Q	heating rate, BTU/hr
R	gas constant, ft-lb/lb-°R, or universal gas constant, R = 1545 lb-ft/mole-°R
R'	R/m
R_w	Specific humidity coefficient
RH	Relative humidity

RP	Vehicle heat rejection penalty, lb/watt or lb/(Btu/hr)
RQ	Respiratory quotient (moles CO_2 produced/moles O_2 consumed)
N_{Sc}	Schmidt number, $\mu/\rho D$, dimensionless
T	temperature, °F or °R
V	volume of compartment, ft^3
$\bar{V}$	velocity, ft/min
$\bar{V}_c$	critical gas velocity, ft/sec
W	weight, lb
$\dot{W}$	mass flow rate, lb/day or lb/min
W_f	weight of fluid at fill, lb
W_T	total weight of pressure vessel and stored fluid, lb
W_u	useful fluid weight, lb
X	system penalty
Y	mole fraction of a gas

$$\alpha = 233 \frac{C_d A}{V} \frac{\sqrt{T_0}}{m} f_1(\gamma)$$

$$\gamma = \frac{C_p}{C_v}$$

ϵ	emissivity
η	efficiency
μ	viscosity, lb/sec-ft
ρ	density, fluid and insulation, lb/ft^3
σ	Stefan-Boltzmann constant (0.1713×10^{-8} Btu/hr-ft^2-°R^4)
τ	time, day or sec
τ	time constant, day or sec
ϕ	specific humidity, lb H_2O/lb gas

Subscripts:

a	atmosphere
acc	accessory
CO_2	carbon dioxide
c	critical or clothing or convection
can	canister
crit	critical
E	equipment
e	system equivalent
F	feed
f	fill state
H	hardware
He	helium
I	inert gas or inspired
in	inner
L	leakage
Ls	lines
l	latent
lk	lock
M	metabolism
MAT	materials

N	nitrogen
Ne	neon
O	oxygen
o	initial value
P	power
Q	of heat
R	residue
r	radiation
S	support
s	skin or sensible
STD	standard conditions
T	total mass
t	total number
u	useful
V	vent
W	water vapor or work
w	wall
*	steady-state value

Superscripts:

·	rate of change with time
'	per person

Conversion Tables

THE MULTIPLE SYSTEMS of units and measures used in the basic biological, physical, and engineering sciences is often confusing to those with interdisciplinary interests. The following tables have been selected from a report by Kinslow and Major.[56] Tables of electrical and thermodynamic units not covered in this extract may be found in the report.

The reader may convert from the measure of quantities in the units listed on the left to those across the top of the page by multiplying by the given factor. The exponent to the numbers indicates the power of 10 by which the factor is to be multiplied. For example, 8.68977^{-2} is equivalent to 0.0868977. Underscores indicate exact values.

Slight numerical differences will be noticed between the values herein and those in most current texts because of the redefinition of the foot in 1960.

Length

	Å	cm	ft	in	km	m	μ	mils	miles (U.S. statute)	mm	miles (nautical)	rods	yd
Å	1.00000	1.00000^{-8}	3.28084^{-10}	3.93701^{-9}	1.00000^{-13}	1.00000^{-10}	1.00000^{-4}	3.93701^{-6}	6.21371^{-14}	1.00000^{-7}	5.39957^{-14}	1.98839^{-11}	1.09361^{-10}
cm	1.00000^{8}	1.00000	3.28084^{-2}	3.93701^{-1}	1.00000^{-5}	1.00000^{-2}	1.00000^{4}	3.93701^{2}	6.21371^{-6}	1.00000^{1}	5.39957^{-6}	1.98839^{-3}	1.09361^{-2}
ft	3.04800^{9}	3.04800^{1}	1.00000	1.20000^{1}	3.04800^{-4}	3.04800^{-1}	3.04800^{5}	1.20000^{4}	1.89394^{-4}	3.04800^{2}	1.64579^{-4}	6.06061^{-2}	3.33333^{-1}
in	2.54000^{8}	2.54000	8.33333^{-2}	1.00000	2.54000^{-5}	2.54000^{-2}	2.54000^{4}	1.00000^{3}	1.57828^{-5}	2.54000^{1}	1.37149^{-5}	5.05050^{-3}	2.77778^{-2}
km	1.00000^{13}	1.00000^{5}	3.28084^{3}	3.93701^{4}	1.00000	1.00000^{3}	1.00000^{9}	3.93701^{7}	6.21371^{-1}	1.00000^{6}	5.39957^{-1}	1.98839^{2}	1.09361^{3}
m	1.00000^{10}	1.00000^{2}	3.28084	3.93701^{1}	1.00000^{-3}	1.00000	1.00000^{6}	3.93701^{4}	6.21371^{-4}	1.00000^{3}	5.39957^{-4}	1.98839^{-1}	1.09361
μ	1.00000^{4}	1.00000^{-4}	3.28084^{-6}	3.93701^{-5}	1.00000^{-9}	1.00000^{-6}	1.00000	3.93701^{-2}	6.21371^{-10}	1.00000^{-3}	5.39957^{-10}	1.98839^{-7}	1.09361^{-6}
mils	2.54000^{5}	2.54000^{-3}	8.33333^{-5}	1.00000^{-3}	2.54000^{-8}	2.54000^{-5}	2.54000^{1}	1.00000	1.57828^{-8}	2.54000^{-2}	1.37149^{-8}	5.05050^{-6}	2.77778^{-5}
miles (U.S. statute)	1.60934^{13}	1.60934^{5}	5.28000^{3}	6.33600^{4}	1.60934	1.60934^{3}	1.60934^{9}	6.33600^{7}	1.00000	1.60934^{6}	8.68977^{-1}	3.20000^{2}	1.76000^{3}
mm	1.00000^{7}	1.00000^{-1}	3.28084^{-3}	3.93701^{-2}	1.00000^{-6}	1.00000^{-3}	1.00000^{3}	3.93701^{1}	6.21371^{-7}	1.00000	5.39957^{-7}	1.98839^{-4}	1.09361^{-3}
miles (nautical)	1.85200^{13}	1.85200^{5}	6.07812^{3}	7.29134^{4}	1.85200	1.85200^{3}	1.85200^{9}	7.29134^{7}	1.15078	1.85200^{6}	1.00000	3.68250^{2}	2.02537^{3}
rods	5.02920^{10}	5.02920^{2}	1.65000^{1}	1.98000^{2}	5.02920^{-3}	5.02920	5.02920^{6}	1.98000^{5}	3.12500^{-3}	5.02920^{3}	2.71555^{-3}	1.00000	5.50000
yd	9.14400^{9}	9.14400^{1}	3.00000	3.60000^{1}	9.14400^{-4}	9.14400^{-1}	9.14400^{5}	3.60000^{4}	5.68182^{-4}	9.14400^{2}	4.93737^{-4}	1.81818^{-1}	1.00000

Area

	acre	in (circular)	mil (circular)	cm²	ft²	in²	m²	mm²	rod²	yd²
Acre	1.00000	7.98657^{6}	7.98657^{12}	4.04686^{7}	4.35600^{4}	6.27264^{6}	4.04686^{3}	4.04686^{9}	1.60000^{2}	4.84000^{3}
Circular in.	1.25211^{-7}	1.00000	1.00000^{6}	5.06707	5.45415^{-3}	7.85398^{-1}	5.06707^{-4}	5.06707^{2}	2.00336^{-5}	6.06017^{-4}
Circular mil.	1.25211^{-13}	1.00000^{-6}	1.00000	5.06707^{-6}	5.45415^{-9}	7.85398^{-7}	5.06707^{-10}	5.06707^{-4}	2.00336^{-11}	6.06017^{-10}
cm²	2.47105^{-8}	1.97353^{-1}	1.97353^{5}	1.00000	1.07639^{-3}	1.55000^{-1}	1.00000^{-4}	1.00000^{2}	3.95368^{-6}	1.19598^{-4}
ft²	2.29568^{-5}	1.83347^{2}	1.83347^{8}	9.29030^{2}	1.00000	1.44000^{2}	9.29030^{-2}	9.29030^{4}	3.67310^{-3}	1.11111^{-1}
in²	1.59423^{-7}	1.27324	1.27324^{6}	6.45160	6.94444^{-3}	1.00000	6.45160^{-4}	6.45160^{2}	2.55076^{-5}	7.71605^{-4}
m²	2.47105^{-4}	1.97353^{3}	1.97353^{9}	1.00000^{4}	1.07639^{1}	1.55000^{3}	1.00000	1.00000^{6}	3.95368^{-2}	1.19598
mm²	2.47105^{-10}	1.97353^{-3}	1.97353^{3}	1.00000^{-2}	1.07639^{-5}	1.55000^{-3}	1.00000^{-6}	1.00000	3.95368^{-8}	1.19598^{-6}
rod²	6.25000^{-3}	4.99161^{4}	4.99161^{10}	2.52929^{5}	2.72250^{2}	3.92040^{4}	2.52929^{1}	2.52929^{7}	1.00000	3.02500^{1}
yd²	2.06611^{-4}	1.65012^{3}	1.65012^{9}	8.36127^{3}	9.00000	1.29600^{3}	8.36127^{-1}	8.36127^{5}	3.30578^{-2}	1.00000

Volume

	cm³	ft³	gal (U.S.)	in³	liter	m³	yd³ (U.S.)
cm³	1.00000	3.53146^{-5}	2.64171^{-4}	6.10236^{-2}	9.99972^{-4}	1.00000^{-6}	1.30794^{-6}
ft³	2.83168^{4}	1.00000	7.48052	1.72800^{3}	2.83161^{1}	2.83168^{-2}	3.70370^{-2}
gal (U.S.)	3.78543^{3}	1.33680^{-1}	1.00000	2.31000^{2}	3.78533	3.78543^{-3}	4.95113^{-3}
in³	1.63871^{1}	5.78704^{-4}	4.32900^{-3}	1.00000	1.63866^{-2}	1.63871^{-5}	2.14335^{-5}
liter	1.00003^{3}	3.53156^{-2}	2.64178^{-1}	6.10253^{1}	1.00000	1.00003^{-3}	1.30798^{-3}
m³	1.00000^{6}	3.53146^{1}	2.64171^{2}	6.10236^{4}	9.99972^{2}	1.00000	1.30794
yd³ (U.S.)	7.64554^{5}	2.70000^{1}	2.01974^{2}	4.66560^{4}	7.64538^{2}	7.64554^{-1}	1.00000

Mass

	grain	gm	kgm	oz (avdp)	lbm	slug	ton (short)
grain	1.00000	6.47988^{-2}	6.47988^{-5}	2.28571^{-3}	1.42857^{-4}	4.44012^{-6}	7.14285^{-8}
gm	1.54323^{1}	1.00000	1.00000^{-3}	3.52739^{-2}	2.20462^{-3}	6.85216^{-5}	1.10231^{-6}
kgm	1.54323^{4}	1.00000^{3}	1.00000	3.52739^{1}	2.20462	6.85216^{-2}	1.10231^{-3}
oz (avdp)	4.37500^{2}	2.83495^{1}	2.83495^{-2}	1.00000	6.25000^{-2}	1.94256^{-3}	3.12500^{-5}
lbm	7.00000^{2}	4.53592^{2}	4.53592^{-1}	1.60000^{1}	1.00000	3.10809^{-2}	5.00000^{-4}
slug	2.25218^{5}	1.45939^{4}	1.45939^{1}	5.14785^{2}	3.21740^{1}	1.00000	1.60870^{-2}
ton (short)	1.40000^{7}	9.07184^{5}	9.07184^{2}	3.20000^{4}	2.00000^{3}	6.21618^{1}	1.00000

Time

	day	hour	μsec	msec	min	sec
day	1.00000	2.40000^{1}	8.64000^{10}	8.64000^{7}	1.44000^{3}	8.64000^{4}
hour	4.16666^{-2}	1.00000	3.60000^{9}	3.60000^{6}	6.00000^{1}	3.60000^{3}
μsec	1.15741^{-11}	2.77778^{-10}	1.00000	1.00000^{-3}	1.66667^{-8}	1.00000^{-6}
msec	1.15741^{-6}	2.77778^{-7}	1.00000^{3}	1.00000	1.66667^{-5}	1.00000^{-3}
min	6.94444^{-4}	1.66667^{-2}	6.00000^{7}	6.00000^{4}	1.00000	6.00000^{1}
sec	1.15741^{-5}	2.77778^{-4}	1.00000^{6}	1.00000^{3}	1.66666^{-2}	1.00000

Angle

	deg	min	quadrant (right angle)	radians	revolutions	sec
deg	1.00000	6.00000^{1}	1.11111^{-2}	1.74533^{-2}	2.77778^{-3}	3.60000^{3}
min	1.66667^{-2}	1.00000	1.85185^{-4}	2.90889^{-4}	4.62963^{-5}	6.00000^{1}
quadrants (right angle)	9.00000^{1}	5.40000^{3}	1.00000	1.57080	2.50000^{-1}	3.24000^{5}
radians	5.72958^{1}	3.43775^{3}	6.36620^{-1}	1.00000	1.59155^{-1}	2.06265^{5}
revolutions	3.60000^{2}	2.16000^{4}	4.00000	6.28320	1.00000	1.29600^{6}
sec	2.77777^{-4}	1.66667^{-2}	3.08642^{-6}	4.84815^{-6}	7.71605^{-7}	1.00000

Velocity

	cm/sec	ft/min	ft/sec	km/hr	knot	m/min	m/sec	mile/hr
cm/sec	1.00000	1.96850	3.28084^{-2}	3.60000^{-2}	1.94384^{-2}	6.00000^{-1}	1.00000^{-2}	2.23694^{-2}
ft/min	5.08000^{-1}	1.00000	1.66667^{-2}	1.82880^{-2}	9.87473^{-3}	3.04800^{-1}	5.08000^{-3}	1.13636^{-2}
ft/sec	3.04800^{1}	6.00000^{1}	1.00000	1.09728	5.92484^{-1}	1.82880^{1}	3.04800^{-1}	6.81818^{-1}
km/hr	2.77778^{1}	5.46807^{1}	9.11344^{-1}	1.00000	5.39957^{-1}	1.66667^{1}	2.77778^{-1}	6.21371^{-1}
knot	5.14444^{1}	1.01268^{2}	1.68781	1.85200	1.00000	3.08667^{1}	5.14444^{-1}	1.15078
m/min	1.66667	3.28084	5.46807^{-2}	6.00000^{-2}	3.23974^{-2}	1.00000	1.66667^{-2}	3.72823^{-2}
m/sec	1.00000^{2}	1.96850^{2}	3.28084	3.60000	1.94384	6.00000^{-1}	1.00000	2.23694
mile/hr	4.47040^{1}	8.80000^{1}	1.46667	1.60934	8.68976^{-1}	2.68224^{1}	4.47040^{-1}	1.00000

Force

	dyne	g_f	kg_f	newton	poundal	lb_f
dyne	1.00000	1.01972^{-3}	1.01972^{-6}	1.00000^{-5}	7.23301^{-5}	2.24809^{-6}
g_f	9.80665^{2}	1.00000	1.00000^{-3}	9.80665^{-3}	7.09316^{-2}	2.20462^{-3}
kg_f	9.80665^{5}	1.00000^{3}	1.00000	9.80665	7.09316^{1}	2.20462
newton	1.00000^{5}	1.01972^{2}	1.01972^{-1}	1.00000	7.23301	2.24809^{-1}
poundal	1.38255^{4}	1.40981^{1}	1.40981^{-2}	1.38255^{-1}	1.00000	3.10809^{-2}
lb_f	4.44822^{5}	4.53594^{2}	4.53594^{-1}	4.44822	3.21740^{1}	1.00000

Pressure

	standard atmosphere	bar [a]	dynes/cm² (barye)	ft H₂O at 60° F [b]	gm/cm²	in. Hg at 32° F [b]	in. H₂O at 60° F [b]	kg/cm²	lb_f/ft²	lb_f/in.²	microns Hg at 32° F [b]	mm Hg at 32° F [b]
standard atmosphere	1.00000	1.01325	1.01325^{6}	3.39320^{1}	1.03323^{3}	2.99213^{1}	4.07184^{2}	1.03323	2.11622^{3}	1.46959^{1}	7.60000^{5}	7.60000^{2}
bar [a]	9.86923^{-1}	1.00000	1.00000^{6}	3.34882^{1}	1.01972^{3}	2.95300^{1}	4.01859^{2}	1.01972	2.08854^{3}	1.45038^{1}	7.50062^{5}	7.50062^{2}
dynes/cm² (barye)	9.86923^{-7}	1.00000^{-6}	1.00000	3.34882^{-5}	1.01972^{-3}	2.95300^{-5}	4.01859^{-4}	1.01972^{-6}	2.08854^{-3}	1.45038^{-5}	7.50062^{-1}	7.50062^{-4}
ft H₂O (at 60° F) [b]	2.94707^{-2}	2.98612^{-2}	2.98612^{4}	1.00000	3.04500^{1}	8.81801^{-1}	1.20000^{1}	3.04500^{-2}	6.23664^{1}	4.33100^{-1}	2.23977^{4}	2.23977^{1}
gm/cm²	9.67841^{-4}	9.80665^{-4}	9.80665^{2}	3.28408^{-2}	1.00000	2.89590^{-2}	3.94089^{-1}	1.00000^{-3}	2.04816	1.42233^{-2}	7.35559^{2}	7.35559^{-1}
in. Hg at 32° F [b]	3.34211^{-2}	3.38639^{-2}	3.38639^{4}	1.13404	3.45315^{1}	1.00000	1.36085^{1}	3.45315^{-2}	7.07262^{1}	4.91154^{-1}	2.54000^{4}	2.54000^{1}
in. H₂O at 60° F [b]	2.45589^{-3}	2.48843^{-3}	2.48843^{3}	8.33333^{-2}	2.53750	7.34834^{-2}	1.00000	2.53750^{-3}	5.19720	3.60917^{-2}	1.86648^{3}	1.86648
kg/cm²	9.67841^{-1}	9.80665^{-1}	9.80665^{5}	3.28408^{1}	1.00000^{3}	2.89590^{1}	3.94089^{3}	1.00000	2.04816^{3}	1.42233^{1}	7.35559^{5}	7.35559^{2}
lb_f/ft²	4.72541^{-4}	4.78803^{-4}	4.78803^{2}	1.60343^{-2}	4.88243^{-1}	1.41390^{-2}	1.92411^{-1}	4.88243^{-4}	1.00000	6.94444^{-3}	3.59131^{2}	3.59131^{-1}
lb_f/in.²	6.80460^{-2}	6.89476^{-2}	6.89476^{4}	2.30894	7.03070^{1}	2.03602	2.77072	7.03070^{-2}	1.44000^{2}	1.00000	5.17149^{4}	5.17149^{1}
microns Hg at 32° F [b]	1.31579^{-6}	1.33322^{-6}	1.33322	4.46474^{-5}	1.35951^{-3}	3.93701^{-5}	5.35768^{-4}	1.35951^{-6}	2.78450^{-3}	1.93368^{-5}	1.00000	1.00000^{-3}
mm Hg at 32° F [b]	1.31579^{-3}	1.33322^{-3}	1.33322^{3}	4.46474^{-2}	1.35951	3.93701^{-2}	5.35768^{-1}	1.35951^{-3}	2.78450	1.93368^{-2}	1.00000^{3}	1.00000

[a] Some writers erroneously use the term "bar" for barye.

[b] For g = 980.665 centimeters per second².

Energy

	Btu	I.T. calorie	electron volt	erg (dyne-cm)	ft-lb$_f$	gm-cm	hp-hr (mech)	absolute joule	kilocalorie	kg-m	kW-hr	watt-hr	ft-poundal
Btu	1.00000	2.51996^{2}	6.58577^{21}	1.05504^{10}	7.78158^{2}	1.07584^{7}	3.93009^{-4}	1.05504^{3}	2.51995^{-1}	1.07584^{2}	2.93067^{-4}	2.93067^{-1}	2.50365^{4}
I.T. calorie	3.96832^{-3}	1.00000	2.61344^{19}	4.18674^{7}	3.08798	4.26928^{4}	1.55958^{-6}	4.18674	1.00000^{-3}	4.26928^{-1}	1.16298^{-6}	1.16298^{-3}	9.93528^{1}
electron-volt	1.51842^{-22}	3.82637^{-20}	1.00000	1.60200^{-12}	1.18157^{-19}	1.63358^{-15}	5.96755^{-26}	1.60200^{-19}	3.82637^{-23}	1.63358^{-20}	4.45000^{-26}	4.45000^{-23}	3.80160^{-18}
erg (dyne-cm)	9.47831^{-11}	2.38849^{-8}	6.24220^{11}	1.00000	7.37562^{-8}	1.01972^{-3}	3.72506^{-14}	1.00000^{-7}	2.38849^{-11}	1.01972^{-8}	2.77778^{-14}	2.77778^{-11}	2.37304^{-6}
ft-lb$_f$	1.28509^{-3}	3.23836^{-1}	8.46328^{18}	1.35582^{7}	1.00000	1.38255^{4}	5.05050^{-7}	1.35582	3.23836^{-4}	1.38255^{-1}	3.76616^{-7}	3.76616^{-4}	3.21740^{1}
gram-cm	9.29505^{-8}	2.34231^{-5}	6.12150^{14}	9.80665^{2}	7.23301^{-5}	1.00000	3.65304^{-11}	9.80665^{-5}	2.34231^{-8}	1.00000^{-5}	2.72407^{-11}	2.72407^{-8}	2.32715^{-3}
hp-hr (mech)	2.54447^{3}	6.41196^{5}	1.67573^{25}	2.68452^{13}	1.98000^{6}	2.73745^{10}	1.00000	2.68452^{6}	6.41196^{2}	2.73745^{5}	7.45700^{-1}	7.45700^{2}	6.37046^{7}
absolute joule (watt-sec)	9.47831^{-4}	2.38849^{-1}	6.24220^{18}	1.00000^{7}	7.37562^{-1}	1.01972^{4}	3.72506^{-7}	1.00000	2.38849^{-4}	1.01972^{-1}	2.77778^{-7}	2.77778^{-4}	2.37304^{1}
kilocalorie	3.96832	1.00000^{3}	2.61344^{22}	4.18674^{10}	3.08798^{3}	4.26928^{7}	1.55958^{-3}	4.18674^{3}	1.00000	4.26928^{2}	1.16298^{-3}	1.16298	9.93528^{4}
kg-m	9.29505^{-3}	2.34231	6.12150^{19}	9.80665^{7}	7.23301	1.00000^{5}	3.65304^{-6}	9.80665	2.34231^{-3}	1.00000	2.72407^{-6}	2.72407^{-3}	2.32715^{2}
kW-hr	3.41219^{3}	8.59858^{5}	2.24719^{25}	3.60000^{13}	2.65522^{6}	3.67098^{10}	1.34102	3.60000^{6}	8.59858^{2}	3.67093^{5}	1.00000	1.00000^{3}	8.54293^{7}
W-hr	3.41219	8.59858^{2}	2.24719^{22}	3.60000^{10}	2.65522^{3}	3.67098^{7}	1.34102^{-3}	3.60000^{3}	8.59858^{-1}	3.67093^{2}	1.00000^{-3}	1.00000	8.54293^{4}
ft-poundal	3.99417^{-5}	1.00651^{-2}	2.63047^{17}	4.21401^{5}	3.10810^{-2}	4.29710^{2}	1.56974^{-8}	4.21401^{-2}	1.00651^{-5}	4.29710^{-3}	1.17056^{-8}	1.17056^{-5}	1.00000

Definitions

$$\frac{1\ \text{Btu}}{°F\ \text{lb}_m} = \frac{1\ \text{I.T. cal}}{°C\ \text{gm}}$$

1 I.T. cal = 1/860 int. W-hr
1 int. watt = 1.000165 ab. watt
1 Btu$_{mean}$ = 1055.8 absolute joules
1 Btu$_{32°F}$ = 1060 absolute joules

1 Btu$_{60°F}$ = 1054.6 absolute joules
I.T. Btu = 1055.04 absolute joules
I.T. cal$_{15}$ °C = 4.1854 absolute joules
I.T. calorie = 4.18674 absolute joules
1 cal$_{mean}$ = 4.190 absolute joules
1 cal$_{20}$ °C = 4.181 absolute joules

1 thermochemical calorie = 4.1840 absolute joules
1 International joule = 1.000165 absolute joules
1 I.T. calorie = 1/860 int. W·hr
Kilocalorie or large calorie = 1000 calories

Power

	Btu/hr	Btu/min	Btu/sec	I.T. cal/hr	I.T. cal/min	I.T. cal/sec	erg/sec	ft-lb/min	ft-lb/sec	hp (elec)	hp (mach)	hp (metric)	kg-m/sec	kW	W
Btu/hr	1.00000	1.66667^{-2}	2.77778^{-4}	2.51996^{2}	4.19993	6.99988^{-2}	2.93067^{6}	1.29693^{1}	2.16155^{-1}	3.92851^{-4}	3.93009^{-4}	3.98460^{-4}	2.98845^{-2}	2.93067^{-4}	2.93067^{-1}
Btu/min	6.00000^{1}	1.00000	1.66667^{-2}	1.51197^{4}	2.51996^{2}	4.19993	1.75840^{8}	7.78158^{2}	1.29693^{1}	2.35711^{-2}	2.35805^{-2}	2.39076^{-2}	1.79307	1.75840^{-2}	1.75840^{1}
Btu/sec	3.60000^{3}	6.0000^{1}	1.00000	9.07183^{5}	1.51197^{4}	2.51996^{2}	1.05504^{10}	4.66894^{4}	7.78158^{2}	1.41426	1.41483	1.43446	1.07584^{2}	1.05504	1.05504^{3}
I.T cal/hr	3.96832^{-3}	6.61387^{-5}	1.10231^{-6}	1.00000	1.66667^{-2}	2.77778^{-4}	1.16298^{4}	5.14663^{-2}	8.57772^{-4}	1.55896^{-6}	1.55958^{-6}	1.58122^{-6}	1.18591^{-4}	1.16298^{-6}	1.16298^{-3}
I.T. cal/min	2.38099^{-1}	3.96832^{-3}	6.61387^{-5}	6.00000^{1}	1.00000	1.66667^{-2}	6.97790^{5}	3.08798	5.14663^{-2}	9.35376^{-5}	9.35751^{-5}	9.48730^{-5}	7.11547^{-3}	6.97790^{-5}	6.97790^{-2}
I.T. cal/sec	1.42859^{1}	2.38100^{-1}	3.96832^{-3}	3.60000^{3}	6.00000^{1}	1.00000	4.18674^{7}	1.85279^{2}	3.08798	5.61225^{-3}	5.61451^{-3}	5.69238^{-3}	4.26928^{-1}	4.18674^{-3}	4.18674
erg/sec	3.41219^{-7}	5.68699^{-9}	9.47831^{-11}	8.59858^{-5}	1.43310^{-6}	2.38849^{-8}	1.00000	4.42537^{-6}	7.37562^{-8}	1.34048^{-10}	1.34102^{-10}	1.35962^{-10}	1.01972^{-8}	1.00000^{-10}	1.00000^{-7}
ft-lb/min	7.71052^{-2}	1.28509^{-3}	2.14181^{-5}	1.94302^{1}	3.23836^{-1}	5.39727^{-3}	2.25970^{5}	1.00000	1.66667^{-2}	3.02909^{-5}	3.03030^{-5}	3.07233^{-5}	2.30425^{-3}	2.25970^{-5}	2.25970^{-2}
ft-lb/sec	4.62631	7.71052^{-2}	1.28509^{-3}	1.16581^{3}	1.94302^{1}	3.23836^{-1}	1.35582^{7}	6.00000^{1}	1.00000	1.81745^{-3}	1.81818^{-3}	1.84340^{-3}	1.38255^{-1}	1.35582^{-3}	1.35582
hp (elec)	2.54549^{3}	4.24249^{1}	7.07081^{-1}	6.41453^{5}	1.06909^{4}	1.78182^{2}	7.46000^{9}	3.30132^{4}	5.50221^{2}	1.00000	1.00040	1.01427	7.60707^{1}	7.46000^{-1}	7.46000^{2}
hp (mech)	2.54447^{3}	4.24079^{1}	7.06798^{-1}	6.41196^{5}	1.06866^{4}	1.78110^{2}	7.45701^{9}	3.30000^{4}	5.50000^{2}	9.99599^{-1}	1.00000	1.01387	7.60402^{1}	7.45701^{-1}	7.45701^{2}
hp (metric)	2.50966^{3}	4.18277^{1}	6.97129^{-1}	6.32424^{5}	1.05404^{4}	1.75673^{2}	7.35500^{9}	3.25486^{4}	5.42476^{2}	9.85924^{-1}	9.86320^{-1}	1.00000	7.50000^{1}	7.35500^{-1}	7.35500^{2}
kg-m/sec	3.34622^{1}	5.57703^{-1}	9.29505^{-3}	8.43233^{3}	1.40539^{2}	2.34231	9.80665^{7}	4.33981^{2}	7.23301	1.31456^{-2}	1.31509^{-2}	1.33333^{-2}	1.00000	9.80665^{-3}	9.80665
kW	3.41219^{3}	5.68699^{1}	9.47831^{-1}	8.59858^{5}	1.43310^{4}	2.38849^{2}	1.00000^{10}	4.42537^{4}	7.37562^{2}	1.34048	1.34102	1.35962	1.01972^{2}	1.00000	1.00000^{3}
W	3.41219	5.68699^{-2}	9.47831^{-4}	8.59858^{2}	1.43310^{1}	2.38849^{-1}	1.00000^{7}	4.42537^{1}	7.37562^{-1}	1.34048^{-3}	1.34102^{-3}	1.35962^{-3}	1.01972^{-1}	1.00000^{-3}	1.00000

Mass Flow Rate

	gm_m/sec	kg_m/sec	lb_m/hr	lb_m/min	lb_m/sec	slug/sec
gm_m/sec	1.00000	1.00000^{-3}	7.93664	1.32277^{-1}	2.20462^{-3}	6.85218^{-5}
kg_m/sec	1.00000^{3}	1.00000	7.93664^{3}	1.32277^{2}	2.20462	6.85218^{-2}
lb_m/hr	1.25998^{-1}	1.25998^{-4}	1.00000	1.66667^{-2}	2.77778^{-4}	8.63360^{-6}
lb_m/min	7.55987	7.55987^{-3}	6.00000^{1}	1.00000	1.66667^{-2}	5.18016^{-4}
lb_m/sec	4.53592^{2}	4.53592^{-1}	3.60000^{3}	6.00000^{1}	1.00000	3.10809^{-2}
slug/sec	1.45939^{4}	1.45939^{1}	1.15826^{5}	1.93044^{3}	3.21740^{1}	1.00000

Pumping Speed or Volume Flow

	cm^3/sec	ft^3/min	ft^3/sec	gal/min	liter/min	liter/sec	m^3/hr	m^3/min
cm^3/sec	1.00000	2.11888^{-3}	3.53147^{-5}	1.58503^{-2}	5.99983^{-2}	9.99972^{-4}	3.60000^{-3}	6.00000^{-5}
ft^3/min	4.71947^{2}	1.00000	1.66667^{-2}	7.48052	2.83160^{1}	4.71934^{-1}	1.69901	2.83168^{-2}
ft^3/sec	2.83168^{4}	6.00000^{1}	1.00000	4.48831^{2}	1.69896^{3}	2.83160^{1}	1.01941^{2}	1.69901
gal/min	6.30902^{1}	1.33680^{-1}	2.22801^{-3}	1.00000	3.78530	6.30884^{-2}	2.27125^{-1}	3.78541^{-3}
liter/min	1.66671^{1}	3.53156^{-2}	5.88594^{-4}	2.64179^{-1}	1.00000	1.66667^{-2}	6.00017^{-2}	1.00003^{-3}
liter/sec	1.00003^{3}	2.11894	3.53156^{-2}	1.58508^{1}	6.00000^{1}	1.00000	3.60010	6.00017^{-2}
m^3/hr	2.77778^{2}	5.88578^{-1}	9.80963^{-3}	4.40287	1.66662^{1}	2.77770^{-1}	1.00000	1.66667^{-2}
m^3/min	1.66667^{4}	3.53147^{1}	5.88578^{-1}	2.64172^{2}	9.99972^{2}	1.66662^{1}	6.00000^{1}	1.00000

Temperature

[Values are based on the thermodynamic temperature scale as defined by the 10th General Conference on Weights and Measures meeting at Paris in October 1954. Temperature of triple point of water $= 273.16°$ K $= 491.688°$ R $= 32.018°$ F $= 0.01°$ C; temperature of ice point of water $= 273.15°$ K $= 491.67°$ R $= 0°$ C $= 32°$ F]

To convert from the units below to those on the right, perform the indicated operations in order.	°C	°F	°K	°R
°C	$\times 1$	$\times 9/5 + 32$	$+ 273.15$	$\times 9/5 + 491.67$
°F	$- 32 \times 5/9$	$\times 1$	$\times 5/9 + 255.372$	$\times 459.67$
°K	$- 273.15$	$\times 9/5 - 459.67$	$\times 1$	$\times 9/5$
°R	$\times 5/9 - 273.15$	$- 459.67$	$\times 5/9$	$\times 1$